Recovery of Transforming Growth Factor-β2 from Whey Growth Factor Extract with Immunoaffinity Techniques

by

Benjamin Matthew Hunt

in the

Department of Chemical Engineering

University of Adelaide

Submitted for the degree of Doctor of Philosophy, February 2000

Table of Contents

Table of Tables

Table of Figures

Abstract

Transforming Growth Factor-β2 (TGF-β2) is a polypeptide with a range of biological activities upon mammalian cells. A great deal of research has indicated a number of possible therapeutic applications for TGF-β2 and as a consequence, it has considerable potential commercial value. A biologically active protein fraction, termed Whey Growth Factor Extract (WGFE), can be derived from cheese whey by using cation-exchange chromatography (Francis et al., 1995). This process has been patented and material is now available from a recently completed GMP pilot-scale facility. Many growth factors have been identified in WGFE and TGF-β2 is the most abundant of these. Its purification from WGFE has been demonstrated with size-exclusion gel filtration and reversed-phase HPLC (Rogers et al., 1996). However, this purification was time-consuming and labour-intensive, and therefore not economically feasible at commercial-scale. Immunoaffinity chromatography has potential for reducing purification costs and was considered as an alternative to the standard purification method.

This thesis describes attempts to develop an immunoaffinity process for the commercial-scale purification of TGF-β2 from WGFE. The standard purification method was used to partially purify TGF-β2. However, much lower specific TGF-β2 activities were observed for the final step of the purification than were reported by Rogers et al. (1996). Two separate immunisation strategies were employed to raise a titre against TGF-β2. One group of mice was immunised with partially purified TGF-β2. The second group was immunised with synthetic peptide that corresponds to amino acids 50-75 of TGF-β2. The second strategy successfully raised a specific titre and fusions generated two specific anti-TGF-β2 positive hybridomas. Antibody 5D4 stains TGF-β2 in western immunoblots and localises TGF-β2 in skin but neither of the antibodies inhibited the biological activity of TGF-β2.

Mathematical models of the immunoaffinity process were developed to identify the best antibody and configuration without the need for experiments that explore every possibility. Simple experiments determined the critical antibody properties to facilitate the modelling and rational design of the immunoaffinity system. Antibody was coupled to membrane and Sepharose but neither of these supports demonstrated specific TGF-β2 binding. However, both supports showed considerable non-specific TGF-β2 binding. Interestingly, Sepharose separated TGF-β2 from partially purified material in the absence of antibody. TGF-β2 was

purified with a combination of acid gel filtration, reversed phase HPLC and Sepharose column chromatography. However, the purification method is complex and offers only modest improvements over the method of Rogers et al. (1996). This work highlights some of the difficulties and pitfalls of immunoaffinity chromatography and it is anticipated that knowledge of these could help future workers to optimise this important technique.

Abbreviations

BCA	bicinchoninic acid
BSA	bovine serum albumin
Chaps	3-(3-chlolamidopropyl)dimethylammonio- 1-propane-sulfonate
CNBr	cyanogen bromide
DMEM	Dulbecco's modified Eagle's medium
DPBS	Dulbecco's phosphate buffered saline
DTT	dithiothreitol
ED_{50}	dose producing 50% maximal inhibition
EDC	1-ethyl-3-(3-dimethylaminopropyl)-carbodiimide
EDTA	ethylenediamine tetra-acetic acid
EGF	Epidermal Growth Factor
ELISA	enzyme-linked immunosorbent assay
FBS	foetal bovine serum
FGF	Fibroblast Growth Factor
G1	gap 1 phase of the cell cycle
G2	gap 2 phase of the cell cycle
GMP	good manufacturing practice
HAT	hypoxanthine-aminopterin-thymidine
HBS	HEPES buffered saline
HEPES	N-(2-hydroxyethyl)piperazine-N'-(2-ethanesulfonic acid)
HFBA	heptafluorobutyric acid
HPLC	high pressure liquid chromatography
HT	hypoxanthine-thymidine
hpTGF-β2	highly purified TGF-β2
IGF	Insulin-like Growth Factor (type I or II)
IgG	Immunoglobulin G
LAP	latency-associated peptide
LTBP	latent TGF-β binding protein
M	mitotic phase of the cell cycle
Mab	monoclonal antibody
MES	2-(N-Morpholino)ethanesulphonic acid

Mv1Lu	mink lung epithelial cell line
MW	molecular weight
NHS	N-hydroxysuccinimide
OPD	o-phenylenediamine
PBS	phosphate buffered saline
PDGF	Platelet-derived Growth Factor
PEG	polyethylene glycol
ppTGF-β2	partially purified TGF-β2
RU	response units
S	DNA synthesis phase of the cell cycle
SDS	sodium dodecyl sulfate
SDS-PAGE	SDS polyacrylamide gel electrophoresis
SPR	surface plasmon resonance
TBS	Tris buffered saline
TCA	trichloroacetic acid
TFA	trifluoroacetic acid
TGF-β	Transforming Growth Factor-β (isotypes 1 or 2)
TGF-β2(50-75)	peptide corresponding to residues 50-75 of TGF-β2
TMB	3,3',5,5'-tetramethyl benzidine
Tris	Tris(hydroxymethyl)aminomethane
UV	ultraviolet light
WGFE	Whey Growth Factor Extract

Statement of originality

This work contains no material which has been accepted for the award of any other degree or diploma in any other University or other tertiary institution and, to the best of my knowledge and belief, contains no material previously published or written by another person, except where due reference has been made in the text. I give consent to this copy of my thesis, when deposited in the University Library, being made available for loan and photocopying.

24/4/01

Ben Hunt

Acknowledgments

I would like to thank the CRC for Tissue Growth and Repair for the opportunity to undertake a PhD in such an exciting field of research. Prior to this project, my background was in chemical engineering with little experience of biochemistry or tissue culture. Their acceptance of a relatively inexperienced student from a different discipline and their receptiveness to ideas from a different field are most encouraging.

I wish to thank my supervisors Dr. Chris Goddard, Dr. Brian O'Neill and Dr. Anton Middelberg for their continual encouragement and excellent advice. Many staff at the CRC contributed to this project in small ways. In particular, I would like to express my gratitude to Dr. Allison Cowin for help with immunohistochemistry work, Sarah Tilley for help with antibody isotyping, and Tina Centofanti for help with antibody purification, western blotting and immunohistochemistry.

One of the strengths of the CRC is the camaraderie between students. I would like to thank Dr. Catherine Yandell, Simon Humphrys, Andrew MacKenzie and Brian Degger for their friendship, advice and good humour.

To my wife, Nicola, and my parents, Tim and Diane, thank you for your faith and words of encouragement during the difficult times and for popping the champagne cork when things worked well.

Chapter One

Introduction

1. Introduction

1.1 General Introduction

The aim of this project has been to develop an immunoaffinity process for the commercial-scale purification of Transforming Growth Factor-β2 (TGF-β2) from Whey Growth Factor Extract (WGFE).

TGF-β2 is a valuable polypeptide that has a wide range of biological activities upon mammalian cells *in vitro* and *in vivo*. It is a highly conserved peptide throughout evolution as its amino acid sequence exhibits a high level of identity between species. It is found in chickens, frog (*Xenopus*) and all mammalian species. Nearly every cell in the human body expresses receptors for TGF-β2 and responds to it in a way defined by the context of the cell type, its state of differentiation and other chemical messages. The effects of TGF-β2 begin at the earliest stages of embryo development and continue throughout adult life. It has potential therapeutic applications in wound healing and it is currently undergoing clinical trials by a number of biotechnology companies.

The gene for TGF-β2 has been cloned and the recombinant production of TGF-β2 has been achieved in Chinese Hamster Ovary cells, *Saccharomyces cerevisiae* and *Escherichia coli.* Patents cover the recombinant production of TGF-β2 and the therapeutic uses of the recombinant peptide.

TGF-β2 has been successfully purified from bovine milk by a combination of ion-exchange chromatography, size-exclusion gel filtration and reversed phase high pressure liquid chromatography (HPLC). TGF-β2 and its isoform, TGF-β1, are present in milk at very low concentrations. The commercial-scale extraction of TGF-β2 from bovine milk is not a viable proposition because huge volumes of milk would have to be processed to satisfy this objective. In addition, milk is a difficult starting material for purification because of the presence of lipids, biological material and high molecular weight proteins, which must be removed prior to the purification process.

Cheese whey is a by-product of the cheese-making process. It consists of 20% of the total milk protein because the fats and casein proteins precipitate in the manufacture of cheese. It is a waste product that constitutes an environmental problem for the cheese industry. It has been

found that TGF-β2 selectively partitions into the whey fraction after the cheese-making process. However, it is still present in cheese whey at concentrations comparable to those in milk.

Whey Growth Factor Extract (WGFE) is the protein fraction derived from the cation-exchange chromatography of cheese whey. In comparison with the predominant protein species in cheese whey, growth factors have a more basic isoelectric point. This means that the predominant protein species are negatively charged whilst growth factors adopt a positive charge. The negative charge of the cation-exchange chromatography media interacts with the positive charge of growth factors but does not impede the passage of the predominant protein species through the column. After the chromatography media has been saturated with positively charged proteins, these proteins are eluted with a high concentration of salt. TGF-β2 is present in this fraction at a specific activity that is much higher than that in cheese whey. The purification of TGF-β2 from WGFE has been demonstrated with a combination of size-exclusion gel filtration and reversed-phase HPLC. GroPep has patented the process for the manufacture of WGFE and a pilot-scale GMP production facility was completed recently in Adelaide.

The purification of biologically active peptides often consists of multiple steps including ion-exchange chromatography, size-exclusion gel filtration or reversed-phase HPLC. In order to purify these peptides to the rigorous specifications imposed by their use as therapeutic agents, low final yields of peptide often result. Therefore there is considerable interest in the development of separation processes that are capable of achieving the required purification whilst conserving the yield of biologically active peptide. Immunoaffinity separations possess an attractive combination of selectivity and yield as they can replace many conventional purification steps with a single step. They rely upon a specific interaction between the biologically active peptide and an immobilised antibody.

There was evidence in the literature that the immunoaffinity separation of TGF-β2 from WGFE would be feasible. The utility of immunoaffinity chromatography in purifying biologically active peptides from the milk of transgenic animals has been demonstrated. In one particular case the concentration of the peptide was similar to that of the concentration of TGF-β2 in WGFE. Monoclonal antibodies have been generated against TGF-β2, immobilised

to chromatographic media and successfully used to affinity purify TGF-β2 from a partially purified preparation from bovine bone.

On the basis of the preceding evidence the potential exists for the development of an immunoaffinity separation process for the purification of TGF-β2 from WGFE. It is likely that the purification technology developed for this specific peptide could be applied to the purification of other biologically active peptides.

The first section of this literature review describes TGF-β2 in the context of the TGF-β family of polypeptides: range of *in vitro* biological activities on mammalian cells, potential clinical applications, chemical structure, natural sources, the latent complex, receptors and the method of recombinant production. Most *in vitro* and *in vivo* studies of TGF-β have concentrated their attention specifically on TGF-β1. In the small number of studies where both TGF-β1 and TGF-β2 were investigated the biological activities were similar. Therefore this literature review includes the details of studies with TGF-β1. The second section focuses on WGFE and specifically describes its major protein species, range of *in vitro* biological activities on mammalian cells and potential clinical applications. The third section describes the general method for generating monoclonal antibodies, the different configurations in which immunoaffinity separations can be performed and specific examples of processes that purify a biologically active peptide from milk.

1.2 Transforming Growth Factor-β2

1.2.1 Transforming Growth Factor-β Supergene Family

The Transforming Growth Factor-β (TGF-β) supergene family of polypeptide growth factors has a wide range of biological activity that occurs from the earliest stages of embryological development and continues throughout adult life. They are key regulators of cell proliferation, differentiation, apoptosis, gene expression and wound healing. Extensive research has identified a number of potential applications for their use in clinical medicine and biotechnology.

The homodimeric isoforms, TGF-β1, TGF-β2 and TGF-β3, have been described in mammals (Roberts and Sporn, 1993) although the heterodimers, TGF-β1.2 and TGF-β2.3, have been purified from bovine bone (Ogawa et al., 1992). TGF-β4 has been identified in chickens

(Jakowlew et al., 1988) and TGF-β5 has been identified in frogs (Roberts et al., 1990). The amino acid sequences of the mature forms of TGF-β share 70-80% identities and nine invariant cysteine residues. The TGF-β supergene family also includes the activins, inhibins, Müllerian inhibitory substance, bone morphogenetic proteins (BMPs), the *Drosophila decapentaplegic* gene product (*dpp*), the *Xenopus laevis* Vg-1 and Vgr-1 and the glial cell line-derived neurotrophic factor (Alevizopoulos and Mermod, 1997). These proteins share 25-50% sequence identities with the TGF-β isoforms and have seven of the nine corresponding cysteine residues conserved. The structure of these proteins is highly similar to that of TGF-β2 (Daopin et al., 1993).

1.2.2 TGF-β2 Structure

TGF-β2 is a homodimeric protein with a molecular weight of 25 kDa. It is expressed as a 442 amino acid precursor, the carboxyl terminus of which is proteolytically cleaved to yield the mature 112 amino acid TGF-β2 monomer (Madisen et al., 1988). The monomeric sub-units are linked together by a disulfide bridge. The amino acid sequences for human, bovine and murine TGF-β2 are shown in Figure 1.1. It is evident from the sequences that TGF-β2 has been highly conserved throughout evolution. The bovine and human forms are identical whereas the murine form differs by three residues.

The 3-dimensional structure of TGF-β2 (Figure 1.2) has been elucidated with X-ray crystallography (Daopin et al., 1993). TGF-β2 is a homodimeric protein stabilised by a single disulfide bridge between Cys^{77} on the respective monomers and paired complementary hydrophobic interfaces between the two sub-units. The TGF-β2 monomer is a flat elongated and slightly bent molecule with an average overall size of 60×20×15 Å. Eight cysteine residues clustered in the core region of each monomer form a compact pattern of intrachain disulfide bridges, termed a "cysteine knot". The receptor-binding region of TGF-β2 has been identified as a contiguous ridge approximately 40 Å long and 15 Å wide. It consists of amino acid residues 92-96 and residues 24-38 of one monomer and residues 56-68 of the other monomer (Griffith et al., 1996).

Bovine	ALDAAYCFRN VQDNCCLRPL YIDFKRDLGW KWIHEPKGYN
Human	ALDAAYCFRN VQDNCCLRPL YIDFKRDLGW KWIHEPKGYN
Murine	ALDAAYCFRN VQDNCCLRPL YIDFKRDLGW KWIHEPKGYN
Bovine	ANFCAGACPY LWSSDTQH**SR** VLSLYNTINP EASASPCCVS
Human	ANFCAGACPY LWSSDTQH**SR** VLSLYNTINP EASASPCCVS
Murine	ANFCAGACPY LWSSDTQH**TK** VLSLYNTINP EASASPCCVS
Bovine	QDLEPLTILY YIG**K**TPKIEQ LSNMIVKSCK CS
Human	QDLEPLTILY YIG**K**TPKIEQ LSNMIVKSCK CS
Murine	QDLEPLTILY YIG**N**TPKIEQ LSNMIVKSCK CS

Figure 1.1: Cross-species comparison of the TGF-β2 amino acid sequences. *The residue differences between the bovine (Cox and Burk, 1991), human (Madisen et al., 1988) and murine (Miller et al., 1989) forms are shown in bold.*

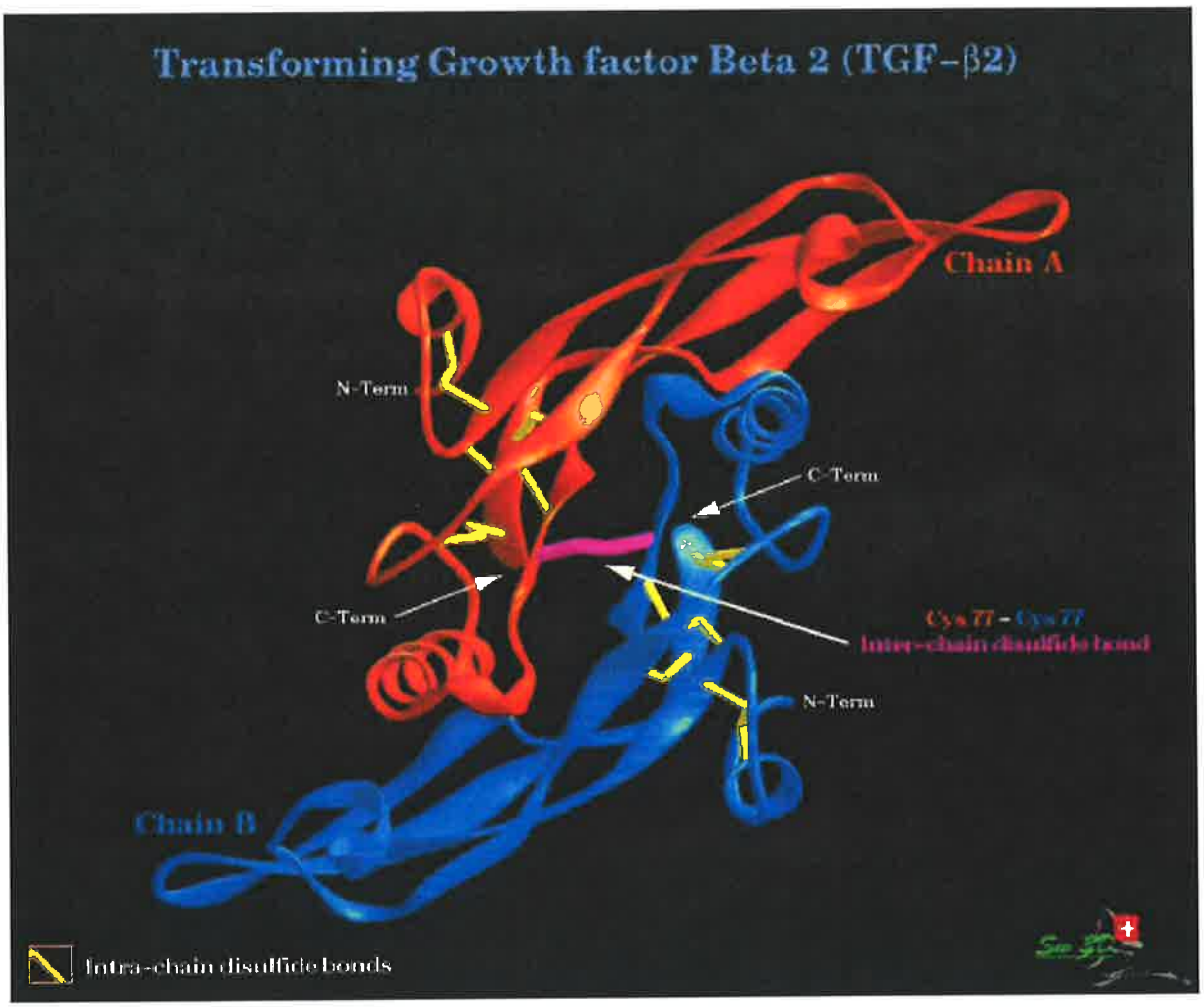

Figure 1.2: Three-dimensional structure of TGF-β2 as determined by X-ray crystallography *(Swiss Protein Databank, 1999a).*

1.2.3 TGF-β Biological Activity

TGF-β has been shown to influence nearly all cell types by inducing proliferation, growth inhibition or differentiation, or other aspects of their function, as reviewed by Sporn et al. (1987). TGF-β1 was initially characterised by its ability to induce the anchorage-independent growth of normal rat kidney cells (Roberts et al., 1981). It is a potent growth inhibitor for many cell types, including normal and transformed epithelial (Laiho et al., 1991), endothelial (Jennings et al., 1988), keratinocyte (Jones et al., 1991), breast cancer cells (Knabbe et al., 1987), B lymphocyte (Kehrl et al., 1986a) and haematopoietic cells (Keller et al., 1990). The growth inhibition effect of TGF-β is not a result of cytotoxicity because it is reversible (Shipley et al., 1986). In contrast, it promotes the proliferation of osteoblasts (Robey et al., 1987), Schwann cells of the peripheral nervous system (Sporn et al., 1987) and fibroblasts (Jones et al., 1991). Most cell lines respond to TGF-β1 and TGF-β2 in an identical manner *in vitro*. Notable exceptions to this include a rat pleuripotent haemopoietic stem cell line (Ohta et al., 1987), endothelial cells (Jennings et al., 1988) and a colon carcinoma cell line that was slightly responsive to TGF-β1 but resistant to TGF-β2 (Suardet et al., 1992). TGF-β stimulates the growth of foetal bovine bone cells *in vitro* without the elaboration of matrix (Robey et al., 1987). TGF-β induces the differentiation of normal bronchial epithelial cells (Masui et al., 1986) and chondrocytes (Seyedin et al., 1986) while it inhibits the differentiation of preadipocytes (Ignotz et al., 1985), B and T lymphocytes (Kehrl et al., 1986a and 1986b), natural killer cells (Rook et al., 1986) and myocytes (Florini et al., 1986).

1.2.4 Potential Clinical Applications of TGF-β

TGF-β is involved in the regulation of cell growth and differentiation and possesses a wide range of biological activities upon the immune system, extracellular matrix proteins, embryonic development, wound healing and tissue homeostasis. Many observations indicate that the action of TGF-β is modified by specific peptides in the extracellular matrix and by certain cell types. Therefore comprehensive *in vivo* experimentation is required to establish the therapeutic utility of TGF-β (Roberts and Sporn, 1991). It has potential therapeutic applications as reviewed in Roberts and Sporn (1993):

- Repair of soft tissue
- Repair of bone
- Treatment of chronic inflammatory fibrotic disorders

- Repair of ischaemic injury
- Treatment of cancer
- Immunosuppression
- Treatment of autoimmune diseases.

There are a number of therapeutic TGF-β agents that are currently undergoing clinical trials (Table 1.1). However, severe secondary effects, such as fibrosis, have been reported following the systemic administration of TGF-β (Alevizopoulos and Mermod, 1997).

Product	Developer	Application	Phase
TGF-β1	Genentech	Chemotherapy-induced mucositis	Pre-clinical
TGF-β1	Genentech	Bone growth	I
TGF-β2	Celtrix Pharmaceuticals	Chronic dermal ulcers	II
TGF-β2	Celtrix Pharmaceuticals	Chemotherapy-induced mucositis	I
TGF-β2	Celtrix Pharmaceuticals	Multiple sclerosis	I
TGF-β2	Collagen	Autoimmune-Immunosuppressives, Cancer, Dermatologic	Lead
Human anti-TGF-β2 monoclonal antibody	Cambridge Antibody Technology	Proliferative vitreoretinopathy	I/II
TGF-β3	OSI Pharmaceuticals	Wound healing and oral mucositis	II
PEG-TGF-β	Enzon	Detached retinas and dermal ulcers	Lead

Table 1.1: Therapeutic TGF-β agents that are currently undergoing clinical trials *(Recombinant Capital, 1999).*

1.2.4.1 Repair of Soft Tissue

An ordered sequence of cellular events takes place during wound healing to restore damaged tissue to its original functional state. These events are partially controlled by growth factors, which induce the early inflammatory responses and the subsequent regeneration. A number of growth factors including TGF-β1, transforming growth factor-α, basic fibroblast growth factor, insulin-like growth factor-1, epidermal growth factor and platelet-derived growth factor accelerate the wound healing process (Beck et al., 1990b). Immediately after wounding, growth factors are secreted at the wound site to enhance healing. TGF-β1 is released by platelets when they are degranulated by thrombin (Assoian et al., 1986) from

activated macrophages (Assoian et al., 1987), T lymphocytes (Kehrl et al., 1986b), endothelial cells (Hannan et al., 1988) and fibroblasts (Roberts et al., 1986). Cell migration and proliferation, synthesis of extracellular matrix, angiogenesis and remodelling are initiated by the release of TGF-β into the wound site. TGF-β increases the rate of healing and the breaking strength of the repaired tissue. Furthermore, it enhances angiogenesis and stimulates the local release of other growth factors, which increases blood flow to dermal wounds (Beck et al., 1990b).

TGF-β controls two separate processes in the wound repair process: synthesis and degradation. It enhances the activity of the promoters for fibronectin, elastin and collagen types I and III genes, thereby increasing synthesis. TGF-β also enhances the transcription of its mRNA and amplifies its own effects (Quaglino et al., 1991). Macrophages and neutrophils are attracted into the wound by TGF-β and they in turn secrete paracrine factors, including transforming growth factor-α, interleukin-1, platelet-derived growth factor A-chain and insulin-like growth factor-1, which also promote synthesis (Jones et al., 1991). Simultaneously, TGF-β blocks degradation by decreasing the secretion of proteases, such as stromelysin (Quaglino et al., 1991), major excreted protein (Chiang and Nilsen-Hamilton, 1986) and plasminogen activator, and by increasing the secretion of plasminogen activator inhibitor (Laiho et al., 1986). This is important because macrophages release cytotoxic agents, such as hydrogen peroxide, at the wound site to defend the host from infection but the excessive production of cytotoxic agents can damage regenerating endothelial cells, fibroblasts and keratinocytes (Jones et al., 1991). In this way the accumulation of matrix proteins is enhanced by TGF-β.

The efficacy of topically or locally applied TGF-β in promoting healing in rats, guinea pigs, rabbits and pigs has been demonstrated by a large literature. Specifically, TGF-β promotes healing in the repair of incisional wounds (Mustoe et al., 1987), excisional wounds (Quaglino et al., 1991), partial thickness wounds (Jones et al., 1991), punch wounds (Beck et al., 1990b), ulcers (Beck et al., 1990a), gastrointestinal incisional wounds (Mustoe et al., 1990) and chorioretinal wounds (Smiddy et al., 1989). Mustoe et al. (1987) showed that a single application of TGF-β to incisional wounds in rats increased breaking strength to 220% of the control after five days and that wound repair was accelerated by three days for at least fourteen days after wounding and TGF-β application. The application frequency of TGF-β in

these animal-wounding models ranged from a single application at the time of wounding to multiple applications throughout the healing period. A single application of recombinant human TGF-β1 enhanced the healing of ulcer wounds placed in the ears of rabbits at levels ranging from 15 to 100 ng per wound. However, the results were biphasic as no enhanced healing was observed for TGF-β1 levels above 100 ng per wound (Beck et al., 1990a). Most of the animal wound healing models investigated only TGF-β1 but Ksander et al. (1990) showed that TGF-β1 and TGF-β2 are equally potent in stimulating wound repair. Human clinical trials showed that a single intraocular application of TGF-β2 to the edge of full-thickness macular holes resulted in a significant improvement in visual acuity (Glaser et al., 1992).

Another potential application of TGF-β is as an anti-psoriatic agent. Psoriasis is a common skin disease and it is characterised by patches, or lesions, of dead skin, which accumulate in layers. A marked increase in the proliferation of keratinocytes in psoriatic lesions relative to healthy skin is evident. Elder et al. (1990) showed that the keratinocytes derived from these lesions are as responsive to TGF-β1 as are normal keratinocytes and that TGF-β1 is a potent inhibitor of the growth of psoriatic keratinocytes.

TGF-β is also effective at increasing the rate of healing of test wounds in a variety of healing impaired models, such as in animals treated with Adriamycin® (Curtsinger et al., 1989), glucocorticoid (Pierce et al., 1989) or radiation (Bernstein et al., 1991). Salomon et al. (1990) showed that Adriamycin® suppressed the expression of TGF-β1 and that the topical application of TGF-β reversed the healing defect. In both normal and healing impaired animals, TGF-β increases the breaking strength of incisional wounds, the influx of fibroblasts and macrophages and the deposition of collagen. The topical application of TGF-β is likely to find clinical use in the treatment of surgical wounds, burns or ulcers in debilitated patients, whose normal wound repair responses are impaired by diabetes, chemotherapy or radiotherapy.

Wound healing in the adult is often accompanied by scar formation whereas wound healing in the foetus is characterised by less inflammation, reduced cytokine response and the absence of scarring. TGF-β1 has been implicated in scar formation (Sullivan et al., 1995). Although increased collagen deposition and tensile strength are usually desirable in wounds,

occasionally excessive scarring can lead to functional impairment, defective growth or poor appearance. Using an incisional wound model in rats, it was found that the application of neutralising antibodies to TGF-β early in the healing process reduced dermal scarring without a decrease in breaking strength (Shah et al., 1992). Furthermore, Ruoslahti et al. (1997) patented the use of the TGF-β antagonist decorin for the prevention or reduction of dermal scar formation. Therefore decorin and antibodies to TGF-β may find application in reducing dermal scarring in normal wound healing.

1.2.4.2 Repair of Bone

The calcified matrix of the skeleton is continuously remodelled by the activity of bone cells. The first phase of bone remodelling is resorption, which is performed by cells called osteoclasts, and then bone is subsequently formed by cells called osteoblasts (Mundy and Bonewald, 1990). After a bone fracture has occurred, platelets and mononuclear cells release TGF-β into the haematoma and it persists there for ten days after the injury (Joyce et al., 1990). TGF-β stimulates mononuclear cells to synthesise it and other growth factors (Wahl et al., 1987). These growth factors then combine to direct the inflammatory response, chondrogenesis and bone formation (Joyce et al., 1990).

The most abundant source of TGF-β in the body is bone and TGF-β is a potent mitogen for osteoblasts *in vitro*, whilst enhancing their collagen production (Robey et al., 1987). Also, TGF-β inhibits osteoclast formation and decreases the rate of bone resorption in prolonged culture (Chenu et al., 1988). Immunohistochemical studies show strong staining of TGF-β1 in chondrocytes, osteoblasts and osteoclasts of developing bone and cartilage (Heine et al., 1987). Repeated injections of TGF-β1 or TGF-β2 on to the periostea of rat parietal bones induced woven bone formation (Noda and Camilliere, 1989).

Ongpipattanakul et al. (1997) combined TGF-β1 with a tricalcium phosphate/amylopectin paste for use as bone defect filler. The efficacy was assessed *in vivo* with a rabbit unilateral segmental defect model. It was demonstrated that there was a higher incidence of radiographic bone union and higher torque strength in the TGF-β1-treated group than the placebo group. Ammann and Rudman (1997) patented the invention of mixing TGF-β with a suitable pharmaceutical carrier and then administering the composition to a wound site to induce the formation of normal adult bone. Examples of these sites include tooth sockets

where healing is impaired by periodontal disease, non-union fractures, large bony defects caused by trauma or surgery, large cranial defects, spinal fusions, surgical correction of severe scoliosis, spinal fractures and artificial prostheses.

1.2.4.3 Treatment of Chronic Inflammatory Fibrotic Disorders

TGF-β is a chemoattractant and an activator of macrophages and fibroblasts. During wound healing, these activities are beneficial and of limited duration. However, a variety of diseases including hepatic cirrhosis, idiopathic pulmonary fibrosis, scleroderma, glomerulonephritis, certain forms of rheumatoid arthritis, schistosomiasis and proliferative vitreoretinopathy are characterised by chronic inflammation and the pathologic accumulation of matrix, which is often accompanied by scarring (Roberts and Sporn, 1993). The overproduction and activation of TGF-β results in the excessive elaboration of connective tissue by activated fibroblasts, which resemble those in healing wounds.

Idiopathic pulmonary fibrosis is a fatal condition characterised by connective tissue deposition in the terminal air spaces resulting in the loss of lung function (Broekelman et al., 1991). In a model of pulmonary fibrosis in rats induced by administration of bleomycin, Khalil et al. (1989) showed that TGF-β is produced by alveolar macrophages at 30-fold elevated levels preceding collagen synthesis. In patients with advanced idiopathic pulmonary fibrosis, both macrophages and epithelial cells in focal lesions stain for TGF-β1 (Broekelman et al., 1991). These results suggest that the progression of the disease may be an aberrant repair process.

Glomerulonephritis is caused by the formation of extracellular matrix within damaged glomeruli and results in impaired filtration and kidney failure (Border et al., 1990). Okuda et al. (1990) found similar TGF-β1 staining in a rat model of glomerulonephritis to that in the pulmonary fibrosis model. Neutralising antibodies to TGF-β1 substantially attenuated glomerulonephritis in a rat model of this disease (Border et al., 1990).

Rheumatoid arthritis is a crippling inflammatory disease of primarily the peripheral joints. Wilder et al. (1990) demonstrated that TGF-β is involved in limiting the formation of synovial stromal connective tissue and stimulating the diseased tissue to fibrose.

TGF-β2 has been implicated in several ocular scarring processes including proliferative vitreoretinopathy, cataract formation and conjunctival wound healing after glaucoma filtration surgery (Connor et al., 1989; Cordeiro et al., 1999). These disorders are characterised by excessive fibrosis and can ultimately result in blindness. Cordeiro et al. (1999) investigated the ability of recombinant human anti-TGF-β2 monoclonal antibodies to inhibit conjuctival scarring after glaucoma filtration surgery. It was found that the treatment significantly affected the surgical outcome by reducing conjuctival scarring both *in vitro* and *in vivo* (rabbit).

The ability of neutralising antibodies against TGF-β to attenuate glomerulonephritis (Border et al., 1990) provides evidence that these antibodies may also alleviate the other chronic inflammatory disorders discussed here. Other potential antagonists for TGF-β include the proteoglycan decorin (Yamaguchi et al., 1990) and the type III TGF-β receptor (Wang et al., 1991).

1.2.4.4 Repair of Ischaemic Injury

Studies on the immunohistochemical staining patterns of TGF-β1 in the heart following experimental myocardial infarction in rats suggest that TGF-β might accelerate repair and restore function to these myocytes (Thompson et al., 1988). The systemic administration of TGF-β following experimental infarction in rats has cardio-protective effects (Lefer et al., 1990). Systemic TGF-β administration suppresses the release of interleukin-1β and tumour necrosis factor-α into circulation after reperfusion. TGF-β preserves and stabilises endothelial function, inhibits endothelial adhesiveness for neutrophils and lymphocytes (Gamble and Vadas, 1991) and reduces the level of superoxide anions in coronary circulation (Lefer et al., 1990).

Angioplasty is a surgical procedure that is used to treat atherosclerotic arteries of the heart. The procedure involves inserting a balloon into the arteries and applying a pressure to increase the cross-sectional area available for blood flow. A complication of the surgery is restenosis where a proliferation of smooth muscle cells can occlude the artery. Grainger et al. (1998) patented the local administration of tamoxifen to the walls of the artery after angioplastic surgery. Tamoxifen has been shown to stimulate the local production of TGF-β1

and does not have an undesirable systemic toxicity. TGF-β1 is a potent inhibitor for the proliferation of smooth muscle cells and can prevent the occlusion of the artery.

1.2.4.5 Treatment of Cancer

Almost all cell types display TGF-β receptors but they have been found to be absent in retinoblastoma tumour cells (Segarini, 1991). This distinguishes these tumour cells from normal retinoblasts, which display significant amounts of all receptors. It has been suggested that the cells of developing retinal tumours gain a replicative advantage by not expressing TGF-β receptors and thereby escape the growth inhibiting effects of TGF-β released by other retinal cells (Roberts and Sporn, 1993). This loss of response to TGF-β has also been observed in a human colon carcinoma cell line (Suardet et al., 1992) and may contribute to tumour progression (Wu et al., 1992). There is evidence that the tumourigenic lesion in some carcinoma cells may be the loss of the ability to activate latent TGF-β so they can no longer limit their own growth. TGF-β is inhibitory for epithelial cells because they can activate the endogenous latent peptide. However, a human lung adenocarcinoma line has lost the ability to activate TGF-β (Wakefield et al., 1987). Tumour cells are known to secrete TGF-β, which suppresses the immune response against those cells. Therefore TGF-β antagonists could be used to enhance cancer therapy by relieving the suppression of immune function associated with malignancies (Lucas et al., 1991).

Many cancer therapies involve the administration of chemotherapeutic agents, which non-selectively kill rapidly proliferating cells including cancerous cells. However, these chemotherapeutic agents have the side effect of also destroying bone marrow cells that are responsible for the production of blood cells. TGF-β inhibits the growth of bone marrow cells and while in this state of suppressed growth they are less susceptible to the toxic effects of chemotherapeutic agents and thus TGF-β has potential as a bone marrow protective agent (Keller et al., 1990). Sonis et al. (1994) found that TGF-β3 is a potential treatment for the attenuation or prevention of ulcerative mucositis, which is a common, dose-limiting problem in patients who are receiving cancer chemotherapy. TGF-β3 inhibits the cell cycling of the oral epithelium *in vivo* and thereby prevents or attenuates oral mucositis in the Syrian golden hamster.

1.2.4.6 Immunosuppression

TGF-β suppresses the *in vitro* proliferation and differentiation of most cells of B and T cell lineages, antagonises the effects of inflammatory effector cytokines such as interleukin-1β, interleukin-6, tumour necrosis factor-α, and interferon-γ, and suppresses the expression of receptors for interleukin-1β and interleukin-2 on cells (Palladino et al., 1990). The production of superoxide and nitric oxide by macrophages is blocked by TGF-β. (Ding et al., 1990). TGF-β also inhibits the adhesion of neutrophils and T-cells to endothelial cells and limits the recruitment of inflammatory cells into a lesion (Gamble and Vadas, 1991). It is speculated that TGF-β antagonists, as discussed in section 1.2.4.3, could be developed to relieve the suppression of immune function that is characteristic of patients with viral and parasitic diseases (Wahl, 1992).

Bacterial infections can progress rapidly to sepsis, cardiovascular collapse, multiple organ failures and ultimately death. A key mediator of septic shock is tumour necrosis factor-α (TNF-α), of which the production is reduced by TGF-β. Palladino et al. (1990) demonstrated that the mortality rate of rats with *Escherichia coli*-induced septic shock was significantly reduced by the intraperitoneal administration of TGF-β1 and TGF-β2.

The recipients of transplanted human organs require chronic immunosuppressive therapy to delay or prevent organ rejection. There is a need for more effective, more specific and less toxic immunosuppressive agents. Palladino et al. (1990) investigated the immunosuppressant activity of TGF-β to prolonging the survival rate of neonatal Balb/c mouse hearts transplanted into the subcutaneous skin of the ears of adult C3H/KM mice. The graft survival rate was found to increase significantly for grafts treated with TGF-β and it thus has a potential clinical application as an agent for the inhibition of organ rejection.

1.2.4.7 Treatment of Autoimmune Diseases

In animal models of multiple sclerosis (experimental autoimmune encephalomyelitis, EAE) and rheumatoid arthritis (collagen-induced arthritis), the systemic administration of TGF-β1 is beneficial in both delaying the onset and reducing the severity of the disease (Kuruvilla et al., 1991). The administration of TGF-β during a remission in the EAE model reduces the severity of subsequent relapses. The administration of neutralising antibodies against TGF-β1 increases the severity of the disease and suggests that endogenous TGF-β1 regulates the

severity of the disease (Miller et al., 1992). In EAE, the oral administration of myelin basic protein prior to the induction of the disease reduces the symptoms. However, the administration of neutralising antibodies to TGF-β1 abrogates this protective effect (Miller et al., 1992). Vitamin D could potentially be used for the treatment of these autoimmune diseases by inducing the expression of endogenous TGF-β (Finkelman et al., 1991) without the side effects of systemically administered peptide.

1.2.5 Latent TGF-β

TGF-β is synthesised in a high molecular weight latent form in human platelets where the active TGF-β molecule is non-covalently associated with the TGF-β propeptide homodimer, called the latency-associated peptide (LAP), which has a molecular weight of ~80 kDa (Miyazano et al., 1990). Latent TGF-β is biologically inactive because it does not bind to cellular receptors. TGF-β must be dissociated from this complex in a process known as activation before TGF-β can exert its action. Therefore the release of active growth factor from the complex is critical in regulating TGF-β availability. Very high concentrations of latent TGF-β1 have been found to have TGF-β1 activity but its potency is 200-fold lower than TGF-β1 itself (Miyazano and Heldin, 1989). Latent TGF-β is targeted to extracellular matrix by the latent TGF-β binding protein (LTBP), which has a molecular weight of 125-160 kDa. A disulfide bridge links one LTBP monomer to LAP (Miyazano et al., 1990). Both LAP and LTBP are highly glycosylated with sialic acid and mannose-6-phosphate residues and the glycosylation has been shown to be involved in rendering TGF-β inactive in the latent complex (Miyazano et al., 1990). Figure 1.3 is a schematic representation of latent TGF-β (Munger et al., 1997).

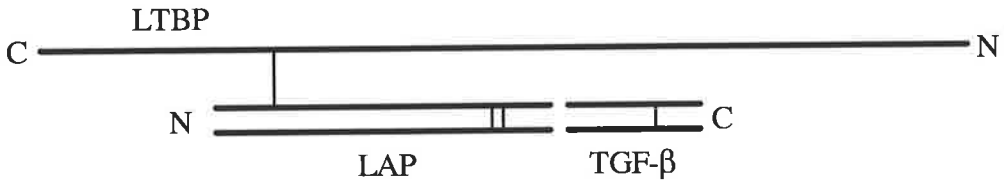

Figure 1.3: Schematic representation of latent TGF-β. *Thin lines indicate disulfide bonds between TGF-β monomers, between LAP monomers and between LAP and LTBP (Munger et al., 1997).*

The *in vitro* activation of TGF-β can be accomplished by heat, detergents (0.02% SDS), pH extremes (below 3.5 and above 12.5), chaotropes (8M urea), radiation, thrombospondin-1, deglycosylation, sialic acid, mannose-6-phosphate, plasmin and cathepsin D (Miyazano et al.,

1990; Munger et al., 1997). Wakefield et al. (1989) demonstrated that the interaction between LAP and TGF-β1 is reversible because after activation, LAP and TGF-β1 reassociate in a time and concentration dependent manner under neutral non-denaturing conditions. The latent complex does not bind to polyclonal antisera raised against TGF-β1. This implies either that LAP is folded to form a cage-like structure around TGF-β1 or that it changes the conformation of exposed TGF-β1 epitopes so they are no longer recognised by the antibodies or the receptor.

1.2.6 TGF-β Receptors and Signal Transduction

Nearly every cell type has been found to possess receptors for TGF-β (Wakefield et al., 1987). The signalling receptors for TGF-β, type I receptors (53 kDa) and type II receptors (70-85 kDa), contain extracellular ligand-binding, transmembrane and intracellular Serine/Threonine kinase domains (Alevizopoulos and Mermod, 1997). The affinity constants are 5-50 pM for the interaction between TGF-β1 and the type I and II receptors (Massague et al., 1990). These receptors have a 10-20 fold higher affinity for TGF-β1 than for TGF-β2 and to compensate there is a smaller number of binding sites per cell (Massague et al., 1990). The type I receptor has a slightly higher affinity for TGF-β1 and TGF-β2 than the type II receptor (Cheifetz et al., 1987). The signalling pathway involves the direct binding of TGF-β to the type II receptor, the formation of a heterodimeric complex between the type I and II receptors and then the recognition of bound TGF-β by the type I receptor. TGF-β is recruited into the complex and becomes phosphorylated by the type II receptor (Wrana et al., 1994). Phosphorylation permits the type I receptor to propagate the signal to downstream substrates. After binding to the receptor, TGF-β is internalised and degraded by lysosomal enzymes. Multiple intracellular pathways mediate the biological response to TGF-β. Protein kinase C, phosphatidylinositol and guanine nucleotide binding proteins (G proteins) are implicated as secondary messenger systems for the biological activity (Segarini, 1991). TGF-β receptor expression is modulated by a range of agents and conditions including high cell density, differentiation, retinoic acid, TGF-β, androgen deprivation, adrenocorticotropic hormone, phytohaemagglutin, parathyroid hormone, interleukin-1 and concanavalin A (Segarini, 1991).

The growth inhibition of mink lung epithelial (Mv1Lu) cells by TGF-β1 is a result of the down-regulation of cyclin-dependent kinase 4 expression, which inhibits the phosphorylation of the retinoblastoma gene product (*Rb*). This occurs in the late G1 part of the cell cycle

(Laiho et al., 1990). In normal cells, *Rb* is expressed throughout the cell cycle but exists in multiple phosphorylated forms for specific phases of the cell cycle (Buchkovich et al., 1989). The more highly phosphorylated forms are found in the S and G2/M phases and the unphosphorylated forms are found during the growth-inhibited G1 phase. Unphosphorylated *Rb* down-regulates c-*myc* activity and subsequently inhibits cell proliferation (Alevizopoulos and Mermod, 1997).

Two other cell-surface TGF-β-binding proteins are betaglycan (type III receptor) (280-330 kDa) and endoglin (190 kDa) (Cheifetz et al., 1987; Cheifetz et al., 1992). Betaglycan is an integral membrane protein that is modified with glycosaminoglycan groups for interaction with extracellular matrix (Segarini and Seyedin, 1988). It displays similar affinity (K_d = 30-300 pM) for both TGF-β1 and 2 (Massague et al., 1990) and is involved in the presentation of TGF-βs to the type I and type II receptors for signalling (Lopez-Casillas et al., 1993). Endoglin is a disulphide-linked homodimeric glycoprotein composed of two subunits of 95 kDa. It only binds to TGF-β1 and TGF-β3 but not to TGF-β2 (Cheifetz et al., 1992).

1.2.7 Natural Sources of TGF-β2

TGF-β2 has been isolated from bovine bone (Seyedin et al., 1985; Ogawa et al., 1992), bovine milk (Cox and Burk, 1991; Jin et al., 1991), cheese whey (Rogers et al., 1996), human glioblastoma cells (Olofsson et al., 1992) and porcine blood platelets (Cheifetz et al., 1987). Cox and Burk (1991) purified TGF-β2 from bovine milk with a combination of strong cation-exchange chromatography, low-pressure hydrophobic interaction chromatography, hydrophobic interaction HPLC and size-exclusion HPLC steps, which separated the protein according to its properties of charge, hydrophobicity and size, respectively. Cox and Burk (1991) also determined that the concentration of TGF-β2 was 115±78 ng/L in bovine milk. Rogers et al. (1996) purified TGF-β2 from cheese whey with a combination of cation-exchange chromatography, acid gel filtration and reversed-phase HPLC. Rogers et al. (1996) ascertained that the TGF-β2 concentration was 3.7±0.7 μg/L in acidified cheese whey and 4.3±0.8 μg/L in acidified bovine milk. The isoforms TGF-β1 and TGF-β2 are both present in bovine milk and cheese whey and TGF-β2 accounts for 85% of the total TGF-β activity (Jin et al., 1991).

1.2.8 Recombinant Production of TGF-β2

TGF-β2 has been expressed recombinantly in Chinese Hamster Ovary cells (Madisen et al. 1990), *Escherichia coli* and *Saccharomyces cerevisiae* (Cerletti et al., 1990). Until recently, the preferred method of recombinant production of TGF-β2 was expression in eukaryotic hosts because of the large number of disulfide bridges in the molecule (Roberts and Sporn, 1993). Production from prokaryotic hosts has proven to be very difficult because of the poor yield of growth-promoting activity after refolding (Cerletti et al., 1990). A novel *E. coli*-based procedure for TGF-β2 now provides enough active substance for clinical development programs.

The method for producing recombinant TGF-β2 in Chinese Hamster Ovary cells is outlined here (Madisen et al. 1990). TGF-β2 was expressed by a Chinese Hamster Ovary cell strain that was transfected with a cDNA clone coding for the 414 amino acid TGF-β2 precursor and subsequently amplified with methotrexate. Serum and cell-free conditioned media from the transfected cells was acidified, dialysed and then the pH was adjusted to 4. TGF-β2 was purified from the supernatant with a CM-Trisacryl column and a reversed phase column.

The method for producing recombinant TGF-β2 in *E. coli* is outlined here according to the patent of Cerletti et al. (1997). TGF-β2 is expressed by an *E. coli* strain K12 LC 137 that is transfected with the pPLMu plasmid. The bacterial cells are disrupted and the non-soluble TGF-β2 is recovered, acidified and subject to gel filtration. The fractions containing monomeric TGF-β2 are pooled and purified on a reversed phase column. TGF-β2 is refolded in 50 mM Tris-HCl pH 8.0, 1M NaCl, 5 mM EDTA, 2 mM reduced glutathione, 1 mM oxidised glutathione and 33 mM Chaps and then purified on a Mono S column and a reversed phase column.

1.3 Whey Growth Factor Extract

Bovine cheese whey is a by-product of the cheese-making process and it consists of proteins, lactose, minerals and water-soluble vitamins that partition into the run-off after the coagulation of casein and fat to produce cheese curd. Whey is essentially without value and actually represents a cost to the industry because it is a pollutant. Therefore it is readily available in tonne amounts from the cheese industry.

Milk-derived fractions of protein have been shown to promote the growth of various mammalian cell types in serum-free culture, including epithelial (Klagsbrun, 1980) and fibroblastic cells (Klagsbrun, 1978). Approximately 20% of the total milk protein partitions in whey and consists mainly of proteins such as β-lactoglobulin, α-lactalbumin, bovine serum albumin and immunoglobulins. Whey also contains less abundant proteins such as lactoferrin, lactollin, glycoprotein and blood transferrin (Marshall, 1982). Whey has been investigated as a source of growth factors that could replace foetal bovine serum in mammalian cell culture (Francis et al., 1995). Cation-exchange chromatography was selected as the enrichment process because, unlike the major whey proteins, β-lactoglobulin, α-lactalbumin and bovine serum albumin, growth factors generally have basic isoelectric points. Whey growth factor extract (WGFE) is the protein fraction that is derived from the cation-exchange chromatography of cheese whey.

WGFE is a complex mixture of proteins that have not as yet been fully characterised. The complexity of the mixture may be appreciated by gel electrophoresis (Figure 1.4). The major protein species of WGFE (Table 1.2) have been characterised by N-terminal sequencing and mass spectroscopy (Australian Proteome Analysis Facility, 1998).

Band number	Name	Molecular weight
1	Xanthine dehydrogenase	146681
2	Hexokinase	103064
3	Poly(A)Polymerase	82310
4	Lactoperoxidase	69460
5	?	55000
6	?	31000
7	?	28000
8	Beta lactoglobulin	18281
9	RNASE 1	13562
10	Angiogenin	14593
11	Calgranulin C	10554
12	Complement C3A anaphylotoxin	9085

Table 1.2: Compositional analysis of WGFE. *The bands of the electrophoresis gel of Figure 1.4 were analysed by N-terminal sequencing and mass spectroscopy. The N-terminal sequences and mass spectroscopy fingerprints of these proteins were compared with those of known proteins in the Swiss Protein Sequence Retrieval System (1999b).*

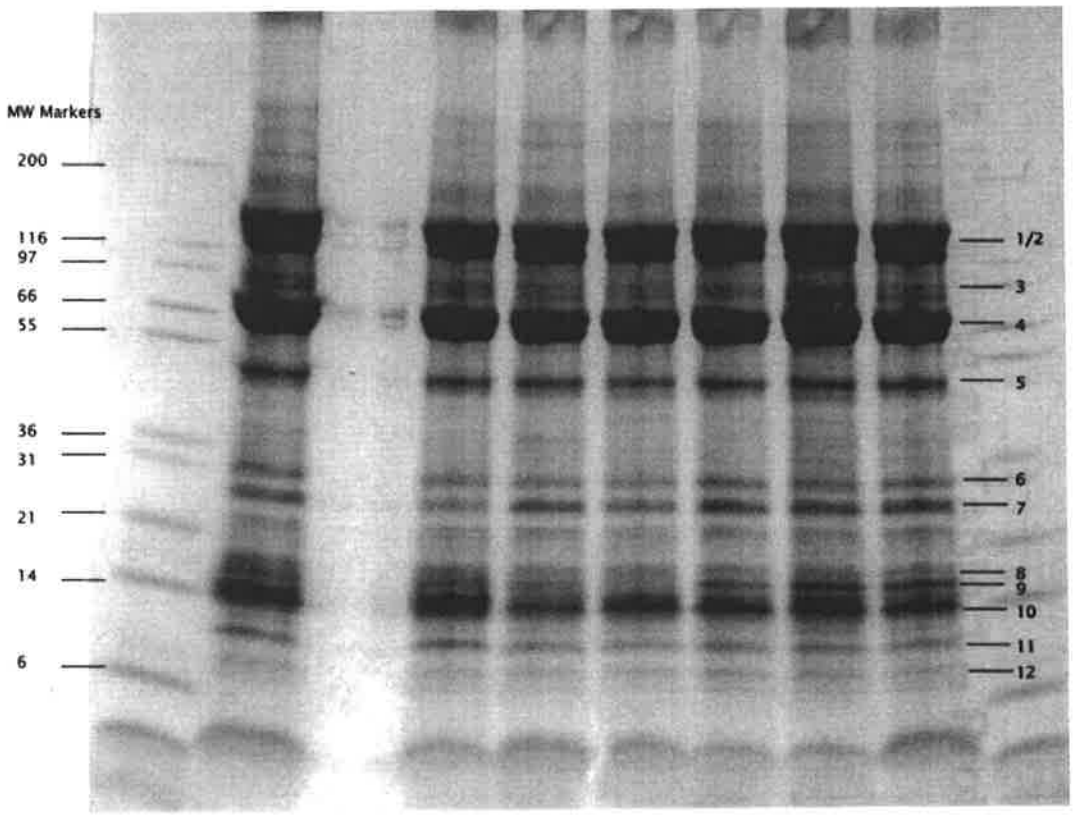

Figure 1.4: SDS-PAGE of WGFE. *The protein was electrophoresed and stained with Coomassie Blue. The major protein bands were identified by N-terminal sequencing and mass spectroscopy (Australian Proteome Analysis Facility, 1998). The numbers in the right margin correspond to the identified protein species in Table 1.2.*

1.3.1 WGFE Biological Activity

WGFE contains only 1-2% of the original whey protein and has substantial growth promoting activities on Balb/c 3T3 cells, L6 myoblasts and human skin fibroblasts (Francis et al., 1995). Lactoperoxidase and immunoglobulin G are abundant in WGFE but no cell growth activity was attributed to them (Francis et al., 1995). The growth factors are present in greatly increased specific activities in WGFE relative to the initial whey material (Francis et al., 1995). The typical growth factor composition of WGFE is summarised in Table 1.3. These growth factors to date include Insulin-like Growth Factor-I and II (Belford et al., 1997), IGF binding proteins-2 and 3 (Belford et al., 1997), acidic and basic Fibroblast Growth Factor (Rogers et al., 1995), Platelet-derived Growth Factor (Belford et al., 1997) and TGF-β1 and 2 (Rogers et al., 1996). However, these growth factors do not account for the total biological activity of WGFE. Belford et al. (1997) cultured Balb/c 3T3 fibroblasts in a mixture of IGF-I, IGF-II, PDGF-AB, TGF-β2 and basic FGF at concentrations commensurate with that found in WGFE and found that the cell growth was only 51% of that for WGFE. This suggests the

presence of additional growth factors in bovine milk. Recently an EGF-like molecule, Betacellulin, has been purified from WGFE and characterised (Dunbar et al., 1999).

Growth Factor	Concentration (ng/mg WGFE)
IGF-I	16.7
IGF-II	6.1
acidic FGF	0.19
basic FGF	0.66
PDGF	4.8
TGF-β1 (active)	0.12
TGF-β2 (active)	0.68
TGF-β1 (total)	7.8
TGF-β2 (total)	44
Betacellulin	27.8

Table 1.3: Growth factor composition of WGFE *(adapted from Belford et al., 1997; Rogers et al., 1995; Dunbar et al., 1999 and Rogers et al., 1996).*

TGF-β is the most abundant growth factor identified so far in WGFE. The specific activity of TGF-β in WGFE has been estimated with a mink lung epithelial cell line bioassay as 0.8±0.1 ng/mg protein. Neutral gel filtration of WGFE has revealed a major peak of latent TGF-β with a molecular weight of 80 kDa and a smaller peak at 600 kDa. The latent TGF-β can be activated by extremes of pH, urea or heat. The stability of the TGF-β latent complex under these conditions is shown in Table 1.4 (Rogers et al., 1996).

Treatment	TGF-β (ng/mg protein)
None	0.8±0.1
Acid (pH2.0)	42.2±6.8
Alkali (pH11)	26.0±6.0
Heat (100°C for 2 min)	9.07
Urea (8M)	52.0±17.0

Table 1.4: Stability of the TGF-β latent complex in WGFE. *TGF-β activity was measured by bioassay in Mv1Lu cells and compared with a recombinant human TGF-β1 standard (Rogers et al., 1996).*

1.3.2 Potential Clinical Applications of WGFE

The mitogenic effects of WGFE suggest that it has potential clinical applications. The oral administration of WGFE in the treatment of patients suffering from intestinal mucositis induced by high dose chemotherapy or radiotherapy has been investigated by Howarth et al. (1996). An animal model for intestinal mucositis, which used methotrexate-treated rats, showed that the co-administration of WGFE in the rat diet improved the integrity of the intestines. WGFE is currently undergoing clinical trials for topical application in the treatment of chronic ulcer wounds. TGF-β is known to promote scarring (Sullivan et al., 1995) and the specific depletion of TGF-β from WGFE could eliminate scar formation with WGFE treatment.

1.4 Immunoaffinity Separations

A plethora of valuable biochemicals is currently recovered from feed streams of either natural or recombinant origin. The economics of such processes are strongly influenced by the cost of the purification step. As a consequence, there is considerable interest in the synthesis of low cost, high efficiency sequences for this fractionation step. Immunoaffinity separations possess an attractive combination of selectivity and yield. Accordingly, they may replace many conventional purification steps by a single step (Chase, 1984).

Immunoaffinity separations rely upon the specific interaction between an antibody and its corresponding antigen. These interactions are characterised by high specificity and very strong binding. Antigen-antibody binding results from a combination of hydrogen bonding, electrostatic attraction, van der Waals forces and hydrophobic interactions between the adjacent amino acid residues. The most widely known immunoaffinity separation technique is packed bed adsorption. A schematic of the steps involved in the immunoaffinity chromatography technique is shown in Figure 1.5. The column consists of a support to which antibody is immobilised (I). When the protein mixture, containing the corresponding antigen, is loaded on to the immunoaffinity column, the antigen binds to the immobilised antibody while contaminating proteins pass through the column unimpeded by the support (II). Loading is continued until the antibody binding sites are saturated or a substantial amount of the antigen is passing through the column and failing to bind. The column is then washed to remove contaminating proteins that remain in the porous interstices or that are non-specifically bound to the support. Washing (III) is continued until an acceptably low quantity of contaminating protein is bound to the support. By changing the solution conditions, it is

then possible to weaken the antibody-antigen interaction and to elute the antigen from the column (IV). Elution is continued until an acceptable proportion of antibody binding sites have been vacated or for a period of time that does not result in the denaturation of the antibody binding capacity or the biological activity of the antigen. After elution, the solution conditions can be returned to the original state in which antibody-antigen binding is favoured and the cycle can be repeated.

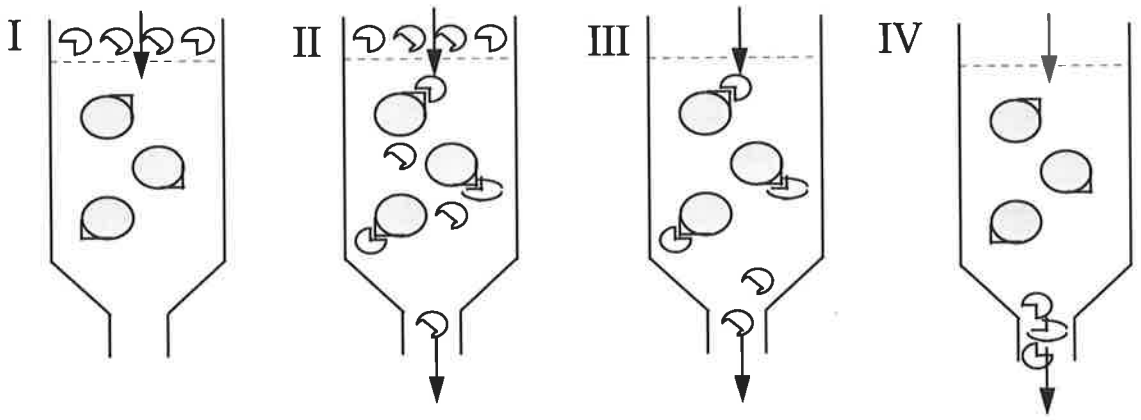

Figure 1.5: The Steps involved in Immunoaffinity Chromatography.

Antibodies may be generated in a variety of ways. A relatively simple method is to generate polyclonal antibodies by immunising an animal with the peptide of interest and periodically taking serum from the animal. The antibodies are then purified from serum with an affinity column to which Protein G or the peptide of interest is coupled. The limitations of this method are that a consistent supply of antibody is not established, GMP quality control is difficult to implement and the avidity of the antibody for the peptide of interest may be so high as to make elution impossible. Monoclonal antibodies do not have these limitations but their generation is a more involved process, which can be achieved by conventional hybridoma technology or phage display affinity maturation and the recombinant production of single chain Fv antibody fragments (Irving and Hudson, 1995).

1.4.1 Hybridoma Technology

The generation of murine hybridomas is a well-established method that was pioneered by Kohler and Milstein (1975). Hybridomas are cells that are the result of a fusion between a cancerous myeloma cell and a spleen derived B lymphocyte. The genes of the myeloma cell bestow immortality upon the genes of the B lymphocyte fusion partner. The genes of the B lymphocyte are expressed by the hybridoma and hence the antibody that was secreted by the

B lymphocyte is also produced by the hybridoma because the myeloma cell does not possess the capacity to secrete antibody. Any given hybridoma cell is the result of a single fusion event. By isolating that cell and growing it in tissue culture, large amounts of antibody of one type, termed monoclonal, may be produced.

The spleen of a mouse contains a heterogeneous population of B lymphocytes and each of these secretes an antibody specific for a different group of amino acids or epitope. B lymphocytes are capable of shuffling the genes that encode for antibody so that the potential number of variations in the binding determinant is very large. Therefore an antibody may be raised against any protein antigen that challenges the immune system of the animal. B lymphocytes, which secrete antibodies against such protein antigens, will proliferate and cells, which produce non-binding antibodies, will acquiesce. By immunising the animal with the protein of interest, B lymphocytes, that secrete protein specific antibodies, will proliferate and a population of these cells will congregate in the spleen. The fusion of a cancerous cell with a B lymphocyte derived from the spleen of an unimmunised animal is likely to produce a panel of hybridomas that secrete antibodies against a wide variety of antigens that have challenged the animal's immune system. In this case, the probability of obtaining an antibody against the protein of interest is very low. Immunising the animal with the protein of interest increases the probability of a fusion event occurring between the myeloma cell and a B lymphocyte that secretes the protein specific antibody.

The general procedure for generating hybridomas is described here. Firstly, the mice are immunised with the protein of interest. The mice are bled from the tail to collect serum. The serum titre is usually determined with enzyme-linked immunosorbent assay (ELISA) or radioimmunoassay. Once a sufficiently high titre or immune response has been obtained the splenocytes may be fused with the myeloma cells. The cells are mixed together in the presence of polyethylene glycol (PEG) which makes the cell membranes more permeable, hence increasing the probability of a fusion event. The fused cell suspension is plated and is maintained in tissue culture until there is evidence of hybridoma growth. The myeloma cells lack an enzyme that is important for growth, usually hypoxanthine-guanine phosphoribosyl transferase (HGPRT). The growth of hybridoma cells can be favoured over myeloma cells by incubating the plated cells in a medium containing hypoxanthine-aminopterin-thymidine (HAT). This medium contains aminopterin, which forces the cells to depend on HGPRT for growth. Therefore the unfused myeloma cells will not grow in this medium and the unfused

mortal B lymphocytes normally die out after a few days. Therefore only hybridomas are capable of colony formation.

The conditioned medium is collected and the titre is determined. Hybridomas that secrete protein specific antibody are transferred from the plates to larger flasks so proliferation can continue. Once there are sufficient cells they are frozen in liquid nitrogen for long-term storage. The primary hybridoma cell line is cloned by diluting the cell suspension at a density of one cell per well. These plates are maintained in tissue culture until the medium has been conditioned sufficiently. The conditioned medium is screened and positive clones are transferred to larger flasks so proliferation can continue. These cells are then frozen for long-term storage.

Two techniques exist for the production of monoclonal antibody: the hybridoma cells can be cultured in the ascitic fluid of mice or *in vitro* tissue culture may be employed. Ascites production involves injecting a quantity of hybridoma cells into the peritoneal cavity of mice. The hybridoma cells proliferate and secrete antibodies into the fluid space. The ascitic fluid can be withdrawn with a hypodermic needle at intervals. Tissue culture systems are largely based on the adherence of the cells to hollow-fibre membranes or microcarriers. Ascites production is relatively simple but the procedure has ethical problems because it is distressing for the mice and eventually results in death. Tissue culture techniques are more complex but do not have these ethical problems.

The antibody can be purified from ascites or conditioned growth medium by Protein G affinity chromatography to an acceptable extent after one step. Any subsequent purification steps, such as ion-exchange chromatography or gel filtration, must be performed under non-denaturing conditions to preserve the binding activity.

1.4.2 Immunoaffinity Separation Configurations

The most commonly investigated adsorption system is the packed bed consisting of Pharmacia Sepharose and the performance of other configurations is often compared with this system. Sepharose is an agarose-based support matrix with high porosity, high antibody immobilisation capacity and low non-specific binding character (Afeyan et al., 1990).

Packed bed adsorption has a number of limitations. The pore diffusion of the biochemical to the antibody-binding sites is often the rate-limiting resistance to adsorption (Arnold et al., 1985b). As well, the productivity of Sepharose is often limited by bed compression (Afeyan et al., 1990). Furthermore, the product streams often contain particles, which can foul and reduce the performance of packed beds. Alternative configurations have been investigated to overcome the limitations of Sepharose. These configurations include continuous stirred-tank adsorption, cross-flow filtration, radial-flow packed beds, magnetically fluidised beds, expanded beds, perfusive beds and membranes (Liu and Fried, 1994). Some of these configurations will be reviewed here.

1.4.2.1 Support Matrices

Support matrices that are suitable for column chromatography possess the following properties:

- Good mechanical and chemical stability.
- An abundance of functional chemical groups.
- Negligible non-specific protein adsorption.
- Relatively inexpensive.
- Good flow characteristics.
- High capacity for the antigen.

Table 1.5 lists a range of support matrices for applications in chromatography and Table 1.6 lists some commercially available membranes.

Support Matrix	**Example**
Agarose	Pharmacia Sepharose CL-6B
Cellulose	
Controlled pore glass and silica	
Polyacrylamide Beads	BioRad Bio-Gel P-200

Trisacryl	IBF Biotechnics Trisacryl GF-2000
Sephacryl	Pharmacia Sephacryl HR series
Ultrogel AcA	IBF Ultrogel AcA 22
Azlactone beads	3M
TSK-Gel Toyopearl HW	Tosoh
HEMA	Alltech HEMA-AFC BIO
Eupergit	Rohm Pharma Eupergit C
Poros	PerSeptive Biosystems

Table 1.5: Support matrices for column chromatography *(as reviewed by Hermanson et al., 1992).*

Membrane Support	Manufacturer
Flat sheet systems	Sartorius, Gottingen, FRG
Stacks of membranes	Millipore, Bedford, MA
Microporous polymer sheets with incorporated cellulose	FMC, Princeton, NJ
Polystyrene	Bio-Rad, Munich, FRG
Silica	Kontes, Vineland, NY
Radial flow cartridges	LKB, Sweden
Hollow-fibre modules	Sepracor, Marlborough, MA

Table 1.6: Commercially available membranes *(as reviewed by Thommes and Kula (1995)).*

1.4.2.2 Membrane Adsorption

Membrane systems have several advantages over the conventional Sepharose extraction systems. The high porosity and near lack of diffusion resistance in membranes enable high flow rates that result in extremely short process times. These membranes, having convective flow properties and lacking dead-end pores, provide a low-pressure system ideal for the processing of large volumes of viscous feed streams. The membrane's high convective mass transfer rates enable one to benefit from the fast adsorption kinetics of the antigen-antibody interaction. The high rates of mass transfer and small thickness permit the elution of adsorbate in very short times. In this way improved yields of active product and useful antibody life can be obtained in cases where the product or antibody would otherwise be degraded by harsh elution conditions (Zale and Colton, 1994).

Soltys and Etzel (1998) immobilised a polyclonal antibody preparation against low-density lipoprotein (LDL) to flat sheet membranes and successfully adsorbed LDL from patient plasma. The membrane volume was 80% smaller than the packed columns while the reduction in patient plasma LDL concentrations was comparable to the levels provided with

packed columns. Nachman (1992) immobilised monoclonal antibodies against interferon-α2a, interleukin-2 and interleukin-2 receptor to hollow fibre membranes. The membranes were well suited to the purification of these recombinant proteins.

1.4.2.3 Expanded Bed Adsorption

In expanded bed adsorption the feed flow rate is reversed and flows upwards. The flow rate is adjusted such that the particles move upwards, the bed expands and the porosity increases in a static state known as fluidisation. The advantage of an expanded bed over a packed bed is that small particles, entrained in the feed, do not plug the spaces between the particles and thereby averts fouling. In this way, centrifugation and filtration are not required prior to separation.

A stable expanded bed has been achieved by using conventional chromatographic supports based on agarose in a column equipped with a purpose designed liquid distribution inlet which gives a plug flow in the column (Chase and Draeger, 1992). However, beds consisting of conventional chromatographic supports used in this way expand too much at low flow velocities due to their low particle density, which results in low productivity. Hjorth et al. (1995) have developed an ion-exchange adsorbent that is an agarose-quartz composite, which possesses the bio-compatibility of agarose and the increased density required for expanded bed supports.

1.4.2.4 Stirred-tank Adsorption

In continuous stirred-tank adsorption, the steps of adsorption, washing, elution and regeneration take place in stirred tanks. The process can be achieved either in batch-mode or operation can be conducted in a continuous fashion (Figure 1.6).

There are many forms of stirred-tank adsorption and the variations are due to the method of separating the immunoadsorbent from solution and the type of immunoadsorbent support. The methods of separation include filtration (Mattiasson and Ling, 1992), sedimentation (Owen et al., 1993) and magnetic separation (Chase, 1984).

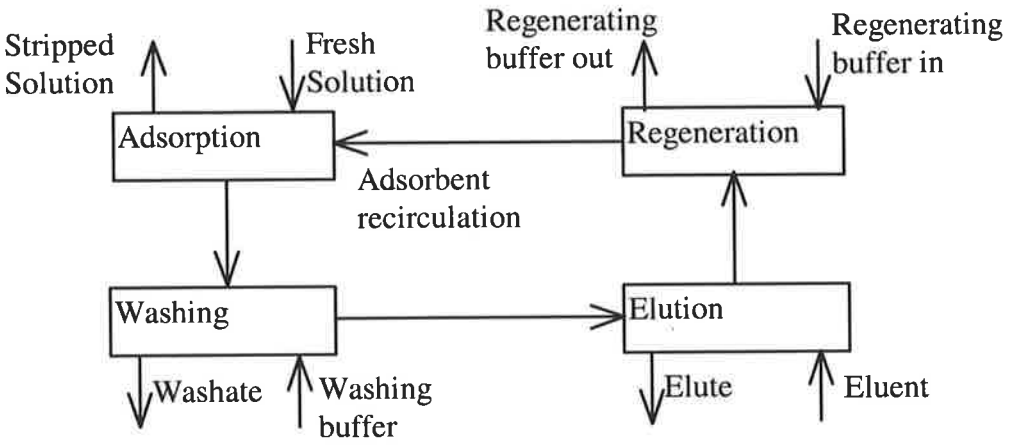

Figure 1.6: Continuous stirred-tank adsorption.

The feed, containing the protein of interest, is contacted with affinity ligands. The ligands bind to the protein of interest before the feed is pumped to the filter. In unbound form, the protein is sufficiently small to permeate through the filter. However, when bound to a large molecular weight ligand or particle, the filter retains the protein. Other proteins, of similar size to the protein of interest, permeate the membrane. The retained ligand-protein complex can then be treated with an appropriate eluent to desorb the protein from the ligand. The ligand can be recycled and reconditioned if necessary. The PERCAS unit (Owen et al., 1993) uses perfluorocarbon emulsion as the support. The PERCAS system consists of four mixer-settler units arranged in a loop. The mixing section of each stage is responsible for the extraction, washing, elution and regeneration steps of each stage, whereas the settler acts as a phase separator, removing the adsorbent particles from their carrying liquid. Chase (1984) suggested the use of magnetic supports for improving the efficiency of batch affinity separations. The use of magnetic traps to separate the immunoadsorbent from solution reduces the time needed to collect the immunoadsorbent.

1.4.2.5 Perfusive Bed Adsorption

Perfusion chromatography (Afeyan et al., 1990) is a relatively new technique for reducing resistance to stagnant mobile phase mass transfer without sacrificing high adsorbent capacity or necessitating extremely high pressure operation. The perfusive particles have throughpores of diameter 6000-8000 Å, which permit liquid flow. In this way, adsorbate can enter the interior of the particles through a combination of convective and diffusion transport. It has been shown that band-spreading, resolution of proteins and dynamic loading capacity are unaffected by increases in mobile phase velocity up to several thousands of centimetres per hour. Using a network of smaller 500-1500 Å interconnecting pores between the

throughpores enhances the surface area of this very large-pore diameter material. Scanning electron micrographs show that the pore network is continuous and that no point in the matrix is more than 5000-10000 Å from a throughpore. Consequently the diffusion path lengths are minimised and the large porous particles take on the transport characteristics of much smaller particles but with a fraction of the pressure drop. Capacity and resolution studies have shown that perfusive supports bind and separate an amount of protein equivalent to that of low performance agarose-based media at greater than 10-100 times the higher mobile phase velocity with no loss in resolution (Afeyan et al., 1990).

1.4.3 Examples of the Immunoaffinity Separation of Proteins from Milk

The commercial extraction of highly pure lactoferrin from bovine milk has been accomplished by immobilised monoclonal antibodies (Kawakami et al., 1987) with a single passage through the column yielding a purity of 98% and a recovery of 80%. Longer-acting tissue-type plasminogen activator (LAtPA) was purified from the milk of a transgenic goat by a scheme including immunoaffinity chromatography (Denman et al., 1991). The scheme extracted LAtPA, present at 3 μg/ml in the milk, with a purity of 98% and 25% yield. Human protein C, secreted in the milk of transgenic pigs, was purified to homogeneity with immobilised monoclonal antibodies (van Cott et al., 1996).

1.5 Project Strategy

The aim of this project has been to develop an immunoaffinity process for the commercial-scale purification of TGF-β2 from WGFE. The strategy that was adopted in order to satisfy this aim is presented here.

- **Purify TGF-β2 from WGFE with Conventional Purification Techniques**

The generation of hybridoma cell lines that secrete monoclonal antibodies against TGF-β2 required milligram quantities of this peptide for the immunisations, the immune response detection and the screening of hybridoma conditioned growth medium. The cost of purchasing recombinant human TGF-β2 from a commercial source was prohibitive in these quantities for it sells for A$250 per μg (1999). The aim was to purify milligram quantities of TGF-β2 to homogeneity for these purposes.

Rogers et al. (1996) demonstrated that TGF-β2 could be purified to homogeneity by a combination of gel filtration and reversed-phase HPLC. The TGF-β2 containing fractions could be identified by a mink lung epithelial cell bioassay. The intention was to follow the procedure of Rogers et al. (1996) to purify milligram quantities of TGF-β2 to homogeneity.

In the event that this procedure should fail to purify TGF-β2 to homogeneity, it was anticipated that an immunoaffinity step could be included to complete the purification. A commercially available anti-TGF-β2 monoclonal antibody would be coupled to NHS-activated Sepharose and used to immunopurify TGF-β2.

- **Generate Hybridoma Cell Lines that Secrete anti-TGF-β2 Monoclonal Antibodies**

The development of a commercial-scale immunoaffinity chromatography process requires gram quantities of antibody. Polyclonal antibodies may be used for the development of such processes and they are considerably easier to generate than monoclonal antibodies. However, in order to obtain significant quantities of the antibody larger animals must be used and correspondingly larger quantities of immunogen are required. Furthermore, polyclonal antibodies often bind to the immunogen with such high avidity that it is difficult or impossible to elute the bound immunogen without denaturing the antibody. For these reasons, a monoclonal antibody-based immunoaffinity process was preferable. A commercially available pan-specific anti-TGF-β monoclonal antibody sells for $1000 per mg (1996) and was therefore prohibitively expensive for a commercial-scale immunoaffinity separation process. Consequently, the generation of hybridoma cell lines was required to produce the required amount of monoclonal antibody.

The steps involved in generating monoclonal antibody-secreting hybridoma cells have been discussed in detail in the literature review section and will not be reiterated here. Two separate immunisation strategies were employed. One group of mice would be immunised with purified TGF-β2. A second group of mice would be immunised with a synthetic peptide that corresponds to amino acid residues 50-75 of TGF-β2 and that has been shown by other researchers to raise a high specific titre for TGF-β2. If either of these immunisation strategies were successful in raising a specific immune response then hybridoma cell lines would be developed from the spleen of the corresponding immune mouse.

- **Produce and Purify Large Amounts of Monoclonal Antibody**

The hybridoma cell lines would be cultured in a CellMax Artificial Capillary Module to produce antibody in the required gram amounts for the immunoaffinity process. It was considered to have advantages over the ascites method of production and other tissue culture systems. The presence of high levels of impurities in the antibody preparation is not acceptable because this would contribute to an increased amount of non-specific binding to the antibody-coupled affinity support. The antibody would be purified from conditioned growth medium by Protein G affinity chromatography because it has been reported to purify antibody to an acceptable extent after one step.

- **Mathematically Model a Hypothetical Immunoaffinity Separation Process**

In order to minimise the costs of purifying TGF-β2 from WGFE an efficient immunoaffinity separation process must be developed. The major costs would be attributable to labour, WGFE, antibody, the equipment and the support for immobilisation. Therefore an efficient immunoaffinity separation process would be fast and require small amounts of WGFE, antibody and support matrix in order to satisfy its design objective. It has been demonstrated by a large literature that the economics of the separation process can be influenced by the configuration of the process, the operating conditions and the characteristics of the antibody. A number of configurations exist for immunoaffinity separation. These include continuous stirred-tank adsorption, cross-flow filtration, axial-flow and radial-flow packed beds, magnetically fluidised beds, expanded beds, perfusive beds and membranes. The operating conditions include the feed flow rate, the dimensions of the immunoaffinity support and the effluent concentration of TGF-β2 at breakthrough. The antibody characteristics include the binding kinetics, the specific binding capacity for TGF-β2 and the rate of binding capacity degradation. Obviously the number of resulting combinations is potentially very large and it would be very time-consuming to investigate all of them in the laboratory. A mathematical model of the immunoaffinity process would be useful in identifying the most promising configurations, operating conditions and antibodies, without having to resort to laboratory experiments that explore every possibility.

- **Characterise the Antibodies and the TGF-β2-Antibody Interactions**

The class and cross-reactivity of the antibody would be ascertained. The ability of the antibody to neutralise the biological activity of TGF-β2 in mink lung epithelial cell assay would be assessed. A variety of chemical eluents would be screened for the ability to dissociate the TGF-β2-antibody interaction, whilst conserving the binding capacity of the antibody. The rate at which eluent-mediated binding capacity degradation occurs would be determined. The binding kinetics of the TGF-β2-antibody interaction would be investigated with the Biacore instrument.

- **Optimise the Activation of TGF-β2 in WGFE**

The optimal method would be found for activating TGF-β2 from WGFE whilst maintaining buffer conditions that are suitable for immunoaffinity chromatography.

- **Immobilise Antibody to a Support**

The most efficient support configuration for immunoaffinity separation, as determined by the mathematical modelling, would be purchased and used to immobilise antibody. The TGF-β2 specific binding capacity of the antibody would be determined by incubating the antibody-coupled support in activated WGFE. The antibody characteristics, the TGF-β2 concentration in activated WGFE and the support dimensions would be fed into the mathematical model to simulate the immunoaffinity separation process. In this way the running costs would be minimised with respect to the operating conditions. The immunoaffinity separation process would then be designed and assembled to these specifications.

Chapter Two

Preparation of Transforming Growth Factor-β2 Immunogen from Whey Growth Factor Extract

2. Preparation of TGF-β2 Immunogen from WGFE

2.1 Introduction

The generation of a hybridoma cell line that produces monoclonal antibodies requires an immunogen for the immunisations and the titre detection. TGF-β2 is commercially available in a pure form and would therefore be the obvious source of antigen. However, the amount of immunogen usually required for hybridoma generation is such that it would be prohibitively expensive to obtain from a commercial source. Therefore, an alternative source of TGF-β2 was required.

TGF-β2 has been identified in a number of natural sources including bovine bone, milk, cheese whey, human glioblastoma cells and porcine blood platelets. The most readily available natural sources of TGF-β2 are clearly bovine milk and cheese whey. Cox and Burk (1991) showed that a purification scheme, consisting of strong cation-exchange chromatography, low-pressure hydrophobic interaction chromatography, hydrophobic interaction HPLC and size-exclusion HPLC, was successful in purifying TGF-β2 to homogeneity. However, milk contains lipids and casein, which make the purification a more difficult task. Presumably, the use of cheese whey would not suffer this limitation because these materials precipitate during cheese manufacture. Rogers et al. (1996) discovered that most of the TGF-β biological activity in milk, as measured by a mink lung epithelial cell line, partitioned into whey after cheese manufacture. Furthermore, this activity could be purified with gel filtration and reversed phase HPLC. The TGF-β2 purification methods of Cox and Burk (1991) and Rogers et al. (1996) from milk and whey respectively are discussed in the following sections.

Cox and Burk (1991) purified TGF-β2 from milk using the following strategy. Pasteurised milk was diluted with distilled water following the addition of protease inhibitor. The diluted milk pH was adjusted to neutrality and then pumped through Dowex AG 50WX2 mesh resin. After loading, the resin was washed with 0.01M NaH_2PO_4 pH 7 to obtain a baseline absorbance. The cation-exchange column was eluted with 0.02M KH_2PO_4 and 0.7M potassium acetate in 40% ethanol pH 7.6 until the absorbance returned to baseline. The eluted fractions were adjusted to pH 5 with acetic acid and the biological activity of the fractions was determined with a fibroblast migration assay. The active fractions were concentrated by rotary evaporation. The next purification step involved hydrophobic interaction

chromatography. Phenyl-Sepharose CL-4B resin was added to a vessel containing the concentrate and stirred gently overnight. The loaded hydrophobic interaction resin was allowed to settle and the biologically inactive supernatant was decanted and discarded. The loaded resin was washed with 0.6M ammonium acetate pH 5 until the effluent was no longer opaque and then transferred to a chromatography column and washed with additional buffer until the absorbance baseline was attained. The column was eluted with 28% ethanol in 0.2M ammonium acetate. The pool of active fractions was lyophilised and resuspended in 42% ethanol, 0.6M ammonium acetate pH 5. Residual particulate matter was removed by centrifugation. Additional ammonium acetate (2M) was added to the pool, which was then pumped on to a butyl-polyol Si500 HPLC column. The column was washed with ammonium acetate pH 5.5 until baseline absorbance was attained. The column was eluted by an increasing stepped ethanol gradient. The pool of biologically active fractions was mixed with ammonium acetate pH 5.5 and then pumped on to an octyl-polyol Si500 HPLC column. The column was washed with ammonium acetate pH 5.5 solution until baseline absorbance was attained. The column was again eluted by an increasing stepped ethanol gradient. The pool of biologically active fractions was lyophilised and resuspended in 42% ethanol-0.6M ammonium acetate pH 5.5. The protein was then injected on to a TSK G2000 SW HPLC size-exclusion column. The biologically active fractions were pooled and lyophilised in a vacuum centrifuge. Jin et al. (1991) further purified TGF-β2 from the pool using reversed phase HPLC with a C4 narrow bore column. The residue was resuspended in 0.1% (v/v) trifluoroacetic acid (TFA) containing 25% acetonitrile (v/v) and injected several times on to the C4 column. The column was eluted with a linear gradient of 28-38% (v/v) acetonitrile over 40 minutes. The fibroblast migration assay detected biological activity that coincided with a protein peak on the chromatogram. These fractions were subject to SDS-PAGE and a single band was revealed. N-terminal sequencing of the protein showed that the material was TGF-β2.

Rogers et al. (1996) purified TGF-β2 from cheese whey using the following purification strategy. Firstly, Whey Growth Factor Extract (WGFE) was prepared from whey by cation-exchange chromatography according to the method of Francis et al. (1995). Briefly, pasteurised whey was filtered and the filtrate pH was adjusted to 6.5 before being loaded on to a column of Sepharose Fast Flow-S resin that had been equilibrated with 50 mM sodium citrate pH 6.5. After washing with equilibration buffer, the protein was eluted with 0.4M

NaCl to yield the WGFE fraction, which was then diafiltered against water and concentrated with a 3 kDa exclusion membrane. The WGFE fraction was loaded on to an Amicon Cellufine column and the protein was eluted with a buffer containing NaCl (0.15 M) and HCl (10 mM) at pH 2.5. The biologically active fractions were identified with TGF-β-responsive mink lung epithelial cells, neutralised with NaOH, diafiltered against water, and then freeze-dried. The protein was resuspended in a buffer containing NaCl (0.15 M), acetic acid (1M) and 10% (v/v) acetonitrile, and was loaded on to a Pharmacia Superdex 75 HR 35/600 size-exclusion column. The pool of TGF-β fractions from the second acid gel filtration step were loaded on to a Deltapak C4 reversed phase HPLC column and eluted with a linear gradient of acetonitrile (0-80%, v/v) over one hour. The TGF-β fractions were then further diluted in 0.1% TFA (v/v), loaded on to the C4 column again, and eluted with a gradient of acetonitrile (0.08% (v/v) per minute over three hours). Rogers et al. (1996) reported that the final reversed-phase HPLC stage yielded two peaks of biological activity, which were eluted at 30-31% and 37-38% acetonitrile (v/v). Most of the TGF-β activity was eluted in the second peak, which was identified as TGF-β2 by N-terminal sequencing. The specific TGF-β activity of this peak was measured by mink lung epithelial cell assay to be 620 μg/mg protein. In view of the relative simplicity of the purification method of Rogers et al. (1996) and the large quantities of WGFE available from the pilot-scale production facility, this purification method was selected for the purification of TGF-β2 immunogen.

2.2 Materials and Methods: Analytical Techniques

2.2.1 Biological Assay for TGF-β Detection

The cell growth inhibition assay for total TGF-β (TGF-β1 and TGF-β2) was performed by the method of Absher et al. (1991) with minor modifications. Jennings et al. (1988) showed that epidermal growth factor, platelet-derived growth factor and insulin-like growth factors-I and -II do not cross-react in this assay. Acidic and basic fibroblast growth factor cross-react in the assay but their concentrations in WGFE are low and are unlikely to significantly influence the extent of TGF-β1 mediated inhibition. Mink lung epithelial cells (Mv1Lu; CCL64) were obtained from the American Type Culture Collection (Rockville, MD, USA). The biological assay is described here in detail.

Mv1Lu cells were cultured in Dulbecco's modified minimal essential Eagle's medium (JRH Biosciences, Lenexa, KS, USA) with the addition of 10% foetal bovine serum (CSL

Biosciences, Parkville, Vic), 1% penicillin-streptomycin-fungizone solution (CSL Biosciences), 0.02M HEPES and 0.044M $NaHCO_3$. The cells were maintained in 75 cm^2 sterile plastic culture flasks (Iwaki, Japan) at 37°C with an atmosphere of 5% CO_2 and 100% relative humidity. Mv1Lu cells adhered to the plastic surface of the flasks and were detached by trypsinisation. This was performed with Dulbecco's phosphate buffered saline (137 mM NaCl, 2.7 mM KCl, 8.1 mM Na_2HPO_4 and 1.5 mM KH_2PO_4, pH 7.4) containing 2.5 mg/ml trypsin (CSL Biosciences) and 1mM EDTA. The culture medium was aspirated from the cell monolayer and replaced with 3 ml of trypsin/EDTA solution, which was also aspirated to remove trace FBS. The cells were incubated in 1 ml of fresh trypsin/EDTA solution for 3 minutes at 37°C. The cells were then detached by agitation and 9 ml of DMEM + 10% FBS was added to the flask in order to neutralise the trypsin activity and form a cell suspension. The cell suspension was centrifuged at 90 g for 5 minutes in a Centaur 2 centrifuge (Sanyo MSE, Leicestershire, U.K.). The supernatant was aspirated from the cell pellet so that the trypsin was removed to prevent damage to the cells. The cell pellet was resuspended in 10 ml of DMEM + 10% FBS and 50 µl samples were taken for cell counting. The samples were mixed with equal volumes of 4% (v/v) trypan blue (Sigma Chemical Co., St. Louis, MO, USA) and the viable cells were counted on a haemocytometer (La Fontaine, France) under a microscope (Olympus CK2, Japan). The cell suspension was diluted with DMEM + 10% FBS such that a cell density of 2×10^5 cells/ml was obtained. One hundred µl of cell suspension was added to each well of a 96-well plate (Iwaki, Japan) and incubated overnight.

The next day, dilutions of recombinant human TGF-β1 (R and D Systems, Oxon, U.K.) were prepared in DMEM + 5% FBS ranging from concentrations of 0.05 to 10 ng/ml. In order to determine the fractions positive for TGF-β, 1:100 or 1:1000 dilutions of sample were made with DMEM + 5% FBS. For determining the TGF-β concentration, serial 1 in 2 dilutions of the pool were prepared. The medium was aspirated from the wells of the plates and replaced with 100 µl/well of DMEM without FBS. This medium was aspirated and replaced with 100 µl/well of the test medium in duplicate. The plates were returned to the incubator for two days. Rogers et al. (1996) demonstrated that rhTGF-β1 and rhTGF-β2 have similar potencies in this assay. Cell growth was quantified using a methylene blue staining method (Oliver et al., 1989). The medium was tipped out of the wells and the plates were washed twice with 0.15 M NaCl. The cells were fixed by incubating the cells in 100 µl/well of methanol for 30 minutes. The methanol was tipped out of the wells and replaced with 100 µl/well of 1% (w/v)

methylene blue (Sigma Chemical Co., St. Louis, MO, USA) in 0.01M sodium tetraborate pH 8.5 buffer. The incubation continued for 30 minutes, after which the methylene blue solution was tipped out of the wells and the wells were washed five times with 0.01M sodium tetraborate pH 8.5. One hundred µl of 50% ethanol-0.05M HCl was dispensed to each well. The plates were agitated on a plate shaker (Ratek Instruments, Borona, Vic) for 10 minutes. The optical density of each well was read with a plate reader (Bio-Rad 450, Hercules, CA, USA) at a wavelength of 655 nm. The pattern of inhibition by TGF-β1 exhibited a truncated sigmoid-shaped concentration-response relationship with a half-maximal inhibition (ED_{50}) at a concentration of 0.4 ng/ml. Absher et al. (1991) reported an ED_{50} of 0.3 ng/ml in their assay. The dose response curve was imported to Tablecurve (Jandel Scientific, San Rafael, CA, USA) and constants *a*, *b*, *c* and *d* were regressed to the four-parameter logistic function (Tijssen, 1985):

$$y = a + \frac{b}{1 + \left(\frac{x}{c}\right)^d} \qquad (2.1)$$

where *x* is the rhTGF-β1 concentration in ng/ml, *y* is the optical density at 655 nm and *c* is the TGF-β concentration for the half-maximal growth response (ED_{50}). The dose response data for the unknown protein sample were imported to Tablecurve and the TGF-β1 concentrations (*x*) were computed from the optical density (*y*) values with the inverse function of Equation 2.1. The TGF-β concentration of the sample was calculated with Lotus 1-2-3 Release 4.01 for Windows application (Lotus Development Corporation, Cambridge, MA, USA).

2.2.2 Enzyme-linked Immunosorbent Assay for TGF-β2 Detection

A commercially available enzyme-linked immunosorbent assay (ELISA) kit (Promega, Madison, WI, USA) was also used to determine the concentration of TGF-β2. A limited number of determinations were also performed with a Quantikine human TGF-β2 Immunoassay (R and D Systems, Oxon, U.K.). The Promega assay was performed according to the manufacturer's instructions, which are described below.

The anti-TGF-β2 monoclonal antibody was diluted 1:1000 in coating buffer (25 mM $NaHCO_3$, 25 mM Na_2CO_3 pH 9.2). One hundred µl of the antibody solution was added to each well of a 96-well ELISA plate (Nunc ALS, Roskilde, Denmark). The plate was

incubated overnight at 4°C while antibody coated the plate. The next day the well contents were discarded. The kit blocking buffer was diluted 1:5 with distilled water. Two hundred and seventy µl of diluted blocking buffer was added to each well of the ELISA plate. The plate was incubated at 37°C for at least 35 minutes while surface hydrophobic residues were blocked to minimise the non-specific binding of TGF-β2 to the plate surface. The kit sample buffer was diluted 1:10 with distilled water. A standard TGF-β2 curve was prepared by diluting the porcine TGF-β2 standard to 1:1000 with sample buffer and then making 1 in 2 serial dilutions to provide duplicate samples for each standard concentration. The unknown protein samples were similarly diluted in sample buffer. The blocking buffer was discarded from the wells and was replaced by 100 µl per well of the protein samples. The plate was incubated for 90 minutes at room temperature on a plate shaker. The wells of the plate were washed five times with ELISA wash buffer (20 mM Tris, 150 mM NaCl, 0.05% (v/v) Tween 20, pH 7.6). The rabbit anti-TGF-β2 polyclonal antibody was diluted 1:2000 with sample buffer. One hundred µl of diluted polyclonal antibody was added to each well of the plate. The plate was incubated for two hours at room temperature on a plate shaker. The wells of the plate were washed five times with ELISA wash buffer. The kit peroxidase-conjugated anti-rabbit antibody was diluted 1:2000 with sample buffer. One hundred µl of diluted anti-rabbit antibody was added to each well of the plate. The plate was incubated for two hours at room temperature on the plate shaker. The wells of the plate were washed five times with ELISA wash buffer. The chromogen TMB (3,3',5,5'-tetramethyl benzidine) was mixed in equal portion with the peroxidase substrate. One hundred µl of substrate was added to each well of the plate. The plate was incubated at room temperature without shaking while the colour developed. After a maximum of 15 minutes, 100 µl of 1M H_3PO_4 was added to each well of the plate to quench the colour reaction.

The optical density of each well was read with a plate reader (Bio-Rad 2550, Hercules, CA, USA) at a wavelength of 450 nm. The dose response curve was imported to Tablecurve and constants *a*, *b* and *c* were regressed to a function of the form:

$$y = a + bx^c \qquad (2.2)$$

where *x* is the porcine TGF-β2 concentration in pg/ml and *y* is the optical density at 450 nm. Equation 2.2 was selected from a number of equations regressed by Tablecurve because it generally gave the best fit to the dose response. Although conventional wisdom dictates that

ELISA dose response curve should be linear, significant non-linearity is often observed. A number of different empirical equations have been regressed to dose response data but there does not appear to be a mechanistic basis for these non-linear equations (Tijssen, 1985). Equation 2.2 was not among those reviewed by Tijssen et al. (1985) but it required less regression parameters than other equations in general use and fitted the data well. The dose response data for the unknown protein sample were imported to Tablecurve and the TGF-β2 concentrations (x) were computed from the optical density (y) values with the inverse function of Equation 2.2. The TGF-β2 concentration of the sample was calculated with Lotus 1-2-3 Release 4.01 for Windows application.

2.2.3 BCA Protein Estimation

The protein concentration of solutions was determined with either the macro BCA Protein Assay kit or the micro BCA Protein Assay kit (Pierce, Rockford, IL, USA). The procedure for the macro BCA Protein Assay is described here.

Standard concentrations of 2 mg/ml bovine serum albumin (Pierce, Rockford, IL, USA) were prepared with protein concentrations in the range of 250 to 2000 μg/ml with distilled water. Ten μl of each BSA concentration was added to the wells of a 96-well microtitre plate (Iwaki, Japan) in triplicate. Serial 1:2 dilutions of the unknown sample were prepared with distilled water and 10 μl of each dilution was added to the wells of the microtitre plate in triplicate. Kit reagents A (Na_2CO_3, $NaHCO_3$, bicinchoninic acid and sodium tartrate in 0.1M NaOH) and B ($CuSO_4$) were mixed together in the proportions of 50:1 and 200 μl of the working reagent was added to each well. The plate was incubated at 37°C for 30 minutes. The optical density of each well was read with a plate reader (Bio-Rad 450) at a wavelength of 570 nm. The dose response curve was imported to Tablecurve and constants a, b and c were regressed to Equation 2.2 where x is the protein concentration in μg/ml and y is the optical density at 570 nm. The dose response data for the unknown protein sample was imported to Tablecurve and the protein concentrations (x) were computed from the optical density (y) values with the inverse function of Equation 2.2. The protein concentration of the sample was calculated with Lotus 1-2-3 Release 4.01 for Windows application.

The procedure for the micro BCA Protein Assay is described here. Standard concentrations of BSA were prepared with protein concentrations in the range of 2.5 to 20 μg/ml with distilled

water. One hundred µl of each BSA concentration was added to the wells of a microtitre plate in duplicate. Serial 1:2 dilutions of the unknown sample were prepared with distilled water and 100 µl of each dilution was added to the wells of the microtitre plate in duplicate. In a limited number of protein assays the same buffer, as that in which the protein was initially dissolved, was used to dilute the samples because undiluted unknown sample was included in the assay. In these cases the standard BSA curve was prepared in the corresponding buffer to account for variations arising from different buffer systems. Kit reagents A (Na_2CO_3, $NaHCO_3$, and sodium tartrate in 0.1M NaOH), B (bicinchoninic acid) and C ($CuSO_4$) were mixed together in the proportions of 50:48:2 and 100 µl of the working reagent was added to each well. The plate was incubated in a water bath at 60°C for 30 minutes. The optical density of each well was read with the plate reader at a wavelength of 570 nm. The protein concentration of the unknown sample was determined in the same manner from the dose response data as described for the macro BCA Protein Assay.

2.2.4 SDS-PAGE

Polyacrylamide gel electrophoresis of the protein was performed with a Pharmacia PhastSystem Separation control and Development unit. Lyophilised samples were reconstituted in loading buffer (10% (w/v) sodium dodecyl sulfate, 20% (v/v) β-mercaptoethanol, 0.04% (w/v) bromophenol blue, 1 mM EDTA, pH 8). The samples were heated at 65°C for 15 minutes and loaded on to an 8-25% gradient polyacrylamide gel. A low molecular weight calibration sample (AMRAD Pharmacia Biotech) was loaded on to the gel for comparison. The protein was electrophoresed and stained with Coomassie blue according to the manufacturer's instructions. The molecular mass of the protein was determined by comparison to molecular weight protein markers.

Alternatively the gel was silver stained according to the modified method of Merril et al. (1984). The gel was fixed with 20% (v/v) trichloroacetic acid for 30 minutes. The gel was subject to two rounds of washing (15 minutes) with 20% TCA, 10% ethanol, 5% acetic acid in water. The gel was incubated in 3.4 mM $K_2Cr_2O_7$, 3.2 mM HNO_3 for 15 minutes. It was then incubated with 12 mM $AgNO_3$ in the dark for 20 minutes. The protein bands were developed with 0.0185% (v/v) formaldehyde in 0.28 M Na_2CO_3. Once the bands had developed sufficiently the stop solution, 3% (v/v) acetic acid, was incubated with the gel for

five minutes. The gel was washed twice with water for 20 minutes per wash. The gel was incubated in 5% (v/v) glycerol for 15 minutes to preserve it.

2.3 Materials and Methods: Purification Techniques

2.3.1 Large-scale Gel Filtration with Cellufine Column

One litre of WGFE was acidified to pH 2.5 with 10 ml of 5M HCl and the solution was incubated overnight at 4°C. On the following day this material was filtered through 1 μm Whatman filter paper and loaded on to a column packed with ~40L of Cellufine media (Amicon Corporation, Danvers, MA, USA) at a flow rate of ~60 ml/min with a peristaltic pump (Watson-Marlow 503U, Cornwall, U.K.). The running buffer consisted of 0.15 M NaCl and 0.01 M HCl. Forty fractions of 450 ml each were collected and they were sampled for the determination of protein and TGF-β concentration. The samples were lyophilised on a centrifugal vacuum drier (Hetovac VR1, Denmark), resuspended in distilled water and subject to the Mv1Lu TGF-β assay and BCA protein assay. Alternatively a crude estimate for protein was gained by measuring the solution absorbance at 450 nm with a spectrophotometer (Cecil Series 1020). In some purifications TGF-β2 ELISA was used to screen for TGF-β2 rather than the Mv1Lu assay. At dilutions greater than 1:100 the acid running buffer did not seriously affect the results of the TGF-β assays and therefore sample freeze-drying was not essential.

Fractions that contained the TGF-β activity were pooled and placed in a DC10L tangential filtration system (Amicon Inc., Beverly, MA, USA). The molecular weight cut-off of the filter was 3 kDa and therefore TGF-β2 (MW 25 kDa) was likely to be retained by the filter. The protein was diafiltered against 20 L of MilliQ water to remove salts and then concentrated to a volume of 1 L. The retentate was further concentrated with four cellulose triacetate membranes in a membrane housing (Sartorius) to a volume of ~300 ml. The molecular weight cut-off of the membranes was 5 kDa. This volume was lyophilised overnight on a Dynavac Freeze Drying Unit. A sample of the lyophilised protein was resuspended in distilled water and its protein and TGF-β concentrations were determined. The sample was also subject to SDS-PAGE.

2.3.2 Small-scale gel filtration with Superdex column

The biologically active lyophilised protein was resuspended in 0.15 M NaCl, 1 M acetic acid buffer and filtered through a 0.45 μm membrane (Millipore, Sydney, NSW). Acetonitrile was then added to the protein solution to give a 10% (v/v) solution. The protein solution was centrifuged (J6, Beckman, USA) at 1700 g for 20 minutes at 4°C and then filtered through a 0.22 μm membrane (Millipore). It was injected on to a Pharmacia Superdex 75 HR 35/600 size-exclusion column at a flow rate of 3.5 ml/min with an FPLC system (AMRAD Pharmacia Biotech). Thirty-six × 5-minute fractions were collected with an FRAC-100 fraction collector (AMRAD Pharmacia Biotech) for each run. The solution absorbance at 280 nm was measured and displayed on a chart recorder. The TGF-β activities for each fraction were determined in a manner similar to that described in section 2.3.1. The fractions containing TGF-β activity were pooled together and a small sample of the pool was lyophilised on the centrifugal vacuum drier. The lyophilised protein was resuspended in distilled water and its protein and TGF-β concentrations were determined.

2.3.3 Reversed-phase HPLC Purification of TGF-β2

The pooled protein was diluted 1:4 with buffer A (0.1% (v/v) TFA in water) and loaded on to a Deltapak C4 column (Waters Chromatography Division, Millipore). The column was washed with buffer A until an absorbance baseline at 214 nm was attained. The buffer system consisted of buffer A and buffer B (0.1% (v/v) TFA and 80% (v/v) acetonitrile in water). A linear gradient of 0-80% acetonitrile over 80 minutes was delivered at a flow rate of 5 ml/min with an HPLC system (GBC Scientific, Australia) and the UV absorbance at 214 nm was recorded. Eighty × 1-minute fractions were collected with an FRAC-100 fraction collector for each run. The fractions were collected in 10 ml tubes that had been exposed to AquaSil siliconising fluid (Pierce, Rockford, IL, USA) to reduce the non-specific adsorption of protein to the tubes. The TGF-β activity of each fraction was determined and the fractions, which contained TGF-β activity, were pooled. A small sample of the pool was lyophilised, resuspended in distilled water and the protein and TGF-β concentrations were determined. The column flow through was diluted at 1:100 with DMEM+5% FBS and included in an Mv1Lu assay to ensure that TGF-β activity bound to the column.

The pooled protein was diluted 1:5 with buffer A and loaded on to the Deltapak C4 column again. The column was washed with buffer A until an absorbance baseline at 214 nm was attained. The linear gradient consisted of 0-20% acetonitrile over 10 minutes, 20-45%

acetonitrile over 250 minutes and finally 45-80% acetonitrile over 10 minutes. The buffer flow was delivered at 5 ml/min with the HPLC system and the UV absorbance at 214 nm was recorded. Two minute fractions were collected in siliconised 10 ml tubes. The TGF-β activity of each fraction was determined and the fractions, corresponding to the second peak of TGF-β activity, were pooled. A small sample of the pool was lyophilised, resuspended in distilled water and its protein and TGF-β concentrations were determined.

2.4 Results and Discussion

An attempt was made to repeat the purification method of Rogers et al. (1996) in order to purify sufficient quantities of TGF-β2 for immunisations and titre detection. Large quantities of WGFE were available from a pilot-scale production facility and the results of Rogers et al. (1996) suggested that milligram quantities of TGF-β2 could be purified to a specific activity of 620 μg/mg protein. Although this purity of TGF-β2 would not be acceptable for polyclonal antisera production it would be acceptable for monoclonal antibody generation. This is because anti-TGF-β2 antibody producing hybridomas can be identified by screening against pure commercially available TGF-β2 and separating them from hybridomas that produce antibodies against contaminants in the crude TGF-β2 preparation. The following sections compare the Mv1Lu assay and the TGF-β2 ELISA, discuss attempts to repeat the purification method of Rogers et al. (1996) and provide possible explanations as to why on this occasion the purifications were not as effective.

The Mv1Lu assay was generally a reliable method for measuring the TGF-β concentration of an unknown sample with low cost consumable materials. However, the assay required four days to perform and scrupulous attention to aseptic technique. A source of inter-assay variation was the cells' gradual decline in TGF-β responsiveness with increasing passage number. In addition, Mv1Lu cells are responsive to both TGF-β1 and TGF-β2 and therefore do not discriminate between the isoforms. Jennings et al. (1988) demonstrated that the known growth factors in WGFE (PDGF, basic FGF, acidic FGF, IGF-I and IGF-II) were unlikely to affect the inhibitory response of Mv1Lu cells to TGF-β. However, unidentified WGFE growth factors may influence the observed response of Mv1Lu cells. Furthermore, the linear portions of the dose response curves for the TGF-β1 standard and the unknown samples often had different slopes, given by parameter *d* in Equation 2.2, and were thus a potential source of error in determining the TGF-β concentration.

The commercially available TGF-β2 ELISA was used to determine the TGF-β2 concentration of unknown samples. Although relatively expensive in comparison with the Mv1Lu assay, it had several advantages over this assay. It is specific for the TGF-β2 isoform, has greater linearity in the dose response curve than the Mv1Lu assay and it uses a porcine TGF-β2 standard with the same amino acid sequence as bovine TGF-β2. Moreover, the ELISA requires only one day to perform and does not require aseptic technique. When an unknown sample of WGFE-derived TGF-β2 was subject to both assays, the Mv1Lu assay determined a TGF-β2 concentration that was higher than that determined by TGF-β2 ELISA (Table 2.1). It was unlikely that TGF-β1 contamination accounted for the higher concentration because the sample had been purified on the 0.1%/min acetonitrile gradient and the second peak of TGF-β activity was pooled. The other sources of error discussed in the preceding paragraph are probably responsible for the discrepancy in TGF-β2 concentration measured by the two techniques.

Protein volume (μl)	**500**	**250**	**Ratio 500:250**
Integrated peak area (V.s)	10.8	4.84	2.23
Mv1Lu Assay (μg)	0.747	0.399	1.87
TGF-β2 ELISA (μg)	0.493	0.207	2.38
Ratio Mv1Lu:ELISA	1.52	1.93	

Table 2.1: Comparison of TGF-β2 measurement by ELISA and Mv1Lu assay. *Partially purified TGF-β2 was subject to reversed phase analytical C4 HPLC at loading volumes of 500 μl and 250 μl. The absorbance peak areas at 214 nm were integrated and the protein in the peaks was assayed in ELISA and for Mv1Lu growth inhibition.*

The purification method of Rogers et al. (1996) was repeated six times with some modifications. The following results correspond to the first purification, which consisted of large-scale Cellufine gel filtration, small-scale Superdex gel filtration and two rounds of reversed phase HPLC. A large-scale Cellufine gel filtration column was used to separate the constituent proteins of WGFE on the basis of molecular size. According to Rogers et al. (1996), TGF-β activity elutes at apparent molecular weights of 80 kDa and 600 kDa under neutral pH conditions because TGF-β2 is bound as a latent complex. The major WGFE proteins, xanthine dehydrogenase, hexokinase and lactoperoxidase, have molecular weights

in the range of 69 to 147 kDa and therefore the latent 80 kDa TGF-β2 complex would co-elute with them when gel filtered under neutral pH conditions. For this reason, WGFE was acidified to dissociate the latent complex thereby releasing active TGF-β2 (25 kDa) at a molecular weight lower than that of the major WGFE proteins. The void volume accessible to TGF-β2 is thus greater than that accessible to the major proteins and TGF-β2 elutes at a greater elution volume (Figure 2.1) when the overall protein concentration is low. The biologically active fractions corresponding to elution volumes 12-16 L were pooled, diafiltered against water, concentrated and lyophilised. The lyophilised protein was subject to SDS-PAGE and a series of bands with molecular weights below 30 kDa were revealed, as shown in the inner lanes of Figure 2.2. Therefore large-scale Cellufine acid gel filtration is a very effective first purification stage.

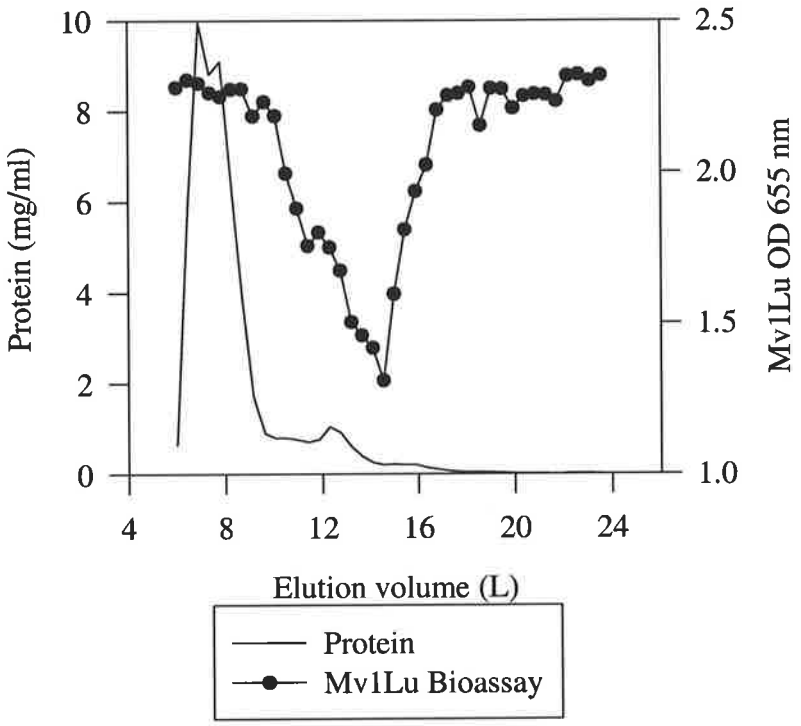

Figure 2.1: Overlay plot of protein concentration and Mv1Lu cell growth versus elution volume for the Cellufine gel filtration step. *Each bioassay point is the mean of six determinations at 1:1000 dilution.*

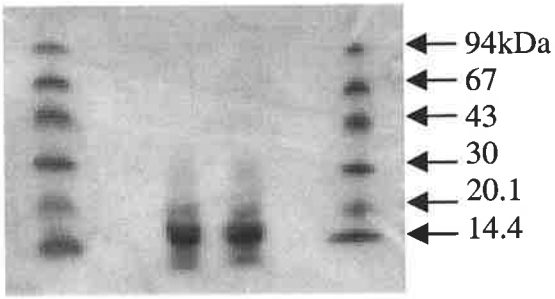

Figure 2.2: SDS-PAGE of Cellufine protein under reducing conditions. *Outer lanes are low molecular weight standard and the inner lanes are Cellufine protein.*

The Cellufine gel filtration column was an effective first purification stage because of its large size (~40L) but Figure 2.1 shows that the resolution of TGF-β activity was poor. This is likely to be due to the mixing that occurs in the column headspace, piping and valves. The Superdex column was selected as a second purification stage because of its improved resolution on the basis of molecular size. However, it has the drawback of being of small size (600 ml) and was therefore unable to separate the same amount of protein as the Cellufine column. The lyophilised protein with TGF-β activity was resuspended in acid running buffer and equal amounts of protein were loaded on to the Superdex column in four separate purification runs. The eluting protein was collected in separate fractions, which were then subject to TGF-β determinations as shown in Figure 2.3. It is evident that the resolution of Superdex acid gel filtration was superior to that of the Cellufine column as the protein was separated into two separate peaks and the peak of biological activity was much sharper.

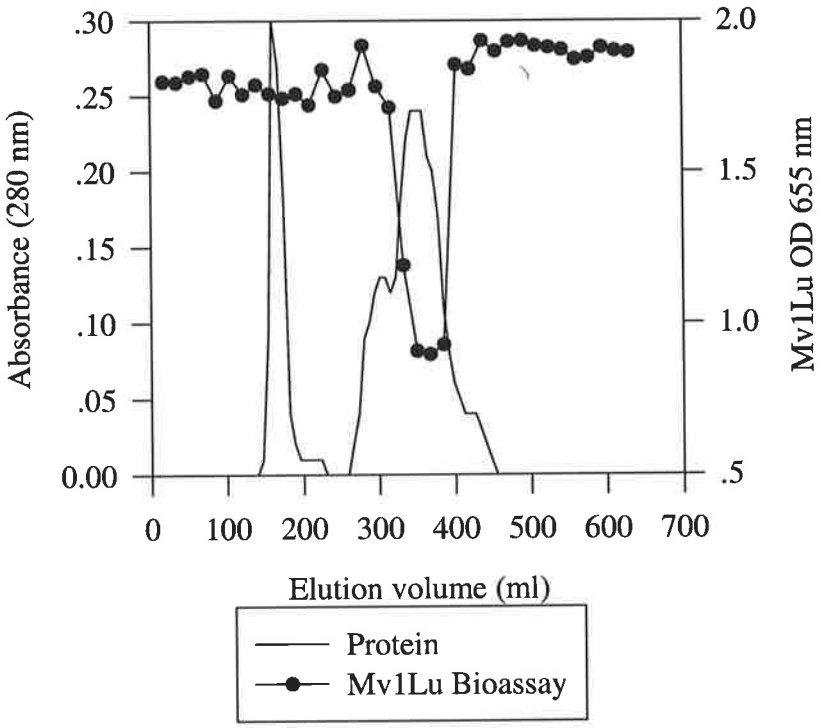

Figure 2.3: Overlay plot of absorbance at 280 nm and Mv1Lu cell growth versus elution volume for the Superdex gel filtration step. *Each bioassay point is the mean of duplicate determinations at 1:1000 dilution.*

Reversed phase HPLC was selected as the next purification stage because it separates proteins on the basis of hydrophobicity. The reversed phase resin consists of spherical particles packed inside a pressure resistant cartridge. The surface of each reversed phase particle is coated with hydrocarbon chains (C4), which are highly hydrophobic. During protein loading, the protein is resuspended in an aqueous phase and injected on to the reversed phase column. Under this condition hydrophobic interactions between the hydrophobic residues of the proteins and the hydrocarbon chains are favoured. It is an entropy driven process because free water molecules are rejected from the hydrophobic interface at a time when the water molecules at the surface of the resin particles are in a state of high organisation (low entropy). By introducing an organic phase (acetonitrile) the entropy at the surface of the resin particles is increased and makes the hydrophobic interactions between proteins and the surface less favourable. A specific acetonitrile concentration exists at which a particular protein desorbs from the column and reversed phase HPLC exploits this phenomenon to purify proteins. The biologically active fractions from the four Superdex gel filtration runs were pooled, divided into three equal volumes and loaded on to the Deltapak C4 column in three separate purification runs. The acetonitrile gradient (1%/min) was

pumped through the column and fractions of the eluting protein were collected. The fractions were subject to TGF-β determination and the results are shown in Figure 2.4.

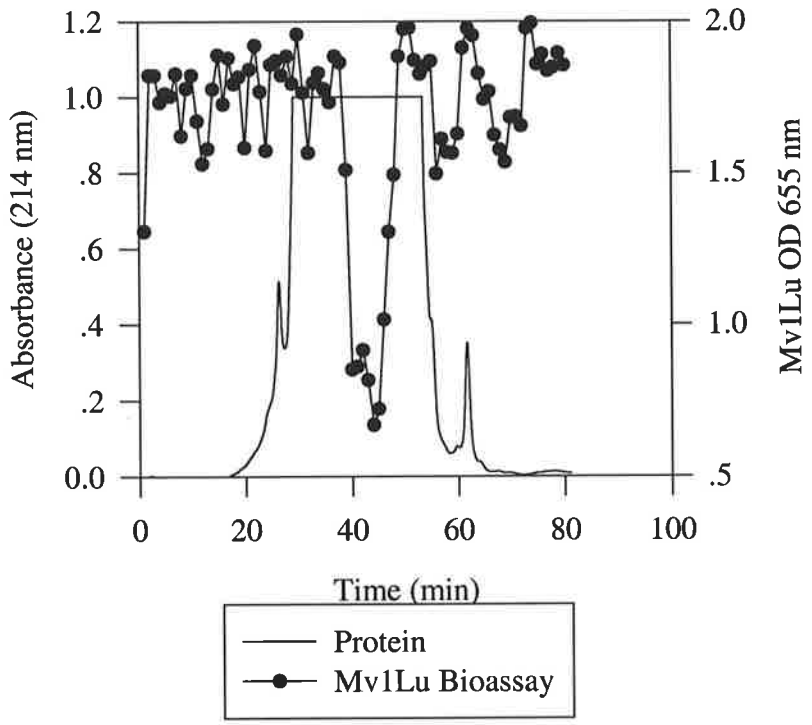

Figure 2.4: Overlay plot of absorbance at 214 nm and Mv1Lu cell growth versus elution volume for the first HPLC step. *Each bioassay point is the mean of duplicate determinations at 1:1000 dilution.*

The biologically active fractions from the three HPLC runs were pooled together and loaded on to the HPLC column again in two separate runs. This time a slower acetonitrile gradient (0.1%/min) was run in order to provide sufficient time for proteins with slightly different hydrophobicities to completely desorb at their critical acetonitrile concentrations. In this way the prevalence of different proteins that co-elute was reduced and the resolution of the separation was increased. For example, the HPLC separation of Figure 2.4 demonstrated a single peak of biological activity but at the slower acetonitrile gradient, two separate peaks of biological activity were resolved (Figure 2.5). The peaks of TGF-β activity were evident at 30-31% and 33-35% acetonitrile from the Mv1Lu bioassay. Previously it was shown that TGF-β activity eluted at 30-31% and 37-38% acetonitrile and that the second peak was TGF-β2 by N-terminal sequencing (Rogers et al., 1996). Presumably the first peak of activity was TGF-β1 (Jin et al., 1991). The corresponding fractions of TGF-β2 activity were pooled.

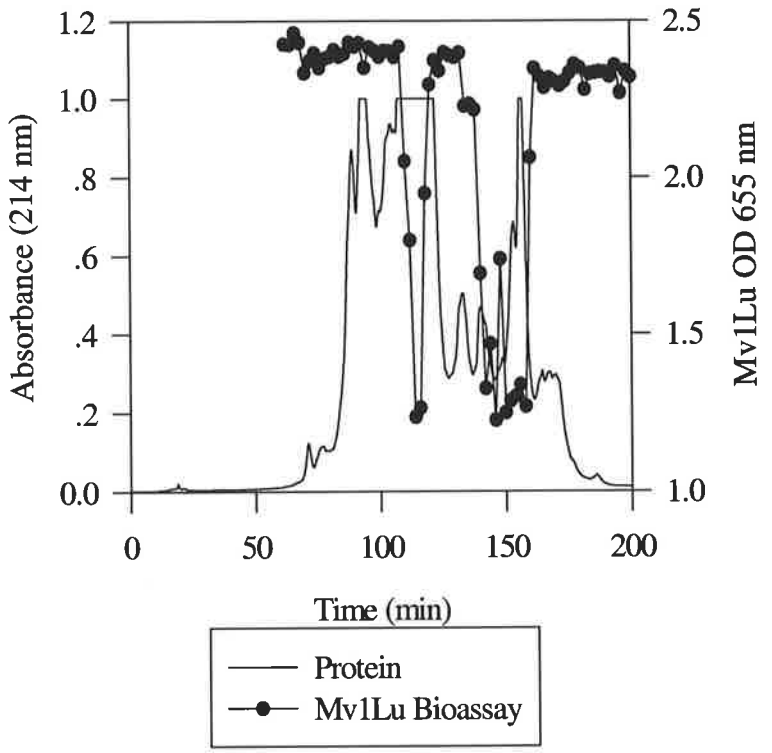

Figure 2.5: Overlay plot of absorbance at 214 nm and Mv1Lu cell growth versus elution volume for the second HPLC step. *Each point is the mean of duplicate bioassay determinations at 1:1000 dilution.*

The TGF-β2 biological activity was loaded on to the HPLC column again and subject to a repeat of the 0.1%/min acetonitrile gradient. The eluting fractions were subject to TGF-β determinations and the results are shown in Figure 2.6. The fractions with TGF-β biological activity were pooled. The pool of material contained 1.08 mg of TGF-β activity and 7.09 mg of protein to give a specific activity of 152000 ng/mg, which compares unfavourably with the previous result of 620000 ng/mg (Rogers et al., 1996). The purified material consisted of proteins of similar molecular size and hydrophobicity to TGF-β2 and therefore additional purification steps that separate proteins on the basis of charge or affinity were required to purify TGF-β2 to homogeneity.

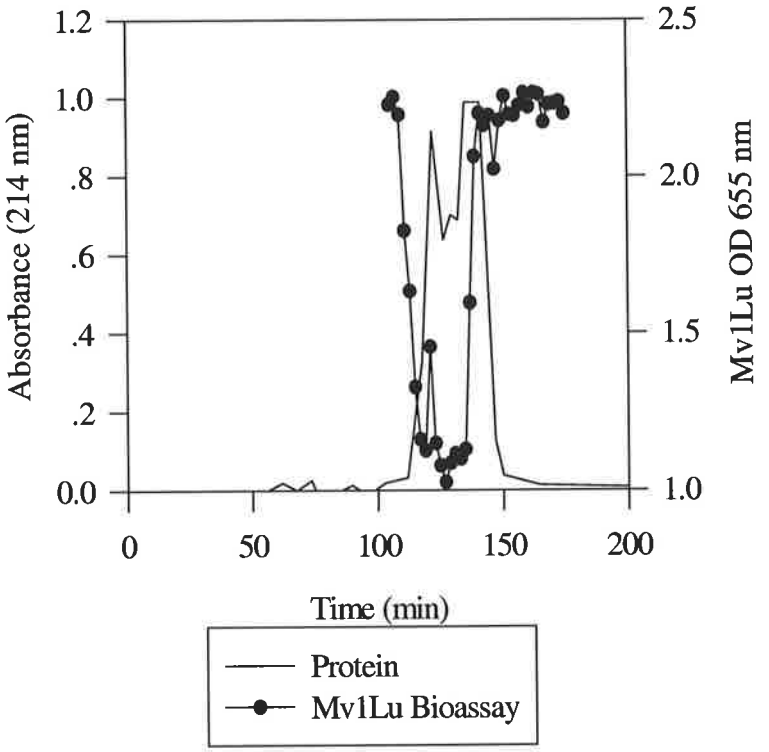

Figure 2.6: Overlay plot of absorbance at 214 nm and Mv1Lu cell growth versus elution volume for the third HPLC step.

The pools of TGF-β activity from each of the purification stages were subject to protein and TGF-β determinations and the results are shown in Table 2.2 for the first purification.

Purification step	Protein (mg)	TGF-β (mg)	Specific activity (ng/mg)
Cellufine	1240	0.915	741
Superdex	621	2.16	3480
HPLC (1%/min)	56.3	0.845	15000
	56.6	2.05	36100
HPLC (0.1%/min)	7.75	0.659	85000
	8.33	0.611	73300
	10.3	0.923	89700
		0.288 (ELISA)	28000 (ELISA)
Repeat HPLC (0.1%/min)	7.09	1.08	152000

Table 2.2: Summary of TGF-β2 purification results for the first TGF-β2 purification. *Mv1Lu bioassay determined TGF-β (TGF-β1 and TGF-β2) concentration, except for those concentrations indicated as having been determined by Quantikine TGF-β2 ELISA.*

Prior to immunising mice, TGF-β2 must be concentrated and formulated in a physiologically compatible solution such as PBS. Therefore the pool was lyophilised on a Dynavac Freeze

Drying Unit and resuspended in PBS. It was determined that 281 μg of TGF-β remained and therefore most of the TGF-β activity was lost through sticking to the glass flask or entrainment with the vacuum.

The preceding purification strategy was repeated twice but without the third HPLC (0.1%/min) step. Summaries of the results for the second and third purifications are shown in Tables 2.3 and 2.4 respectively.

Purification step	Protein (mg)	TGF-β (mg)	Specific activity (ng/mg)
Cellufine	1140	1.22	1080
Superdex	598	2.79	4660
HPLC (1%/min)	45.4	2.25	49400
HPLC (0.1%/min)	11.7 12.6	1.11 6.74 0.575 (ELISA)	94100 528000 49000 (ELISA)

Table 2.3: Summary of TGF-β2 purification results for the second TGF-β2 purification.

Purification step	Protein (mg)	TGF-β (mg)	Specific activity (ng/mg)
Cellufine	609	2.04	3350
Superdex	291	9.36	32200
HPLC (1%/min)	35.8	2.21	65600
HPLC (0.1%/min)	4.68	2.49	531000

Table 2.4: Summary of TGF-β2 purification results for the third TGF-β2 purification.

As for the first pool, the third pool was lyophilised and resuspended in PBS for the immunisation of mice. It was determined that 299 μg of TGF-β remained and again most of the TGF-β activity was lost through freeze-drying.

SDS-PAGE was conducted on the second and third pools to reveal the following bands with silver staining (Figure 2.7). The expected molecular weight of reduced TGF-β2 is 12.5 kDa.

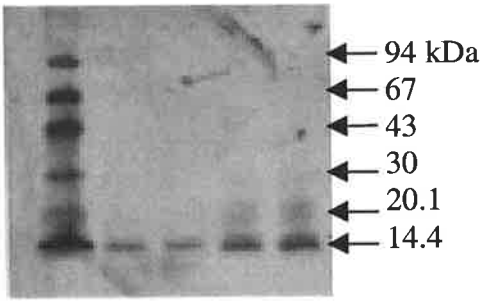

Figure 2.7: SDS-PAGE of pool 2 and pool 3 protein under reducing conditions with silver staining. *The first lane from the left is low molecular weight marker, lanes 2-3 are pool 3 and lanes 4-5 are pool 2.*

The purification strategy described above was conducted three more times but only one HPLC step was performed at 0.1%/min acetonitrile gradient with no 1%/min gradient. A summary of the results is shown in Tables 2.5, 2.6 and 2.7.

Purification step	Protein (mg)	TGF-β (mg)	Specific activity (ng/mg)
Cellufine	813	3.01	3690
HPLC (0.1%/min)	4.07	0.196	48200 (ELISA)

Table 2.5: Summary of TGF-β2 purification results for the fourth TGF-β2 purification. *Determinations of the Superdex pool protein and TGF-β were not performed.*

Purification step	Protein (mg)	TGF-β (mg)	Specific activity (ng/mg)
Cellufine	702	2.37	3380
HPLC (0.1%/min)	3.53	0.156 0.285	44200 (ELISA) 80700

Table 2.6: Summary of TGF-β2 purification results for the fifth TGF-β2 purification.

Purification step	Protein (mg)	TGF-β (mg)	Specific activity (ng/mg)
Unacidified WGFE	13100	0.0807	6.16 (ELISA)
Acidified WGFE	37200	6.60	177 (ELISA)
Cellufine pool before concentration	4250	4.72	1110 (ELISA)
Cellufine pool after concentration	2000	2.24	1120 (ELISA)
Superdex pool	1680	2.62	1560 (ELISA)
HPLC 0.1%/min	39.6	1.86	47100 (ELISA)
		1.77	44800 (Bioassay)

Table 2.7: Summary of TGF-β2 purification results for the sixth purification. *Additional protein and TGF-β2 determinations were performed on unacidified and acidified WGFE and the Cellufine pool after ultrafiltration and lyophilisation.*

It is evident from Table 2.7 that the acidification of WGFE is very effective in dissociating the TGF-β2 latent complex because the active TGF-β2 specific activity increased from 6.16 to 177 ng/mg. This compares with the TGF-β increase of 0.8±0.1 to 42.2±6.8 ng/mg that was reported by Rogers et al. (1996) after acidification. A source of protein loss is the concentration step after Cellufine gel filtration. In the case of the sixth purification, 53% of the protein and TGF-β2 were lost when the Cellufine pool was concentrated by ultrafiltration and freeze-drying. Protein may have been lost in the permeate, the interstitial volume of the membranes or by entrainment in the freeze-drier. It is likely that this protein loss was suffered by all of the purification attempts.

A comparison of the first purification with the purification of Rogers et al. (1996) is shown in Table 2.8. The TGF-β specific activities of the purification steps for the first purification are consistently greater than the specific activities of the Rogers et al. (1996) purification. However, Rogers et al. (1996) obtained much greater resolving power for the second HPLC step (3200 to 620000 ng/mg).

Purification step	Specific activity (ng/mg) (First purification)	Specific activity (ng/mg) (Rogers et al., 1996)
Cellufine pool	741	70
Superdex pool	3480	150
HPLC 1%/min	15000	3200
HPLC 0.1%/min	85000	620000
Repeat HPLC 0.1%/min	152000	-

Table 2.8: Purification of TGF-β from whey reported by Rogers et al. (1996) and compared with the first purification.

There are a number of possible explanations as to why the TGF-β2 purification in this work was not as effective as it was for Rogers et al. (1996). The quality of the whey may have differed for the two cases. For example, the whey of Rogers et al. (1996) may have had less protein, of similar molecular size and hydrophobicity to that of TGF-β2, than the whey in this instance. It is possible that the reversed phase column resolution degraded with age and therefore the purification of Rogers et al. (1996) could not be duplicated. Also the test, for selecting which TGF-β positive fractions to pool, was largely subjective because Rogers et al. (1996) did not publish the extent of Mv1Lu growth inhibition required to distinguish positive from negative fractions.

Generally the best immunogen, with which to immunise mice for the generation of a titre, is homogeneous. Several repetitions of the purification method of Rogers et al. (1996) were performed but none of them yielded homogeneous TGF-β2. Nevertheless, partially purified TGF-β2 was used as an immunogen because authentic anti-TGF-β2 antibody producing hybridomas can theoretically be detected by screening the hybridoma culture medium against commercially available pure TGF-β2. Small amounts of commercially available pure TGF-β2 were required to confirm specificity but only once the hybridoma culture medium had tested positive for the partially purified TGF-β2 preparation. Therefore the TGF-β2 purity for use as an immunogen and ELISA plate-coating antigen is not critical but it does influence the probability of obtaining an anti-TGF-β2 antibody producing hybridoma.

Chapter Three

Generation of Anti-TGF-β2 Monoclonal Antibody

3. Generation of Anti-TGF-β2 Monoclonal Antibody

3.1 Introduction

The development of a commercial-scale immunoaffinity separation process requires gram quantities of antibody. A commercially available anti-TGF-β monoclonal antibody (Genzyme, MA, USA) costs $1000 per mg (1996) and is therefore prohibitively expensive for a commercial-scale process. A hybridoma (1D11.16.8) cell line (Dasch et al., 1989) is commercially available from the American Type Culture Collection (Rockville, MD, USA). However, the monoclonal antibody produced by this hybridoma is not specific for TGF-β2 because it cross-reacts with TGF-β1, which is also a constituent of WGFE. Consequently, a hybridoma cell line was required to produce a monoclonal antibody against TGF-β2.

Dasch et al. (1989) generated monoclonal antibodies against TGF-β2 with conventional hybridoma techniques. A group of female Balb/c mice was injected intraperitoneally with 10 μg of native TGF-β2 purified from bovine bone. The mice were boosted, bled and the serum antibody titres against TGF-β2 were determined. The animal with the highest titre was euthanased and the spleen cells were fused with SP2/0-Ag14 myeloma cells in the presence of polyethylene glycol. The hybridomas were cultured and tested for the production of anti-TGF-β2 monoclonal antibodies. In this way, four monoclonal antibodies against TGF-β2 were obtained. All four antibodies recognised dimeric TGF-β2 in Western blots and were found to immunoprecipitate ^{125}I-TGF-β2. One of the antibodies (1D11.16) was able to neutralise the *in vitro* biological activity of TGF-β1 and TGF-β2 in an IL-1, PHA-dependent thymocyte mitogenic assay. This antibody cross-reacted with TGF-β1 unlike the other three, which were specific for TGF-β2. One of the three other antibodies was coupled to CNBr-activated Sepharose (Pharmacia) and was used to immunoaffinity purify TGF-β2 from partially purified TGF-β2 (10-20 μg/mg protein).

An animal may fail to raise antibodies against an immunogen if the protein is identical or very similar to a self-antigen. The animal avoids responding against itself by acquiring self-tolerance. During the development of self-tolerance B and/or T cells are eliminated if they secrete antibodies against a self-antigen. In this way an immunogen may be ignored by the immune system and fail to raise a titre (Harlow and Lane, 1988). TGF-β2 is highly conserved in mammals and therefore the bovine form is likely to be recognised as self in the mouse. Furthermore, TGF-β2 is a potent immunosuppressant and can inhibit the immune response of

an animal (Palladino et al., 1990; Ding et al., 1990; Gamble and Vadas, 1991). It is therefore surprising that Dasch et al. (1989) were able to raise four monoclonal antibodies using a conventional technique. The fact that it has not been reported again reinforces the difficulty in raising monoclonal antibodies to TGF-β2. As a consequence other methods have been attempted.

Thompson et al. (1999) circumvented these problems by selecting single chain antibody fragments (scFv) specific for TGF-β2 from repertoires displayed on the surface of filamentous bacteriophage. The most potent neutralising scFv antibodies were converted into the human IgG4 format because their intended use was as a therapeutic for the treatment of fibrotic disorders. The IgG4 antibody with the highest affinity was determined to have a dissociation constant of 0.89 nM with the Biacore biosensor and also neutralise (ED_{50} = 2 nM) the anti-proliferative effect of TGF-β2 in a TF1 human erythroleukaemia cell bioassay. This human anti-TGF-β2 antibody is currently undergoing clinical trials for the treatment of proliferative vitreoretinopathy.

Lucas et al. (1991) attempted to produce monoclonal antibodies against TGF-β1 using intraperitoneal and subcutaneous immunisation and conventional fusion procedures but were unsuccessful. Monoclonal antibody producing hybridomas were raised successfully by immunising mice with TGF-β1 using footpad injections and then fusing their draining inguinal and popliteal lymph nodes to the mouse myeloma X63-Ag8.653 cell line.

Flanders et al. (1990) raised polyclonal antibodies to synthetic peptides corresponding to several regions of TGF-β2. The peptides were coupled to ovalbumin with diazotised benzidine or left uncoupled prior to immunisation. The antisera raised to a peptide corresponding to residues 50-75 of TGF-β2, TGF-β2(50-75), had the highest titre against TGF-β2 in ELISA. Figure 3.1 shows the 3-dimensional structure of the TGF-β2 monomer and highlights the structure of sequence 50-75. The antisera were tested for their reactivity with either the native or reduced forms of both TGF-β1 and TGF-β2 in ELISA, Western blots and immunoprecipitation assays. On Western blots, anti-TGF-β2(50-75) specifically detected 5 ng of TGF-β2, while antisera raised to TGF-β2(1-30) and TGF-β2(79-108) cross-reacted with TGF-β1. Anti-TGF-β2(50-75) localised TGF-β2 in murine placenta in immunohistochemical studies. None of the peptide antibodies immunoprecipitated more than

20% of ^{125}I-TGF-β2. However, when the reducing agent, dithiothreitol, was added to the antisera, the reactivity of the antibody decreased but there was an increase in the amount of ^{125}I-TGF-β2 immunoprecipitated by anti-TGF-β2(50-75) and anti-TGF-β2(79-108). Presumably the reducing agent opens the structure of TGF-β2 and makes these regions of the molecule more accessible to the peptide antisera. None of the antisera were as effective at immunoprecipitating ^{125}I-TGF-β2 as antisera raised against native TGF-β2. The anti-peptide antisera were unable to block receptor binding of either ^{125}I-TGF-β1 or ^{125}I-TGF-β2 to normal rat kidney cells.

In view of the successes of these researchers, it was decided that intraperitoneal immunisations and conventional fusion protocols would be used for two immunisation strategies. Firstly, mice would be injected with partially purified TGF-β2 from Chapter 2 in an attempt to raise an immune response. If this method is unsuccessful, mice would be immunised with the synthetic peptide corresponding to the 50-75 sequence, TGF-β2(50-75).

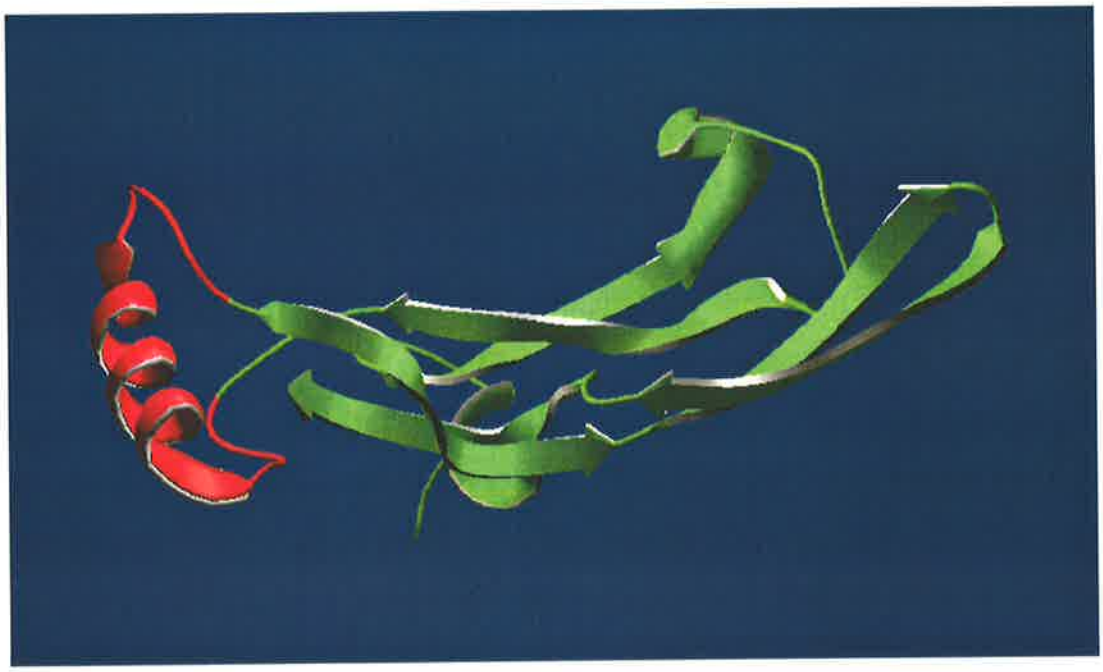

Figure 3.1: The 3-dimensional structure of the TGF-β2 monomer as determined by X-ray crystallography. *The structure (Protein Databank, 1999) was modelled with Swiss PDB Viewer software and TGF-β2(50-75) is shown in red.*

3.2 Materials and General Methodology

Four separate attempts were made to generate monoclonal antibodies against TGF-β2. The following immunogens were employed in each of the attempts:

1. Partially purified TGF-β2 (ppTGF-β2)
2. Highly purified TGF-β2 (hpTGF-β2)
3. Synthetic peptide TGF-β2(50-75) conjugated to ovalbumin
4. Synthetic peptide TGF-β2(50-75) conjugated to diphtheria toxoid

A general methodology is described in the following sections and it was used for each of the attempts, subject to minor modifications. Section 3.3 discusses the modifications to the methodology for each individual attempt.

3.2.1 Immunogens

Five female six-week-old Balb/c mice (IMVS Animal House, Gilles Plains, SA) were housed in the CSIRO Human Nutrition Animal House. The appropriate ethics committees approved all experimental procedures (Ethics Approval numbers: M/46/97 (University of Adelaide), 438 and 534 (CSIRO)). Animals were each immunised with 50-200 µl of immunogen by intraperitoneal injection with a 30 gauge needle. The immunogens used in each attempt are described in the following sections.

- Partially purified TGF-β2

The pool of ppTGF-β2 from the final HPLC step of the third purification (Table 2.1) was lyophilised on a Dynavac Freeze Drying Unit. The lyophilised protein was resuspended in 3 ml of Dulbecco's phosphate buffered saline (DPBS) overnight and 2 ml of protein solution was recovered. On day 161 mouse 9 was immunised with hpTGF-β2 as purified in section 6.3.1. The immunogen was prepared by thawing the immunogen and delivering it to a 10 µg vial of Gerbu adjuvant (Gerbu Biotechnik GmbH, Heidelberg, Germany). The solution was agitated in the vial to resuspend the lyophilised adjuvant (2 µg/mouse). The immunogen was taken into a 1 ml syringe and tapped to dislodge bubbles prior to injection.

- Highly purified TGF-β2

The hpTGF-β2 immunogen was prepared with the methods of section 6.3.1, lyophilised, resuspended in DPBS and mixed with adjuvant (1 μg/mouse). After day 61 the immunogen was mixed with adjuvant (2 μg/mouse). On days 82, 96, 135 and 142 the mice were injected with the ppTGF-β2 pool from the fifth purification (Table 2.6).

- Synthetic peptide TGF-β2(50-75) conjugated to ovalbumin

Synthetic peptide YLWSSDTQHSRVLSLYNTINPEASAS(Y) was supplied by Chiron Technologies (Clayton, Victoria, Australia). The residue (Y) denotes a C-terminal tyrosine that does not correspond to the residue at this position in native TGF-β2. The batch of 5.4 mg was greater than 80% pure by mass spectrometer analysis. The peptide was dissolved in 0.1M Tris-0.15M NaCl pH 8 (TBS) to give a concentration of 4 mg/ml. TBS (5.5 ml) was used to form a 2 mg/ml solution of ovalbumin (gift from the Department of Obstetrics and Gynaecology, University of Adelaide). These solutions were mixed in a small glass beaker. Glutaraldehyde (0.13M) in 2.7 ml of TBS was gradually added to the protein mixture over a period of 20 minutes and stirring was continued for 90 minutes. The reaction mixture was transferred to CelluSep dialysis tubing (Membrane Filtration Products Inc., San Antonio, TX, USA) with a molecular weight cut off of 3500. The solution was dialysed overnight against 4L of TBS at 4°C. The dialysed conjugate was stored in siliconised tubes at -20°C. Conjugated TGF-β2(50-75) was mixed with adjuvant (2 μg/mouse) prior to injection.

- Synthetic peptide TGF-β2(50-75) conjugated to diphtheria toxoid

Chiron Technologies supplied 1.9 mg of TGF-β2(50-75) (purity 95% by HPLC analysis) that was conjugated to 4 mg of diphtheria toxoid by a glutaraldehyde linker. Conjugated TGF-β2(50-75) was mixed with adjuvant (2 μg/mouse) prior to injection. Unconjugated TGF-β2(50-75) (purity 95% by HPLC analysis) was also supplied for the titre detection.

3.2.2 Detection of Anti-TGF-β2 Antibodies by ELISA

Blood was taken from the mice for titre determinations. The mice were anaesthetised with fluothane, the tail was swabbed with ethanol and a small portion of tail was removed. Blood was collected from the wound site and placed in 1.5 ml conical tubes. The mice were monitored for signs of distress after the procedure. The blood samples were allowed to clot and spun in a Hermle Z233M microcentrifuge (Hermle-Labortechnik, Germany) at 12000 g

for five minutes. The serum was collected with a pipette, diluted 1:10 in DPBS and stored frozen at -20°C.

The screening ELISA was conducted as follows. Immunogen was resuspended in 10mM HCl and then further diluted with coating buffer (15mM Na_2CO_3, 35mM $NaHCO_3$ pH 9.6) to a concentration of 1 μg/ml. Half of 3×96 well ELISA plates (Nunc ALS, Roskilde, Denmark) were coated with 100 μl per well of the TGF-β2 solution. One hundred microlitres of coating buffer alone was added to each of the wells in the other halves of the plates. The plates were incubated at 37°C for 3 hours. The plates were washed four times with wash buffer (1.5mM KH_2PO_4, 6.5mM Na_2HPO_4, 0.5M NaCl+0.05% tween 20, pH 7.6) using the Immunowash system (Nunc ALS, Roskilde, Denmark). The plates were blocked by adding 100 μl of 2% (w/v) bovine serum albumin (Sigma, St. Louis, MO, USA) in wash buffer to each well and incubating overnight at 4°C.

The serum from each mouse was diluted approximately 1:400 with DPBS. The serum from a normal mouse was included in each assay as a negative control. Anti-TGF-β1,2,3 monoclonal antibody (Genzyme, MA, USA) was diluted 1:1000 with DPBS and included as a positive control. Seven serial 1 in 2 dilutions were made from each 1:400 dilution with DPBS. Each dilution was delivered to three wells on the coated side and to three wells on the uncoated side with 100 μl per well. The plates were incubated at 37°C for three hours. The plates were washed six times in wash buffer and 100 μl of rabbit anti-mouse immunoglobulin antibody conjugated to horseradish peroxidase (DAKO Corp., CA, USA) diluted 1:2000 in 0.5% BSA in wash buffer was added to each well. The plates were incubated at 37°C for 90 minutes. The plates were washed six times. One hundred microlitres of substrate solution (1 mg/ml o-phenylene diamine (Sigma Chemical Co., St. Louis, MO, USA), 0.03% (v/v) H_2O_2 in 34.7mM citric acid, 67mM Na_2HPO_4, pH 5) was added per well and the plates were incubated at 37°C for 30 minutes. The enzyme reaction was stopped with the addition of 50 μl of 1M H_2SO_4 per well. The optical densities of the wells were measured at 490 nm with a plate reader 450 (Bio-Rad, Hercules, CA, USA). The titre for each dilution was determined by subtracting the optical density of the uncoated wells from the optical density of the TGF-β2 coated wells.

3.2.3 Detection of Anti-TGF-β2 Antibodies by Mv1Lu Bioassay

The Mv1Lu assay was used to determine if neutralising antibodies were present in the mouse sera. The Mv1Lu assay was conducted according to the methods described in section 2.2.1 with the following modifications. Serial 1:2 dilutions of TGF-β2 immunogen were prepared with DMEM+5% FBS in the range of 0.006 to 6 ng/ml TGF-β2. The mouse sera were diluted 1:1000 in DMEM+5% FBS and added to the dilutions of TGF-β2. The Mv1Lu cells were cultured in these dilutions of TGF-β2 and mouse sera. The dose response curves of Mv1Lu cells to dilutions of TGF-β2 alone and TGF-β2+mouse sera were compared.

3.2.4 Hybridoma Production

The methodology employed to generate anti-TGF-β2 antibodies was performed essentially as described in Zola (1987). The mouse, with the highest titre for TGF-β2, was immunised without adjuvant by intraperitoneal injection three days prior to the fusion. A non-immunised donor mouse was killed two days later. The spleen was extracted and it was cleaned of connective tissue. Incisions were made in the spleen before it was placed in a loose Teflon glass homogeniser filled with 10 ml of pre-warmed DPBS+2% FBS. The mixture was gently homogenised until a uniform cell suspension was achieved. The homogeniser contents were transferred to a 50 ml centrifuge tube. The homogeniser was washed with 10 ml of DPBS+2% FBS and it was also transferred to the centrifuge tube. The spleen capsule was removed from the cell suspension. The cell suspension was spun at 90 g for three minutes in a Centaur 2 centrifuge (Sanyo MSE, Leicestershire, U.K.). The supernatant was aspirated from the tube. The cell pellet was resuspended in 10 ml of DPBS+2% FBS and spun again at 90 g for three minutes. The supernatant was aspirated from the tube. The cell pellet was resuspended in 10 ml of DPBS+2% FBS and transferred to a bottle containing 250 ml of DMEM+20% FBS. One ml of cell suspension was delivered to each well of 10×24-well flat-bottomed tissue culture plates (Nunc ALS, Roskilde, Denmark). The plates were incubated at 37°C with an atmosphere of 5% CO_2 and 100% humidity.

The mouse myeloma cell line SP2/0-Ag14 was obtained from the American Type Culture Collection (Rockville, MD, USA). One week prior to the fusion, the myeloma cells were thawed from frozen stocks and grown in DMEM+10% FBS. On the day of the fusion the SP2/0 cells were in exponential phase growth. The SP2/0 cell suspension was transferred to

50 ml centrifuge tubes and was spun at 260 g for five minutes. The supernatant was aspirated. The cell pellets were resuspended in 2×50 ml centrifuge tubes filled with DPBS. The cell suspension was spun again at 260 g for five minutes. The supernatant was aspirated and the cell pellets were resuspended in 10 ml of DMEM without FBS. SP2/0 cells were counted according to the procedure of section 2.2.1. Splenocytes were prepared from the spleen of the immune mouse according to the procedure above and suspended in 10 ml of DMEM without FBS. Small samples of SP2/0 cells and immune splenocytes were reserved for the control wells. The extent of SP2/0 cell proliferation in the control wells provided an indication as to the effectiveness of the HAT selection medium. Blood was taken from the immune mouse upon death and it was screened with ELISA plates that were coated with TGF-β2 to confirm the titre.

Cells were cultured in DMEM with the addition of 20% FBS, 1% penicillin-streptomycin-fungizone solution, 0.02M HEPES and 0.044M $NaHCO_3$. HAT selection medium was prepared by adding 100 μM hypoxanthine, 400 μM aminopterin and 16 μM thymidine (Boehringer Mannheim, Germany) to the standard medium while HT medium was prepared by adding 100 μM hypoxanthine and 16 μM thymidine (Sigma Chemical Co., St. Louis, MO, USA). Approximately equal numbers of splenocytes and SP2/0 cells were combined in a 50 ml centrifuge tube. The suspension was spun at 90 g for three minutes and the supernatant was aspirated from the cell pellet. One ml of polyethylene glycol 1500 (Boehringer Mannheim, Germany) was added to the cell pellet as the timer was started. The contents of the centrifuge tube were gently agitated while the lower half of the tube was immersed in a water bath at 37°C. After one minute the gradual addition of DMEM without FBS was started at the rate of 1 ml per minute and continued for seven minutes. After a total of eight minutes had elapsed, 8 ml of DMEM without FBS was added to the cells. The fused cell suspension was spun at 40 g for ten minutes. The supernatant was aspirated from the cell pellet, which was then resuspended in 250 ml of DMEM+20% FBS+HT. One millilitre of cell suspension was delivered to each well of the spleen conditioned tissue culture plates without prior removal of the spleen cell suspension. Five wells were filled with 1 ml of splenocyte suspension per well and another five wells were filled with 1 ml of SP2/0 cell suspension per well. The 24-well plates were returned to the incubator. On the next day the medium was aspirated from the wells and was replaced with 2 ml of DMEM+20% FBS+HAT per well. The plates were returned to the incubator.

3.2.5 Tissue Culture

Every two weeks after the fusion, the medium was aspirated from the wells and 2 ml of fresh DMEM+20% FBS+HAT was delivered to each well in order to replenish the nutrients. After the conditioned medium was sampled, a pipette was used to agitate the cells in an attempt to detach them from the surface of the wells. The cell suspension was transferred to 25 cm^2 tissue culture flasks filled with fresh DMEM+20% FBS+HAT. When the cells reached confluence in the 25 cm^2 flasks they were transferred to 75 cm^2 flasks and given fresh DMEM+20% FBS+HAT. The cells that did not detach from the well were provided with fresh DMEM+20% FBS+HAT. The hybridomas were maintained in tissue culture until all of the live hybridomas had been screened. Hybridoma cells that tested negative twice to the TGF-β2 preparation were discarded.

The medium from rapidly growing colonies was sampled and screened with ELISA plates that were coated with TGF-β2 immunogen. Anti-TGF-β1,2,3 monoclonal antibody (dilution 1:1000) was included as the positive control and unconditioned medium was included as the negative control. Positive hybridomas were grown in tissue culture flasks and cryopreserved when the cells reached a sufficient number. The flasks were agitated to detach the cells from the surface. The cells were counted to ascertain the cell density before the cell suspension was spun at 90 g for five minutes. The cryopreserving medium was a 10% solution of dimethyl sulfoxide (Sigma, St. Louis, MO, USA) in FBS. The supernatant was collected and the cell pellet was resuspended in cryopreserving solution to obtain a cell density of 10^7 cells/ml. Cryovials (Iwaki, Japan) were filled with 0.5 ml of cell suspension each and then placed between two polystyrene tube racks. The racks were taped shut and left overnight in a -80°C freezer (Hetofrig CL410, Denmark). On the following day the cryovials were transferred to liquid nitrogen tanks for long term storage. At least ten vials of positive primary hybridomas and primary and secondary hybridoma clones were frozen down. The viability of the frozen cells was routinely checked by thawing one vial on the next day and culturing.

3.2.6 Cloning by Limiting Dilution

The positive hybridomas were cloned by diluting and plating the cell suspension in DMEM+20% FBS+HAT at a cell density of one cell per well. Two 96 well plates of each cloned hybridoma were maintained in tissue culture and fresh medium was added to the wells when evaporation had depleted the medium level. The conditioned media from the wells with

live cells were screened against TGF-β2 immunogen. The three most vigorous positive clones for each primary hybridoma were expanded to larger wells with 2 ml of DMEM+20% FBS+HAT each. When the positive clones had grown sufficiently they were subject to a second round of cloning. The three positive clones for each primary hybridoma were then transferred to larger flasks so proliferation could continue for their eventual cryopreservation.

The three most vigorous positive clones for each primary hybridoma were each cloned again into two 96 well plates with DMEM+20% FBS+HAT. The conditioned media from the wells with live cells were screened against TGF-β2 immunogen. The three most vigorous positive secondary clones for each hybridoma were expanded to larger wells with 2 ml of DMEM+20% FBS+HAT. These clones were then transferred to larger flasks so proliferation could continue for their eventual cryopreservation. Upon each expansion DMEM+20% FBS+HAT was replaced with DMEM+20% FBS+HT, then DMEM+10% FBS+HT and then DMEM+10% FBS in order to gradually wean the cells on to the new medium. The conditioned media were screened against TGF-β2 immunogen before cryopreservation to ensure that the secondary clones did not lose their antibody production during the weaning process.

3.2.7 Large Scale Production of Monoclonal Antibody

The CellMax™ artificial capillary cell culture system (Cellco Inc., Germantown, MD, USA) was used for the large scale production of monoclonal antibody from hybridoma cell lines. Figure 3.2 shows a schematic diagram of the CellMax™. The hybridoma cells are inoculated into the module and they reside on the surface of the capillaries. Fresh growth medium is pumped through the capillaries by a peristaltic pump. Glucose and other essential nutrients diffuse through the pores in the capillaries. Cell waste products diffuse through the pores to be carried away by the flow of recirculating growth medium. Oxygen and carbon dioxide exchange is facilitated by a long section of silicone tubing which is permeable to these gases. The system is maintained in an incubator at 37°C in an atmosphere of 5% CO_2 and 100% humidity. This system sustains high numbers of cells within a small volume and consequently the proportion of serum in the growth medium may be reduced without a decrease in metabolic activity. Serum contains proteins that bind to Protein G and their presence in the conditioned medium complicates the purification of monoclonal antibody by Protein G affinity chromatography. Therefore a reduction in serum content improves the quality of the

antibody purification. The CellMax™ Artificial Capillary Module Cellulosic -MPS was chosen because its pore size is such that it excludes the antibody from the lumen of the hollow fibres. In this way, the antibody may be partitioned on the outside of the capillaries and a small volume of conditioned medium of high antibody concentration can be harvested periodically.

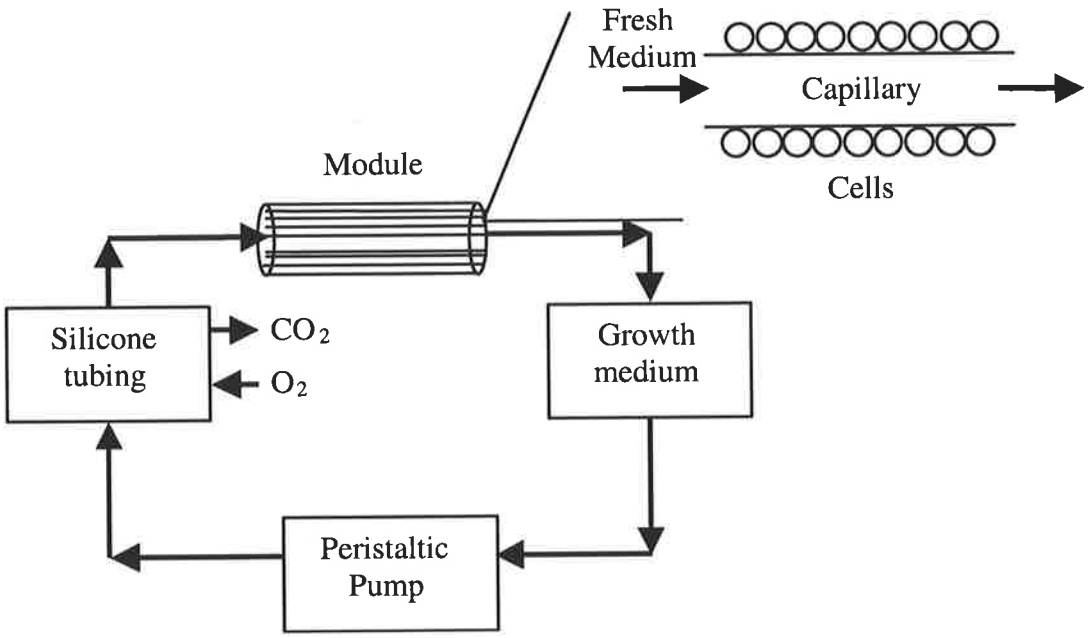

Figure 3.2: Schematic diagram of the CellMax™ Artificial Capillary Module *(adapted from CellMax™ instruction manual).*

The manufacturer's instructions were followed in the use of the CellMax™. Hybridoma cells were cultured in DMEM with the addition of FBS, 1% penicillin-streptomycin-fungizone solution, 0.02M HEPES and 0.044M $NaHCO_3$. The peristaltic pump was set to the high flow rate setting. Every day the glucose concentration in the growth medium was measured using BM-Test Glycemie 20-800 glucose strips (Boehringer Mannheim, Australia) that were read with an Omniscan Blood Glucose Monitor (CXG Systems). When the glucose concentration was determined to have fallen to half of its starting value (25 mM), then the medium was replaced. During the start-up period when glucose consumption was low, the medium was replaced weekly but once the cells reached higher densities, the glucose consumption was such that 500 ml bottles of medium were replaced daily. To encourage the cells to grow during the start-up period 10% FBS was added to the growth medium. Once glucose consumption rose to approximately 500 mg/day, stepwise daily reductions in serum content were made so that the cells were not shocked by a sudden transition (10%, 7.5%, 5%, and

then 2.5%). Glucose consumption dropped dramatically when FBS-deficient DMEM was used as a growth medium. For this reason the proportion of FBS in growth medium was not reduced below 2.5%.

Three times per week the conditioned medium inside the CellMax™ module but external to the capillaries was flushed and collected (5-7 ml). This collected medium was called the first flush. Twenty ml of fresh growth medium was then used to wash the remaining conditioned medium from the module. This was also collected and termed the second flush. The space external to the capillaries was then filled with fresh growth medium. Flushes were performed routinely to collect the conditioned medium, prevent the build-up of toxic cell waste products and determine the cell viability. Samples were taken from the first and second flush and mixed with trypan blue. The dead cells, which absorb the blue stain, and the live cells, which do not absorb, were counted separately with a haemocytometer under a microscope. In this way the percentage cell viability was calculated. If the percentage cell viability for a particular flush was determined to be less than 50% then the flush was spun down at 810 g for five minutes, the supernatant was frozen at -20°C for storage and the cell pellet was discarded. If the percentage cell viability for a flush was determined to be greater than 50% then the flush was spun down at 90 g for five minutes, the supernatant was frozen at -20°C for storage and the cell pellet was resuspended in fresh growth medium and reinoculated into the module. This proved to be an acceptable compromise between ensuring that a dense build-up of dead cells did not hinder the transfer of gases and nutrients between the lumen and the live cells while not removing too many productive cells. The glucose consumption rate and percentage cell viability were good indications as to the health and metabolic activity of the cells. If the glucose consumption rate and percentage cell viability decreased rapidly, the remedial actions were to increase the FBS content of the growth medium or to reinoculate the flush cell pellets back into the module.

3.2.8 Antibody Purification

The affinity adsorbent Prosep-G (Bioprocessing Ltd., Durham, UK) was purchased for the purification of monoclonal antibody from the antibody conditioned medium. A column (Vantage L 11×250, Amicon, Beverly, MA, USA) was packed with 10 ml of Prosep-G affinity adsorbent.

The conditioned media of the first and second flushes were filtered through a 0.45 μm membrane. All flows were delivered at 2 ml/min by an FPLC system. The adsorbent was equilibrated with loading buffer (8.38mM Na_2HPO_4, 1.47mM KH_2PO_4, 2.68mM KCl, 137mM NaCl, 500mM glycine, pH 7.4) until UV absorbance baseline was attained. Regenerating buffer (0.03 M HCl) was pumped through the adsorbent until UV absorbance baseline was attained. Filtered conditioned medium was loaded on to the adsorbent and the flow through was collected. Once the conditioned medium had finished loading, a flow of loading buffer was maintained until UV absorbance baseline was attained. The adsorbent was washed with 0.1M citric acid pH 5 until UV absorbance baseline was attained. Bound antibody was eluted from the adsorbent with a flow of 0.1M citric acid pH 2. Additional bound antibody was eluted from the adsorbent with 0.03M HCl. The antibody elution peaks, corresponding to 0.1M citric acid pH 2 and the 0.03M HCl, were dialysed immediately after collection in separate dialysis tubes against 1L of dialysis buffer (83.8mM Na_2HPO_4, 14.7mM KH_2PO_4, 2.68mM KCl, 137mM NaCl, pH 7.4). After the overnight dialysis at 4°C, the antibody solutions were filtered through 0.22 μm membranes to minimise the chance of microbial contamination.

The original conditioned medium, the column flow through, the material eluting in 0.1M citric acid pH 5, in 0.1M citric acid pH 2 and in 0.03M HCl were screened against the TGF-β2 pool from the sixth purification. Dilutions of these samples (1:10, 1:20, 1:40, 1:80, 1:160 and 1:320) were prepared with DPBS and added to the ELISA plate in duplicate. A sample of bottle growth medium was taken after the cells had depleted the glucose over one day of culture. This sample was included in the screening ELISA and its antibody activity was compared to that of the conditioned medium recovered from the space that was external to the capillaries.

For every antibody purification run the purity of the antibody in the 0.1M citric acid pH 2 and 0.03M HCl fractions was ascertained by running the protein under reducing conditions on a Tricine 10-20% gel (Novex, San Diego, CA, USA) according to the method of section 3.2.10. The protein concentrations of the antibody preparations were determined using the micro BCA protein assay of section 2.2.3. The eluting protein peaks from the Prosep-G purifications were combined into two separate pools for the individual antibodies. The pools were lyophilised with the centrifugal vacuum drier for long-term storage.

Biochemical analysis of the FBS batch used in the growth medium demonstrated that 6% of the total protein was gammaglobulin, of which immunoglobulin is a major constituent (personal communication with John Sharpe, CSL Limited, Parkville, Vic). Bovine immunoglobulin binds to protein G at least as well as murine immunoglobulin (Hermanson et al., 1992) and therefore the potential existed for the monoclonal antibody to be contaminated with bovine immunoglobulin. To determine the extent to which the monoclonal antibody was contaminated, 40 ml of unconditioned DMEM+10% FBS was loaded on to the Prosep-G column and was subject to the same purification procedure as conditioned medium. The amount of protein eluting in 0.1M citric acid pH 2 and 0.03M HCl was determined with the micro BCA protein assay. The approximate purity of the antibody pools was estimated by comparing the amount of protein eluted in this instance with the amount of protein eluted after adsorption from conditioned medium. The eluting protein was electrophoresed on a Tricine 10-20% gel under reducing conditions.

3.2.9 Determination of Antibody Specificity

The possibility existed that antibodies had been generated against contaminants in the partially purified TGF-β2 and therefore they were screened against recombinant human TGF-β2 (Sigma, St. Louis, MO, USA). The amino acid sequences of human TGF-β2 and bovine TGF-β2 are identical (Cox and Burk, 1991; Madisen et al., 1988) and therefore this is a valid method for ascertaining TGF-β2 specificity. ELISA plates were coated with 100 ng/well of rhTGF-β2 and the conditioned media (100 µl/well) of the positive hybridomas were screened against this material. A 1:1000 dilution of anti-TGF-β1,2,3 monoclonal antibody (positive control) and unconditioned growth medium (negative control) were included in the assays. The cross-reactivity of the antibodies with TGF-β1 was also investigated. The amino acid sequences of human TGF-β1 and bovine TGF-β1 are identical (Swiss Protein Sequence Retrieval System, 1999b). An ELISA plate was coated with 100 ng/well of recombinant human TGF-β1 (R and D Systems, Oxon, U.K.). The conditioned media of the hybridomas (100 µl/well) were screened against this material to check for cross-reactivity.

3.2.10 Determination of Antibody Class

A commercially available ELISA kit (Bio-Rad, Hercules, CA, USA) was used to determine the immunoglobulin class of the monoclonal antibodies in conditioned medium. Isotype

specific rabbit polyclonal antibodies against IgG1, IgG2a, IgG2b, IgG3, IgM, IgA, κ chain and λ chain were available from the kit. Three ml of the ppTGF-β2 pool from the sixth purification were dialysed overnight against 1L of 0.01M phosphate buffer pH 7.2 with 0.01% thimerosal. All solutions were prepared with 0.01% thimerosal. The solution was further diluted with the dialysis buffer to 5 μg/ml TGF-β2. One hundred microlitres of the TGF-β2 solution was added to each of 24 wells of an ELISA plate. The plate was covered and incubated at room temperature for one hour. The plate was washed twice with 0.01M phosphate buffer pH 7.2 by incubating for 15 seconds per wash. Three hundred microlitres of 1% BSA in 0.01M phosphate buffer pH 7.2 was added to each well. The incubation continued for 30 minutes at room temperature. The plate was washed three times with 0.01M phosphate buffer pH 7.2 to which 0.05% tween 20 was added. One hundred microlitres of undiluted culture medium from the hybridomas was added to each of eight wells that were coated with ppTGF-β2. Incubation continued for one hour at room temperature. The plate was washed three times with wash buffer (0.01M phosphate, 0.15M NaCl pH 7.2 + 0.05% tween 20). One hundred microlitres of the isotype specific antibodies was added to a well for each sample of hybridoma medium. Incubation continued for one hour at room temperature. The plate was washed five times with wash buffer. Goat anti-rabbit antibody conjugated to horseradish peroxidase was diluted 1:3000 in wash buffer. One hundred microlitres of the conjugate was added to each of the wells. After one hour of incubation at room temperature, the plate was washed four times with wash buffer and an additional time with wash buffer without tween 20. One hundred microlitres of peroxidase substrate was added to each well. After 30 minutes of incubation at room temperature, the colour reaction was stopped with the addition of 100 μl of 2% (w/v) oxalic acid to each well. The optical density of each well was read with a 2550 plate reader (Bio-Rad, Hercules, CA, USA) at a wavelength of 414 nm. The monoclonal antibody isotype was determined with the generation of a coloured product.

3.2.11 Western Immunoblot

TGF-β2 preparations were electrophoresed under reducing or non-reducing conditions and electroblotted to nitrocellulose membranes. The membranes were incubated in the monoclonal antibody and then in an anti-mouse antibody conjugated to peroxidase. The presence of bound antibody was viewed with enhanced chemiluminescence. The details of the procedure are described in the following paragraphs.

Non-reducing loading buffer (40% (v/v) glycerol, 10% (w/v) sodium dodecyl sulfate, 0.04% (w/v) Coomassie blue, 0.2 M Tris, pH 6.8) or reducing loading buffer (as above with the addition of 2% (v/v) β-mercaptoethanol) was added to TGF-β2 preparations in the volume ratio of 1:4. The samples were vortexed and then transferred to a water bath at 80°C for 10 minutes. The samples were pulse spun at 7000 g in the microcentrifuge.

The protein was injected in to the lanes of a Tricine 10-20% gel. [^{14}C] molecular weight calibration markers (Amersham, Little Chalfont, Buckinghamshire, UK) or Mark 12 molecular weight calibration markers (Novex, San Diego, CA, USA) were included for comparison. The gel was run on a SE250 system (Hoefer Scientific Instruments, San Francisco, CA, USA) with an EC-600-90 power supply (EC Apparatus Corporation, USA). The operating conditions were 125V, 80 mA and 90 minutes run time.

The protein bands on the gel were transferred to Hybond C nitrocellulose paper (Amersham Pharmacia Biotech, Little Chalfont, Buckinghamshire, UK) with an Electrotransfer Multiphor 2 electrophoresis system (AMRAD Pharmacia Biotech). The operating conditions were 125V, 86 mA and one hour run time. A discontinuous buffer system was used. Six cards of Whatman paper were soaked in 0.03M Tris pH 10.4 (anode 1), three cards and the nitrocellulose paper were soaked in 0.025M Tris pH 10.4 (anode 2), and nine cards were soaked in 4mM 6-amino-n-hexanoic acid pH 7.6 (cathode). The six anode 1 cards were placed on the bottom graphite surface, followed by three anode 2 cards, the nitrocellulose paper, the Tricine gel, the nine cathode cards and then the top graphite surface. After transfer, the blotted protein bands were visualised by staining the nitrocellulose with Ponceau reagent (Sigma, St. Louis, MO, USA). The MW markers were visible and the staining pattern was scanned (Deskscan II, Hewlett Packard) for future reference.

All incubations were performed for one hour at room temperature on a plate shaker (Ratek Instruments, Borona, Vic). The blotted nitrocellulose paper was blocked overnight in TBS+3% BSA solution. The blocking solution was removed and the paper was briefly washed twice with TBS+0.05% tween 20, followed by a 15 minute and 2×5 minute washes. The nitrocellulose paper was incubated in undiluted conditioned media, purified monoclonal antibody or positive control anti-TGF-β1,2,3 monoclonal antibody diluted 1:1000 in wash buffer. The antibody solutions were removed and the nitrocellulose was washed as previously

described. The nitrocellulose paper was incubated in dilutions of goat anti-mouse immunoglobulin antibody conjugated to horseradish peroxidase (Amersham Pharmacia Biotech). The antibody solutions were again removed and the nitrocellulose was washed as previously described.

The bands were detected by enhanced chemiluminescence (Pierce, Rockford, IL, USA) according to the manufacturer's instructions. The luminescent nitrocellulose was exposed to Hyperfilm (Amersham Pharmacia Biotech) which was developed on a developing machine (AGFA CURIX 60 Type 9462/100/140). The Tricine gel was stained with Coomassie blue for 40 minutes on a plate shaker. The Coomassie blue was removed and the gel was destained with 30% (v/v) methanol, 10% (v/v) acetic acid in water. The gel was incubated in drying solution (5% (v/v) glycerol, 35% (v/v) ethanol in water) for 40 minutes and then placed between two pieces of cellophane and air-dried.

3.2.12 Immunohistochemical Localisation of TGF-β2

Dr. Allison Cowin of the Child Health Research Institute (Adelaide) generously donated slide-mounted sections of human skin. The slides were washed three times with PBS. Monoclonal antibody was prepared by large-scale production in the CellMax™ Artificial Capillary Module and purified from culture medium by Protein G affinity chromatography. Antibody was prepared at dilutions of 50, 10, 5 and 2.5 μg/ml in PBS. Each section of human skin was incubated in 100 μl of antibody dilution for one hour at room temperature. The slides were washed three times with PBS. A 1:200 dilution of biotinylated anti-mouse IgG antibody (Vector Laboratories, CA, USA) in PBS was incubated with the slides for one hour at room temperature. The slides were washed three times with PBS. A 1:300 dilution of streptavidin CY3 conjugate (Sigma, St. Louis, MO, USA) in PBS was incubated with the sections for 40 minutes at room temperature in the dark. The slides were washed four times with PBS. The human skin sections were then observed under a fluorescence microscope (Leica Leitz DMRD) and the images were converted to a digital format with Image ProPlus 4.0 software (Media Cybernetics, Silver Spring, MD, USA). The above staining procedure was repeated by substituting monoclonal antibody with an anti-TGF-β2 rabbit polyclonal antibody (R and D Systems, Oxon, UK) at 1:100 dilution and substituting biotinylated anti-mouse IgG antibody with biotinylated anti-rabbit IgG antibody to serve as a positive control. Two negative control slides were included for which (1) only the biotinylated anti-mouse IgG

antibody was added with no monoclonal antibody incubation and (2) only monoclonal antibody was added with no biotinylated anti-mouse IgG antibody incubation.

Competition experiments were performed to determine whether solution phase TGF-β2 competes with TGF-β2 in the skin for monoclonal antibody. The 50 μg/ml solution of monoclonal antibody in PBS was judged to give the best contrast and intensity for the dilutions investigated. The TGF-β2 pool from the sixth purification was added to monoclonal antibody (50 μg/ml) at dilutions of 0.001, 0.01, 0.1 and 1 μg/ml TGF-β2. The mixture was pre-incubated at room temperature for one hour before being added to the skin sections. The skin sections were then subject to the same procedure of incubations as described above.

3.3 Results and Discussion

3.3.1 Immunisation with WGFE-Derived TGF-β2

Mice were immunised with TGF-β2 that had been partially purified from WGFE in an attempt to raise a titre against the native molecule. Five mice were immunised according to the schedule in Table 3.1 with partially purified TGF-β2 (ppTGF-β2) pool from the third purification (Table 2.2) and highly purified TGF-β2 (hpTGF-β2) as purified in section 6.3.1.

Time (day)	Activity
0	Injected four mice with 4.0 μg of ppTGF-β2 and one mouse with 6.4 μg.
14	Injected three mice with 6.4 μg of ppTGF-β2 and two mice with 3.2 μg.
29	Injected three mice with 6.4 μg of ppTGF-β2 and two mice with 4.8 μg.
63	Injected five mice with 5.6 μg of ppTGF-β2 each.
72	Mice were bled and serum was screened against hpTGF-β2.
149	Injected two mice with 6.4 μg of ppTGF-β2, two mice with 4.8 μg and one mouse with 3.2 μg.
161	Injected immune mouse with 9.8 μg of hpTGF-β2 without adjuvant.
163	Plated a spleen cell feeder layer with the spleen of a non-immune mouse.
164	Fusions between immune mouse splenocytes and SP2/0 cells.

Table 3.1: Timetable for immunising mice with WGFE-Derived TGF-β2.

The day 72 mouse sera were screened against hpTGF-β2 with an ELISA detection system as shown in Figure 3.3. The ability of the mouse sera to inhibit the biological activity of TGF-β2 in a Mv1Lu assay was investigated (Figure 3.4). The TGF-β2 dilution corresponding to half-maximal response, ED_{50}, was $1:3.42\times10^5$ in the absence of serum. The addition of mouse 9 serum to the dose response increased the ED_{50} to $1:1.29\times10^5$ by presumably blocking the type II receptor-binding site of TGF-β2. However, the addition of sera from the other mice did not significantly affect the ED_{50} at a 5% level of significance. The neutralisation of TGF-β2 biological activity is evidence that the immune response of mouse 9 was specific for TGF-β2.

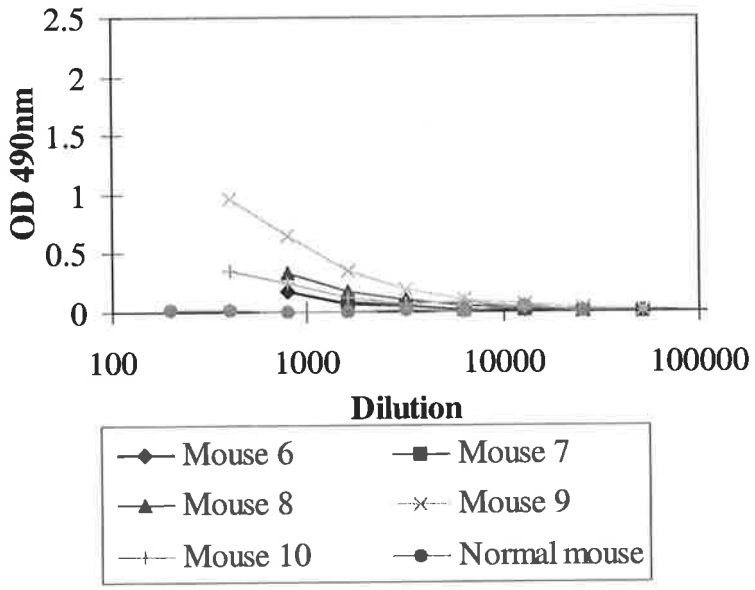

Figure 3.3: Screening ELISA results of mouse sera against hpTGF-β2 on day 72. *Each data point is the average of triplicate determinations of the optical density (490 nm) for TGF-β2 coated wells less the optical density (490 nm) for uncoated wells. These values are displayed as a function of serum dilution and are plotted on the same scale for comparison.*

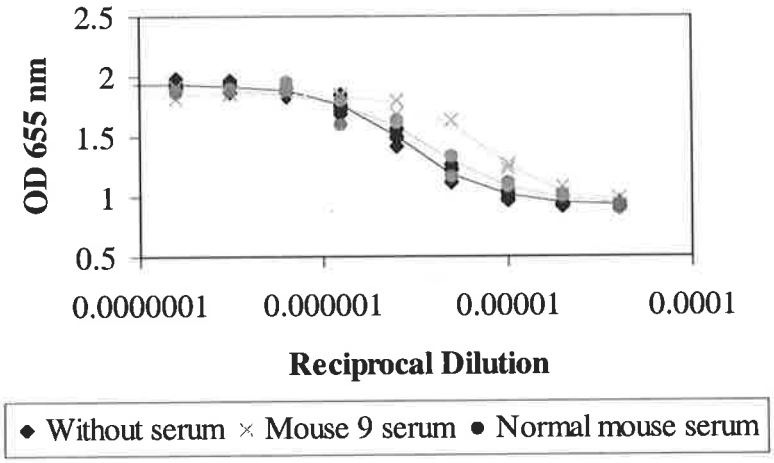

Figure 3.4: Neutralisation of TGF-β2 biological activity in a Mv1Lu assay by the addition of mouse serum.

Although not a particularly high titre, the response of mouse 9 was considered sufficient to justify a fusion. Three days prior to the fusion, mouse 9 was given an intraperitoneal injection of 9.8 μg hpTGF-β2. Blood was taken from mouse 9 upon death on day 164 and the serum was again screened against hpTGF-β2 (Figure 3.5). The titre of mouse 9 had increased since day 72 and was therefore a suitable candidate for fusion.

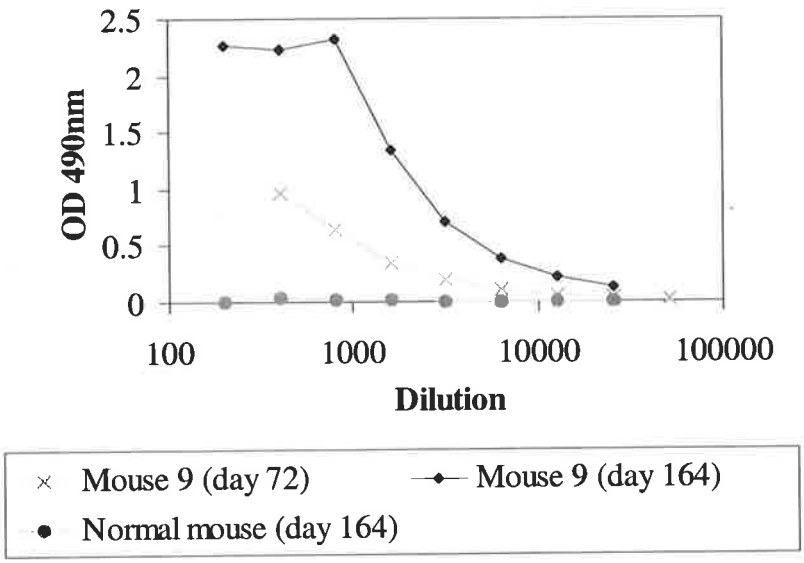

Figure 3.5: Screening ELISA results of mouse 9 serum against TGF-β2 on days 72 and 164.

The fusion between mouse 9 splenocytes and SP2/0 cells, yielded 44 colonies. The conditioned medium from 36 wells was screened but none tested positive. The fusion failed

to yield a hybridoma that secreted anti-TGF-β2 antibody because either the number of anti-TGF-β2 antibody secreting B lymphocytes in the immune spleen was insufficient or the number of fused cells was too low.

Five different mice were immunised according to the schedule in Table 3.2 with ppTGF-β2 from the final HPLC step of the fifth purification (Table 2.6) and hpTGF-β2 as purified in 6.3.1.

Time (day)	Activity
0	Injected five mice with 9 μg of hpTGF-β2.
18	Injected five mice with 10 μg of hpTGF-β2.
28	Mice were bled and serum was screened against hpTGF-β2.
47	Injected five mice with 10 μg of hpTGF-β2.
61	Injected five mice with 10 μg of hpTGF-β2.
76	Mice were bled and serum was screened against hpTGF-β2.
82	Injected five mice with 52.4 μg of ppTGF-β2.
96	Injected five mice with 73.1 μg of ppTGF-β2.
110	Mice were bled and serum was screened against ppTGF-β2.
135	Injected immune mouse in the tail vein with 10 μg of ppTGF-β2 without adjuvant.
142	Injected immune mouse intraperitoneally with 10 μg of ppTGF-β2 without adjuvant.
144	Plated a spleen cell feeder layer with the spleen of a non-immune mouse.
145	Fusions between immune mouse splenocytes and SP2/0 cells.

Table 3.2: Timetable for the second attempt at immunising mice with WGFE-Derived TGF-β2.

The sera from bleeds on days 28, 76 and 110 were screened against TGF-β2 in the ELISA format. No significant titres were measured on days 28 and 76 and therefore hpTGF-β2 had failed to raise a titre according to the method of Dasch et al. (1989). It was thought that titres had not been elicited because of the small amounts of TGF-β2 used for immunisation. The purification of hpTGF-β2 was a very time consuming process that resulted in a small yield. Larger amounts of ppTGF-β2 were available and, despite the potential for titres to be raised against contaminants, were used for the immunisations. On day 110 all of the mice showed titres for ppTGF-β2 (Figure 3.6) with mouse 13 displaying the highest. However, the mouse sera (day 110) did not inhibit the biological activity of TGF-β2 in the Mv1Lu assay at a dilution of 1:1000 and did not confirm that the titre was TGF-β2 specific. By comparison,

mouse 9 serum inhibited TGF-β2 biological activity in this assay at a dilution of 1:470. Although the titre of mouse 13 was not particularly high and its specificity was doubtful, it was considered as sufficient evidence to justify another attempt at a fusion.

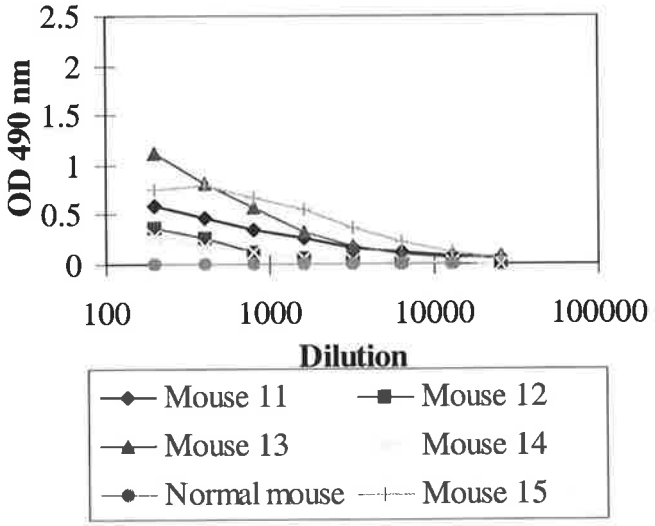

Figure 3.6: Screening ELISA results of mouse sera against TGF-β2 on day 110.

3.3.2 Generation of Cell Line 9B1-1D9-1C4

Ten days prior to the fusion, mouse 13 was given an intravenous injection of 10 μg ppTGF-β2 and then boosted a week later with an intraperitoneal injection of 10 μg ppTGF-β2. The fusion between mouse 13 splenocytes and SP2/0 cells, yielded 230 colonies. The conditioned media from 60 wells tested negative only once and the conditioned media from 70 wells tested negative more than twice. Five wells initially tested positive but later tested negative. One well (9B1) tested positive and was cloned twice by limiting dilution (Figure 3.7).

A commercially available ELISA was used to determine the immunoglobulin class of the monoclonal antibody. Hybridoma 9B1 was determined to produce an antibody of isotype IgG1 that possesses κ light chains. No reaction was observed for the remaining IgG subclasses tested nor the IgA or IgM isotype specific antibodies.

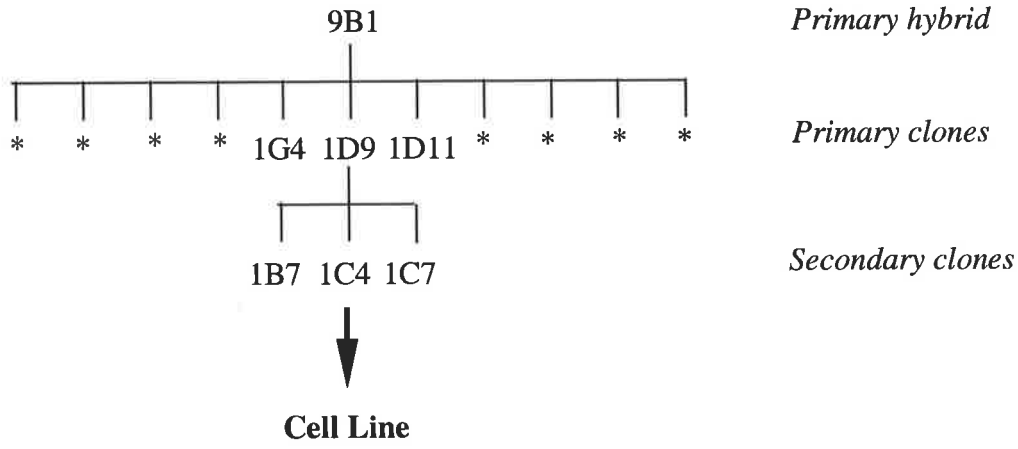

Figure 3.7: Summary of the cloning history of the 9B1 hybridoma cell line. *From the first round of cloning eleven colonies were identified to be positive for binding to TGF-β2. From the second round of cloning three positive clones were identified. The 1C4 secondary clone was established as the cell line. The probability that cell line 9B1-1D9-1C4 is monoclonal was calculated to be 99.7% by the statistical analysis of Coller and Coller (1983).*

The immune response of mouse 13 was generated against an impure TGF-β2 preparation and the titres were determined with the same preparation. Therefore the possibility existed that a monoclonal antibody against a contaminant had been generated. To check for this an ELISA plate was coated with commercially available recombinant human TGF-β2 that was 95% pure. The conditioned medium of 9B1-1D9-1C4 was screened against this material. The ELISA included a 1:1000 dilution of anti-TGF-β1,2,3 monoclonal antibody as a positive control and a negative control (unconditioned growth medium). The results of the ELISA are shown in Figure 3.8.

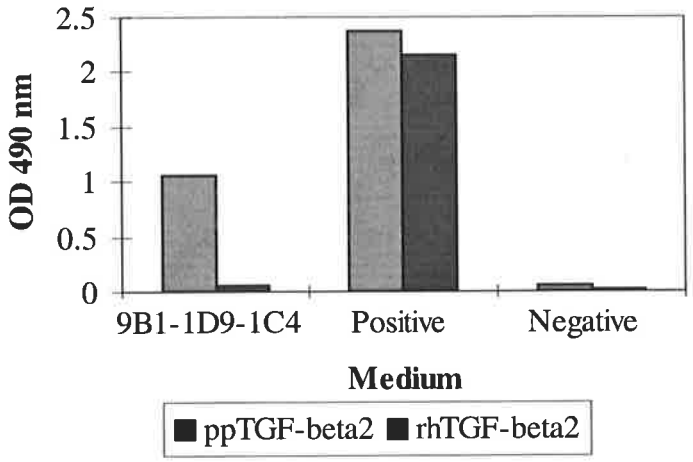

Figure 3.8: Screening of Hybridoma 9B1 Conditioned Medium against TGF-β2. *ELISA plates were coated with the TGF-β2 pool from the sixth purification (specific activity 47100 ng/mg TGF-β2) and rhTGF-β2. Conditioned medium from 9B1-1D9-1C4, a 1:1000 dilution of anti-TGF-β1,2,3 monoclonal antibody and unconditioned medium were screened against these TGF-β2 preparations.*

The antibody of 9B1-1D9-1C4 does not bind to rhTGF-β2 whereas the control anti-TGF-β1,2,3 monoclonal antibody binds strongly. Therefore the antibody of 9B1-1D9-1C4 is not specific for TGF-β2 but is rather specific for a contaminant in ppTGF-β2. The conditioned medium of 9B1 was used to probe a nitrocellulose membrane blotted with ppTGF-β2 to determine the molecular weight of the contaminant to which the antibody binds (Figure 3.9). ppTGF-β2 pool was run on a Tricine gel under non-reducing conditions and electroblotted on to nitrocellulose paper at 1.55 μg TGF-β2 per lane. The conditioned medium of 9B1 was concentrated two times by drying on a centrifugal vacuum drier. The blotted protein was probed with anti-TGF-β1,2,3 antibody (1 μg/ml) or conditioned medium for 20 hours. The blotted protein was then incubated with peroxidase conjugated anti-mouse antibody (1:800) for 20 hours and viewed with enhanced chemiluminescence.

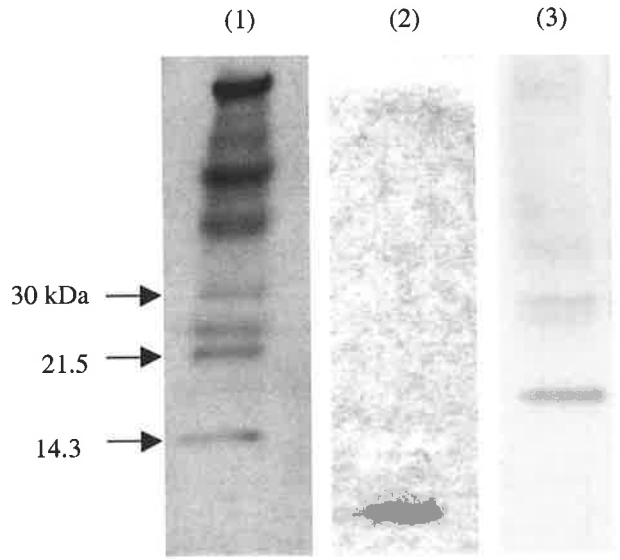

Figure 3.9:Western Immunoblots of TGF-β2. *Comparison of the western immunoblots of ppTGF-β2 (1.55 μg/lane) probed with conditioned medium from hybridoma 9B1-1D9-1C4 (2) and 1:1000 anti-TGF-β1,2,3 monoclonal antibody (3). The stained Tricine gel is included to show the [^{14}C] molecular weight markers (1).*

When blotted ppTGF-β2 was probed with antibody 9B1-1D9-1C4, the immunoblot revealed a band at a molecular weight of approximately 10 kDa. This confirms that the antibody of 9B1-1D9-1C4 is specific for a contaminant of lower molecular weight than TGF-β2 or a fragment of TGF-β2.

The immunisation of mice with native TGF-β2 was not successful in raising a monoclonal antibody against TGF-β2. Presumably this is due to the immunosuppressive and highly conserved natures of TGF-β2 as noted by Thompson et al. (1999). Animals occasionally fail to respond to a given molecule because the appropriate B and/or T cells have been eliminated during the development of self-tolerance. Therefore the injection of a molecule that is identical or very similar to a host molecule can not stimulate an immune response. Lucas et al. (1991) immunised a variety of animals (rabbits, goats, turkeys and guinea pigs) by several immunisation procedures, including alum-precipitated TGF-β1 or TGF-β1 in detox adjuvant or Freund's adjuvant. They reported that most animals produced titres against TGF-β1 but the

titres were not very high or sustained for long. Therefore TGF-β isoforms are not highly immunogenic polypeptides.

3.3.3 Immunisation with TGF-β2(50-75)

In view of the difficulties experienced in raising a titre against native TGF-β2 an alternative immunogen was used. Flanders et al. (1990) reported that immunisation with the synthetic peptide corresponding to amino acid residues 50-75 of the native molecule, TGF-β2(50-75), raised a specific titre for native TGF-β2.

Five new mice were immunised according to the schedule in Table 3.3 with TGF-β2(50-75) conjugated to ovalbumin.

Time (day)	Activity
0	Injected five mice with 90 μg of peptide each.
28	Injected four mice with 80 μg and one mouse with 45 μg.
52	Mice were bled and serum was screened against ppTGF-β2.
112	Injected three mice with 90 μg and one mouse with 45 μg.
126	Injected four mice with 70 μg.
141	Injected four mice with 90 μg.
175	Injected four mice with 90 μg.
184	Mice were bled and serum was screened against ppTGF-β2.

Table 3.3: Timetable for immunising mice with TGF-β2(50-75) conjugated to ovalbumin.

The sera from bleeds on days 52 and 184 were screened against the ppTGF-β2 pool from the third purification. None of the mice demonstrated significant titres for ppTGF-β2. The sera were also screened against ovalbumin to investigate whether the immunisation procedure and the general ELISA method were valid. Some of the mice showed very high titres against ovalbumin (Figure 3.10) but this was expected because ovalbumin is highly immunogenic in mammals. Therefore the immunisation procedure and the general ELISA method were valid.

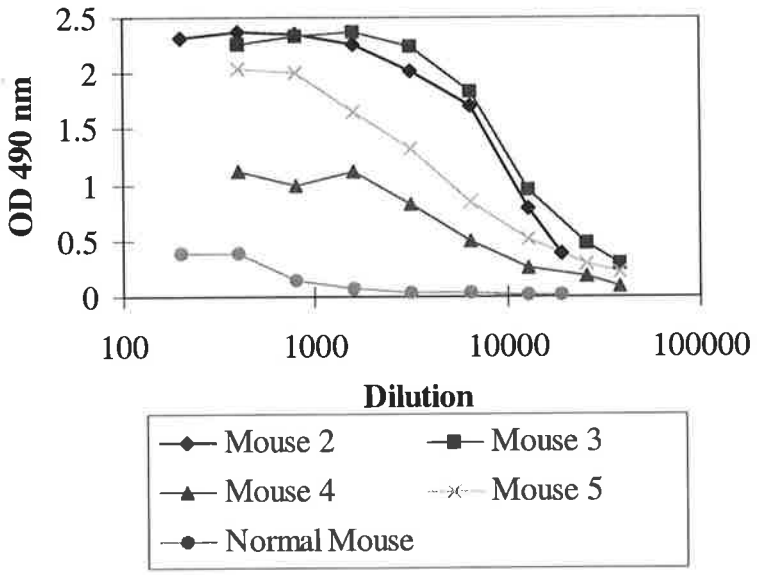

Figure 3.10: Screening ELISA of mouse serum against ovalbumin on day 112.

Immunisation with TGF-β2(50-75) conjugated to ovalbumin failed to elicit a significant titre as determined by screening sera against ppTGF-β2 in an ELISA format. By comparison, Flanders et al. (1990) raised polyclonal antisera against TGF-β2 by immunising rabbits with TGF-β2(50-75) that had been coupled to ovalbumin with diazotised benzidine. Possible reasons why a titre against ppTGF-β2 was not detected in this case are discussed in the following section.

The method of immunisation and the general ELISA method were validated because a high serum titre to ovalbumin was demonstrated so alternative explanations must be sought. There is a possibility that covalently coupling TGF-β2(50-75) to ovalbumin with glutaraldehyde links the peptide to the carrier in an orientation that does not present an immunogenic epitope. Glutaraldehyde reacts covalently with the amine group at the N-terminal of TGF-β2(50-75) and cross-links it to lysine residues of ovalbumin. Flanders et al. (1990) synthesised TGF-β2(50-75) with terminal tyrosines to enable coupling to ovalbumin via a diazonium linkage. This procedure was thought to anchor both ends of the peptide and make the structure of TGF-β2(50-75) more like the corresponding region of TGF-β2. In addition, the immunogenicity of TGF-β2(50-75) may not have been as great in mice as in rabbits. After TGF-β2(50-75) had been coupled to ovalbumin with glutaraldehyde no experiment was performed to confirm that the coupling reaction had actually occurred. If the coupling reaction had not taken place, unconjugated TGF-β2(50-75) was of sufficiently small

molecular size (MW 3103) to have diffused through the pores of the dialysis tubing (molecular weight cut off 3500) during the dialysis. In this way the peptide may have been lost. However, this is unlikely because a well-established procedure was used.

The next TGF-β2(50-75) immunisation attempt used a different carrier protein, diphtheria toxoid, to raise a titre against TGF-β2. Five new mice were immunised with this material according to the schedule in Table 3.4.

Time (day)	Activity
0	Injected five mice with 78.3 μg of peptide each.
14	Injected mice with 78.3 μg.
28	Injected mice with 78.3 μg.
43	Injected mice with 78.3 μg.
57	Mice were bled and serum was screened against ppTGF-β2.
176	Injected immune mouse with 18.9 μg.
192	Immune mouse was bled and serum was screened against peptide.
195	Immune mouse was bled and serum was screened against ppTGF-β2.
202	Injected immune mouse with 18.9 μg.
204	Plated a spleen cell feeder layer with the spleen of a non-immune mouse.
205	Fusions between immune mouse splenocytes and SP2/0 cells.

Table 3.4: Timetable for immunising mice with TGF-β2(50-75) conjugated to diphtheria toxoid.

Day 57 sera were screened against unconjugated TGF-β2(50-75) in an ELISA format (Figure 3.11). Mouse 16 demonstrated a high titre against unconjugated TGF-β2(50-75) unlike the other mice, which did not demonstrate a response above that of the normal mouse. It was then necessary to confirm that TGF-β2(50-75) was an effective mimic for the epitope of native TGF-β2. Mouse 16 serum was screened against the ppTGF-β2 pool from the fifth purification and a significant titre was observed (Figure 3.12). It was therefore highly likely that the titre was specific for TGF-β2.

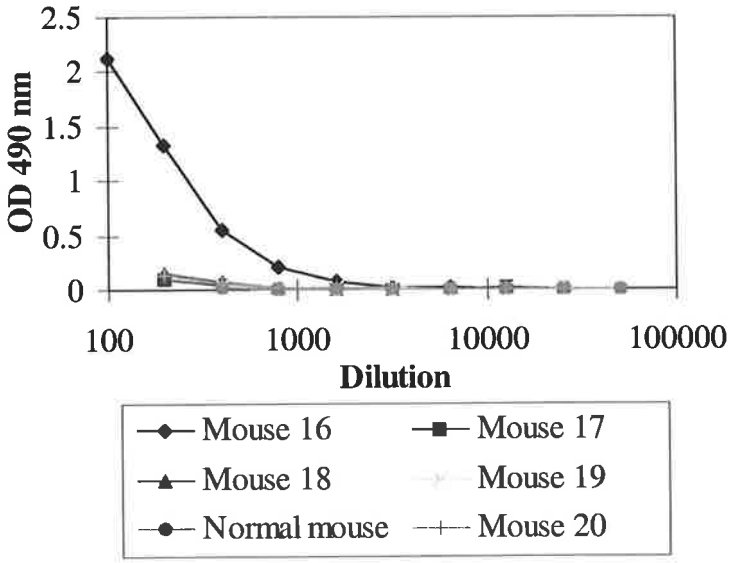

Figure 3.11: Screening ELISA results of mouse sera against unconjugated TGF-β2(50-75) on day 57.

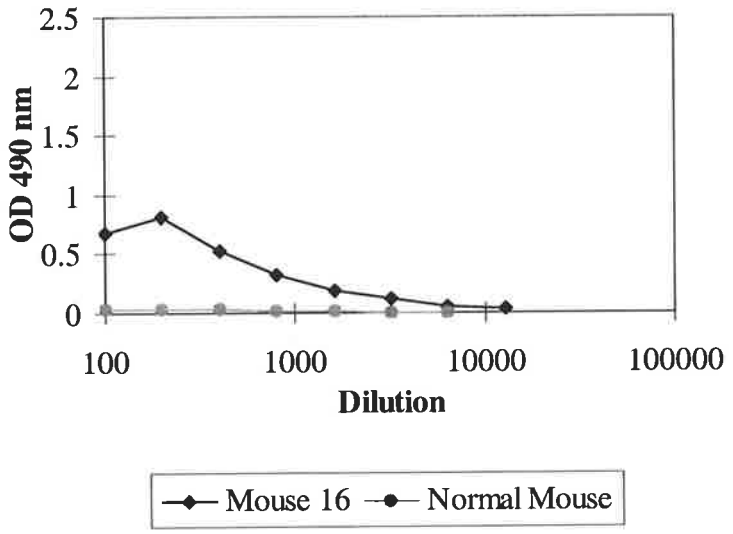

Figure 3.12: Screening ELISA results of mouse 16 serum against ppTGF-β2 on day 57.

A delay of 119 days followed while the hybridoma tissue culture of cell line 9B1 was performed. Mouse 16 was then immunised with 18.9 μg of TGF-β2(50-75) conjugate and 4 μg of adjuvant. The immune mouse was bled sixteen days later and its serum was screened against rhTGF-β2 and unconjugated TGF-β2(50-75) (Figure 3.13). Mouse 16 was bled again three days later and its serum was screened against the ppTGF-β2 pool from the sixth purification (Figure 3.14). Significant titres were observed against all of these

preparations, thereby confirming that the titre was specific for TGF-β2 and that ppTGF-β2 was a valid screening antigen.

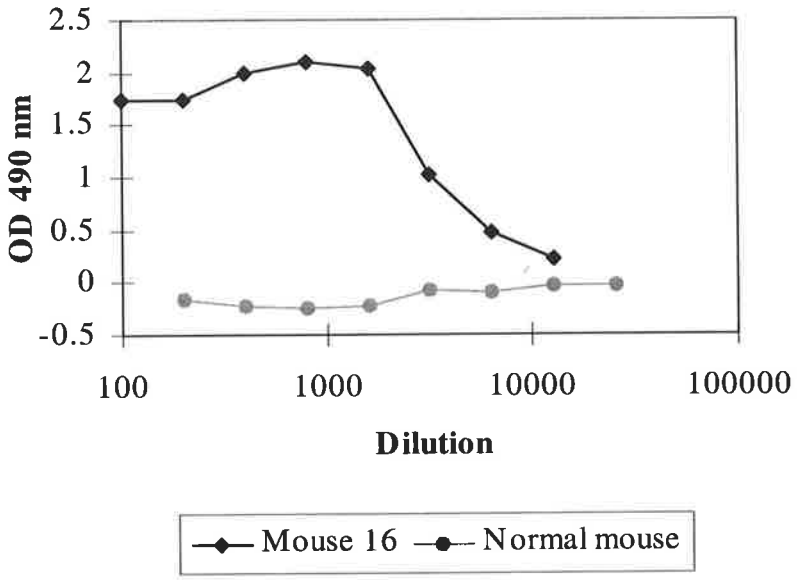

Figure 3.13: Screening ELISA results of mouse 16 serum against unconjugated TGF-β2(50-75) on day 192.

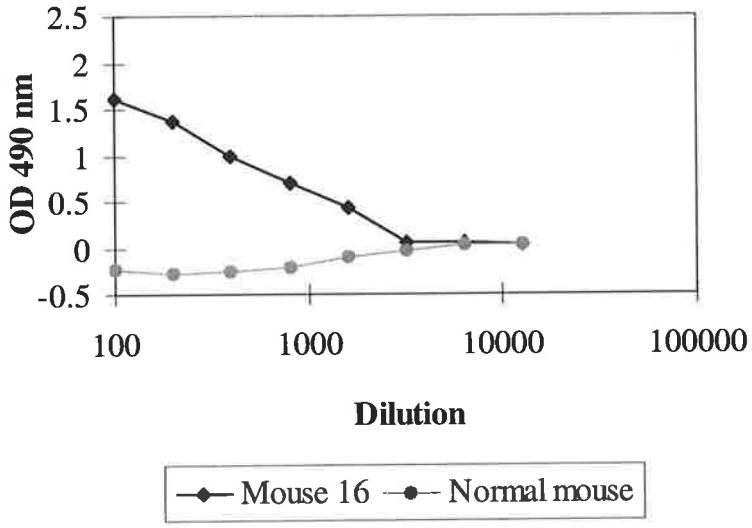

Figure 3.14: Screening ELISA results of mouse 16 serum against ppTGF-β2 on day 195.

3.3.4 Generation of Cell Lines 5D4-1D9-A7 and 8A3-1G3-E9

Three days prior to the fusion, mouse 16 was given an intraperitoneal injection of 18.9 μg TGF-β2(50-75) conjugate without adjuvant. After the fusion, colonies were observed in 47 wells and the conditioned media were screened against the ppTGF-β2 pool from the sixth

purification. One well (4B5) tested positive but later tested negative. Fazekas de St. Groth and Scheidegger (1980) have previously noted this eventual loss of antibody production with SP2/0 derived hybridomas. Two wells (5D4 and 8A3) tested positive and were cloned twice by limiting dilution. A summary of the cloning histories of hybridomas 5D4 and 8A3 are presented in Figures 3.15 and 3.16 respectively.

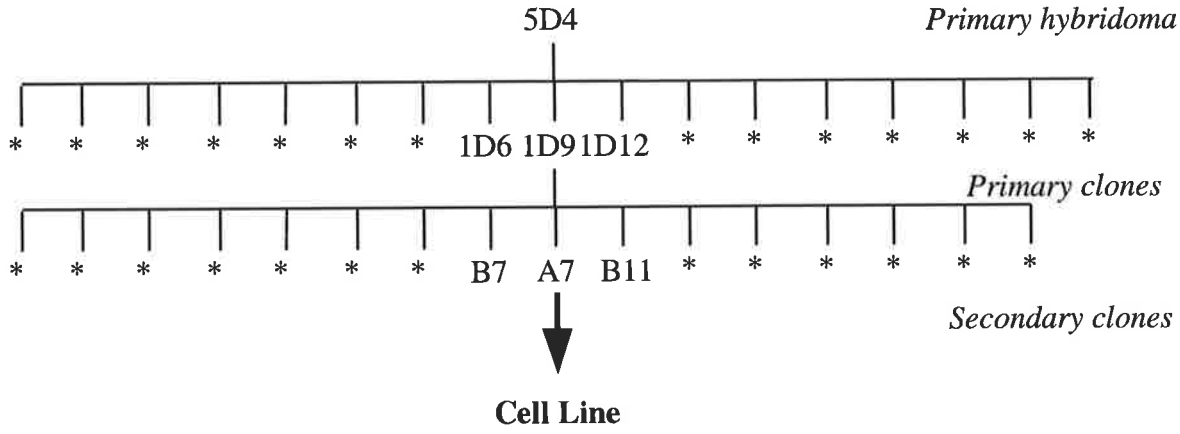

Figure 3.15: Cloning of the 5D4 primary hybridoma. *From the first round of cloning seventeen colonies were identified to be ppTGF-β2 positive. From the second round of cloning sixteen positive clones were identified. The secondary clone 5D4-1D9-A7 was established as a cell line. The probability that cell line 5D4-1D12-A7 is monoclonal was calculated to be 98.5% by the statistical analysis of Coller and Coller (1983).*

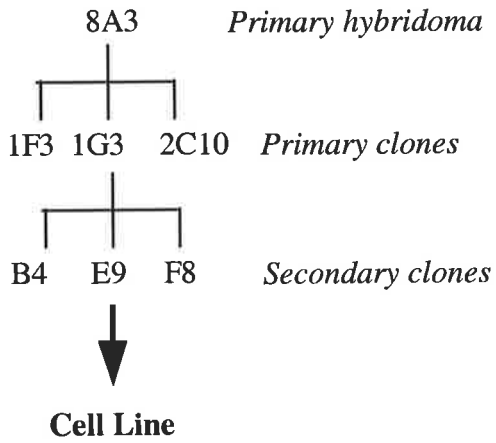

Figure 3.16: Cloning of the 8A3 primary hybridoma. *From the first round of cloning three colonies were identified to be ppTGF-β2 positive. From the second round of cloning three positive clones were identified. The secondary clone 8A3-1G3-E9 was established as a cell line. The probability that cell line 8A3-1G3-E9 is monoclonal was calculated to be 99.9% by the statistical analysis of Coller and Coller (1983).*

A commercially available ELISA was used to determine the immunoglobulin class of the monoclonal antibodies. Hybridomas 5D4 and 8A3 were determined to produce antibodies of isotype IgG1 that possess κ light chains. No reaction was observed for the remaining IgG subclasses tested nor the IgA or IgM isotype specific antibodies.

The possibility existed that the generated monoclonal antibodies were specific for both the unconjugated TGF-β2(50-75) and a contaminant in the ppTGF-β2 pool. To check for this, an ELISA plate was coated with recombinant human TGF-β2 and the conditioned media of hybridomas 4B5, 5D4 and 8A3 were screened against this material. The assay included a 1:1000 dilution of anti-TGF-β1,2,3 monoclonal antibody as a positive control and a negative control (unconditioned growth medium).

Figure 3.17 compares the sequences of TGF-β2 and TGF-β1 in the 50-75 residues region. The sequences of TGF-β1(50-75) and TGF-β2(50-75) are 65% homologous and therefore the potential for cross-reactivity between the generated antibodies and bovine TGF-β1 existed.

TGF-β2 Y **L** W S **S** D T Q **H** S **R** V L **S** L Y N **T** **I** N P **E** A S A **S**

TGF-β1 Y **I** W S **L** D T Q **Y** S **K** V L **A** L Y N **Q** **H** N P **G** A S A **A**

Figure 3.17: Comparison of TGF-β1 and TGF-β2 in the 50-75 residues region *(Swiss Protein Sequence Retrieval System, 1999b). The residue differences between sequences are shown in bold.*

The amino acid sequences of human TGF-β1 and bovine TGF-β1 are identical (Swiss Protein Sequence Retrieval System, 1999b). To check for cross-reactivity, an ELISA plate was coated with recombinant human TGF-β1 (R and D Systems, Oxon, U.K.) and the conditioned media were screened against this material. The assay included a 1:1000 dilution of anti-TGF-β1,2,3 monoclonal antibody as a positive control and a negative control (unconditioned growth medium). Figure 3.18 shows the reactivities of the conditioned media against unconjugated TGF-β2(50-75), ppTGF-β2, rhTGF-β2 and rhTGF-β1.

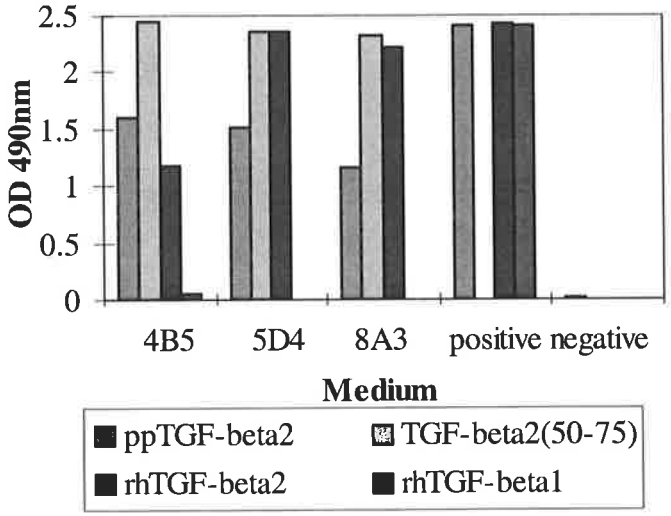

Figure 3.18: Screening of Hybridoma Conditioned Media against TGF-β. *The specificity of the monoclonal antibodies was investigated by screening the conditioned media of hybridomas 4B5, 5D4 and 8A3, 1:1000 dilution of anti-TGF-β1,2,3 monoclonal antibody (positive control) and unconditioned medium (negative control) against ppTGF-β2, rhTGF-β2, unconjugated TGF-β2(50-75) and rhTGF-β1.*

Figure 3.18 shows that the monoclonal antibodies derived from hybridomas 4B5, 5D4 and 8A3 are specific for TGF-β2 and that they display no cross-reactivity with TGF-β1. The positive control antibody (anti-TGF-β1,2,3 monoclonal antibody) was observed to bind to both TGF-β1 and TGF-β2 as expected but did not bind to unconjugated TGF-β2(50-75). Flanders et al. (1990) also found that the polyclonal antisera raised against TGF-β2(50-75) did not cross-react with TGF-β1 and is therefore in agreement with these results. In spite of the 65% homology between TGF-β1(50-75) and TGF-β2(50-75), the structures are sufficiently different for TGF-β2 specific antibodies to be raised to this region.

The CellMax™ artificial capillary cell culture system was used for the large-scale production of monoclonal antibody from hybridomas 5D4-1D12-A7 and 8A3-1G3-E9. During the operation of these systems the glucose consumption rate and the cell viability were determined as described in section 3.2.7 and were correlated with the proportion of FBS in the medium (Figures 3.19 and 3.20). It should be noted that the measured cell viability of the module flushes is not synonymous with the cell viability remaining in the module because live cells adhere to the capillaries more firmly than non-viable cells.

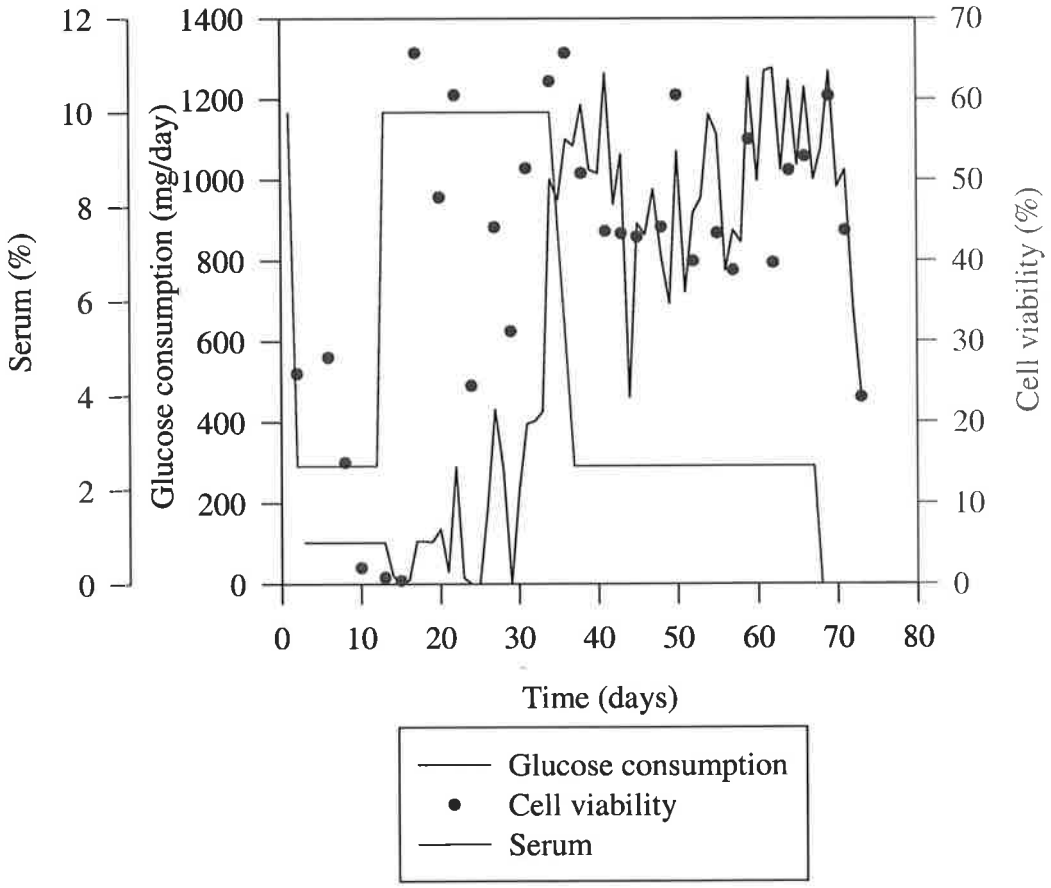

Figure 3.19: Summary of the glucose consumption rate, cell viability and FBS percentage in the growth medium for hybridoma 5D4-1D12-A7 in the CellMax™ system. *On day 0, 1.4×10^8 cells were inoculated into the CellMax™ and on day 13, a further 2.27×10^7 cells were inoculated. The cell line was cultured for 75 days in which time 456 mg of antibody was produced.*

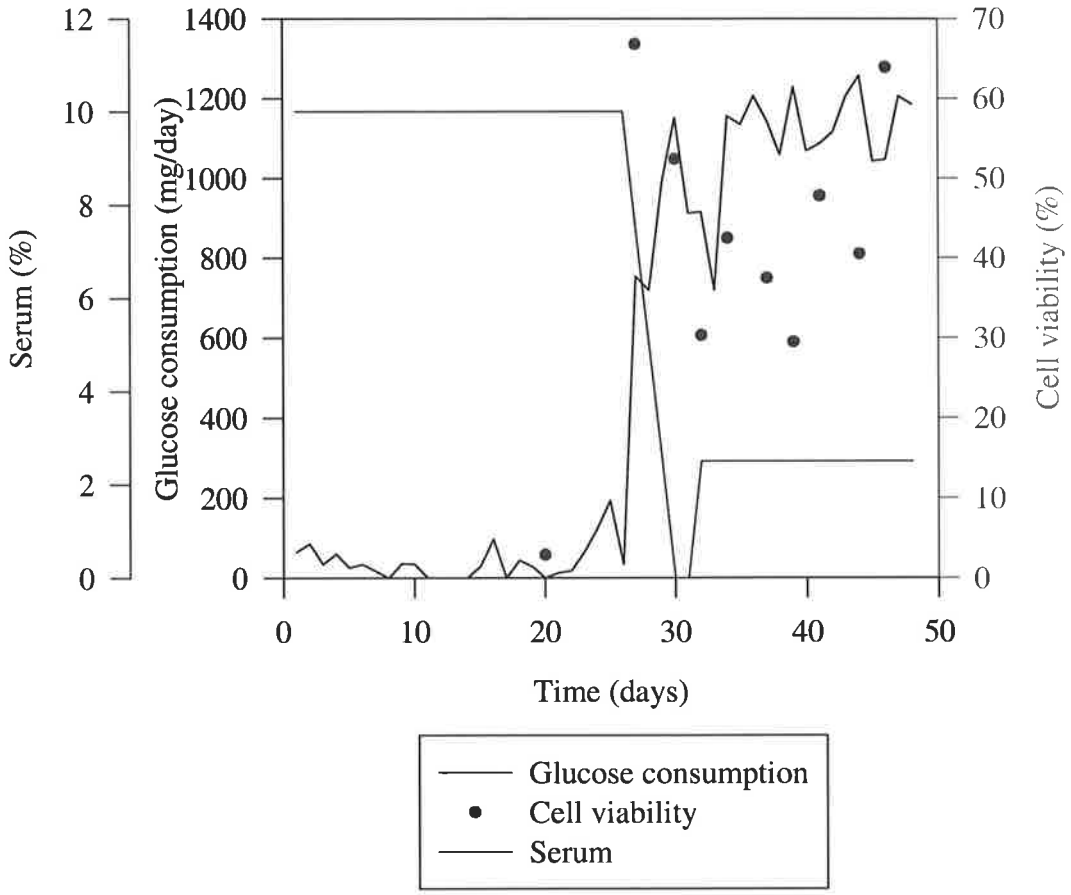

Figure 3.20: Summary of the glucose consumption rate, cell viability and FBS percentage in the growth medium for hybridoma 8A3-1G3-E9 in the CellMax™ system. *On day 0, 1.24×10^{8} cells were inoculated into the CellMax™ and on day 13, a further 2.08×10^{7} cells were inoculated. The cell line was cultured for 47 days in which time 189 mg of antibody was produced.*

It was found that collecting the conditioned medium from the module external to the capillaries was an acceptable harvest method. Approximately 80% of the antibody was concentrated in the space external to the capillaries because the molecular weight cut-off of the membrane was less than the molecular weight of the antibody. The cells used 500 ml of DMEM+2.5% FBS per day at their maximum metabolic rate, which compares with the 25 ml of conditioned medium recovered from the space external to the capillaries every 2-3 days. In this way the highly concentrated antibody was recovered in a small volume.

The affinity adsorbent Prosep-G (Bioprocessing Ltd., Durham, UK) was used to purify monoclonal antibody from the antibody conditioned medium. A typical chromatogram for the purification is shown in Figure 3.21.

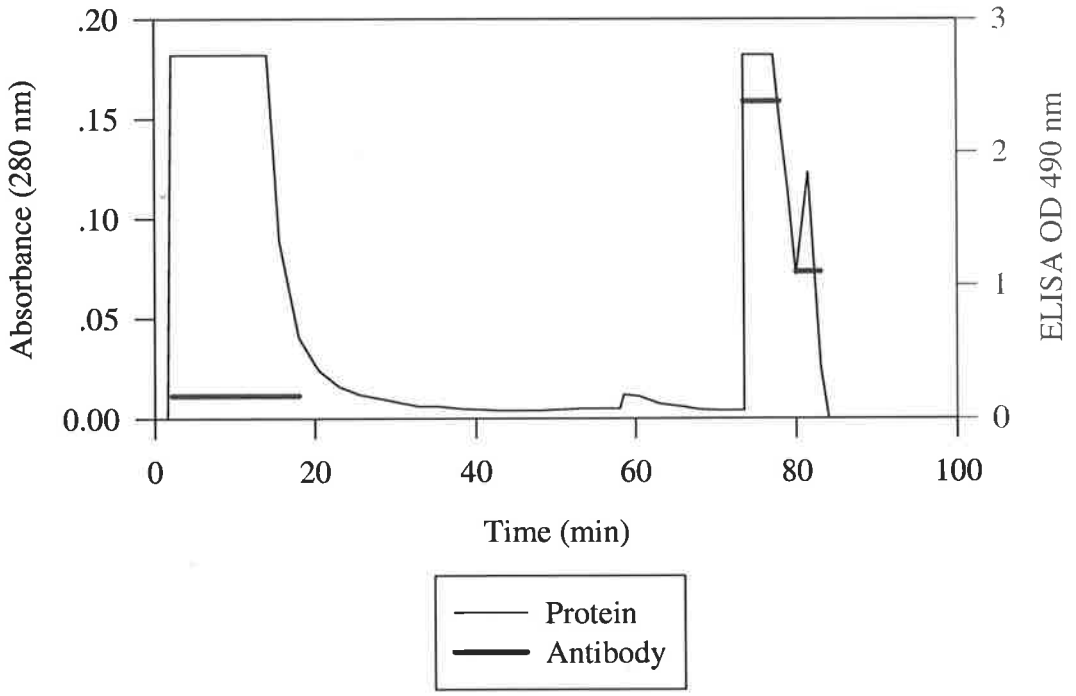

Figure 3.21: Typical chromatogram for the Prosep-G affinity adsorption of antibody from conditioned medium. *Conditioned medium was loaded on the column (20 min), the column was washed with loading buffer (38 min) and 0.1M citric acid pH 5 (15 min), and then eluted with 0.1M citric acid pH 2 (7 min) and 0.03M HCl (10 min). The eluted protein was screened against ppTGF-β2 in ELISA and the optical densities are included for comparison.*

The original conditioned medium, the column flow through, the material eluting in 0.1M citric acid pH 5, 0.1M citric acid pH 2 and 0.03M HCl were screened against the ppTGF-β2 pool from the sixth purification. In comparison with the antibody activity in the original conditioned medium, the antibody activity in the flow through was negligible. No antibody activity was detected in the 0.1M citric acid pH 5 fraction and this buffer was subsequently used as a wash buffer. Antibody eluted in the 0.1M citric acid pH 2 and the 0.03M HCl fractions. For every antibody purification run the purity of the antibody in the 0.1M citric acid pH 2 and the 0.03M HCl fractions was ascertained by running the protein on a Tricine 10-20% gel. Figure 3.22 shows a typical protein-staining pattern when the antibody was electrophoresed on the Tricine gel under reducing conditions.

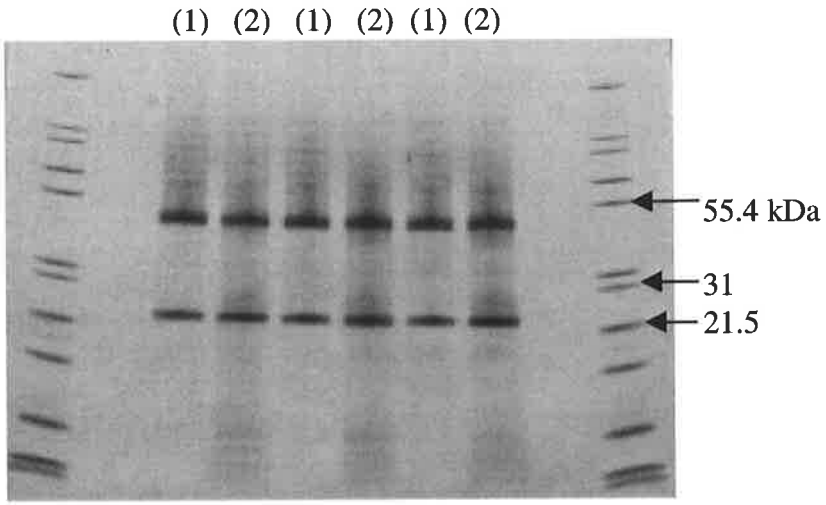

Figure 3.22: Typical Tricine gel when the antibodies were loaded under reducing conditions. *Mark 12 molecular weight markers occupied the outer lanes. The antibody 8A3-1G3-E9 was purified by Protein G affinity chromatography in three separate runs. Two inner lanes correspond to each run. The antibody was eluted with 0.03M HCl (1) and 0.1M citric acid pH 2 (2).*

When run electrophoretically under reducing conditions, both antibodies 5D4-1D12-A7 and 8A3-1G3-E9 displayed two separate bands that corresponded to the antibody fragments. β-mercaptoethanol reduced the interchain disulfide bonds to sulfydyls thereby dissociating the heavy (53 kDa) and light (21 kDa) chains. The approximate molecular weights of intact antibodies 5D4 and 8A3 were calculated by plotting the distance that the molecular weight marker proteins migrated from the origin versus $\log_{10}$(MW) and regressing a straight line through the data with Excel 97. The molecular weights of the antibody heavy and light chains were determined with the inverse function of the regressed straight line. An intact IgG molecule consists of two heavy and two light chains and therefore the molecular weights of antibodies 5D4 and 8A3 were 148 kDa and 149 kDa respectively. The apparent purity of the antibody in Figure 3.22 was typical for all of the purification runs.

To determine the extent to which the monoclonal antibody was contaminated with FBS, 40 ml of unconditioned DMEM+10% FBS was loaded on to the Prosep-G column and was subject to the same purification procedure as conditioned medium. According to the increases in absorbance at 280 nm, protein eluted in the 0.1M citric acid pH 2 and 0.03M HCl fractions. Approximately 5.1 mg of protein eluted in these fractions. The protein from the peaks was run on a Tricine gel under reducing conditions; bands corresponding to the heavy and light chains of immunoglobulin were observed but other bands accounted for most of the

protein. Based on the observation that 1.3 mg of contaminating protein co-eluted with monoclonal antibody for each ml of FBS loaded, the approximate purity of the antibody pools was determined. This calculation assumes that the only source of contamination is due to FBS proteins and not hybridoma-secreted proteins. Therefore the purity of monoclonal antibody 5D4-1D12-A7 was 91% (40.8 mg contaminating protein/456 mg total protein) and the purity of monoclonal antibody 8A3-1G3-E9 was 96% (8.1 mg contaminating protein/189 mg total protein). Although contaminants were still present, the purity of the eluting antibody was deemed sufficient for the purposes of this study.

The ability of the purified antibodies to inhibit the biological activity of TGF-β2 in a Mv1Lu assay was investigated. Dilutions of the ppTGF-β2 pool from the sixth purification were prepared in DMEM+5% FBS in the range of 0.05 to 10 ng/ml TGF-β2. Monoclonal antibody was prepared by large-scale production in the CellMax™ Artificial Capillary Module and purified from culture medium by Protein G affinity chromatography. Antibody 5D4 was added to the dilutions of TGF-β2 to give a final concentration of 100 μg/ml. Antibody 8A3 was added to the dilutions of TGF-β2 to give a final concentration of 25 μg/ml. The mixtures were vortexed and then placed in a water bath at 37°C and incubated for twenty minutes. The Mv1Lu cells were cultured in these dilutions but TGF-β2 biological activity was not inhibited in the presence of these antibodies. This result agrees with the finding of Flanders et al. (1990) because antisera against TGF-β2(50-75) did not block the binding of ^{125}I- TGF-β2 to normal rat kidney cells. By comparison, Dasch et al. (1989) developed an anti-TGF-β2 monoclonal antibody (1D11.16) that inhibited the biological activity of TGF-β2 in an interleukin-1, PHA-dependent thymocyte mitogenic assay at a concentration of 10 μg/ml. Also, Thompson et al. (1999) developed a human antibody that neutralised the biological activity of TGF-β2 in a bioassay using TF1 human erythroleukemia cells with an ED_{50} of 0.3 μg/ml.

Antibodies 5D4 and 8A3 were subject to western immunoblots for further confirmation of TGF-β2 specificity. The ppTGF-β2 pool from the sixth purification was run on a Tricine gel under non-reducing conditions and electroblotted on to nitrocellulose paper at ~25 ng TGF-β2 per lane. Monoclonal antibody was prepared by large-scale production in the CellMax™ Artificial Capillary Module and purified from culture medium by Protein G affinity chromatography. The blotted protein was probed with anti-TGF-β1,2,3 antibody (1 μg/ml),

purified antibody 5D4 (60.8 ng/ml) or purified antibody 8A3 (61.2 ng/ml). The blotted protein was then probed with peroxidase conjugated anti-mouse antibody (1:8000 dilution for anti-TGF-β1,2,3 antibody, 1:3000 for others) and viewed with enhanced chemiluminescence. A single band was revealed for anti-TGF-β1,2,3 monoclonal antibody and antibody 5D4 but not for antibody 8A3. The band ran at the expected molecular weight for dimeric TGF-β2 (25 kDa).

Recombinant human TGF-β2 (100 ng) was run under reducing conditions on a Tricine gel and electroblotted on to nitrocellulose paper. The blotted protein was probed with purified antibody 5D4 (0.5 μg/ml) for two hours. The membrane was then incubated with peroxidase conjugated anti-mouse antibody (1:10000 dilution) for 30 minutes and visualised with enhanced chemiluminescence (Figure 3.23)

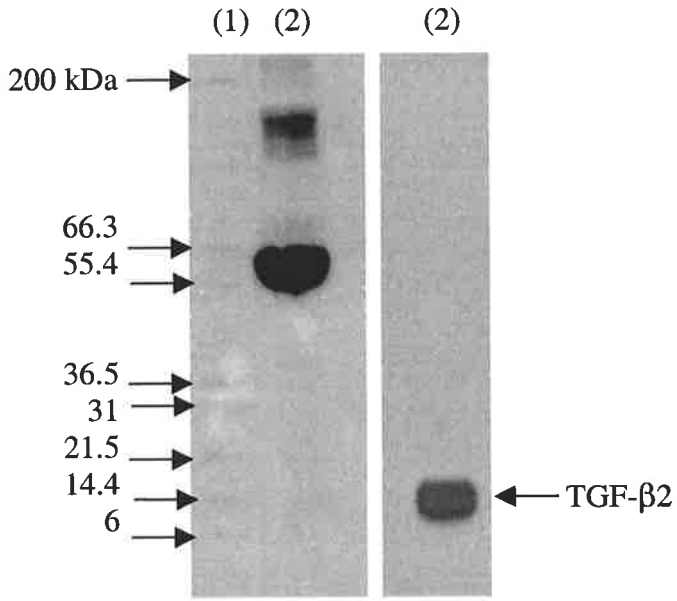

Figure 3.23: Western Immunoblot of Recombinant Human TGF-β2 with Antibody 5D4. *The Tricine gel was stained with Coomassie Blue (left). The blotted protein was probed with purified antibody 5D4 (right). The lanes are (1) molecular weight markers and (2) 100 ng recombinant human TGF-β2 with 50 μg BSA under reducing conditions.*

Figure 3.23 shows a protein band at ~60 kDa which corresponds to the BSA carrier protein. Insufficient rhTGF-β2 was present for it to be visible as a protein band. The Western blot shows a band at ~12.5 kDa which corresponds to the expected molecular weight of the reduced monomer of rhTGF-β2.

The technique of indirect immunofluorescence was used to localise TGF-β2 in human skin sections. The stained skin samples were observed to fluoresce strongly in the basal layer and to a lesser degree in the epidermis as shown in Figures 3.24 (1:100 dilution of anti-TGF-β2 polyclonal antibody) and 3.25 (50 μg/ml antibody 5D4). An acceptable level of fluorescence was provided by concentrations of 10-50 μg/ml antibody 5D4. No fluorescence was observed for the negative control slides. A reduction in fluorescence intensity was evident when TGF-β2 was added to antibody 5D4 at concentrations of 0.001, 0.01 and 0.1 μg/ml. Figure 3.26 clearly shows that 0.1 μg/ml TGF-β2 reduces the fluorescence intensity in comparison with the intensity observed in Figure 3.25. These results agree with Flanders et al. (1990) who also found that antisera raised against TGF-β2(50-75) localised TGF-β2 in murine placenta.

Figure 3.24: Immunohistochemical staining pattern when human skin was incubated with a 1:200 dilution of commercially available rabbit anti-TGF-β2 polyclonal antibody. *This fluorescence image was captured with a magnification of 400 times and a gate setting of four. Staining was observed in the basal layer.*

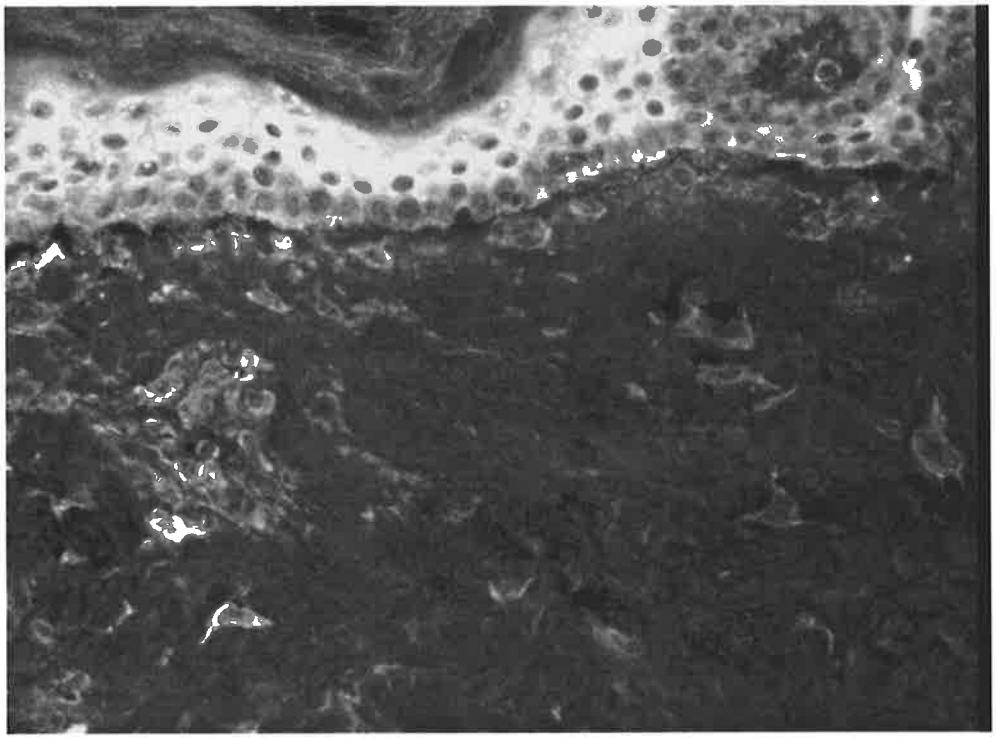

Figure 3.25: Immunohistochemical staining pattern when human skin was incubated with 50 μg/ml monoclonal antibody 5D4. *This fluorescence image was captured with a magnification of 400 times and a gate setting of four. Staining is observed in the basal layer and to a lesser degree in the epidermis.*

Figure 3.26: Immunohistochemical staining pattern when human skin was incubated with 50 μg/ml antibody 5D4 and 0.1 μg/ml TGF-β2. *This fluorescence image was captured with a magnification of 400 times and a gate setting of four.*

Considerable difficulties were encountered in raising a titre against native TGF-β2 and this finding is in agreement with reports in the literature (Flanders et al., 1990; Lucas et al., 1991; Thompson et al., 1999). Presumably the immunosuppressive properties and highly conserved nature of the peptide act to dampen the immune response. A monoclonal antibody was generated against a low molecular weight protein contaminant in ppTGF-β2. The identity or nature of this protein is as yet unknown. Flanders et al. (1990) reported that immunisation with the peptide TGF-β2(50-75) raised a specific titre against native TGF-β2. This alternative strategy was employed and was found to be successful. Two anti-TGF-β2 monoclonal antibodies were generated with conventional hybridoma technology. The CellMax™ Artificial Capillary Module was used to produce large quantities of antibody 5D4 (456 mg) and 8A3 (189 mg). Protein G affinity chromatography purified the antibodies from conditioned medium. Antibodies 5D4 and 8A3 bind to TGF-β2 in the ELISA format and do not show any cross-reactivity with TGF-β1. Antibody 5D4 also binds specifically to TGF-β2 in western immunoblots and in the immunohistochemical staining of human skin. The following chapters investigate whether antibodies 5D4 and 8A3 are suitable for immunoaffinity chromatography.

Chapter Four

Mathematical Modelling of Immunoaffinity Separations

4. Mathematical Modelling of Immunoaffinity Separations

4.1 Introduction

In developing an efficient immunoaffinity separation process for the commercial-scale purification of TGF-β2 from WGFE, the major costs must be identified and minimised. It has been demonstrated by a large literature that the economics of the separation process can be influenced by the configuration of the process, the operating conditions and the characteristics of the antibody. A number of configurations exist for immunoaffinity separation. These include continuous stirred-tank adsorption, cross-flow filtration, axial-flow and radial-flow packed beds, magnetically fluidised beds, expanded beds, perfusive beds and membranes (Liu and Fried, 1994). The operating conditions include the feed flow rate, the dimensions of the immunoaffinity support and the effluent concentration of the adsorbate at breakthrough. The antibody characteristics include the binding kinetics, the specific binding capacity for adsorbate and the rate of binding capacity degradation. Obviously the number of resulting combinations is potentially very large and it would be very time-consuming to investigate all of them in the laboratory. A mathematical model of the immunoaffinity process would be useful in identifying the most promising configurations, operating conditions and antibodies, without having to resort to laboratory experiments that explore every possibility.

The most commonly investigated adsorption system is the packed bed consisting of Pharmacia Sepharose™ and the performance of other configurations is often compared with this system. Sepharose™ is an agarose-based support matrix with high porosity, high antibody immobilisation capacity and low non-specific binding character (Afeyan et al., 1990). However, the pore diffusion of the biochemical to the antibody-binding sites is often the rate-limiting resistance to adsorption (Arnold et al., 1985b). As well, the productivity of Sepharose™ is often limited by bed compression (Afeyan et al., 1990). The recent developments of perfusive particle technology (Afeyan et al., 1990) and hollow-fibre membrane technology (Charcosett et al., 1995) do not have these disadvantages as perfusive particles and membranes do not compress and have negligible mass transfer resistance. Therefore intrinsic binding kinetics control the rate of adsorption in these new technologies.

Intuitively, one would expect that the economic performance of these new technologies would be superior to that of a Sepharose™ packed bed. Studies have been conducted that demonstrate the increased productivity per unit time per unit volume, Ψ_{prod} for the new

technologies relative to Sepharose™ (Brandt et al., 1988; Fulton et al., 1992). Maximising Ψ_{prod} should mean less immunoadsorbent and fewer columns are required and should result in the lowest possible cost. However, Colby (1997) demonstrated that high Ψ_{prod} is not necessarily synonymous with good economic performance, particularly when the chromatographic resin and columns are not the dominant cost drivers.

An economic analysis has been performed for the operation of a Sepharose packed bed, a perfusive bed and a hollow-fibre membrane in an attempt to determine the optimal operating conditions for each of these configurations in a hypothetical extraction system. In this way the most efficient configuration and operating conditions can be identified. In addition, a sensitivity analysis on parameters that are associated with the adsorbate-antibody interaction has been performed. The effects of variations in specific binding capacity (n), equilibrium association constant (K_{sa}), forward rate constant (k_{1sa}) and binding capacity degradation rate constant (k_{deg}) on the dimensionless annual operating cost (ϕ_{tot}) and the adsorbent productivity (Ψ_{prod}) have been investigated for the Sepharose packed bed.

It is intended that this simulation be used to model the operation of the TGF-β2-anti-TGF-β2 monoclonal antibody system. However, the interaction kinetics of this system were not characterised prior to this investigation. Therefore the simulation has been based on a hypothetical immunoaffinity system. The bovine serum albumin (BSA)- anti-BSA monoclonal antibody system was chosen because it has been thoroughly characterised in the literature (Antonsen et al., 1991; Olson et al., 1989). The feed concentration of contaminant and adsorbate are characteristic of WGFE and TGF-β2 respectively.

In the hypothetical extraction system 1 gram of BSA is to be extracted per year from a feed consisting of a mixture of proteins, where BSA constitutes 0.01% (w/w) of total protein. The eluted biochemical product must be >10% pure because a purification factor of 1000 is reasonable for immunoaffinity separations. Realistically, the partially purified adsorbate would be subject to polishing by reversed phase HPLC after immunoaffinity chromatography. It is assumed that the immunoaffinity step is the most expensive and therefore the most critical process in determining economic viability. For this reason, the analysis focuses on the costs involved with immunoaffinity chromatography. The system is expected to be under the control of an automated FPLC unit (Pharmacia, Upssala, Sweden) and runs continuously throughout each batch run. Four batches are run per year and each is of two weeks duration.

The model of the hypothetical system was developed with the following characteristics:

- Simulates the chromatographic behaviour during the adsorption, washing, elution and regeneration steps.
- Sufficiently flexible to predict the outcome of changes in operating conditions.
- Easily solved in a short period of time (5-10 minutes) on a 486 computer.
- Considers the effects of long-term binding capacity degradation and antibody leakage.

Three models were chosen to simulate the chromatographic behaviour:

- Hiester and Vermeulen (1952) model of frontal adsorption
- Goldstein (1953) model of zonal elution
- Arnold and Blanch (1985b) model of frontal elution

The models were modified to account for the different mass transfer characteristics of perfusive beds (Afeyan et al., 1990) and membranes (Sarfert and Etzel, 1997). These simple analytical models were solved with MathCad 6+ (MathSoft Corporation).

4.2 Theory

4.2.1 Simulation of Immunoaffinity Adsorption in a Packed Bed

4.2.1.1 Adsorption Model

The following model development is based on the work of Boyer and Hsu (1992). The adsorbate is assumed to interact with the antibody by a monovalent second-order reversible interaction, which has a characteristic binding energy as described by Equation 4.1.

$$A + B \underset{k_{l2}}{\overset{k_{l1}}{\rightleftharpoons}} A.B \qquad (4.1)$$

where A is the adsorbate in solution, B is the immobilised antibody binding site and A.B is the antibody-adsorbate complex. The rate constants k_{l1} and k_{l2} are not the intrinsic rate constants for the interaction, but rather are lumped parameters which reflect the contributions of mass transport as well. The rate of adsorption for this type of interaction is given by:

$$\frac{\partial q}{\partial t} = k_{l1} C_i (q_m - q) - k_{l2} q \qquad (4.2)$$

Consider a fixed bed of uniform spherical particles, having radius R, which has a uniform cross-section of length L and void fraction ε. Liquid flows through the bed at a superficial velocity of U_0, and initially the column is devoid of adsorbate. At time zero the inlet concentration of adsorbate in the mobile phase to the column is changed to C_0. A material balance of the adsorbate in the mobile phase for such a system can be written as:

$$U_0 \frac{\partial C}{\partial z} + \varepsilon \frac{\partial C}{\partial t} + (1-\varepsilon)\frac{\partial q}{\partial t} = 0 \tag{4.3}$$

Arnold et al. (1985a) found that axial dispersion is negligible in these systems and therefore does not appear in Equation 4.3. Thomas (1944) first derived the analytical solution to Equations 4.2 and 4.3 for the frontal analysis of an ion-exchange column. Arnold and Blanch (1986) found that it was convenient to transform the equations to the following dimensionless variables:

$$\begin{aligned} x &= C/C_0 \\ y &= \frac{q(K^{-1} + C_0)}{q_m C_0} \\ r &= 1 + KC_0 \\ N &= \frac{k_{11}(1-\varepsilon)q_m L}{U_0} \\ T &= \frac{(K^{-1} + C_0)}{q_m(1-\varepsilon)}\left(\frac{U_0 t}{L} - \varepsilon\right) \end{aligned} \tag{4.4}$$

The variables x and y are the dimensionless adsorbate and bound concentrations, where N is a dimensionless number of transfer units for the adsorption process, r is a separation factor, and T is the throughput or dimensionless effluent volume. After these transformations, equations 4.2 and 4.3 may be written, respectively, as:

$$\frac{\partial y}{\partial NT} = x(1-y) + \frac{1}{r}(x-1)y \tag{4.5}$$

$$\frac{\partial x}{\partial N} + \frac{\partial y}{\partial NT} = 0 \tag{4.6}$$

The solution of these equations for frontal analysis is:

$$C(L,t)/C_0 = \frac{J\left(\frac{N}{r}, NT\right)}{J\left(\frac{N}{r}, NT\right) + \left[1 - J\left(N, \frac{NT}{r}\right)\right]\exp\left[\left(1-\frac{1}{r}\right)(N-NT)\right]} \tag{4.7}$$

where the function J is given by Hiester and Vermeulen (1952):

$$J(a,b) = 1 - \int_0^x \exp(-b-\xi) I_0\left(2\sqrt{b\xi}\right) d\xi \qquad (4.8)$$

where I_0 refers to a zero-order modified Bessel function of the first kind.

As mentioned earlier, the rate constants k_{l1} and k_{l2} are lumped parameters which contain the effects of both the intrinsic kinetics and mass transfer. Arnold and Blanch (1986) have described a method of estimating the relative magnitudes of these processes. This method is based on a mass transfer rate equation having the following form:

$$(1-\varepsilon)\frac{\partial q}{\partial t} = K_{mt} a_p (C - C_i) \qquad (4.9)$$

It has been shown that if this equation is substituted for Equation 4.2, after appropriate transformation, dimensionless equations of exactly the same form as Equations 4.5 and 4.6 are obtained (Hiester and Vermeulen, 1952). In this derivation the number of transfer units for mass transfer is given by:

$$N_{mt} = \frac{2K_{mt} a_p rL}{(r+1)U_0} \qquad (4.10)$$

It should be noted that Hiester and Vermeulen (1952) made the assumption that $x = 0.5$ in Equations 4.5 and 4.6 to convert the Thomas solution into an explicit form. This is an approximation because it actually increases from 0 to 1 during adsorption.

The mass transfer coefficient is estimated with Equation 4.11:

$$\frac{1}{K_{mt} a_p} = \frac{R^2}{15(1-\varepsilon)}\left(\frac{1}{D_i} + \frac{5}{k_f R}\right) \qquad (4.11)$$

Substitution into Equation 4.9 gives:

$$N_{mt} = \frac{30(1-\varepsilon) rL}{(r+1)R^2 U_0\left(\frac{1}{D_i} + \frac{5}{k_f R}\right)} \qquad (4.12)$$

The fluid film mass transfer coefficient, k_f, can be estimated from the equation of Foo and Rice (1975):

$$\frac{2k_f R}{D_L} = 2 + 1.45\left(\frac{2RU_0\rho}{\mu}\right)^{0.5}\left(\frac{\mu}{\rho D_L}\right)^{0.33} \tag{4.13}$$

An expression for the number of transfer units due to the intrinsic adsorption kinetics has exactly the same form as the lumped model.

$$N_k = \frac{k_1(1-\varepsilon)q_m L}{U_0} \tag{4.14}$$

In this equation, k_1 is the intrinsic rate constant for the adsorption process. Arnold and Blanch (1986) proposed that the mass transfer and kinetic number of transfer units, N_{mt} and N_k, respectively, can be combined as resistances in series to yield the overall number of transfer units:

$$N = \left(\frac{1}{N_k} + \frac{1}{N_{mt}}\right)^{-1} \tag{4.15}$$

This assumption was made in the work of Boyer and Hsu (1992) in the treatment of dye-ligand adsorption. However, this assumption is not strictly correct; individual transfer unit heights (*HTU*'s) may only be added directly in the case of linear equilibrium (Vermeulen et al., 1984). In these simulations the equilibrium dissociation constant is 2.77 mg/L which is approximately the same as the adsorbate concentration C_0 = 2 mg/L. Therefore adsorption occurs along the linear portion of the Langmuir isotherm.

The number of transfer units due to axial dispersion, N_d, was derived by Arnold et al. (1985b).

$$N_d = \frac{PeL}{2R} \tag{4.16}$$

Miller and King (1966) made the observation that in packed beds of spherical particles at low Reynolds numbers, $\varepsilon Pe \approx 0.2$. Therefore Equation 4.16 becomes:

$$N_d = \frac{L}{10\varepsilon R} \tag{4.17}$$

It was found that for all of the operating conditions simulated $N_d >> N_{mt}$; therefore axial dispersion does not affect the rate of adsorption in this packed bed configuration.

In a chromatography system mixing in the tubing, valves, connections and distributors can seriously degrade the separation efficiency by peak spreading (Arnold et al., 1985a). The

effects of this external source of peak spreading can be measured by observing the spread of solute pulses in the system in the absence of immunoadsorbent. Arnold et al. (1985a) injected 1 ml pulses of BSA onto a Pharmacia column of 1.6 cm diameter with no adsorbent in which the two distributors were pushed together. The resulting peaks were highly non-gaussian and showed considerable tailing. To estimate the *HTU* due to external sources of peak spreading from the bandwidth of the 1 ml pulse, the variance of the peak values, σ^2, were obtained from the exiting peak widths. The contribution to the total *HTU* for a given bed and adsorbate can be calculated from:

$$\Delta HTU = \frac{\sigma^2 U_0^{\,2}}{L[\varepsilon + (1-\varepsilon)\beta]^2} \tag{4.18}$$

Therefore the number of transfer units due to external sources of peak spreading is defined by:

$$N_{ext} = \frac{L^2[\varepsilon + (1-\varepsilon)\beta]^2}{\sigma^2 U_0^{\,2}} \tag{4.19}$$

Accounting for the additional sources of transfer units:

$$N = \left(\frac{1}{N_k} + \frac{1}{N_{mt}} + \frac{1}{N_d} + \frac{1}{N_{ext}} \right)^{-1} \tag{4.20}$$

The breakthrough time, *bt*, was determined by using MatchCad 6+ to find the root, *t*, of the equation:

$$C(t,L)/C_0 - X = 0 \tag{4.21}$$

The amount of adsorbate that is bound or present in the pore spaces after the adsorption step, Φ, is given by:

$$\Phi = C_0 \cdot f \cdot bt - f\int_{t\,limit}^{bt} C(t,L)dt \tag{4.22}$$

where t_{limit} is the dead time that accounts for the time taken for the feed front to traverse the length of the bed:

$$t_{limit} = \frac{\varepsilon L}{U_0} \tag{4.23}$$

The equations developed above are applicable to both the specific adsorption of the adsorbate and non-specific adsorption of the contaminant. MathCad 6+ encountered difficulties in accurately calculating the mass of contaminant bound to the bed after adsorption; the

numerical integration would terminate prematurely and yield a value smaller than expected. It is thought that this was due to the very sharp breakthrough curve for the contaminant. When numerical integration was completed successfully, the bed was saturated and the mass of contaminant was proportional to the bed volume.

4.2.1.2 Washing Model

The model for zonal elution (Goldstein, 1953; Arnold and Blanch, 1986) was modified for use as a washing model. In zonal elution, a pulse of adsorbate is fed to the bed, after which the buffer flows and a peak of adsorbate elutes from the column. This is analogous to the loading and wash steps. This model only provides *C(L,t)* for *t* greater than the pulse time and therefore the model for frontal elution must be used for the adsorption step.

For a pulse of duration t_0 a dimensionless pulse time is defined as:

$$T_0 = \frac{\left(K^{-1} + C_0\right)}{q_m\left(1-\varepsilon\right)}\left(\frac{U_0 t_0}{L}\right) \tag{4.24}$$

In this case t_0 is equivalent to the breakthrough time, *bt*. The exiting concentration profile is given by:

$$C/C_0 = \frac{1}{1 + \dfrac{P(t,L)}{\int_0^{\frac{N}{r}} \exp\left[\left(-N\left(T-T_0\right)-\xi\right)+\omega\right]\cdot I_0\left[2\sqrt{N\xi\left(T-T_0\right)}\right] - \exp\left[\left(-NT-\xi\right)+\omega\right]\cdot I_0\left(2\sqrt{N\xi T}\right)d\xi}} \tag{4.25}$$

where

$$P = exp\left[\left(1-\frac{1}{r}\right)\left(N-NT+\omega\right)\right]\left[1-J\left(N,\frac{NT}{r}\right)\right] + exp\left[\left(1-\frac{1}{r}\right)\left(N-NT+NT_0\right)+\omega\right]J\left(N,\frac{N\left(T-T_0\right)}{r}\right) \tag{4.26}$$

and ω is a number sufficiently large such that it permits the numerical integration of Equation 4.25 with MathCad 6+.

It is assumed that *C(L,t)* is maintained at the breakthrough concentration for the duration of the dead time, t_{limit}. This model was useful for predicting the amount of adsorbate that desorbs during the wash step. The amount of adsorbate remaining on the column after the wash step, Ω, is given by:

$$\Omega = \Phi - f\int_{bt}^{twash} C(t,L)dt \qquad (4.27)$$

The duration of the adsorption and wash steps, t_{wash}, was calculated by solving the root of the following equation with MathCad 6+ for a target ratio of specifically bound material to non-specifically bound material, Ψ_{pure}:

$$\Phi_{nw} - f\int_{bt}^{twash} C_w(t,L)dt - \frac{\Phi_{sw}}{\Psi_{pure}} + \Phi_{sw} = 0 \qquad (4.28)$$

where the subscript *n* denotes non-specifically bound material and the *s* subscript denotes specifically bound material. Once t_{wash} is known, the amount of adsorbate washed off the bed may be determined in a similar manner.

4.2.1.3 Elution Model

The following model was adapted from the work of Arnold and Blanch (1985b). It is assumed that there is no barrier to the entrance and distribution of eluent within the pores and therefore there is no time delay as the eluent diffuses through the particle to reach the adsorbed material. If the elution conditions are effective, it is reasonable to expect that adsorbate, once it has desorbed, will not readsorb to a significant extent on the support.

The initial and boundary conditions are:

$$\left.\begin{aligned} C(z,0) &= 0 \\ q(z,0) &= q_{ads} \end{aligned}\right\} 0 < z < L$$
$$C(0,t) = 0 \quad t \geq \{\varepsilon + (1-\varepsilon)\beta\}\frac{z}{U_0} \qquad (4.29)$$

In many cases of adsorption $q(z,0)$ varies along the length of the column as most of the adsorbed material will be located predominantly at the inlet side of the bed. The requirement that the surface concentration of adsorbate is constant throughout the column at the end of washing is difficult to fulfil unless dimensionless breakthrough concentrations, that approach one, are used. Sarfert and Etzel (1997) encountered a similar problem in their treatment of mass transfer-limited elution from a membrane. Sarfert and Etzel (1997) divided the mass of protein that adsorbed to the membrane by the membrane solid volume to yield the average desorbable protein concentration, q_{ads}. This was the solution that was employed.

A modified form of the equation derived by Arnold and Blanch (1985b) for elution is:

$$C_e(t) = \frac{k_{12e} q_{ads} L}{U_0} exp\left(-\frac{k_{2e} L}{U_0} \frac{\{U_0 At - [\varepsilon + (1-\varepsilon)\beta]v\}}{v} \right) \quad (4.30)$$

where k_{12e} is the lumped desorption rate. The number of kinetic transfer units is given by:

$$N_{ke} = \frac{k_{2e} L}{U_0} \quad (4.31)$$

The number of mass transfer units is given by:

$$N_{mte} = \frac{15(1-\varepsilon)L}{R^2 U_0 \left(\frac{1}{D_i} + \frac{5}{k_f R} \right)} \quad (4.32)$$

The number of transfer units due to mass transfer, kinetics, axial dispersion and external sources of peak spreading can be combined as resistances in series to yield the overall number of transfer units (Arnold and Blanch, 1986):

$$N_e = \left(\frac{1}{N_{ke}} + \frac{1}{N_{mte}} + \frac{1}{N_d} + \frac{1}{N_{ext}} \right)^{-1} \quad (4.33)$$

The lumped desorption rate is then calculated:

$$k_{12e} = \frac{U_0 N_e}{L} \quad (4.34)$$

Over the period of time, t_{limit}, in which the eluent front migrates the length of the column, it is assumed that the effluent concentration is zero. The elution duration, t_{elute}, corresponds to the time at which 99.99% of the bound material has eluted. Equation 4.30 is integrated so that t_{elute} may be determined for a given elution efficiency:

$$t_{elute} = \frac{-\frac{U_0 v}{k_{12e} L} ln(0.0001) + [\varepsilon + (1-\varepsilon)\beta]v}{U_0 A} \quad (4.35)$$

4.2.1.4 Regeneration Model

In the regeneration step, adsorption buffer is introduced to the column in order to flush the eluent from the pore spaces. The aim of the model is to determine the regeneration time that

is required to saturate the pore spaces with adsorption buffer. The regeneration time, t_{regen}, is defined as the time required for the column effluent to be 99.99% adsorption buffer. Regeneration is mathematically analogous to that of adsorption; instead of having an adsorbate, which adsorbs to the surface of the particles the regenerant particle, $H_2PO_4^-$, diffuses into the pore spaces within the particles. The throughput ratio, T, is defined according to the relation of Vermeulen et al. (1984):

$$T = \frac{V - \varepsilon v}{V_{stoic}} \tag{4.36}$$

where V is the throughput volume *and* V_{stoic} is the fluid volume holding enough adsorbate to saturate packed volume v completely if all the solute were transferred to it. For regeneration, V_{stoic} is the intraparticle pore volume, $\beta_r(1-\varepsilon)v$.

Therefore:
$$T_r = \frac{V - \varepsilon v}{\beta_r(1-\varepsilon)v} \tag{4.37}$$

The number of mass transfer units is given by:

$$N_{mtr} = \frac{15(1-\varepsilon)L}{R^2 U_0\left(\frac{1}{D_{ir}} + \frac{5}{k_{fr}R}\right)} \tag{4.38}$$

Accounting for the other transfer unit contributions:

$$N_r = \left(\frac{1}{N_{mtr}} + \frac{1}{N_d} + \frac{1}{N_{ext}}\right)^{-1} \tag{4.39}$$

With reference to Equation 4.4, the dissociation equilibrium constant for regenerant is infinity because the regenerant does not partition into one phase. Therefore $r = 1$ and linear equilibrium is observed. Under the condition of linear equilibrium, the dimensionless solid phase concentration, Y_r, is given by Vermeulen et al. (1984):

$$Y_r(t, L) = 1 - J(N_r T_r, N_r) \tag{4.40}$$

The regeneration time, t_{regen}, is calculated by solving for the root of the equation:

$$Y_r(t_{regen}, L) - 0.9999 = 0 \tag{4.41}$$

4.2.1.5 Adsorbate Recovery

The adsorbate recovery is the total amount of purified adsorbate that is eluted from the column for a given number of cycles whilst accounting for antibody leakage and the degradation in binding capacity that occurs as a result of antibody contact with the eluent. It was assumed that the binding capacity degradation rate could be approximated by a first order rate expression as a function of cycle number, Ψ_{cyc}, and batch number, Ψ_{batch}:

$$Q_m(\Psi_{cyc},\Psi_{batch}) = q_m \exp\left[-k_{deg}\cdot\Psi_{cyc}\cdot t_{elute} - k_{leak}\left(t_{store}+t_{run}\right)\left(\Psi_{batch}-1\right)\right] \qquad (4.42)$$

where k_{deg} is the binding capacity degradation rate constant, k_{leak} is the antibody leakage rate constant and t_{store} is the storage time between batches. During a production run, binding capacity degradation and leakage occur simultaneously whereas leakage only occurs during storage. The production time line for one year of operation is shown in Figure 4.1.

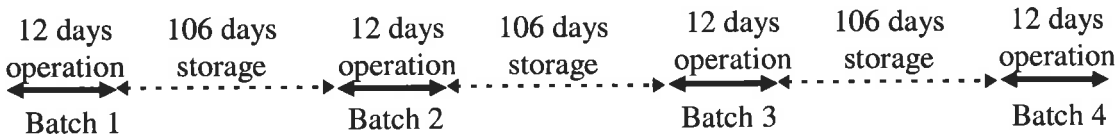

Figure 4.1: The production time line for one year of operation of the hypothetical packed bed immunoaffinity separation system.

The effects of binding capacity degradation upon operation are summarised in Table 4.1 for the operating conditions: L = 0.08 m, f = 12 ml/min and X = 0.05.

Q_m (g/L)	*bt* (s)	*BU* (%)	*AU* (%)
0.372	4388	16.56	98.45
0.157	1718	15.36	98.34
0.066	609	12.91	98.11
0.028	177	8.86	98.03

Table 4.1: Summary of the effects of binding capacity degradation upon breakthrough time, *bt*, bed utilisation, *BU*, and adsorbate utilisation, *AU*. *The operating conditions were L = 0.08 m, f = 12 ml/min and X = 0.05.*

As binding capacity degrades, the breakthrough time, *bt*, decreases if adsorption is terminated at the specified X for each cycle. A linear correlation exists between Q_m and *bt* with R^2 =

0.9942 for the data of Table 4.1. If a constant breakthrough time is maintained throughout the immunoadsorbent life then the adsorption will be very wasteful of feed as the immunoadsorbent ages. Feed may be conserved by decreasing the adsorption time as a linear function of Q_m. Bed utilisation decreases with Q_m and it is therefore not possible to simplify the calculation by assuming that adsorbate recovered per cycle is proportional to q_m. Adsorbate recovery may only be determined by repeating the calculation of Φ for a large number of cycles whilst Q_m is modified by Equation 4.42.

The dimensionless parameters are redefined:

$$N_{k\,deg}(\Psi_{cyc},\Psi_{batch}) = \frac{k_1(1-\varepsilon)Q_m(\Psi_{cyc},\Psi_{batch})\cdot L}{U_0}$$

$$T_{deg}(t,\Psi_{cyc},\Psi_{batch}) = \frac{\left(K^{-1}+C_0\right)}{Q_m(\Psi_{cyc},\Psi_{batch})\cdot(1-\varepsilon)}\left(\frac{U_0 t}{L}-\varepsilon\right) \qquad (4.43)$$

$$N_{deg}(\Psi_{cyc},\Psi_{batch}) = \left(\frac{1}{N_{mt}}+\frac{1}{N_{k\,deg}(\Psi_{cyc},\Psi_{batch})}+\frac{1}{N_d}+\frac{1}{N_{ext}}\right)^{-1}$$

and the exit concentration is given by:

$$C_{deg}(\Psi_{cyc},\Psi_{batch},t)/C_0 = \frac{J\left(\frac{N_{deg}}{r},N_{deg}T_{deg}\right)}{J\left(\frac{N_{deg}}{r},N_{deg}T_{deg}\right)+\left[1-J\left(N_{deg},\frac{N_{deg}T_{deg}}{r}\right)\right]exp\left[\left(1-\frac{1}{r}\right)\left(N_{deg}-N_{deg}T_{deg}\right)\right]} \qquad (4.44)$$

The amount of adsorbate, that is bound or present in the pore spaces after the adsorption step for a given cycle, is given by:

$$\Phi_{deg}(\Psi_{cyc},\Psi_{batch}) = \frac{C_0\cdot f\cdot bt\cdot Q_m\left(\Psi_{cyc},\Psi_{batch}\right)}{q_m} - f\int_{t\,limit}^{\frac{bt\cdot Q_m(\Psi cyc,\Psi batch)}{qm}} C_{deg}(t,\Psi_{cyc})dt \qquad (4.45)$$

A mathematical problem can result when $\frac{bt\cdot Q_m\left(\Psi_{cyc},\Psi_{batch}\right)}{q_m} \le t_{limit}$. It is obviously uneconomic to use the immunoadsorbent when binding capacity has degraded to this extent. Therefore operation is terminated when this condition occurs irrespective of whether all of the production runs have been completed.

The recovery is given by: $$\Psi_{rec} = 15\frac{\Omega}{\Phi}\sum_{i=1}^{\Gamma}\Phi_{deg}(15i) \quad (4.46)$$

where Γ is the total number of cycles in the immunoadsorbent life. The fraction Ω/Φ for the first cycle has been included to account for the difference between the amount of adsorbate recovered after elution and the amount of adsorbate that is bound and present in the pore spaces at the end of adsorption. It was assumed that this ratio is constant throughout the immunoadsorbent life. The number of numerical integrations for $\Phi_{deg}(j)$ can become large for high numbers of cycles, resulting in long calculation times. The number of numerical integrations was reduced by assuming that one value of $\Phi_{deg}(j)$ was the same for the next 15 cycles so the adsorbate recovered for this number of cycles was $15\Phi_{deg}(j)$. The preceding 15 cycles and the degradation it has caused were accounted for by the next integration: $\Phi_{deg}[15(j+1)]$. It was assumed that there is no retention of bound adsorbate after the elution step despite the earlier constraint of eluting 99.99% of bound material. The results of varying the partition size are shown in Table 4.2. The percentage error was measured relative to the Ψ_{rec} determined with the partition size of 3.75.

Partition size (cycles)	Ψ_{rec} (g)	% error
120	1.078	+21.0
60	0.989	+11.0
30	0.937	+5.16
15	0.911	+2.24
7.5	0.898	+0.786
3.75	0.891	0

Table 4.2: The effect of varying the partition size on Ψ_{rec} determined by numerical integration of Equation 4.46. *The % error was measured relative to the Ψ_{rec} determined with the partition size of 3.75.*

A program was written in MathCad 6+ to calculate Ψ_{rec}, Γ and the total elapsed time of operation, t_{total}. The program structure is shown in the flow diagram of Figure 4.2.

The number of columns that are required to purify M_{prod} grams of adsorbate pa is given by:

$$N_{col} = \frac{M_{prod}}{\Psi_{rec}} \quad (4.47)$$

The average adsorbate recovery per day per unit adsorbent volume, or productivity (Ψ_{prod}) is defined by:

$$\Psi_{prod} = \frac{M_{prod}}{N_{col} \cdot t_{run} \cdot B \cdot v} \tag{4.48}$$

where B is the number of production batches per annum.

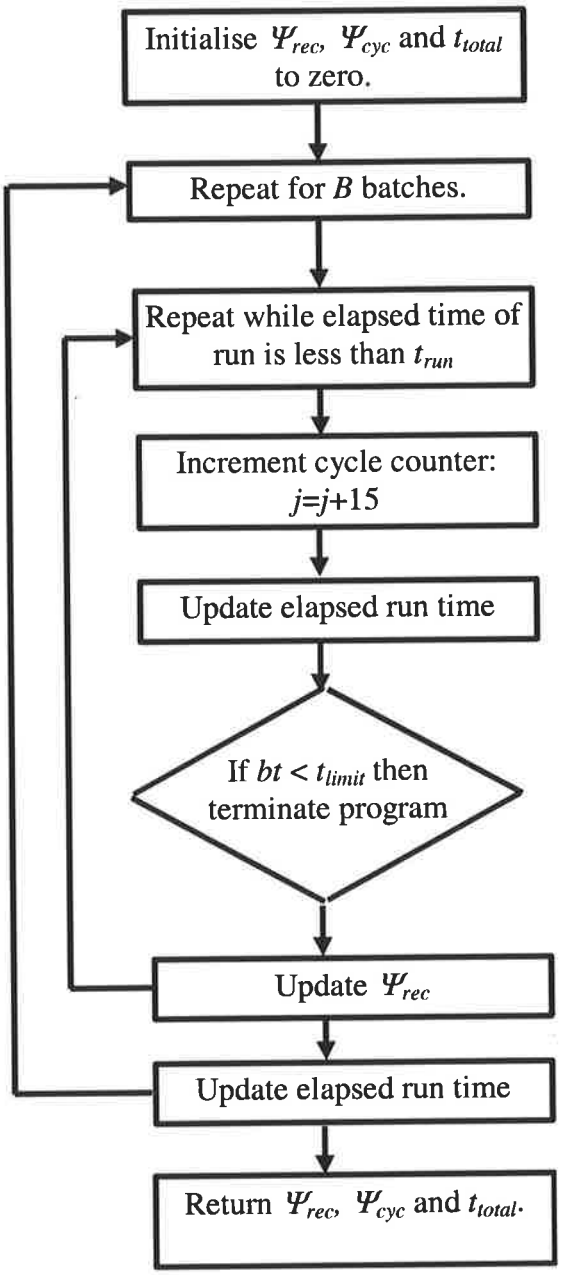

Figure 4.2: Flow diagram of the MathCad 6+ program that was written to calculate Ψ_{rec}, Ψ_{cyc} and the total elapsed time of operation, t_{total}.

4.2.1.6 Antibody Leakage

According to Antonsen et al. (1991) the antibody leakage rate can be approximated by a first order rate expression:

$$\eta(t) = \eta(0)\exp(-k_{leak}t) \tag{4.49}$$

where η is the amount of antibody immobilised to the support. Antibody leakage has two undesirable effects, namely the loss of adsorbate binding capacity and the contamination of the product with antibody.

4.2.1.7 Economic Analysis

The economic analysis was conducted in a similar manner to the analysis of Colby (1997). In this optimisation, the objective function is the total dimensionless operating cost, ϕ_{tot}, as derived by Middelberg (1996):

$$\phi_{tot} = \frac{\phi_{dfc} + \phi_{con}}{\phi_{ch}} \tag{4.50}$$

where ϕ_{dfc} is the amortised annual cost for direct-fixed-capital (DFC) dependent items including maintenance, depreciation, insurance and local taxes; ϕ_{con} is the annual cost of consumables; and ϕ_{ch} is the characteristic cost. It is assumed that labour costs are insensitive to operating conditions and changes of scale.

The DFC-dependent cost can be related to the total equipment purchased cost, ϕ_{ep}, of individual items using a simple factor, ζ (Middelberg, 1996):

$$\phi_{dfc} = \zeta\phi_{ep} \tag{4.51}$$

ϕ_{ep} includes the cost of the columns (γ_{col}) and the cost of an automated FPLC system (γ_{pcs}):

$$\phi_{dfc} = \zeta(N_{col}\gamma_{col} + \gamma_{pcs}) \tag{4.52}$$

Consumable costs include recurrent expenditure on the chromatographic resin, ϕ_r, antibody, ϕ_a, WGFE feed, ϕ_f, wash and regenerant solution, ϕ_w, and eluent costs, ϕ_e.

$$\phi_{con} = \phi_r + \phi_a + \phi_f + \phi_w + \phi_e \tag{4.53}$$

A characteristic cost, ϕ_{ch}, is used to non-dimensionalise the annual operating cost. This cost must be constant and independent of scale variations in the affinity system with flow rate,

bed height and breakthrough concentration. For the purposes of this study, the cost of an automated FPLC system was selected as the characteristic cost. The FPLC system consists of a controller, two pumps, valves, UV monitor and a fraction collector.

4.2.1.8 Pressure Drop

A critical superficial velocity exists during the operation of Sepharose packed beds (Soriano et al., 1997); as the superficial velocity exceeds this value column pressure tends to infinity and the resulting compression damages separation performance. Therefore a check must be performed to ensure that the operating conditions do not exceed this critical superficial velocity. The axial profile of pressure can be described by the system of differential equations (Soriano et al., 1997):

$$\frac{dP_s}{dz} = \Delta\rho(1-\varepsilon)g + \frac{\mu U_0}{K_m \exp\left(-\frac{P_s}{P_{s0}}\right)} - P_s k_m \left(\frac{4}{D}\right)\tan\xi$$

$$\frac{dP_f}{dz} = \frac{\mu U_0}{K_m \exp\left(-\frac{P_s}{P_{s0}}\right)} \qquad (4.54)$$

where P_s is the vertical solid pressure in the bed, P_f is the fluid pressure in the bed, $\Delta\rho$ is the density difference between the gel and the fluid, K_m is the permeability of the matrix, P_{s0} is the matrix rigidity, ξ is the angle of wall friction, D is the column diameter and k_m is a constant. MathCad 6+ was used to solve this system with an adaptive Runge-Kutta function.

4.2.2 Simulation of Immunoaffinity Adsorption in a Perfusive Bed

The mathematical equations that were developed for the packed bed case are generally applicable to perfusion chromatography. The modifications to these equations are discussed below.

4.2.2.1 Momentum and Mass Transport in a Perfusive Bed

The following theoretical derivations are from the work of Afeyan et al. (1990). The ratio of the flow through the column relative to flow through the particles is obtained by treating both as packed beds of particles. The Blake-Kozeny Equation (Bird et al., 1960) relates the permeability (K_m) of a packed column to its void fraction (ε) as:

$$K_m = \frac{\varepsilon^3}{150(1-\varepsilon)^2} \tag{4.55}$$

where

$$K_m = \frac{\mu U_0}{4R^2\left(\frac{dP}{dR}\right)} \tag{4.56}$$

The driving force for perfusive flow across a particle is the column pressure gradient, which imposes a pressure difference $2R\left(\frac{dP}{dR}\right)$ across each particle. Therefore the flow through a permeable particle can be modelled by using the correlation above. Although the exact flow through particles in a packed column will be influenced by the pressure distribution around a particle which in turn is heavily influenced by neighbouring particles, a first approximation can be derived by treating the particle as a loosely packed agglomerate of smaller particles (microspheres). Thus, the flow channels are the interstices formed between microspheres. It is assumed that the column pressure drop is mainly due to the interstitial flow around particles. In other words, the flow rate through the particle is much smaller than that around the particle. Therefore the flow through the particle is given by:

$$U_{pore} = \frac{K_p d_m{}^2\left(\frac{dP}{dx}\right)(1-\varepsilon)}{\mu\beta} \tag{4.57}$$

where d_m is the nominal microsphere diameter and K_p is the permeability of the particle. In addition:

$$K_p = \frac{\beta^3}{150(1-\beta)^2} \tag{4.58}$$

and

$$d_m = \kappa d_{pore} \tag{4.59}$$

where d_{pore} is the nominal throughpore diameter and κ is a constant related to the closeness of the packing (tortuosity). By combining Equations 4.56-4.59:

$$\frac{U_{pore}}{U_0} = \frac{K_p}{K_m}\left(\frac{d_m}{2R}\right)^2 \frac{(1-\varepsilon)}{\beta} \tag{4.60}$$

In the simulation of a packed bed composed of Sepharose particles it was only necessary to consider diffusive transport into the stagnant mobile phase. In order to adapt the existing equations for application to the perfusive case, the effective diffusivity can be modified to include a convective enhancement factor.

$$D_{eff} = D_i + U_{pore} \cdot R \tag{4.61}$$

The preceding equation is based on the assumption that the concentration terms governing diffusion and convection can be treated as approximately equal. Mechanistically, this is not accurate because diffusion depends on a concentration gradient while convection is related to the average concentration across the channel. However, this assumption is valid at the limit where the maximum driving force for diffusion and convection are considered, that is, where the pore exit concentration is zero. POROS 20 tolerates pressures up to 17 MPa (Perseptive Biosystems) and was treated as an incompressible material.

4.2.2.2 Numerical Integration Problems

MathCad 6+ encountered difficulties in accurately calculating the mass of contaminant bound to the bed after adsorption with Equation 4.22; the numerical integration would terminate prematurely and yield a value smaller than expected. It was thought that this was due to the very sharp breakthrough curve for the contaminant. When the numerical integration was completed successfully, the bed was saturated and the mass of contaminant was proportional to the bed volume.

In the washing model, MathCad 6+ was unable to solve for t_{wash} with Equation 4.28. The error message "not converging" was returned repeatedly. It is thought that this was due to the very sharp washing curve of Equation 4.25. An alternative washing model was developed to determine t_{wash}. Generally the number of mass transfer units, N_{mtw}, is much larger than the number of kinetic transfer units, N_{kw}, and therefore the rate of washing is desorption-controlled. Additionally the bed is saturated with contaminant after the adsorption step and therefore when washing begins a volume of feed solution, undepleted of contaminant, flows through the bed for a duration $t_{limit} = \varepsilon L/U_0$. This situation is very similar to the elution of bound adsorbate and can be represented by modification of Equation 4.30:

$$C_w(t) = \frac{k_{2n}\left(\Phi_w - C_0 \cdot f \cdot t_{limit}\right)}{U_0 \cdot A} exp\left\{-\frac{k_{2n} L}{U_0}\frac{\left[U_0 At - \varepsilon v\right]}{v}\right\} \tag{4.62}$$

Equation 4.62 was integrated to determine t_{wash} subject to the purity constraint on the adsorbate:

$$t_{wash} = t_{limit} + bt - \frac{1}{k_{2n}} ln \left(\frac{\frac{\Phi}{\Psi_{pure}} + C_0 \cdot f \cdot t_{limit} - \Phi}{\Phi_w} \right) \tag{4.63}$$

4.2.2.3 Adsorbate Recovery

The adsorbate recovery was calculated with the method of section 4.2.1.5. The results of varying the cycle partition size are shown in Table 4.3. The percentage error was measured relative to the Ψ_{rec} determined with the partition size of 7.5.

Partition size (cycles)	Ψ_{rec} (g)	% error
120	4.528	+2.12
60	4.478	+0.992
30	4.453	+0.429
15	4.44	+0.135
7.5	4.434	0

Table 4.3: The effect of varying the partition size on Ψ_{rec} determined by numerical integration of Equation 4.46. *The % error is measured relative to the Ψ_{rec} determined with the partition size of 7.5.*

The partition size of 60 was selected because it integrated Equation 4.46 in an acceptable period of time with sufficient accuracy.

4.2.3 Simulation of Immunoaffinity Adsorption in a Hollow-fibre Membrane

4.2.3.1 Momentum and Mass Transport in a Membrane

In order to use the Thomas solution (Thomas, 1944) for the prediction of the breakthrough curves it must be shown that both axial and radial dispersion are negligible in the membrane. Mathematical models have been developed which account for axial and radial dispersion (Suen and Etzel, 1992) but these require more complex numerical solution procedures. Suen and Etzel (1992) showed that axial dispersion could be neglected above a critical axial Peclet number, Pe_z of 40 for a BSA-monoclonal antibody system. Above this Pe_z the breakthrough curve approaches the Thomas solution. Liu and Fried (1994) performed a similar study for the lysozyme-Cibacron Blue affinity system. They also considered radial dispersion, ie. the

occurrence of a concentration profile perpendicular to the convective flow through the membrane pores. They found that the conditions at which dispersion could be neglected were $Pe_r < 0.04$ and $Pe_z > 25$. In this work it was assumed that dispersion was negligible for the conditions of:

$$Pe_z = \frac{\varepsilon U_0 L}{D_L} \geq 40$$
$$Pe_r = \frac{U_0 r_0^2}{L D_L} \leq 0.04 \qquad (4.64)$$

Suen and Etzel (1992) reported that variations in membrane thickness and porosity significantly degrade performance by broadening the breakthrough curve. Liu and Fried (1994) also reported that variations in pore size significantly degrade performance. The extent to which a membrane is affected by these variations is dependent on its thickness. A single hollow-fibre membrane is therefore more susceptible to performance degradation from such variations than is a stack of thick membranes. The effects of the variations in thickness, porosity and pore size were neglected in this simulation.

The number of kinetic transfer units is defined by:

$$N_k = \frac{k_1 q_m L}{U_0} \qquad (4.65)$$

Sarfert and Etzel (1997) investigated mass transfer phenomena for the adsorption of BSA to an ion-exchange membrane; breakthrough curves were analysed with the Thomas solution by regressing the overall solid-phase mass transfer coefficient to the data. They found that solid-phase diffusion is unimportant and that film mass transfer resistance is dominant. The number of mass transfer units is given by:

$$N_{mt} = \frac{(1-\varepsilon) k_f a_m L}{U_0} \qquad (4.66)$$

where k_f is the film mass transfer coefficient and a_m is the ratio of surface area to solid volume. k_f may be evaluated by using the relation:

$$k_f \propto \left(\frac{U_0}{\varepsilon}\right)^{\frac{1}{3}} \left(\frac{D_L}{2r_0}\right)^{\frac{2}{3}} \qquad (4.67)$$

and a_m is defined by:

$$a_m = \frac{6\varepsilon}{2r_0(1-\varepsilon)} \tag{4.68}$$

where r_0 is the mean pore radius. The overall number of transfer units is defined by:

$$N = \left(\frac{1}{N_k} + \frac{1}{N_{mt}} \right)^{-1} \tag{4.69}$$

Washing the membrane entails flushing the shell-side of the module, which has a considerable dead volume in comparison with the membrane. Therefore the duration of the wash step and the regeneration step were assumed to be equivalent to the dead time.

4.2.3.2 Adsorbate Recovery

The adsorbate recovery was calculated with the method of section 4.2.1.5. The results of varying the cycle partition size are shown in the Table 4.4. The percentage error is measured relative to the Ψ_{rec} determined with the partition size of 7.5.

Partition size (cycles)	Ψ_{rec} (g)	% error
120	11.564	+1.02
60	11.503	+0.489
30	11.472	+0.218
15	11.456	+0.0786
7.5	11.447	0

Table 4.4: The effect of varying the partition size on Ψ_{rec} determined by numerical integration of Equation 4.46. *The % error is measured relative to the Ψ_{rec} determined with the partition size of 7.5.*

The partition size of 60 was selected because it integrated Equation 4.46 in an acceptable period of time with sufficient accuracy.

4.3 Parameter Values used in the Models

4.3.1 Packed Bed System Constants and Costs

Arnold and Blanch (1985a) determined the interstitial void fraction, ε, of Sepharose CL-4B to be 0.34 by measuring the retention time of Dextran Blue in a column. Using a similar method, it was determined that the particle porosity, β, and particle diffusivity, D_i, for BSA were 0.52 and 9.6×10^{-8} cm^2s^{-1} respectively. The bulk diffusivity of BSA, D_L, is 6.7×10^{-7} cm^2s^{-1} (Creighton, 1984).

Horstmann and Chase (1989) determined the particle size distribution for Sepharose by using an OPTOMAX V image analyser. The particles were found to be spherical and have almost uniform size distribution. The particle radius value of 50 μm is within the bounds of their calculated value of 45±12.5 μm.

The bulk diffusivity of $H_2PO_4^-$, D_{Lr}, was estimated to be 6.1×10^{-6} cm^2s^{-1}using the semi-empirical equation of Polson (1950):

$$D_{Lr} = 9.4\times10^{-11}\frac{T}{\mu(MW)^{1/3}} \tag{4.70}$$

The particle diffusivity of $H_2PO_4^-$, D_{ir}, was estimated to be 9.3×10^{-7} cm^2s^{-1} from the relation:

$$D_{ir} = D_{Lr}\times\frac{Di}{D_L} \tag{4.71}$$

The particle porosity of Sepharose with respect to $H_2PO_4^-$, β_r, was assumed to be 0.96 because this value was estimated from a knowledge of the overall agarose content (Horstmann and Chase, 1989).

It was assumed that the density (ρ = 1000 kgm^{-3}) and viscosity (μ = 0.001 Pa.s) of water were unaffected by the presence of protein at a temperature of 25°C.

The purity of BSA in the feed (Ψ_{feed}) was assumed to be 100 μg/g protein because this is the approximate purity of TGF-β2 in WGFE. The protein concentration of the feed (C_0) was assumed to be 20 g/L.

The particle density of Sepharose CL-6B is 1059 kgm^{-3} (Soriano et al., 1997). Therefore the density difference, $\Delta\rho$ = 1059 - 1000 = 59 kgm^{-3}. The permeability of uncompressed gel matrix, K_m, is defined by the equation of Soriano et al. (1997) and was calculated to be 6.02×10^{-12} m^2. The matrix rigidity, P_{s0}, the value of the coefficient k_m and the wall friction angle, φ, of Sepharose CL-4B are 23.6 kPa, 0.758 and 7° respectively (Soriano et al., 1997).

Arnold et al. (1985a) injected 1 ml pulses of BSA onto a Pharmacia column of 1.6 cm diameter with no adsorbent in which the two distributors were pushed together. The resulting

peaks were highly non-gaussian and showed considerable tailing. To estimate the *HTU* due to external sources of peak spreading from the bandwidth of the 1 ml pulse, the variance of the peak values, σ^2, were obtained from the exiting peak widths at a corresponding height of $e^{-0.5}c_{max}$. The results showed that $\sigma^2_{ext}U_0^2 \approx 10^{-5}$ m^2. It was assumed that the peak spreading for a 2.6 cm column is identical to that for a 1.6 cm column.

The DFC-dependent cost is related to the total equipment purchased cost, ϕ_{ep}, of individual items using a simple factor, ζ, with the value of 1.45 (Middelberg, 1996). Additional costs are shown in Table 4.5.

Item	Source	Cost (Year)
Pharmacia XK 26/100 Column	Amrad Pharmacia Biotech	$761 (1997)
automated FPLC system	Amrad Pharmacia Biotech	$52138 (1997)
CNBr Activated Sepharose Fast Flow	Amrad Pharmacia Biotech	$4705/250 g (1997)
anti-TGF-β1,2,3 monoclonal antibody	Genzyme	$1000/mg (1996)
WGFE	GroPep	$500/L (1997)
0.1M glycine pH2.5 eluent	Sigma Chemical Co.	$1.68/L (1997)
phosphate buffer	Sigma Chemical Co.	$0.75/L (1997)

Table 4.5: Costs involved in the economic analysis of a packed bed.

4.3.2 Perfusive Bed System Constants and Costs

Unless otherwise stated the system constants are identical to those for the packed bed simulation. According to Afeyan et al. (1990), the interstitial void fraction, ε, of POROS 20 is 0.35, the nominal throughpore diameter, d_{pore}, is 7×10^{-7} m, the particle porosity, β, is 0.5, and the constant relating microsphere diameter to throughpore diameter, κ, is 2. The particle diameter of POROS 20 is 20 μm (Perseptive Biosystems Inc., Camridge, MA, USA). The particle porosity of POROS 20 with respect to $H_2PO_4^-$, β_{ir}, was assumed to be 0.5 (Afeyan et al., 1990). The cost of this support is $2595 per 125 ml (AdeLab Scientific, Adelaide).

4.3.3 Membrane System Constants and Costs

Unless otherwise stated the system constants are identical to those for the packed bed simulation. The properties of the hollow-fibre module are shown in Table 4.6. The values in brackets are those which were used in the simulation.

Thickness	240-250 (245) μm
Total membrane volume	0.38-0.44 (0.32) ml
Total lumen surface area	13.1 (13.06) cm^2
Mean pore diameter	0.75 μm
Porosity	0.75-0.8 (0.775)
Hydraulic permeability	1.3-1.8 (1.55) cm/min.psi

Table 4.6: Properties of the hollow-fibre membrane *(Charcosset et al., 1995).*

Amicon (Danvers, MA, USA) manufactures a hollow-fibre membrane similar to that used by Charcosset et al. (1995). The smallest hollow-fibre membrane cartridge available from Amicon is the H1MP01-43 cartridge, which has an area of 0.03 m^2. The geometry of Table 4.6 has been scaled up to an area of 0.03 m^2 while holding thickness, mean pore diameter, porosity and hydraulic permeability constant. The dead volume of the system was estimated to be 41.2 ml.

Analysis of the breakthrough curves for the adsorption of BSA to an ion-exchange membrane provided a value for k_f (Sarfert and Etzel, 1997). The membrane pore size was 150 μm, the interstitial velocity was 2.26×10^{-4} ms^{-1} and k_f was 2.8×10^{-8} ms^{-1}. Therefore the following relationship holds:

$$k_f = 2.8\times10^{-8}\cdot\left(\frac{U_0}{2.26\times10^{-4}\,\varepsilon}\right)^{\frac{1}{3}}\left(\frac{1.5\times10^{-4}}{2r_0}\right)^{\frac{2}{3}} \qquad (4.72)$$

The listed price of Amicon cartridge H1MP01-43 is $731 (AdeLab Scientific, Adelaide).

4.3.4 Antibody Properties

Antonsen et al. (1991) and Olson et al. (1989) provided the values for the equilibrium association constant (K_{sa}), the association rate constant (k_{1sa}) and dissociation rate constant (k_{2sa}) constant for the BSA-anti-BSA antibody system. The maximum bounds of variation for the sensitivity analysis were determined by these values. Below is a brief account of the experimental procedure of Olson et al. (1989).

Superose 6 (11-15 μm porous agarose particles) was used because intraparticle diffusion times are estimated to be less than 5 s and were thus small compared with the observed monoclonal antibody dissociation times. The buffer used for kinetic and thermodynamic

experiments was 0.01M potassium phosphate buffer pH 7.4. Monoclonal antibody was covalently immobilised to Superose 6 using CNBr activation. Varying amounts of the immunoadsorbent and ^{125}I-BSA were added to centrifuge tubes and rotated for 2 hours. The bead suspension was then precipitated via low speed centrifugation. The supernatant was transferred to a fresh tube and both supernatant and precipitate tubes were counted for ^{125}I activity. Non-specific adsorption of ^{125}I-BSA onto the adsorbents was negligible for these conditions, as determined by performing control assays with immobilised mouse immunoglobulins. Monoclonal antibody equilibrium association constants and specific binding capacity were obtained by fitting the data to the Langmuir isotherm.

To determine the dissociation rate constants, the immunoadsorbent was incubated with ^{125}I-BSA, rapidly washed and contacted with a vast excess of unlabelled BSA. Periodically, samples of the suspension were withdrawn and filtered to determine the fraction of bound ^{125}I-BSA. The reaction vessel was a 50 ml stirred ultrafiltration cell. The thermodynamic and kinetic measurements were carried out at room temperature. The panel of 12 monoclonal antibodies demonstrated K_{sa} in the range 2.5×10^{7} to 1.2×10^{8} M^{-1} and k_{2sa} in the range of 4.07×10^{-5} to 7.94×10^{-3} s^{-1} (Olson et al., 1989).

The specific binding capacity (n), leakage rate constant (k_{leak}), binding capacity degradation rate constant (k_{deg}), association equilibrium constant during elution (K_{se}) and non-specific equilibrium constant (K_{na}) for the BSA-anti-BSA system were determined by Antonsen et al. (1991). The support consisted of cyanogen bromide-activated Sepharose 4B. A similar procedure to that described above by Olsen et al. (1989) was used to determine the binding capacity (n) and equilibrium association during adsorption (K_{sa}). The panel of six monoclonal antibodies demonstrated K_{sa} in the range 9.5×10^{6} to 5.7×10^{7} M^{-1} and n in the range of 0.5 to 1.3 (Antonsen et al., 1991).

The BSA binding capacity per unit particle volume was determined from the equation:

$$q_{ms} = \frac{AD \cdot n}{(1-\varepsilon)} \cdot \frac{MW(BSA)}{MW(IgG)} \tag{4.73}$$

where AD is the antibody coupling density.

Mouse IgG was immobilised to Sepharose and used as a control for the non-specific binding of BSA in the work of Antonsen et al. (1991). From this data, the equilibrium association constant for the non-specific binding of BSA to the adsorbent (K_{na}) was calculated to be 4.04×10^5 M^{-1}. It was assumed that the association rate constant for non-specific adsorption is identical to that of specific adsorption.

Antonsen et al. (1991) also estimated the association equilibrium constant (10^5 M^{-1}) during elution (K_{se}) for antibody 9.1 in 0.1M glycine pH 2.5. It was assumed that the association rate constant is unchanged from that in binding buffer and that the dissociation rate constant varies to satisfy the new lower equilibrium constant.

Antonsen et al. (1991) performed cycling experiments to simulate the repeated use of immunoadsorbents. The various solutions used for adsorption, washing or elution were passed sequentially through the column. Periodically, after a predetermined number of adsorption-elution cycles had passed, the flow was halted and the column was disconnected. A sample was removed from the column and its binding capacity was measured with radioimmunoassay. After each sample was taken, the column was reconnected so that the remaining immunoadsorbent could be subjected to further adsorption-elution cycles. Each cycle consisted of one hour of exposure to the eluent followed by one hour of washing with binding buffer. Antonsen et al. (1991) found that there was no significant change in K_{sa} during cycling but there was significant degradation in binding capacity, n, as a function of cycle number. It was assumed that binding capacity degrades as a function of the contact time with the eluent (Tejeda et al., 1998):

$$n = n_0 \exp(-k_{\text{deg}} t) \tag{4.74}$$

The values of k_{deg} were calculated with Equation 4.74 to range between 0 to 0.0978 hr^{-1} for the antibody panel (Antonsen et al., 1991).

Antonsen et al. (1991) also measured the rate of antibody leakage from the support matrix in the following way. Immobilised radiolabelled antibody was confined in a glass tube with frits at either end. The buffer was passed continuously through the tube in a closed loop. Periodic samples were taken and counted for ^{125}I activity. The data of Antonsen et al. (1991) were regressed to the leakage rate Equation 4.49 and it was found that k_{leak} was 1.35×10^{-8} s^{-1}.

The maximum non-specific binding capacity, q_{mn}, was estimated from the work of Kennedy and Barnes (1983). The contribution of ethanolamine-substituted CNBr-activated Sepharose 4B to the non-specific adsorption of human serum IgG was demonstrated by a plot of the IgG adsorbed by and eluted from the gel as a function of serial adsorption-elution cycles. The non-specific binding capacity, q_{mn}, was estimated to be 3.04 mg/ml.

A summary of the properties of antibody 9.1 is presented in Table 4.7.

Property	Value
Equilibrium affinity constant for BSA, K_{sa}	2.5×10^{7} M^{-1}
Equilibrium affinity constant during elution, K_{se}	10^{5} M^{-1}
Specific binding capacity, n	0.55
Association rate constant, k_{1sa}	1.3×10^{5} $M^{-1}s^{-1}$
Antibody leakage rate constant, k_{leak}	1.35×10^{-8} s^{-1}
Binding capacity degradation rate constant, k_{deg}	1.053×10^{-5} s^{-1}

Table 4.7: Summary of the properties of antibody 9.1 used in the operating condition optimisation study.

POROS 20 may be purchased in a pre-activated state (Perseptive Biosystems). The literature did not describe the antibody properties for this panel of anti-BSA monoclonal antibodies when it was coupled via hydrazide chemistry to POROS 20. It was assumed that the antibody properties are unchanged when the antibodies are immobilised to POROS.

The Sepracor hollow-fiber membrane can be activated by two different chemistries: hydrazide (Nachman et al., 1992) and 2-fluoro-1-methylpyridinium toluene-4-sulfonate (FMP) (Charcosset et al., 1995). Analysis of the data of Nachman et al. (1992) showed that the BSA-anti-BSA antibody system provided kinetic parameters that were realistic for the hollow-fibre membrane. In addition, the specific binding capacity, n, of the membrane-immobilised antibody was determined to be in the range of 0.49 to 1.79 and was subsequently used as the bounds for the sensitivity analysis.

4.4 Results

4.4.1 Optimisation of Operating Conditions

4.4.1.1 Packed Bed

Simulations have been performed with the model presented in the preceding sections. The immunoadsorption process was designed to extract one gram of adsorbate per annum at a purity of <10%. In one year, the process is to be run in four batches that are each of two

weeks duration. Approximately four months separates each of the batches. It is not necessary that 250 mg be recovered from each batch as binding capacity degradation will progressively reduce production throughout the year. When the breakthrough time for a given cycle number falls below the dead time (t_{limit}), production is terminated irrespective of whether all the batches have been completed.

The operating conditions of bed depth (L), flow rate (f) and dimensionless breakthrough concentration (X) were varied in an attempt to locate the optimal operating conditions that minimises ϕ_{tot}. The simulations examined the results of varying L between 2 and 10 cm and X between 0.05 and 0.8. For a given combination of L and X the upper bound for f is either limited by the critical superficial velocity at which bed compression occurs or the flow rate at which $\frac{C(L,t_{limit})}{C_0} = X$. At low flow rates the numerical integrations of Equations 4.22 and 4.27 give spurious results or take long times to complete. The dimensions of the optimisation problem were limited by assuming that the flow rate is constant throughout the cycle although practically this limitation would not exist. The properties of antibody 9.1 were assumed in these simulations.

The dimensionless annual operating cost, ϕ_{tot}, and the productivity, Ψ_{prod}, are presented in Figures 4.3 to 4.10. Table 4.8 shows some trends that are observed in Figures 4.3 to 4.10.

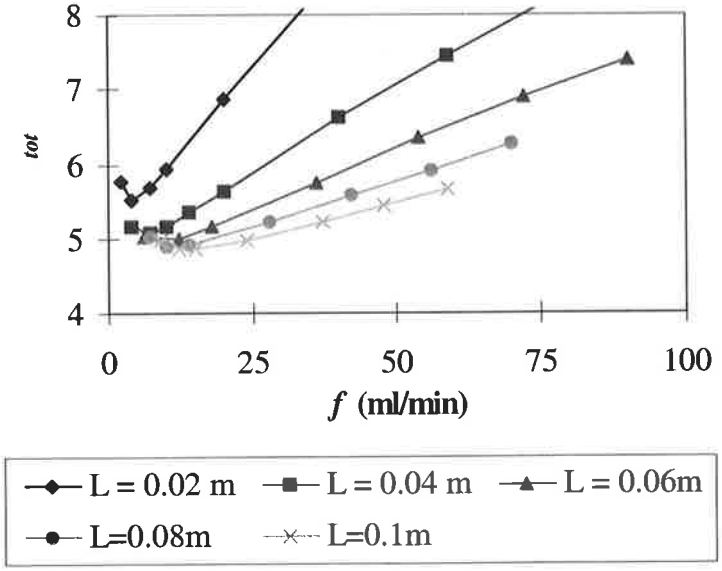

Figure 4.3: Variation of the dimensionless annual operating cost, ϕ_{tot}, with flow rate, f, and bed depth, L, at a dimensionless breakthrough concentration, X, of 0.8.

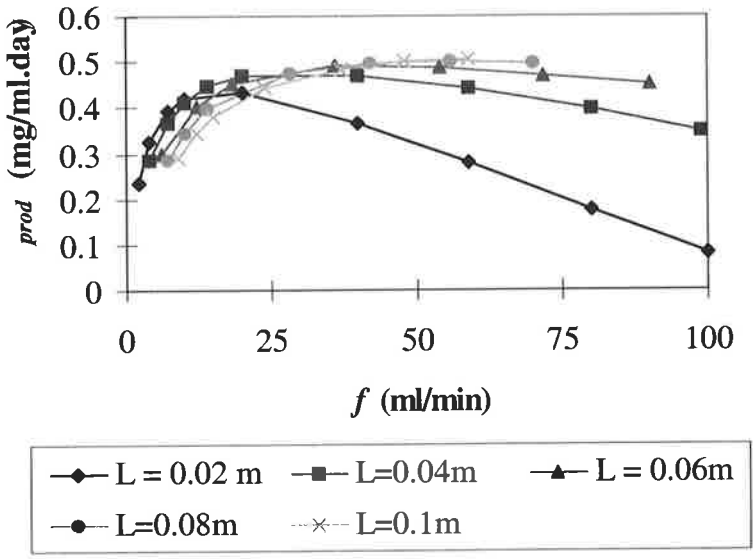

Figure 4.4: Variation of the productivity, Ψ_{prod}, with flow rate, f, and bed depth, L, at a dimensionless breakthrough concentration, X, of 0.8.

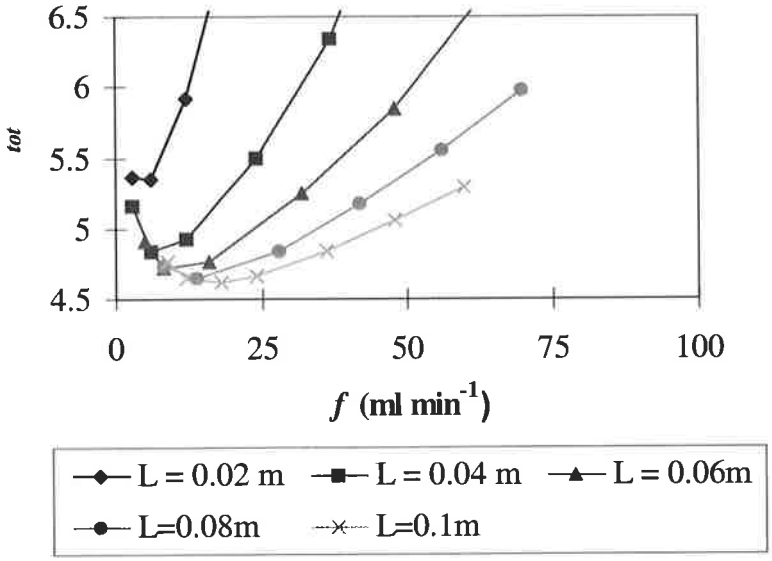

Figure 4.5: Variation of the dimensionless annual operating cost, ϕ_{tot}, with flow rate, f, and bed depth, L, at a dimensionless breakthrough concentration, X, of 0.5.

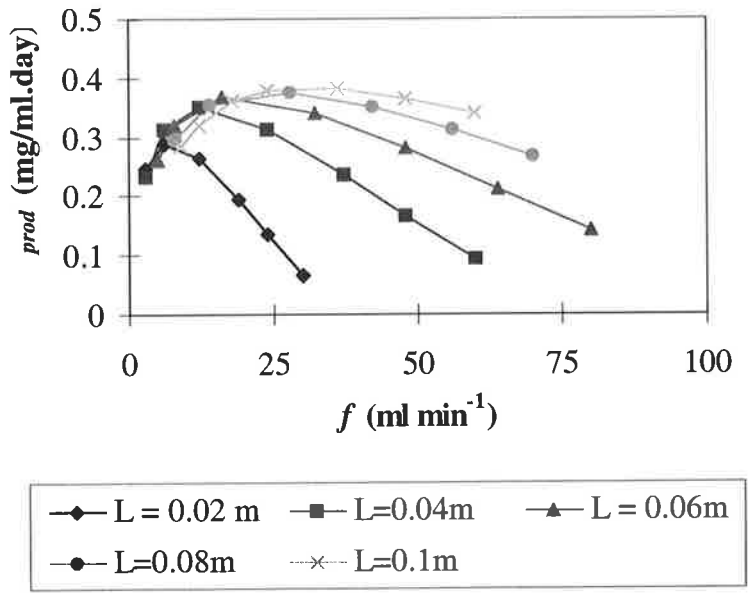

Figure 4.6: Variation of the productivity, Ψ_{prod}, with flow rate, f, and bed depth, L, at a dimensionless breakthrough concentration, X, of 0.5.

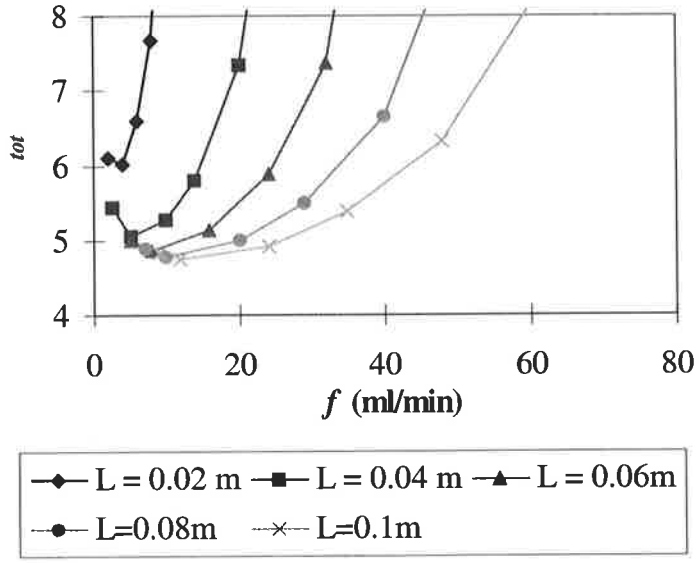

Figure 4.7: Variation of the dimensionless annual operating cost, ϕ_{tot}, with flow rate, f, and bed depth, L, at a dimensionless breakthrough concentration, X, of 0.2.

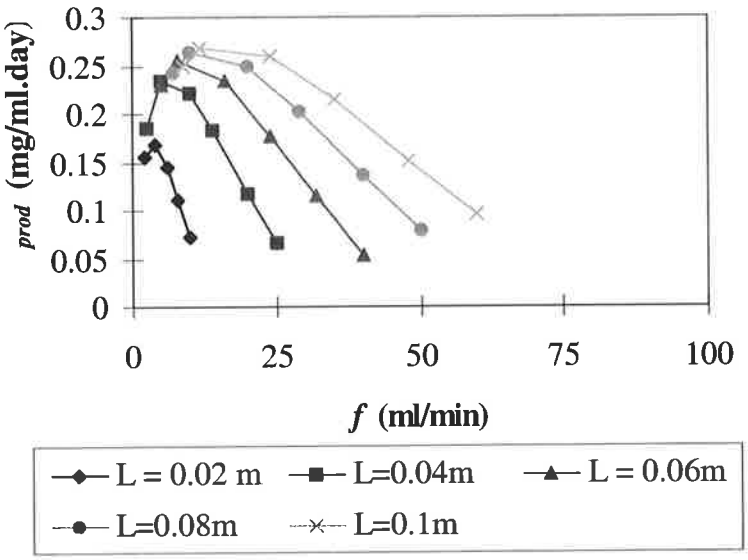

Figure 4.8: Variation of the productivity, Ψ_{prod}, with flow rate, f, and bed depth, L, at a dimensionless breakthrough concentration, X, of 0.2.

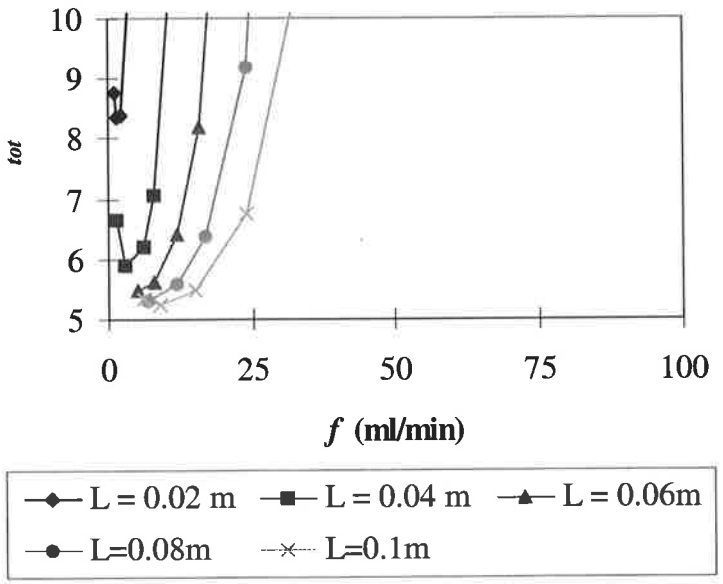

Figure 4.9: Variation of the dimensionless annual operating cost, ϕ_{tot}, with flow rate, f, and bed depth, L, at a dimensionless breakthrough concentration, X, of 0.05.

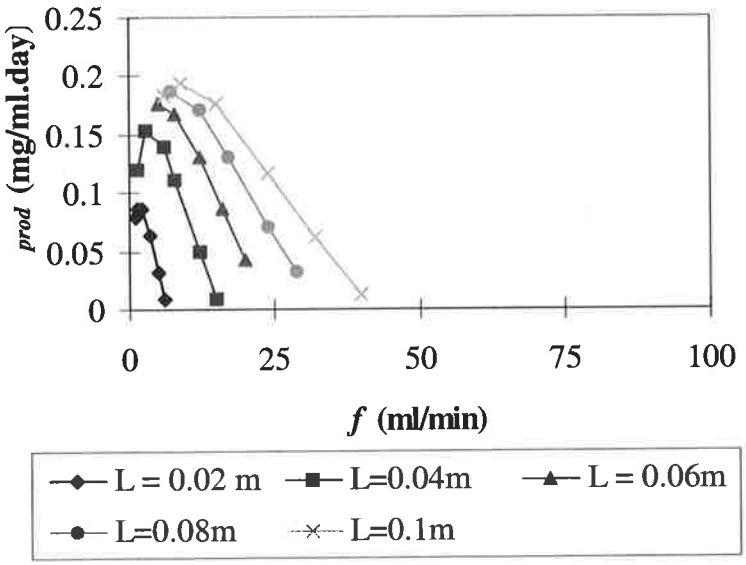

Figure 4.10: Variation of the productivity, Ψ_{prod}, with flow rate, f, and bed depth, L, at a dimensionless breakthrough concentration, X, of 0.05.

Parameter	Variation in f	Variation in L	Variation in X
ϕ_{tot}	Convex plot with a local minimum	ϕ_{tot} ↓ as L ↑	Convex plot with a local minimum
Ψ_{prod}	Concave plot with a local maximum	Ψ_{prod} ↑ as L ↑	Ψ_{prod} ↑ as X ↑

Table 4.8: Trends that are observed in Figures 4.3 to 4.10.

The optimal operating conditions were determined to be L = 10 cm, f = 18 ml.min^{-1} and X = 0.5 which gave ϕ_{tot} = 4.628. An example of the simulation output for these conditions is presented in the Appendix.

4.4.1.2 Perfusive Bed

The operating conditions of bed depth (L), flow rate (f) and dimensionless breakthrough concentration (X) were varied in an attempt to locate the optimal operating conditions that minimise ϕ_{tot}. The simulations examined the results of varying L between 2 and 10 cm and X between 0.01 and 0.8. For a given combination of L and X the upper bound for f is limited to the flow rate at which $\frac{C(L,t_{limit})}{C_0} = X$; at low flow rates the numerical integration of Equations 4.22 and 4.27 give spurious results or take long times to complete. The dimensions of the optimisation problem were limited by assuming that the flow rate is constant throughout the cycle although practically this limitation would not exist.

The behaviour of the perfusive bed was similar to that of the packed bed as shown in Figures 4.3 to 4.10. Table 4.9 shows some trends that are observed in the dimensionless annual operating cost, ϕ_{tot}, and the productivity, Ψ_{prod}, as f, L and X vary.

Parameter	Variation in f	Variation in L	Variation in X
ϕ_{tot}	Convex plot with a local minimum	ϕ_{tot} ↓ as L ↑	ϕ_{tot} ↑ as X ↑
Ψ_{prod}	Concave plot with a local maximum	Ψ_{prod} ↑ as L ↑	Ψ_{prod} ↑ as X ↑

Table 4.9: Trends that are observed in the dimensionless annual operating cost, ϕ_{tot}, and the productivity, Ψ_{prod}, as f, L and X vary.

The optimal operating conditions were found to be $L = 8$ cm, $f = 60$ ml.min^{-1} and $X = 0.01$ which gave $\phi_{tot} = 3.334$.

4.4.1.3 Membrane

The operating conditions of flow rate (f) and dimensionless breakthrough concentration (X) were varied in an attempt to locate the optimal operating conditions that minimises ϕ_{tot}. The simulations examined the results of varying X between 0.01 and 0.8; the lower bound for f is limited by the relation $Pe_z > 40$ which ensures that the Thomas solution is valid for predicting breakthrough curves. The dimensions of the optimisation problem were limited by assuming that the flow rate is constant throughout the cycle although practically this limitation would not exist.

The behaviour of the membrane was similar to that of the packed bed as shown in Figures 4.3 to 4.10. Table 4.10 shows some trends that are observed in the dimensionless annual operating cost, ϕ_{tot}, and the productivity, Ψ_{prod}, as f and X vary.

Parameter	Variation in f	Variation in X
ϕ_{tot}	Convex plot with a local minimum	Convex plot with a local minimum
Ψ_{prod}	Concave plot with a local maximum	$\Psi_{prod} \uparrow$ as $X \uparrow$

Table 4.10: Trends that are observed in the dimensionless annual operating cost, ϕ_{tot}, and the productivity, Ψ_{prod}, as f and X vary.

The optimal operating conditions were determined to be $f = 100$ ml.min^{-1} and $X = 0.05$ which gave $\phi_{tot} = 3.334$.

4.4.2 Operating Cost Sensitivity to Antibody Properties

Olson et al. (1989), Antonsen et al. (1991) and Nachman et al. (1992) demonstrated that, within a panel of antibodies, there is considerable variation in specific binding capacity (n), binding capacity degradation rate constant (k_{deg}), association equilibrium constant (K_{sa}) and association rate constant (k_{1sa}). The aim of this study was to examine whether realistic variations in some key antibody properties significantly affect ϕ_{tot}.

The operating conditions L = 10 cm, f = 18 ml.min^{-1} and X = 0.5 were used in the simulation of the Sepharose packed bed. Although these operating conditions are not necessarily optimal for each of the antibody property variations they are an approximation. Each of the antibody properties n, k_{deg}, K_{sa}, k_{1sa} and the association equilibrium constant during elution (K_{se}) were varied in turn while holding the others constant at antibody 9.1 values.

The dimensionless annual operating cost, ϕ_{tot}, is presented in Figures 4.11 to 4.15 for the antibody property variations. Table 4.11 shows some trends that are observed in Figures 4.11 to 4.15.

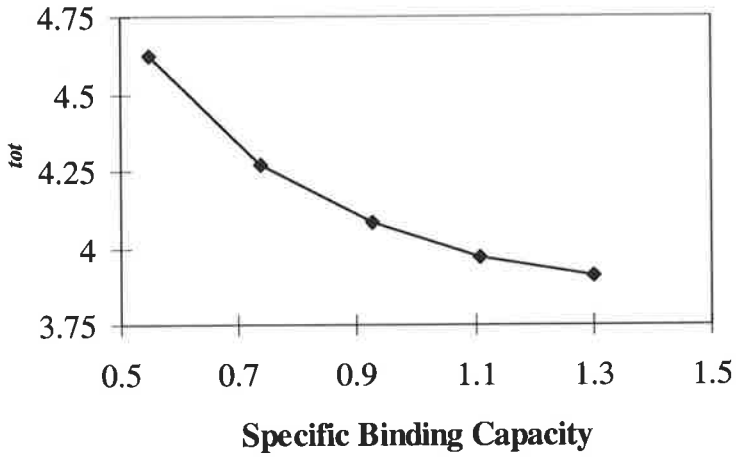

Figure 4.11: Effect of Specific Binding Capacity, n, upon the dimensionless operating cost, ϕ_{tot}.

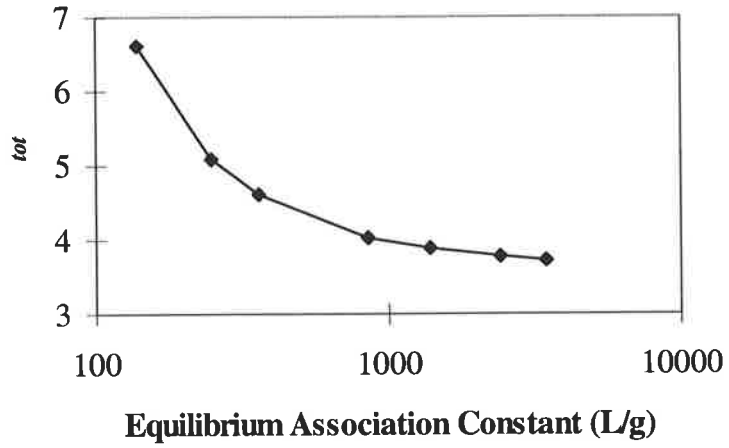

Figure 4.12: Effect of Equilibrium association constant, K_{asa}, upon the dimensionless operating cost, ϕ_{tot}.

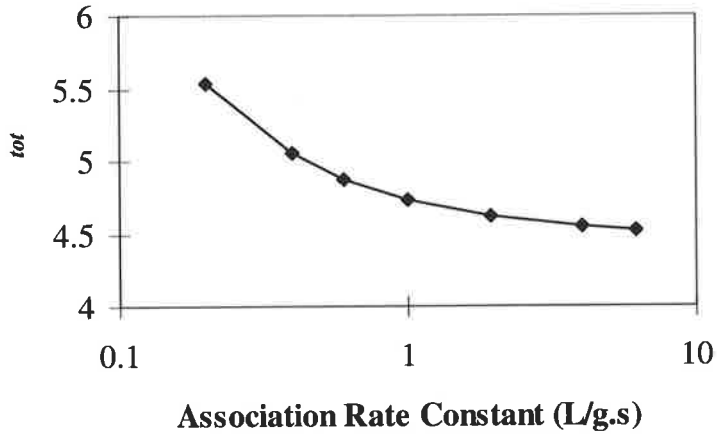

Figure 4.13: Effect of association rate constant, k_{1sa}, upon the dimensionless operating cost, ϕ_{tot}.

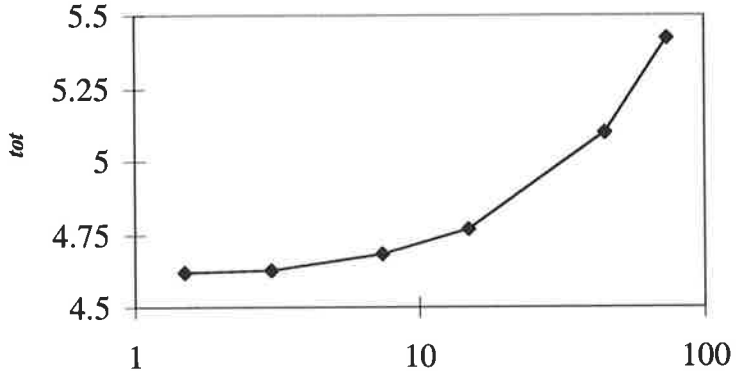

Figure 4.14: Effect of equilibrium association constant during elution, K_{ase}, upon the dimensionless operating cost, ϕ_{tot}.

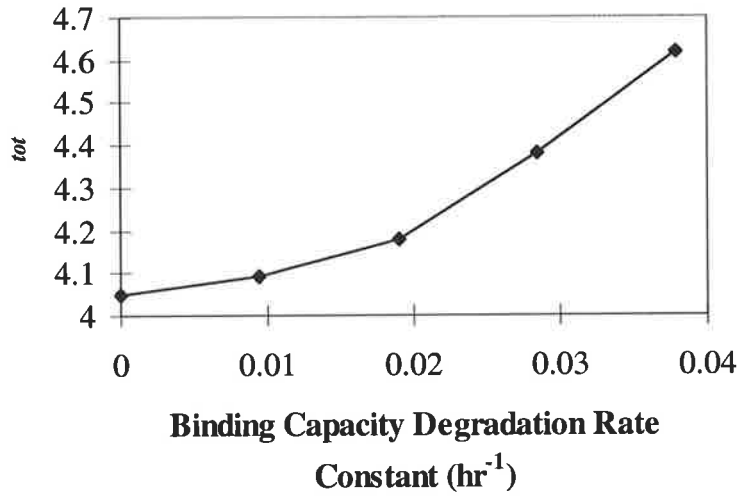

Figure 4.15: Effect of binding capacity degradation rate constant, k_{deg}, upon the dimensionless operating cost, ϕ_{tot}.

	Range	Trend	% Change
n	0.55 to 1.3	ϕ_{tot} ↓ as n ↑	0 to -15.4%
K_{sa} (L.g^{-1})	137 to 3450	ϕ_{tot} ↓ as K_{sa} ↑	+43.3% to -19.3%
k_{1sa} (L.g^{-1}.s^{-1})	0.2 to 6.18	ϕ_{tot} ↓ as k_{1sa} ↑	+19.7% to -2.2%
K_{se} (L.g^{-1})	1.49 to 74.7	ϕ_{tot} ↑as K_{se} ↑	0 to +17.3%
k_{deg} (hr^{-1})	0 to 0.0379	ϕ_{tot} ↑as k_{deg} ↑	-12.3% to 0

Table 4.11: Trends that are observed in Figures 4.11 to 4.15. *The % Change in ϕ_{tot} is calculated relative to the ϕ_{tot} for the antibody properties assumed in the optimisation problem.*

4.5 Discussion

The behaviour of a packed bed consisting of Sepharose, a perfusive bed consisting of Perfusive Biosystems POROS and a hollow-fiber membrane were simulated by solving a modified Hiester and Vermeulen chromatographic model with MathCad 6+ on a 486 computer. Typically the simulation took 5-10 minutes to run.

At low f the adsorbent is fully saturated for a given cycle but the rate at which adsorbate is fed to the column is lower than the potential adsorption rate. Production time is wasted and this is therefore a sub-optimal operating condition. At high f the adsorbate is fed to the column at a rate higher than the potential adsorption rate and unbound adsorbate breaks through to the effluent before the adsorbent is fully saturated. The adsorbent is not fully utilised and this operating condition is sub-optimal. Therefore an optimum flow rate, $f_m(\phi_{tot})$, exists which minimises ϕ_{tot} and an optimal flow rate, $f_m(\Psi_{prod})$, exists which maximises Ψ_{prod}.

At low L the resistances to adsorption characterised by N_d and N_{ext} become high relative to N_{mt} and this broadens the breakthrough curve to a greater extent than is observed for high L. The broadening of the breakthrough curve decreases BU for a specified X, increases ϕ_{tot} and decreases Ψ_{prod}. At L = 8-10 cm the resistances due to N_d and N_{ext} become negligible and this reduces the effect of L on ϕ_{tot} and Ψ_{prod}.

At low X the feed is conserved but the short adsorption time results in low BU. In addition this operating condition minimises ϕ_{tot} when the feed cost dominates the operating costs. At high X feed is wasted but the adsorbent is fully saturated which maximises Ψ_{prod}; this

operating condition minimises ϕ_{tot} when the adsorbent cost dominates. The optimal X is dictated by the relative costs for adsorbent and feed.

Yamamoto and Sano (1992) sought to maximise Ψ_{prod} in an attempt to minimise the objective function, ϕ_{tot}. However, it has been shown that maximising Ψ_{prod} may adversely affect economics in the case of the WGFE ion-exchange system (Colby, 1997). It is evident from Figures 4.3 to 4.10 that the f values that minimise ϕ_{tot}, do not necessarily maximise Ψ_{prod}. Therefore maximising Ψ_{prod} does not always minimise the operating costs, ϕ_{tot}, which agrees with the finding of Colby (1997).

Table 4.12 presents a comparison between the optimised operation of the hollow-fibre membrane, the packed bed and the perfusive bed.

Parameter	Membrane	Packed Bed	Perfusive Bed
Annual feed throughput (L)	521	630	529
Number of batches run	4	3.2	2.98
Number of cycles run	5839	1083	9882
Bed Utilisation (%)	22.4	34.5	21.1
Adsorbate Utilisation (%)	98.9	84.2	99.8
Antibody required (mg)	11.2	58.3	9.47
ϕ_{tot}	3.334	4.628	3.334

Table 4.12: Comparison between the optimised operation of the hollow-fibre membrane, the packed bed and the perfusive bed.

It is evident from Table 4.12 that the economic performance of the perfusive bed and the membrane is superior to that of the packed bed because they utilise feed more efficiently, run for a longer period of time before binding capacity is degraded and require less antibody. The perfusive bed and the membrane operate with sharper breakthrough curves than the packed bed because mass transfer resistance is much lower in these systems. The perfusive bed is incompressible and withstands higher operating pressures than the packed bed. The membrane operates efficiently at lower operating pressures. Therefore higher flow rates may be used without the occurrence of premature breakthrough. Consequently the bed utilisation and adsorbate utilisation are higher for a shorter adsorption time. The faster flow rate permits washing and regeneration to be accomplished in shorter time periods. The lower mass transfer resistance results in faster elution rates so all of the adsorbate can be recovered in a

short pulse of eluent. This minimises the time for which the eluent is in contact with the antibody and hence increases the operating life of the antibody.

The economic performance of purifying BSA from a feed was quantified using a dimensionless annual operating cost, ϕ_{tot}, for each of the configurations. The effects of variations in bed depth (L), flow rate (f) and dimensionless breakthrough concentration (X) upon economics were determined. The optimal operating conditions for each of these configurations were identified. Under these conditions, the dimensionless operating cost for the perfusive bed and the hollow-fibre membrane were comparable and approximately 40% lower than that for the packed bed configuration. This model system may be used to analyse the purification cost of the TGF-β2 separation system and help in the design of the system. This study also shows that a considerable saving in operating costs may be gained by choosing an antibody with high n, K_{sa}, k_{1sa} and low k_{deg}. It suggests that a decrease in operating costs would accompany efforts to optimise the binding and eluting conditions of a panel of prospective antibodies; the simulation may be used to choose the most suitable antibody from a panel of anti-TGF-β2 antibodies. The rate constants, the specific binding capacity and the binding capacity degradation rate constant for the TGF-β2-anti-TGF-β2 antibody interaction will be determined in the following chapters.

4.6 Nomenclature

A	column cross-sectional area	m^2
AD	antibody density	gL^{-1}
a_m	membrane surface area per unit membrane volume	m^2m^{-3}
a_p	particle surface area per unit bed volume	m^2m^{-3}
AU	proportion of adsorbate depleted from the column feed	%
bt	breakthrough time	s
B	number of production batches per annum	
BU	proportion of antibody binding sites associated with adsorbate	%
C	bulk liquid concentration	gL^{-1}
C_i	concentration at the interface	gL^{-1}
C_0	feed concentration	gL^{-1}
d_m	microsphere diameter	m
d_{pore}	particle throughpore diameter	m
D	column diameter	m

D_{eff}	modified adsorbate diffusivity	m^2s^{-1}
D_i	effective particle diffusivity for adsorbate	m^2s^{-1}
D_L	bulk diffusivity for adsorbate	m^2s^{-1}
f	flow rate	$ml.min^{-1}$
HTU	individual transfer unit height	m
k	intrinsic kinetic rate constant	s^{-1}
k_{deg}	binding capacity degradation rate constant	s^{-1}
k_f	film mass transfer coefficient	ms^{-1}
k_{leak}	rate constant for antibody leakage	s^{-1}
k_m	constant for equation (4.54)	
K	equilibrium association constant	Lg^{-1}
K_m	permeability of the matrix	m^2
K_{mt}	overall mass transfer coefficient	ms^{-1}
K_p	permeability of the particle	m^2
L	bed length	m
M_{prod}	adsorbate production quota per annum	g
n	specific binding capacity	
N	overall number of transfer units	
N_d	number of transfer units due to axial dispersion	
N_{ext}	number of transfer units due to external sources of peak spreading	
N_k	number of kinetic transfer units	
N_{mt}	number of mass transfer units	
P_f	fluid pressure in the bed	Pa
P_s	vertical solid pressure in the bed	Pa
P_{s0}	matrix rigidity	Pa
Pe	axial Peclet number	
q	concentration of adsorbed material	gL^{-1}
q_{ads}	concentration of adsorbed material after wash step	gL^{-1}
q_m	initial binding capacity	gL^{-1}
Q_m	time dependent binding capacity	gL^{-1}
r	dimensionless parameter defined by equation (4.4)	
r_0	mean pore radius	m
R	particle radius	m
t	time	s

t_0	pulse time	s
t_{cyc}	duration of a cycle	s
t_{elute}	time at which elution is complete	s
t_{limit}	time taken for feed to traverse bed	s
t_{regen}	time taken for column to regenerate	s
t_{run}	duration of a batch run	s
t_{store}	duration of storage between batches	s
t_{total}	total elapsed time of operation	s
t_{wash}	duration of the adsorption and wash steps	s
T	dimensionless effluent volume defined by equation (4.4)	
T_0	dimensionless pulse time defined by equation (4.24)	
T_r	dimensionless effluent volume defined by equation (4.37)	
U_0	superficial velocity	ms^{-1}
U_{pore}	intraparticle fluid velocity	ms^{-1}
v	bed volume	m^3
V	throughput volume	m^3
V_{dead}	dead volume in membrane system	m^3
V_{stoic}	fluid volume required to saturate the packed bed	m^3
x	dimensionless parameter defined by equation (4.4)	
X	dimensionless breakthrough time	
y	dimensionless parameter defined by equation (4.4)	
Y_r	dimensionless solid phase concentration of regenerant	
z	axial position within bed	m

Greek

β	particle porosity for adsorbate	
β_r	particle porosity for regenerant	
ΔP	pressure drop across column	Pa
$\Delta\rho$	density difference between gel and liquid	kgm^{-3}
ε	void fraction	
ϕ_a	unit cost of antibody	$\$g^{-1}$
ϕ_{ch}	characteristic cost	$
ϕ_{con}	annual cost of consumables	$
ϕ_{dfc}	amortised annual cost for direct fixed capital	$

ϕ_e	unit cost of eluent cost	$\$L^{-1}$
ϕ_{ep}	total equipment purchased cost	\$
ϕ_f	protein feed cost	$\$g^{-1}$
ϕ_r	chromatographic resin cost	$\$L^{-1}$
ϕ_{tot}	dimensionless annual operating cost	
ϕ_w	wash and regenerant solution cost	$\$L^{-1}$
Φ	adsorbate that is bound or present in pores after adsorption	g
γ_{col}	unit cost of the columns	\$
γ_{hold}	unit cost of membrane cartridge holder	\$
γ_m	cost of the membrane per unit area	$\$m^{-2}$
γ_{pcs}	unit cost of automated FPLC system	\$
Γ	total number of cycles in the adsorbent life	
κ	relates microsphere diameter to throughpore diameter	
μ	liquid viscosity	Pa.s
η	amount of antibody immobilised to the support	
ρ	liquid density	kgm^{-3}
σ^2	variance of gaussian peak	s^2
Ω	adsorbate remaining on column after the wash step	g
ξ	angle of wall friction	rad
Ψ_{batch}	batch number	
Ψ_{cyc}	number of cycles	
Ψ_{feed}	proportion of adsorbate in the feed	
Ψ_{prod}	productivity per unit adsorbent	$gL^{-1}day^{-1}$
Ψ_{pure}	purity of adsorbate after the wash step	
Ψ_{rec}	total recovery of adsorbate over adsorbent life	g
ζ	simple factor (Middelberg, 1996)	

Subscipts

1	denotes association rate
2	denotes dissociation rate
a	denotes condition during adsorption
deg	denotes condition of binding capacity degradation
e	denotes condition during elution

l	denotes lumped effects of intrinsic kinetics and mass transfer
n	denotes non-specific interaction
r	denotes condition during regneration
s	denotes specific interaction
w	denotes condition during washing

Chapter Five

Characterisation of the Antibody-Antigen Interaction required for the Immunoaffinity Separation of TGF-β2 from WGFE

5. Characterisation of the Antibody-Antigen Interaction required for the Immunoaffinity Separation of TGF-β2 from WGFE

5.1 Introduction

It was demonstrated in Chapter 2 that the purification of TGF-β2 from whey with size-exclusion gel filtration, ion-exchange chromatography and reversed phase HPLC was refractory. Therefore it was likely that a considerable improvement could be achieved by including an immunoaffinity step in the purification. In Chapter 3, two anti-TGF-β2 monoclonal antibodies were generated and produced in the amounts required by a commercial-scale immunoaffinity chromatography process. The optimisation of such a process is complex because the configuration, operating conditions and antibody properties contribute to the operating cost. Chapter 4 showed that a mathematical model could predict the effect of changes in these parameters on the operating cost. Furthermore, the models showed that the operating cost could be predicted by knowing the feed antigen concentration, antigen-antibody interaction kinetics, specific binding capacity and binding capacity degradation rate. These fundamental parameters can be determined with simple experiments and used in the mathematical model, hence obviating the need for exhaustive bench-scale testing with the immunoaffinity chromatography process. The model can also be used to identify the antibody with the greatest commercial potential from a panel of antibodies. The aim of Chapter 5 is thus to determine the feed antigen concentration, the antigen-antibody interaction kinetics, the specific binding capacity of the antibody and the binding capacity degradation rate with simple experiments.

5.2 Materials and Methods

5.2.1 Activation of WGFE

Wakefield et al. (1989) demonstrated that the TGF-β1 latent complex does not bind to polyclonal antisera raised against TGF-β1. This implies either that the latency-associated peptide is folded to form a cage-like structure around TGF-β1 or that it changes the conformation of exposed TGF-β1 epitopes so they are no longer recognised by the antibodies. It was therefore highly unlikely that a monoclonal antibody against active TGF-β2 would bind to TGF-β2 in the latent complex. Most of the TGF-β2 in WGFE is present as a latent complex and activation can be accomplished non-biochemically by exposure to acid (pH 2.0), alkali (pH 11), urea (8M) or heat (100°C) (Rogers et al., 1996). To optimise the efficiency of an immunoaffinity separation it will be necessary to dissociate the latent complex such that a

high concentration of active TGF-β2 is in solution. However, the conditions under which TGF-β2 is activated are not conducive to antigen-antibody binding (Yarmush et al., 1992). Therefore the conditions of WGFE must be returned to a favourable state for antigen-antibody binding after TGF-β2 activation. An additional factor to consider is that increasing the pH of WGFE above 4 after the overnight acidification results in protein precipitation (G. Regester and C. Goddard, personal communication). Protein precipitates could plug and foul the immunoaffinity support and must be removed by centrifugation or filtration prior to the column separation. Therefore the aim of this section was to activate WGFE in such a way as to maximise the TGF-β2 concentration and then retain that concentration after the solution pH has been neutralised.

5.2.1.1 Acid Activation and Reneutralisation of WGFE

Previous studies showed that the optimal pH for TGF-β2 activation was 2.5 (G. Regester and C. Goddard, personal communication). WGFE (batch number D15157) was acidified to pH 2.5 with HCl and incubated overnight at 4°C. The next day the acidifed WGFE was divided into four samples and they were each diluted to protein concentrations of 30.1, 22.6, 15.0 and 7.52 mg/ml with 150 mM NaCl. Each of the four samples was then further divided into four sub-samples (10 ml). Sodium hydroxide was added to the sub-samples to increase the pH to 4, 5, 6 and 7 and they were incubated overnight at 4°C. The next day the sub-samples were centrifuged (J6, Beckman, USA) at 1700 g for 20 minutes at 4°C because protein had precipitated. An aliquot from the supernatant of each sub-sample was filtered through 0.22 μm membranes (Millipore, Sydney, NSW). Each aliquot was subject to macro BCA protein assay and TGF-β2 ELISA (Promega, Madison, WI, USA).

In view of the loss of WGFE protein to precipitation, the potential existed for resuspending the precipitate in acidic buffer to reduce WGFE wastage. This was investigated by decanting the supernatant and adding 150 mM NaCl pH 2.5 to each sub-sample precipitate to give a volume of 10 ml. The precipitates were resuspended by vortexing and then incubated overnight at 4°C. The next day the sub-samples were reneutralised to their original pH with NaOH and incubated overnight at 4°C. On the following day the sub-samples were centrifuged (J6, Beckman, USA) at 1700 g for 20 minutes at 4°C. An aliquot from the supernatant of each sub-sample was filtered through a 0.22 μm membrane and subject to macro BCA protein assay.

The preceding investigations revealed that precipitation was unlikely to be the only source of TGF-β2 depletion from the supernatant. The reneutralised supernatant sub-samples were reacidified to pH 2.5 with HCl and incubated overnight at 4°C. ELISA was used to determine the TGF-β2 concentrations of the reacidified samples.

5.2.1.2 Alkaline Activation and Reneutralisation of WGFE

The first experiment endeavoured to determine the optimal alkaline activation pH. WGFE (30.1 mg/ml) was divided into five samples and the pH of each was adjusted to 9, 10, 11, 12 and 13 with NaOH. The samples were incubated overnight at 4°C, filtered through 0.22 μm filters and subject to macro BCA assay and TGF-β2 ELISA.

Having determined the optimal alkaline activation pH, the second experiment characterised the extent of protein precipitation after reneutralisation. The pH of WGFE (30.1 mg/ml) was increased to 11 with NaOH and incubated overnight at 4°C. The next day the alkaline WGFE was divided into four samples and HCl was added to decrease the pH to 10, 9, 8 and 7 respectively. The samples were incubated overnight at 4°C and then treated with the same procedure as section 5.2.1.1 on the following day.

5.2.1.3 Estimation of Confidence Intervals for TGF-β2 Concentration

Estimates of the confidence intervals on the TGF-β2 and protein concentrations are required in order to conclude that one activation condition is better than another at a given level of significance (95%). The standard curves in the TGF-β2 ELISA and the BCA protein assay were imported to Tablecurve and constants *a*, *b* and *c* were regressed to Equation 2.2:

$$y = a + bx^c \tag{2.2}$$

where x is the TGF-β2/protein concentration and y is the optical density. The dose response data for the unknown sample were imported to Tablecurve and the concentrations (x') were computed from the optical density (y) of each well, after accounting for the sample dilution d, with the inverse function Equation 5.1.

$$x' = d\left(\frac{y-a}{b}\right)^{\frac{1}{c}} \tag{5.1}$$

The 95% confidence intervals of x' are given by:

$$\sigma_{x'} = \sqrt{\left(\frac{\partial x'}{\partial a}\sigma_a\right)^2 + \left(\frac{\partial x'}{\partial b}\sigma_b\right)^2 + \left(\frac{\partial x'}{\partial c}\sigma_c\right)^2} \qquad (5.2)$$

where σ_a, σ_b and σ_c are the 95% confidence interval values on the parameters a, b and c provided by Tablecurve after the regression. The average concentration of a sample was then calculated by taking the average of m individual concentrations (x'). The 95% confidence interval on the average TGF-β2 concentration, $\overline{\sigma}_{x'}$, is given by:

$$\overline{\sigma}_{x'} = \sqrt{\sum_{i=1}^{m}\left(\frac{\sigma_{xi'}}{m}\right)^2} \qquad (5.3)$$

These calculations were performed with Excel 97 and the results were included as error bars on the average concentrations.

5.2.1.4 TGF-β2-Antibody Association at pH 4

It was found that acidifying WGFE to pH 2.5 and then adjusting the pH to 4 provided the highest active TGF-β2 concentration. According to Antonsen et al. (1991) antigen-antibody association is poor at pH less than 4. Therefore an association experiment was performed to determine the extent of TGF-β2 -antibody association at pH 4. If the extent of association at pH 4 was comparable to that at pH 7 then acid activation followed by adjustment to pH 4 would be the preferred activation method.

The association buffer selected was 50mM sodium acetate-150mM NaCl pH 4. The wells used in this experiment were included with the ELISA plates of section 5.2.2. The TGF-β2 coated and uncoated wells were prepared as for the standard association wells of section 5.2.2. The antibody samples were diluted to a concentration of 1 μg/ml with pH 4 buffer and 1 μg/ml with 10 mM Na_2HPO_4, 150 mM NaCl pH 7 buffer (control). The antibody samples (100 μl/well) were added to the ELISA plates and incubated for three hours at 37°C. The wells incubated with pH 4 buffer were washed six times with pH 4 buffer and the control wells were washed six times with phosphate wash buffer. The ELISA plates were then incubated on a shaker for fifteen minutes at room temperature with pH 4 buffer and phosphate wash buffer in the test and control wells respectively. The wells were washed three

times with phosphate ELISA wash buffer. Horseradish peroxidase-conjugated rabbit anti-mouse immunoglobulin antibody was diluted 1:2000 with 0.5% BSA in phosphate ELISA wash buffer. The secondary antibody was added to the plates at 100 µl/well and incubation continued for 90 minutes at 37°C. All of the wells were washed six times with phosphate ELISA wash buffer. o-phenylenediamine (OPD) solution was added to the plates at 100 µl/well and incubation continued for ten minutes at room temperature. The colour reaction was stopped with 50 µl/well of 1M H_2SO_4. The optical densities of the wells were measured at 490 nm with a plate reader. The corrected optical densities were determined by subtracting the optical densities of the uncoated wells from the optical densities of the TGF-β2 coated wells.

5.2.2 Eluent Screening

The immunoaffinity purification of TGF-β2 from WGFE requires a condition under which the TGF-β2 may be dissociated from the immobilised monoclonal antibody and recovered. This condition is termed elution and can be achieved by pressure, temperature, electrophoretic or chemical means (Yarmush et al., 1992). Special cases have been reported in the literature where the first three have been successful, however, chemical elution is the most commonly employed technique because it is generally simple and effective. Chemical eluents can be divided into the general classes of pH extremes, chaotropes, solvents and high ionic strength solutions. The ideal eluent for this system would quickly elute all of the bound TGF-β2 from the immobilised monoclonal antibody. Unfortunately, satisfying this condition can lead one to select a harsh eluent that rapidly denatures the binding capacity of the monoclonal antibody or denatures the biological activity of the recovered antigen. Therefore an eluent must be found that compromises on the conflicting objectives of effectiveness and the conservation of long-term binding capacity and antigen biological activity.

The eluent screening consists of identifying effective eluents from a large number of potential eluents and then measuring the decrease in binding capacity over long times of incubation in the effective eluents. In this way an effective eluent can be selected that conserves the antibody long-term binding capacity. The ELISA technique (Pepper, 1992) was adapted to the task of eluent screening because it is relatively quick and simple. In the experience of Pepper (1992), eluents that are capable of eluting in the ELISA format make suitable eluents in practical immunoaffinity separations. When screening for elution in the ELISA format, the

appropriate controls must be included to account for the dissociation of coated antigen from the polystyrene surface and the degradation of the antibody constant regions. Eluents from each of the general classes were included in the screening. Specifically they were potassium iodide, lithium 3,5-diiodosalicylate (chaotropes), glycine (pH extremes), magnesium chloride (ionic strength), isopropanol and dimethyl sulfoxide (solvents).

The TGF-β2 pool from the sixth purification was dialysed overnight against coating buffer pH 9.6. The dialysed TGF-β2 was then diluted to 1 μg/ml TGF-β2 with additional coating buffer and 100μl was added to each well of one half of the ELISA plates. Coating buffer (100μl/well) was delivered to the other halves of the ELISA plates and were incubated for three hours at 37°C after which they were washed four times with wash buffer (1.5mM KH_2PO_4, 6.5mM Na_2HPO_4, 0.5M NaCl+0.05% tween 20, pH 7.6). Each eluent test consisted of standard association wells, eluent pre-incubation wells and eluent test wells, each of which were conducted in triplicate wells on the TGF-β2 coated side and the blank side.

The pre-incubation wells were each filled with 100μl of eluent and the other wells were each filled with 100μl of wash buffer. The plates were incubated on a plate shaker for fifteen minutes at room temperature after which all of the wells were washed three times. The ELISA plates were blocked overnight at 4°C with 100μl per well of 2% BSA in wash buffer. The pre-incubation samples were prepared by adding eluent to monoclonal antibody solution (~400 μg/ml) in the ratio of 9:1. These samples were incubated for fifteen minutes with shaking at room temperature and then the samples were further diluted to an antibody concentration of 1 μg/ml with 10mM Na_2HPO_4, 150mM NaCl pH 7 (PBS). In this way, the robustness of the TGF-β2- monoclonal antibody binding, the robustness of the rabbit anti-mouse antibody-monoclonal antibody binding and the strength of TGF-β2 coating to the ELISA plate in the presence of the eluents were ascertained. Antibody was diluted to a concentration of 1 μg/ml with PBS for the standard association samples and the eluent test samples. The standard association samples were made up by adding eluent at a dilution commensurate with the eluent dilution in the pre-incubation samples. In this way it was ensured that the dilution of the eluent after the eluent pre-incubation was sufficient for binding to be unaffected relative to binding in the absence of eluent.

The next day the antibody samples (100 µl/well) were added to the ELISA plates and incubated for three hours at 37°C. All of the wells were washed six times but wash buffer was allowed to remain in all of the wells except the eluent test wells to which were added 100 µl/well of eluent. The ELISA plates were incubated on the plate shaker for fifteen minutes at room temperature after which all of the wells were washed three times with wash buffer. Horseradish peroxidase-conjugated rabbit anti-mouse immunoglobulin antibody was diluted 1:2000 with 0.5% BSA in wash buffer. The secondary antibody was added to the plates at 100 µl/well and incubation continued for 90 minutes at 37°C. All of the wells were washed six times with wash buffer. o-phenylenediamine (OPD) solution was added to the plates at 100 µl/well and incubation continued for ten minutes at room temperature. The colour reaction was stopped with 50 µl/well of 1M H_2SO_4. The optical densities of the wells were measured at 490 nm with a plate reader (Bio-Rad 450, Hercules, CA, USA). The corrected optical densities were determined by subtracting the optical densities of the uncoated wells from the optical densities of the TGF-β2 coated wells.

5.2.3 Long-term Binding Capacity Degradation

The experiment described in section 5.2.2 provided a crude measure of the degradation in binding capacity that occurs upon contact with various eluents. A method was developed to quantify this degradation as a function of time without interference from stripping of TGF-β2 from the ELISA plate or degradation of the antibody constant regions. According to Antonsen et al. (1991) binding capacity degradation occurs by the irreversible denaturation of the antigen-binding site. This does not result in a partial retention of binding capacity by the degraded site but in a total loss of capacity. This conclusion was made because eluent contact did not change the equilibrium association constant but did reduce the binding capacity over a period of time for the BSA-antibody system of Antonsen et al. (1991).

The test samples were prepared by adding eluent to antibody solution (~400 µg/ml) in the ratio of 9:1. At the same time, negative control samples were prepared by adding diluent (PBS+0.5% BSA) to antibody solution (~400 µg/ml) in the same ratio. Precautions were taken to prevent microbial contamination of the samples and non-specific adsorption of TGF-β2 to the tubes. The tubes were exposed to ultraviolet light for ten minutes, the caps were only opened in a laminar flow hood and all solutions were filtered through 0.22 µm

membranes. To minimise non-specific binding of TGF-β2, the tubes were siliconised and BSA was included in the diluent buffer. The tubes were capped and incubated at room temperature. At ten time points an aliquot was taken from each antibody-eluent sample and diluted with diluent to 1 μg/ml antibody. The zero time point binding capacity was represented by the negative control samples.

The ELISA technique was used to measure the concentration of viable antibody after the eluent incubations. ELISA plates were prepared as described in section 5.2.2 and samples were added in triplicate (100 μl/well) to the coated and uncoated sides. Standard curves of viable antibody were included so that the optical densities of the samples could be related to viable antibody concentrations. Tablecurve was used to fit Equation 2.2, $y = a + bx^c$, to the viable antibody concentration (x) versus OD 490nm (y) plot. The dose response data for the denatured antibody sample were imported to Tablecurve and viable antibody concentrations (x) were computed from the optical density (y) values with the inverse function of Equation 2.2. The viable antibody concentrations were plotted as a function of eluent incubation time.

5.2.4 Kinetics of the TGF-β2-Antibody Interaction

5.2.4.1 Biacore 2000 Instrument

The Biacore 2000 (Pharmacia Biosensor AB, Uppsala, Sweden) is an instrument that is designed to measure the rates of binding interaction between a solid phase ligand and a solution phase analyte. The solid phase ligand is chemically immobilised to carboxymethylated dextran that is linked to a gold surface (Figure 5.1). Changes in the refractive index, close to the sensor surface, are monitored using surface plasmon resonance (SPR) detection as a function of time. The change in refractive index is proportional to the accumulation of mass at the surface. In a typical experiment, the association phase consists of pumping a laminar flow of analyte solution over the surface while the analyte binds to the immobilised ligand. In the dissociation phase the analyte is eluted from the surface by buffer and the loss of bound analyte is monitored. In this way the kinetic rate constants for the antibody-antigen interaction can be determined. The advantages of using the Biacore to measure interaction rate constants relative to other techniques is that it monitors binding in real time, it is automated and it requires relatively small amounts of the antibody and antigen.

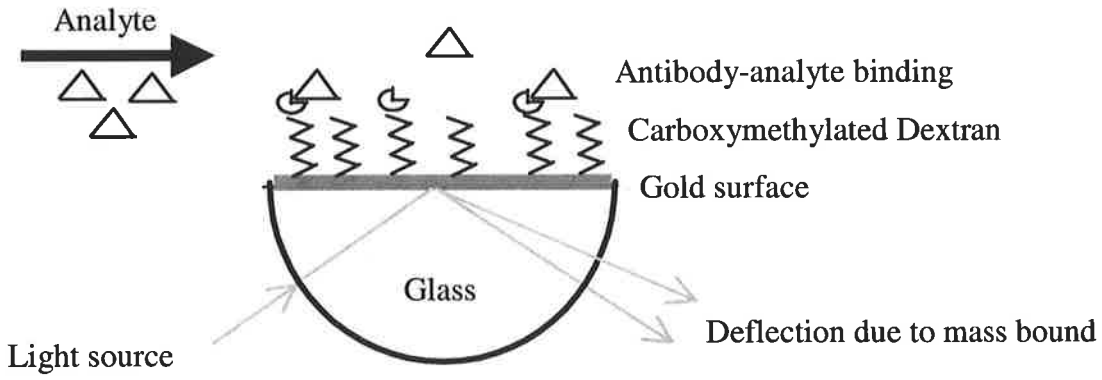

Figure 5.1: Schematic diagram of the principles involved in the Biacore instrument. *A laser light source is directed through a glass prism at the angle of total internal reflection. A quantum mechanical phenomenon, known as a plasmon, develops at the gold surface and resonates in proportion to the mass of material deposited at the surface. This results in a deflection in the totally internally reflecting light beam, which is measured by the instrument.*

5.2.4.2 TGF-β2 Immobilisation to the Sensor Chip

It was preferable for TGF-β2 to be immobilised to the chip surface because larger amounts of pure antibody are available than pure TGF-β2 and also TGF-β2 is more resistant to harsh regenerant conditions than the antibody. Recombinant human TGF-β2 (Sigma, St. Louis, MO, USA) was immobilised to a CM5 sensor chip (Pharmacia Biosensor AB, Uppsala, Sweden) with N-hydroxysuccinimide (NHS)/1-ethyl-3-(3-dimethylaminopropyl)-carbodiimide (EDC) chemistry in a method recommended by the manufacturers. The immobilisation reaction chemistry is shown in Figure 5.2. Two flow paths on the chip surface were utilised; no antibody was immobilised to the first (blank flow path) and TGF-β2 was immobilised to the second. HBS buffer (10 mM HEPES pH7.4, 150 mM NaCl, 3.4 mM EDTA, 0.005% Surfactant P20) was pumped over the surface of the Biacore sensor chip at 5 µl/min. Fifty µl of NHS stock solution and 50 µl of EDC stock solution were mixed and 35 µl of the mixture was injected over the surface of the chip. TGF-β2 was diluted 1:2 from an original concentration of 20 µg/ml in 30% acetonitrile/ 0.1% TFA with 10 mM sodium acetate pH 5. The pH of the solution was adjusted to ~6 and 95 µl of the TGF-β2 solution was injected on to the chip surface. Unused NHS moieties were then blocked with a 35 µl pulse of 1M ethanolamine pH 8.5. An increase in the instrument response of 1657 RU after the procedure indicated that TGF-β2 had immobilised. This response corresponds to an adsorbed protein surface concentration of 1.657 ng/mm^2 according to Stenberg et al. (1991)

who found that a correlation exists between the SPR signal response and the protein surface concentration. The blank flow path was prepared in a similar manner to the preceding immobilisation but 35 µl of 10 mM sodium acetate pH 5 was injected in place of TGF-β2 solution.

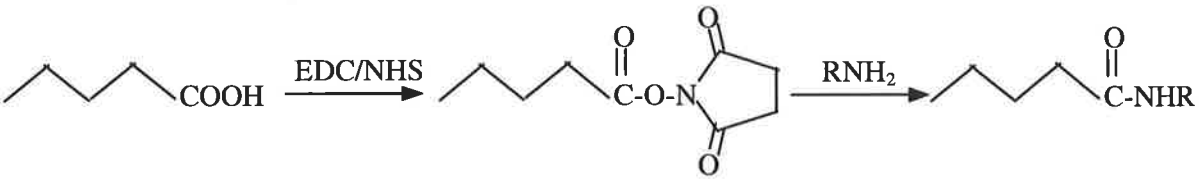

Figure 5.2: NHS/EDC immobilisation chemistry for coupling antibody, R, to the carboxymethylated sensor chip surface *(BIAapplications Handbook, 1995).*

5.2.4.3 Binding to Surface TGF-β2

Fifteen µl of 100 µg/ml anti-TGF-β1,2,3 monoclonal antibody (Genzyme, MA, USA) in HBS was injected at 5 µl/min over the surface of both flow paths. After the injection, the chip surface was washed with HBS and the remaining bound material was desorbed from the surface by injecting 15 µl of 0.1M HCl because TGF-β2 was known to be acid resistant. The chip surface was washed again with HBS to equilibrate the immobilised TGF-β2. Fifteen µl of 10 µg/ml anti-TGF-β1,2,3 antibody was injected, the surface was washed with HBS and then regenerated with 0.1M HCl.

Fifteen µl of conditioned medium from hybridoma 5D4-1D9 was injected at 5 µl/min over the surface of both flow paths. The surface was washed with HBS and regenerated. Fifteen µl of conditioned medium from hybridoma 8A3-1G3 was injected. The surface was then similarly washed with HBS and regenerated.

The sensorgram data were processed with Biaevaluation 3.0 software (Pharmacia Biosensor AB, Uppsala, Sweden). The sensorgrams were transformed to zero baseline by selecting the portion of the sensorgram prior to analyte injection and using the function "Y-transform to average of selection". To account for the delay that occurs as the TGF-β2 solution front reaches the flow paths sequentially, the sensorgrams were transformed in the time axis so that the binding curves commenced at the same time point. To account for the response artefacts

of solution refractive indices and non-specific binding, the response of the blank flow path was subtracted from the antibody immobilised flow path responses for all time points.

5.2.4.4 Antibody Immobilisation to the Sensor Chip

It was found that immobilising TGF-β2 to the chip surface was unsuitable for the elucidation of the TGF-β2-antibody reaction kinetics. Anti-TGF-β1,2,3 monoclonal antibody was immobilised to a CM5 sensor chip with NHS/EDC chemistry in the method recommended by the manufacturers. Two flow paths were utilised on the chip surface; no antibody was immobilised to the first (blank flow path) and monoclonal antibody was immobilised to the second. Fifty µl of NHS stock solution and 50 µl of EDC stock solution were mixed and 35 µl of the mixture was injected over the surface of the chip. Antibody was diluted 1:20 from an original concentration of 1 mg/ml with 10 mM sodium acetate pH 5. Thirty-five µl of the antibody solution was injected on to the chip surface and unused NHS moieties were blocked with a 35 µl pulse of 1M ethanolamine pH 8.5. An increase in the instrument response of 14200 RU after the procedure indicated that antibody had immobilised. The blank flow path was prepared in a similar manner to the preceding immobilisation by injecting 35 µl of 10 mM sodium acetate pH 5 in place of antibody solution.

Antibodies 5D4 and 8A3, that had been purified by Protein G affinity chromatography, were immobilised to another CM5 sensor chip with NHS/EDC chemistry. Three flow paths on the chip surface were utilised; no antibody was immobilised to the first (blank flow path), 5D4 antibody was immobilised to the second and 8A3 antibody was immobilised to the third. Fifty µl of NHS stock solution and 50 µl of EDC stock solution were mixed and 35 µl of the mixture was injected over the surface of the chip. Antibody 5D4 was diluted from an original concentration of approximately 400 µg/ml to a concentration of 100 µg/ml with 10 mM sodium acetate pH 5. Fourteen µl of the antibody solution was injected on to the chip surface. Unused NHS moieties were then blocked with a 35 µl pulse of 1M ethanolamine pH8.5. An increase in the instrument response of 2281 RU after the procedure indicated that antibody had immobilised. Antibody 8A3 was immobilised to another flow path in a similar manner by injecting 23 µl of 100 µg/ml on to the chip surface. An increase in response of 915 RU indicated that antibody had immobilised. The blank flow path was prepared in a similar manner to the preceding immobilisation but 70 µl of 10 mM sodium acetate pH 5 was

injected in place of antibody solution. An increase in response of 175 RU was negligible in comparison to the response increases observed for the antibody immobilisations.

5.2.4.5 Surface Regeneration

After having bound analyte to the surface it must be desorbed so that the original binding capacity is regained and another binding cycle can be conducted. This rate of desorption is slow in binding buffer and therefore an eluent must be selected for the fast regeneration of the surface. The Biacore manufacturers suggest the use of eluents such as 0.1M HCl and 1.5M glycine pH 2.5. However, these eluents are harsh and the binding capacity would have been rapidly degraded. It is shown in sections 5.3.2 and 5.3.3 that 0.1M glycine pH 3.5 and 0.1M glycine pH 3 were effective eluents for antibodies 5D4 and 8A3 and yet retained their binding capacities for TGF-β2 after long-term exposure to these eluents. An experiment was conducted to assess the effectiveness of these eluents for the regeneration of the sensor chip.

The sixth pool of TGF-β2 activity (Table 2.7) was dialysed overnight against 1L of PBS. TGF-β2 ELISA (Promega, Madison, WI, USA) demonstrated a TGF-β2 concentration with a 95% confidence interval of 0.908±0.226 μg/ml. The running buffer was changed to PBS because Biacore HBS was not considered to be a realistic buffer system for a large-scale purification process. Fifty μl of 0.908 μg/ml TGF-β2 was injected over the surface for all flow paths. Relative to the blank flow path, the antibody immobilised flow paths showed a binding response. After the injection, PBS began to wash the chip surface and the amount of bound material began to decrease. The flow rate was increased to 40 μl/min in order to simulate the conditions during the kinetic study. A series of prospective eluents of volume 200 μl were injected on to the chip surface; the eluents were 0.1M glycine pH 4.5, 0.1M glycine pH 4.0, 0.1M glycine pH 3.5, 0.1M glycine pH 3.0, 0.1M glycine-0.5M NaCl pH 3.5 and 0.1M glycine-0.5M NaCl pH 3.0.

5.2.4.6 Kinetic Study for Binding to Surface Antibody

The fourth pool of TGF-β2 activity (Table 2.5) was lyophilised, resuspended in HBS and injected on to the chip surface coupled with anti-TGF-β1,2,3 monoclonal antibody. Ten μl of 1, 5, 10, 20 and 50 μg/ml TGF-β2 in HBS was injected sequentially at 5 μl/min over the

surface of both flow paths. After each injection, the chip surface was washed with HBS and the remaining bound material was desorbed from the surface by injecting 5 µl of 1.5M glycine pH 2.5. No study was undertaken to determine whether more gentle eluents were effective in regenerating the chip surface.

A method program was written for the collection of sensorgrams from the injection of eight samples on to the chip coupled with antibodies 5D4 and 8A3. Four different concentrations of TGF-β2 were made up with PBS in duplicate: 5.81 nM, 8.94 nM, 17.88 nM and 35.76 nM. The instrument selected the samples randomly and injected 240 µl of each sample at a rate of 40 µl/min over all flow paths. After the injection, PBS was pumped over the chip for ten minutes at 40 µl/min and the surface was regenerated with a 200 µl pulse of 0.1M glycine-0.5M NaCl pH 3.0. After the regeneration, PBS was pumped over the chip prior to the next sample injection. The sensorgram data were processed with Biaevaluation 3.0 software as described in section 5.2.4.3.

The kinetic study experiment was repeated with recombinant human TGF-β2 (Sigma, St. Louis, MO, USA) at similar sample concentrations to determine whether contaminating proteins in the partially purified TGF-β2 preparation were responsible for the observed binding curves. The recombinant human TGF-β2 was dialysed against PBS and the TGF-β2 concentration was assayed with TGF-β2 ELISA. Partially purified TGF-β2 was injected on to the chip surface to ensure that the binding capacity of the immobilised antibody did not significantly differ from that in the previous binding study.

5.2.4.7 Regression of Sensorgrams to Kinetic Models

The sensorgram curves of antibodies 5D4 and 8A3 for the binding of partially purified TGF-β2 were regressed using two different pre-defined models with Biaevaluation 3.0. The first was a Langmuir 1:1 binding interaction model and the second was a heterogeneous ligand model with parallel reactions. The reaction schemes and the corresponding rate equations for each of these models are described below. The pre-defined models contain an additional regression constant that accounts for the change in the response when a solution with a refractive index different to that of the running buffer passes over the chip surface. The blank flow path response was subtracted from the antibody immobilised flow paths in order to

negate the bulk effects. The pre-defined models were edited to remove the bulk effect regression constant from the analysis.

In a Langmuir 1:1 binding interaction analyte *A* binds immobilised molecule *B*:

$$A + B \underset{k_d}{\overset{k_a}{\rightleftharpoons}} AB \tag{5.4}$$

The following rate equations may be written for the immunocomplex concentration, [*AB*]:

$$\frac{d[AB]}{dt} = k_a[A][B] - k_d[AB] \tag{5.5}$$

In terms of parameters measured by the Biacore:

$$\frac{dR}{dt} = k_a C(R_{\max} - R) - k_d R \tag{5.6}$$

where R is the response, C is the analyte concentration and R_{max} is the analyte binding capacity of the immobilised antibody.

In the heterogeneous ligand model, two different ligands, B_1 and B_2 compete for binding to the same analyte, *A*:

$$A + B_1 \underset{k_{d1}}{\overset{k_{a1}}{\rightleftharpoons}} AB_1 \tag{5.7}$$

$$A + B_2 \underset{k_{d2}}{\overset{k_{a2}}{\rightleftharpoons}} AB_2 \tag{5.8}$$

The following rate equations may be written for the immunocomplexes, $[AB_1]$ and $[AB_2]$:

$$\frac{d[AB_1]}{dt} = k_{a1}[A][B_1] - k_{d1}[AB_1] \tag{5.9}$$

$$\frac{d[AB_2]}{dt} = k_{a2}[A][B_2] - k_{d2}[AB_2] \tag{5.10}$$

In terms of parameters measured by the Biacore:

$$\frac{dR}{dt} = k_{a1}C(R_{\max 1} - R_1) + k_{a2}C(R_{\max 2} - R_2) - k_{d1}R_1 - k_{d2}R_2 \tag{5.11}$$

where R is the total response, R_1 and R_2 are the individual responses for ligands B_1 and B_2, C is the analyte concentration and R_{max1} and R_{max2} are the analyte binding capacities of ligands B_1 and B_2 respectively.

The goodness of fit between the fitted curve and the experimental data is expressed in terms of the χ^2-test:

$$\chi^2 = \frac{\sum_{1}^{n}(r_f - r_x)^2}{n - p} \qquad (5.12)$$

where r_f is the fitted value at a given point, r_x is the experimental value at the same point, n is the number of data points and p is the number of degrees of freedom.

5.2.5 Antigen Capture ELISA

The commercially available TGF-β2 ELISA (Promega, Madison, WI, USA) was employed to determine whether antibodies 5D4 or 8A3 could be coated on to an ELISA plate and used for the capture of TGF-β2. The wells of an ELISA plate were coated with 100 µl per well of 1, 10 and 100 µg/ml antibody 5D4, 1, 10 and 100 µg/ml antibody 8A3, 1 µg/ml Promega anti-TGF-β2 monoclonal antibody and coating buffer (25 mM $NaHCO_3$, 25 mM Na_2CO_3 pH 9.2). These solutions coated the ELISA plate overnight at 4°C and on the next day the plate was blocked for 50 minutes at 37°C. Dilutions of the following solutions of TGF-β2 were prepared with sample buffer: Promega porcine TGF-β2 standard (1 ng/ml), the sixth TGF-β2 pool (6.2 ng/ml), activated WGFE (1.2 ng/ml), activated WGFE (700 ng/ml) and sample buffer (0 ng/ml). Each sample (100 µl per well) was added to seven wells, each of which were coated with a different antibody or antibody concentration. The ELISA was subsequently performed as described in section 2.2.2.

Flanders et al. (1990) reported that the addition of 40 mM dithiothreitol to buffer enhanced the amount of immunoprecipitation of ^{125}I-TGF-β2 with polyclonal antisera against synthetic peptides of TGF-β2. Theoretically dithiothreitol reduces and partially unfolds the TGF-β2 molecule thereby exposing linear epitopes to which the antibodies have been raised. The antigen capture ELISA was repeated by coating the ELISA plate with 100 µl per well of 1 µg/ml Promega antibody, 1 µg/ml antibody 5D4 and 1 µg/ml antibody 8A3. Dilutions of 18 ng/ml TGF-β2 were prepared in 0, 1, 5, 10, 40 and 100 mM dithiothreitol. The ELISA plate

was blocked and samples (100 µl) of the dilutions were added to coated and uncoated wells. The ELISA was subsequently performed as described in section 2.2.2. The extent of specific binding was determined by subtracting the optical density of the uncoated well from the optical density of the corresponding coated well. This was done to account for increases in non-specific binding in the presence of dithiothreitol.

5.2.6 Antibody Immobilisation to Ultrabind Membrane

Chapter 4 showed that the economic performance of an affinity membrane is theoretically superior to a column of Sepharose particles. In view of this considerable potential, attempts were made to immobilise antibody to Ultrabind US450 membrane (Gelman Sciences, Ann Arbor, MI, USA). The membrane is manufactured from polyethersulfone with a pore size of 0.45 µm and has aldehyde groups that permit the covalent immobilisation of proteins (Pemawansa et al., 1990).

5.2.6.1 Immobilisation Chemistry

The Ultrabind membrane has a high density of aldehyde sites available for covalent bonding with amine groups. The manufacturers claim that the bond with polyamines, such as proteins, is very stable even without cyanoborohydride reduction. Immobilisation chemistries that have proven successful for membrane systems include the hydrazide activation chemistry (Nachman et al., 1992), tosyl chloride activation chemistry (Kasper et al., 1997) and EDC activation chemistry (Suen and Etzel, 1994). The activation mechanisms for these chemistries are shown in Figures 5.3 to 5.6.

- Aldehyde coupling chemistry

A modified method of Pemawansa et al. (1990) was used to immobilise antibody to the Ultrabind membrane. Three square pieces (2×2 cm) were cut from the Ultrabind membrane sheet. Antibody 5D4 was resuspended from a lyophilised preparation to a concentration of ~5 mg/ml with 300 µl of distilled water. Similarly, antibody 8A3 was resuspended to a concentration of ~5 mg/ml with 333 µl of distilled water. Two of the membrane pieces were placed in small petri dishes (Costar, Cambridge, MA, USA). One membrane piece was spot-wetted with 45 µl of 5 mg/ml antibody 5D4 and the other was spot-wetted with 45 µl of 5 mg/ml antibody 8A3. The antibody was distributed uniformly over the surface of the membrane pieces and was allowed to dry overnight at room temperature.

The next day, the three membrane pieces were incubated in 10 ml of 1M ethanolamine pH 9 for 2.5 hours with shaking at room temperature in order to block residual aldehyde groups. The blocking solution was discarded and replaced with 10 ml wash buffer (1.5mM KH_2PO_4, 6.5mM Na_2HPO_4, 0.5M NaCl+0.05% tween 20, pH 7.6) to wash any non-covalently bound antibody from the membrane. Incubation continued for two hours with shaking at room temperature and then the membranes were stored in PBS+0.02% sodium azide at 4°C.

Figure 5.3: Aldehyde coupling chemistry of Ultrabind membrane *(Pemawansa et al., 1990).*

- Hydrazide coupling chemistry

A modified method of Hermanson et al. (1992) was used to immobilise antibody to Ultrabind membrane. Adipic acid dihydrazide (Fluka Chemie AG, Switzerland) was dissolved to a concentration of 0.5M in 0.1M 2-(N-Morpholino)ethanesulphonic acid (MES) buffer pH 4.75. Three pieces (3.1×3.1 cm) were cut from the Ultrabind membrane sheet and were incubated in 0.5M adipic acid dihydrazide for four hours with shaking at room temperature. After this time, the solution was drained off, washed three times with distilled water, three times with 1M NaCl and three times again with distilled water.

The cis-diols in the Fc portion of the antibodies were oxidised to aldehydes with sodium metaperiodate in the following manner. Lyophilised antibody 5D4 (9 mg) was resuspended with distilled water to a concentration of ~5 mg/ml. Lyophilised antibody 8A3 (10.4 mg) was resuspended with distilled water to a concentration of ~5 mg/ml. The pools of antibody were dialysed overnight at 4°C against 1L of 0.1M KH_2PO_4 pH 5.5. The next day, the dialysis membranes were opened and their contents were filtered through 0.2 µm filters and placed into siliconised tubes. One-tenth the volume of 0.1M sodium metaperiodate (Sigma, St. Louis, MO, USA) solution was added to each of the antibody solutions. The tubes were wrapped in aluminium foil to prevent the admittance of light and placed on a shaker at room

temperature. Antibody 5D4 was oxidised for 90 minutes and antibody 8A3 was oxidised for 155 minutes.

A column (Vantage L 11×250, Amicon, Beverly, MA, USA) was packed to a height of 11 cm with fine Sephadex G25 (AMRAD Pharmacia Biotech). Approximately 3.5 ml of the oxidation mixture (antibody 5D4) was loaded on to the desalting column at 1 ml/min with an FPLC unit (AMRAD Pharmacia Biotech). A 1 ml/min flow of 0.1M KH_2PO_4 was maintained after the oxidation mixture had loaded and a volume of 10 ml was collected that corresponded to the absorbance peak at 280 nm. Approximately 5 ml of the oxidation mixture (antibody 8A3) was loaded on to the desalting column. A volume of 10 ml was collected that corresponded to the absorbance peak.

The three membrane pieces were placed in separate weigh boats. To each was added 10 ml of 0.1M KH_2PO_4 pH 5.5, 10 ml of desalted oxidised antibody 5D4 and 10 ml of desalted oxidised antibody 8A3. Incubation continued overnight with shaking at room temperature. The solutions were removed from the membranes and a 50mM sodium cyanoborohydride (Sigma, St. Louis, MO, USA) solution was prepared with 0.1M KH_2PO_4 pH 5.5. To each membrane piece was added 3.3 ml of 50mM sodium cyanoborohydride and the incubations continued for two hours with shaking at room temperature. The membrane pieces were each washed nine times with 0.1M KH_2PO_4 pH 5.5 before use in the binding capacity experiment.

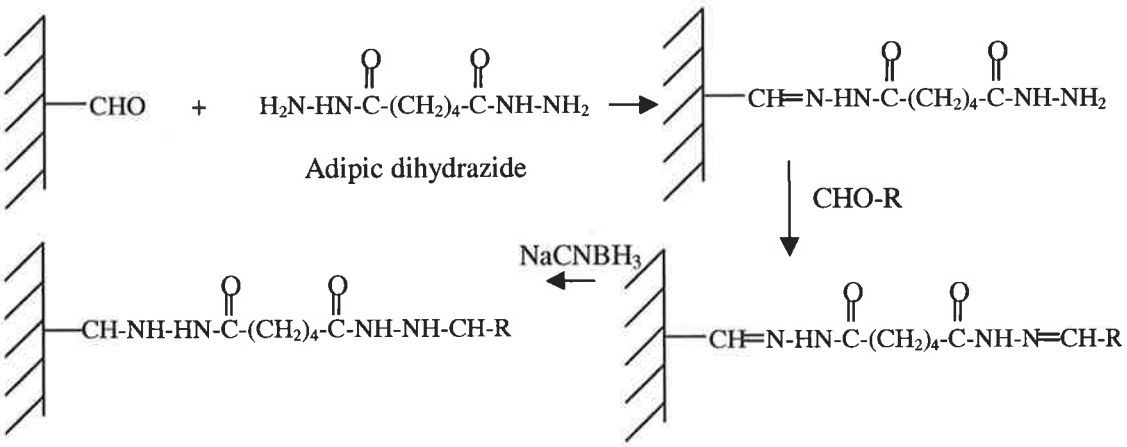

Figure 5.4: Hydrazide coupling chemistry of Ultrabind membrane *(Hermanson et al., 1992).*

- Tosyl chloride coupling chemistry

A modified method of Hermanson et al. (1992) was used to immobilise antibody to Ultrabind membrane. Three square pieces of membrane (3.1×3.1 cm) were cut from the Ultrabind membrane sheet. The membrane pieces were incubated in 10 ml of 1M ethanolamine pH 9 for two hours with shaking at room temperature. The membrane pieces were washed three times with distilled water, and then with 10 ml of 30:70, 10 ml of 60:40 and 10 ml of 80:20 (v/v) acetone: distilled water mixtures. The membrane pieces were then washed five times with pure acetone. A 6% (w/v) solution of p-toluenesulfonyl chloride (Sigma, St. Louis, MO, USA) in acetone was prepared. The membrane pieces were soaked in this solution for one hour at room temperature. During this time, 100 µl of pyridine was added to the reaction mixture every six minutes to neutralise the liberated HCl. The activated membrane pieces were washed with 10 ml of 30:70, 50:50 and 70:30 (v/v) 1 mM HCl: acetone mixtures. The membrane pieces were then washed with pure 1 mM HCl.

Lyophilised antibody 5D4 (4.6 mg) and lyophilised antibody 8A3 (5.3 mg) were each resuspended in 1 ml of distilled water. Each antibody solution was adjusted to pH~8 with NaOH. The membrane pieces were incubated overnight separately in 1 mM HCl, 1 ml of 4.6 mg/ml antibody 5D4 and 1 ml of 5.3 mg/ml antibody 8A3 with shaking at room temperature. The next day, the solutions were drained and replaced with 1M ethanolamine pH 9 in order to block the unreacted tosylate groups. The incubations continued for 2.5 hours with shaking at room temperature. The membrane pieces were washed three times in 0.25M Na_2CO_3 pH 9.5, 1M NaCl and 0.25M Na_2CO_3 pH 9.5 again.

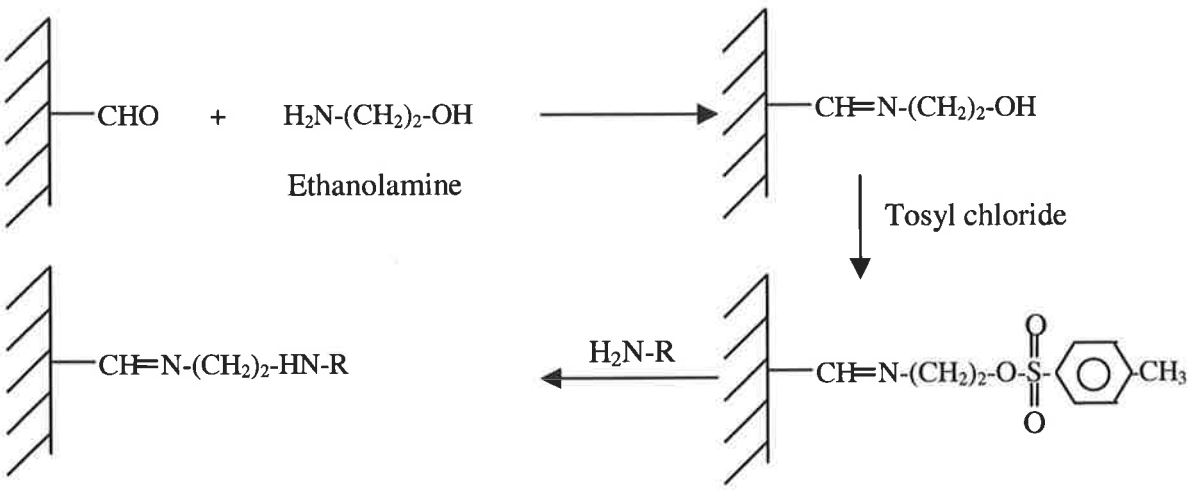

Figure 5.5: Tosyl chloride coupling chemistry of Ultrabind membrane *(Hermanson et al., 1992).*

- EDC coupling chemistry

A modified method of Hermanson et al. (1992) was used to immobilise antibody to Ultrabind membrane. Three square pieces of Ultrabind membrane (3.1×3.1 cm) were cut from the Ultrabind membrane sheet. A solution of 6-aminocaproic acid (0.763M) was prepared in 0.1M K_2HPO_4 pH 7.5. The membrane pieces were incubated overnight in this solution with shaking at room temperature. On the following day the pieces were washed three times with distilled water, 1M NaCl and again with distilled water. Lyophilised antibody 5D4 (4.6 mg) and lyophilised antibody 8A3 (5.3 mg) were each resuspended in 1 ml of 0.1M MES pH 4.75 buffer. Thirty mg of 1-ethyl-3-(3-dimethylaminopropyl)-carbodiimide (Sigma, St. Louis, MO, USA) was dissolved in each of the antibody solutions and in 1 ml of 0.1M MES pH 4.75 buffer. The membrane pieces were incubated in these solutions for 4.5 hours with shaking at room temperature. They were then washed twice in 0.1M MES pH 4.75 buffer, three times in 1M NaCl and twice again in 0.1M MES pH 4.75.

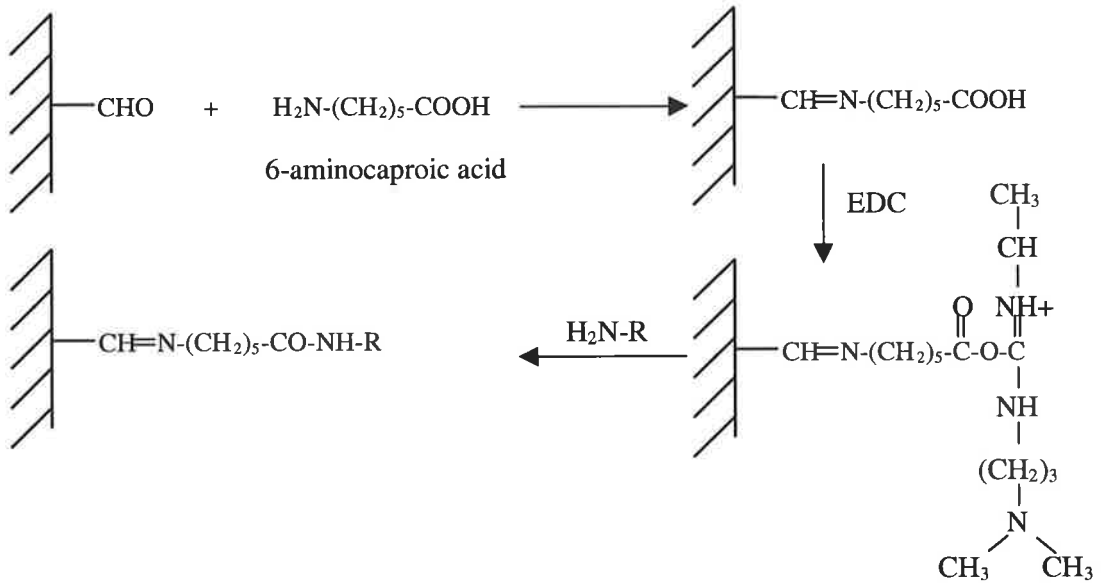

Figure 5.6: EDC coupling chemistry of Ultrabind membrane *(Hermanson et al., 1992).*

5.2.6.2 Antibody Coupling Density

The macro BCA Protein Assay kit (Pierce, Rockford, IL, USA) of section 2.2.3 was used to determine the antibody coupling density on the membranes. Dilutions of BSA ranging in protein concentration from 0 to 2 mg/ml were prepared from a 2 mg/ml BSA stock (Pierce, Rockford, IL). Ten µl of each dilution was added to the wells of a 96-well microtitre plate (Iwaki, Japan) and 200 µl of BCA working reagent was added to each well. Sections with the dimensions 0.5×0.5 cm were cut from the negative control membrane and the antibody

coupled membranes. The sections were placed in 1.5 ml conical tubes with 1 ml of BCA working reagent each and the tubes were capped. The standards and samples were incubated at room temperature for at least four hours. The next day, 50 µl samples from each BSA dilution were delivered to three new wells. In addition, 18×50 µl samples of the BCA reagent from each membrane piece were transferred to wells of the 96-well plate. The optical density of each well was read with a plate reader (Bio-Rad 450, Hercules, CA, USA) at a wavelength of 570 nm. The dimensions of the membrane sections were measured in order to determine the area, *A*.

The standard dose response curve was imported to Tablecurve and constants *a*, *b* and *c* were regressed to Equation 2.2 where *x* is the protein concentration in µg/ml and *y* is the optical density at 570 nm. The dose response data for the membranes were imported to Tablecurve and the protein concentrations (*x*) were computed from the optical density (*y*) values with the inverse function of Equation 2.2. The quantity of protein coupled to each membrane was calculated with Excel 97. It was found that the negative control membranes also reacted with the BCA reagent to give an absorbance at 570 nm. However, the antibody-coupled membranes always gave a higher absorbance than the negative control membranes. It is thought that ethanolamine and adipic acid dihydrazide were responsible for this artefact. The antibody coupling density, *AD*, was calculated with Equation 5.13:

$$AD = \left(\frac{Concentration}{Membrane\ Area} - \frac{Negative\ control\ concentration}{Negative\ control\ membrane\ Area} \right) \times Volume \qquad (5.13)$$

5.2.6.3 Static Binding Capacity for TGF-β2

Static incubation experiments were performed to determine whether TGF-β2 specifically binds and elutes from antibody coupled membrane. A method similar to that of Soltys and Etzel (1998) was employed. The sixth TGF-β2 pool was dialysed overnight against 10 mM Na_2HPO_4, 150 mM NaCl pH 7 (PBS) at 4°C. The uncoupled membrane piece (negative control) and the antibody coupled membrane pieces were incubated overnight in the TGF-β2 preparation with agitation at room temperature. The next day, the TGF-β2 preparation was drained from the membrane pieces, which were then dipped into wash buffer (1.5mM KH_2PO_4, 6.5mM Na_2HPO_4, 0.5M NaCl+0.05% tween 20, pH 7.6) and then placed into separate fresh weigh boats. Ten ml of eluent (0.1M glycine, 0.5M NaCl pH 3) was placed into

each weigh boat and the membrane pieces were incubated in this solution for one hour with shaking at room temperature. After the incubation, the TGF-β2 concentrations of the eluents were determined with TGF-β2 ELISA (Promega, Madison, WI, USA).

5.3 Results and Discussion

5.3.1 Activation of WGFE

WGFE was subject to various activating conditions in order to find the condition that maximised the active TGF-β2 concentration. Table 5.1 shows the active TGF-β2 concentration measured by TGF-β2 ELISA when WGFE was heated or subject to pH adjustment.

Conditions	Exposure time	TGF-β2 specific activity (ng/mg)
No activation		3.7±2.0
Acid HCl (pH 2.5)	Overnight	120±60
Acid HCl (pH 2.5)	Transient- adjusted to pH 7	14.2±4.0
Alkali NaOH (pH 13)	Overnight	0
Alkali NaOH (pH 12)	Overnight	25±19
Alkali NaOH (pH 11)	Overnight	28±20
Alkali NaOH (pH 10)	Overnight	17±13
Alkali NaOH (pH 9)	Overnight	7.1±4.6
Heat (80°C)	5 minutes- cooled to room T	2.5±0.7

Table 5.1: Active TGF-β2 concentration measured by TGF-β2 ELISA when WGFE (Lot D15157) was subject to various activating conditions. *Confidence intervals of 95% are shown.*

Rogers et al. (1996) reported specific activities of 0.8 ng/mg for unactivated WGFE, 42.2 ng/mg for acidification to pH 2.0, 26.0 ng/mg for alkaline conditions (pH 11) and 9.07 ng/mg for heat (100°C) as measured by Mv1Lu bioassay. These specific activities are of similar magnitude to the specific activities shown in Table 5.1.

Antonsen et al. (1991) found that poor antigen-antibody binding occurred outside the pH range of 4 to 11 for a BSA-anti-BSA monoclonal antibody system. As shown in section 5.3.2 extremes of pH are effective eluents for this immunoaffinity system. It is therefore important

that after activation, the WGFE is returned to a state at which antibody-TGF-β2 binding can take place.

5.3.1.1 Acid Activation and Reneutralisation of WGFE

WGFE was diluted to protein concentrations of 30.1, 22.6, 15.0 and 7.52 mg/ml with 150 mM NaCl. The four samples were acidified to pH 2.5 with HCl and incubated overnight at 4°C. The next day each sample was further sub-divided into four sub-samples. Sodium hydroxide was added to the sub-samples to increase the pH to 4, 5, 6 and 7. The sub-samples were incubated overnight at 4°C and, on the following day, the sub-samples were centrifuged. The supernatants were decanted, filtered and subjected to protein and TGF-β2 determinations. Figure 5.7 shows the TGF-β2 concentration in the supernatant of each sub-sample from the 30.1 mg/ml sample as a function of the final adjusted pH.

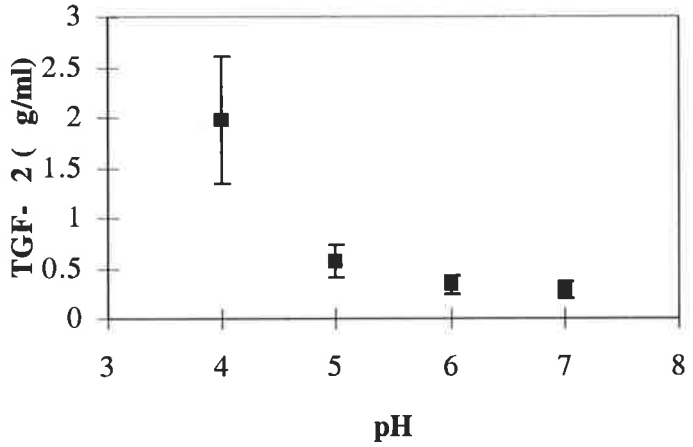

Figure 5.7: TGF-β2 concentration in the supernatant of each sub-sample from the 30.1 mg/ml sample that was acidified to pH 2.5 with HCl. *The sub-samples were reneutralised to the pH as shown. The error bars refer to the 95% confidence interval on each concentration.*

The TGF-β2 concentration in the supernatant decreased substantially as the pH increased (Figure 5.7). This trend was typical for all of the WGFE protein concentrations. Figure 5.8 shows the proportion of total protein that was lost as precipitate after the pH increase overnight. At pH 4 an insignificant amount of protein was lost and a high TGF-β2 concentration was measured but at pH above 4 substantial amounts of protein precipitated and low TGF-β2 concentrations were measured. There was evidence that a lower starting protein concentration prior to activation resulted in a slightly lower percentage protein loss.

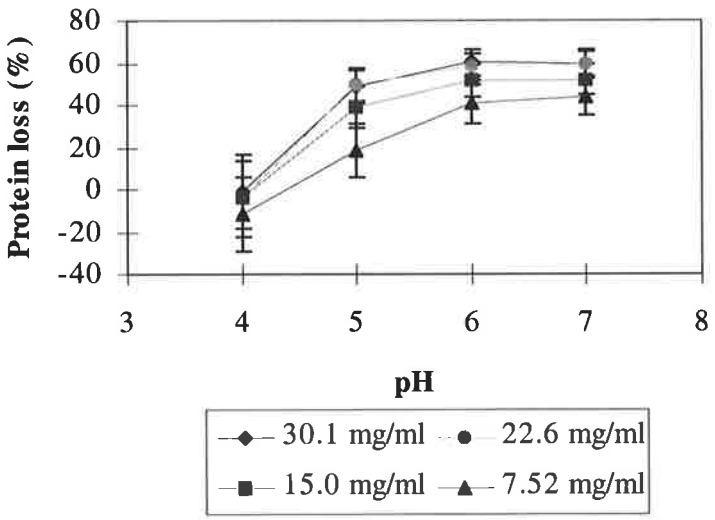

Figure 5.8: Proportion of the total protein (%) that was lost as precipitate. *The error bars refer to the 95% confidence interval on each protein loss (%).*

Figure 5.9 shows the specific activity of TGF-β2 per unit of protein in the sub-sample supernatant. It is evident that the specific activity decreases as the pH is adjusted upwards. Therefore protein precipitation is not the only source of the decrease in TGF-β2 concentration observed in Figure 5.9 and another mechanism is likely to be at work.

Wakefield et al. (1989) demonstrated a time-dependent relationship of latent complex conversion when the TGF-β1 latent complex was acidified and then abruptly reneutralised. It is therefore likely that the re-association of TGF-β2 with the latency-associated peptide (LAP) decreases the concentration of active TGF-β2 in the supernatant. It was found that re-acidifying the supernatant samples to pH 2.5 resulted in an increase in TGF-β2 concentration (data not shown) lending support to this proposal.

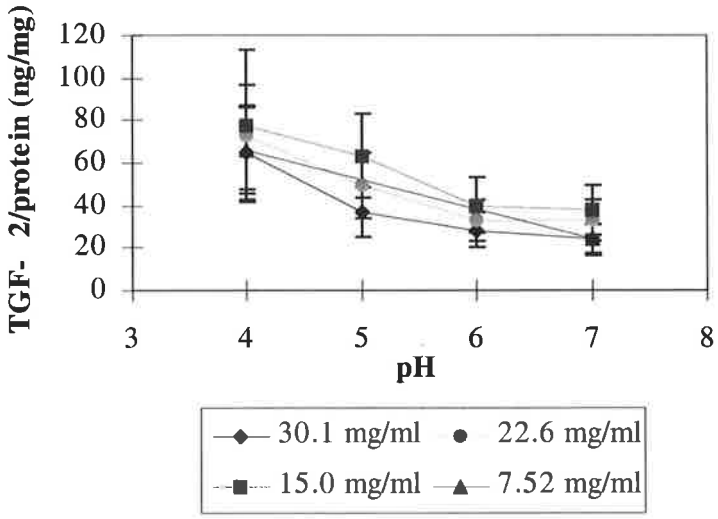

Figure 5.9: Specific activity of TGF-β2 per unit of protein in the sub-sample supernatant. *The error bars refer to the 95% confidence interval on each specific activity (ng/mg).*

The possibility that the acidified WGFE could be reneutralised and then quickly injected on to an affinity support before the TGF-β2 latent complex could re-associate was investigated. The time-dependent TGF-β1 latent complex re-association data of Wakefield et al. (1989) was analysed by assuming second order kinetics and the rate constant was estimated to be 1.6 $nM^{-1}hr^{-1}$. At this rate it would take 8.5 seconds for the TGF-β2 concentration (6.6 μg/ml, 264 nM) in acidified WGFE to decrease to 3.3 μg/ml. It is therefore likely that the rate of re-association is too fast for the proposed method to be viable.

A small proportion of the WGFE protein precipitate resuspended (8.3 and 22%) when acidic buffer was added to the precipitates. Therefore it is difficult to recover the TGF-β2 that precipitated during reneutralisation and hence this treatment wastes large amounts of WGFE and would be unlikely to yield an economic process.

5.3.1.2 Alkaline Activation and Reneutralisation of WGFE

The pH of WGFE was increased to pH 11 with NaOH and incubated overnight at 4°C. The next day the sample was divided into four samples and the pH of each was adjusted to 10, 9, 8 and 7 respectively. Macro BCA protein assay of the supernatant demonstrated that no significant protein precipitation occurred. In Figure 5.10, the TGF-β2 concentration did not decrease significantly when the pH was adjusted to neutrality, as is the case in Figure 5.7.

Furthermore, the TGF-β2 concentration at pH 7 was higher for alkaline activation than for acid activation despite the more effective acid activation prior to reneutralisation (Table 5.1).

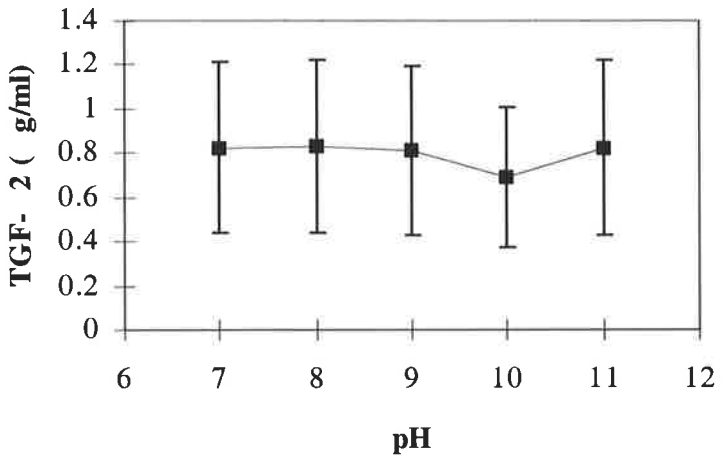

Figure 5.10: TGF-β2 concentration in the supernatant of each sub-sample from the 30.1 mg/ml sample after alkaline pH adjustment. *The error bars refer to the 95% confidence interval on each concentration.*

It is unusual that protein precipitation did not occur when WGFE was activated at pH 11 and then reneutralised because the isoelectric points (pI) of xanthine dehydrogenase, lactoperoxidase and TGF-β2 are 8.06, 8.27 and 7.69 respectively (Swiss Institute of Bioinformatics, 1999). Theoretically these proteins should precipitate when they acquire a neutral charge during the pH adjustment from 11 to 7.

5.3.1.3 TGF-β2-Antibody Association at pH4

Section 5.3.1.1 demonstrated that acidifying WGFE to pH 2.5 and then adjusting the pH to 4 provided the highest active TGF-β2 concentration. Therefore an ELISA was performed to determine the extent of TGF-β2-antibody association at pH 4. It is evident from Figure 5.11 that a comparable amount of antibody binds at pH 4 to that which remains after elution at pH 3 for antibodies 5D4 and 8A3. Acid activation followed by reneutralisation to pH 4 is not a viable method for activating WGFE prior to the immunoaffinity purification of TGF-β2 because of the poor TGF-β2-antibody binding at pH 4. Therefore alkaline activation followed by adjustment to pH 7 is the preferred method of WGFE activation.

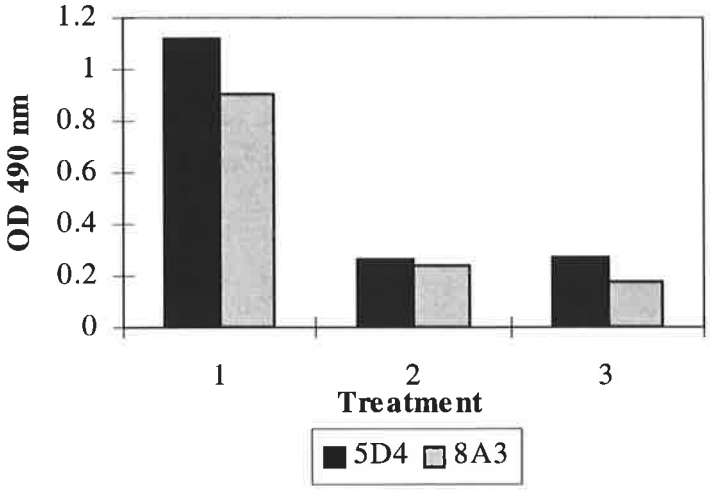

Figure 5.11: Association of antibodies 5D4 and 8A3 with TGF-β2 in the ELISA format. *The treatments were association at pH 7 without elution (1), association at pH 4 (2) and association at pH 7 with elution at pH 3 (3) included for comparison.*

5.3.2 Eluent Screening

A range of eluents was screened for the ability to dissociate the TGF-β2-antibody complex. The optical density at 490 nm indicated the amount of antibody remaining bound to the wells after incubation with the eluents. Specifically, this measure was obtained by subtracting the optical density at 490 nm for the wells on the uncoated side from the OD 490 nm for the TGF-β2 coated wells and taking the average of these three values. Figures 5.12 and 5.13 show the binding capacity retained after pre-incubation with various eluents. The binding capacity after pre-incubation is expressed as a percentage after dividing the OD 490 nm for the pre-incubation wells by the OD 490 nm for the standard association wells. It is a measure of the antibody robustness under various elution conditions. Figures 5.14 and 5.15 show the antibody bound after elution that is expressed as a percentage by dividing the OD 490 nm for the eluent test wells by the OD 490 nm for the pre-incubation wells. It is an indicator of the effectiveness of the eluent because it measures the amount of antibody that may be eluted reversibly without denaturation. A summary of the eluents used in this study is included in Table 5.2.

Key	Definition
pH 1.5	0.1M glycine pH 1.5
pH 2.0	0.1M glycine pH 2.0
pH 2.5	0.1M glycine pH 2.5
pH 3.0	0.1M glycine pH 3.0

pH 3.5	0.1M glycine pH 3.5
pH 4.0	0.1M glycine pH 4.0
pH 4.5	0.1M glycine pH 4.5
pH 5.0	0.1M glycine pH 5.0
pH 11	0.1M glycine pH 11
pH 12	0.1M glycine pH 12
Iso	30% (v/v) Isopropanol
DMSO	50% (v/v) Dimethyl sulfoxide
2M $MgCl_2$	2M Magnesium chloride
4M $MgCl_2$	4M Magnesium chloride
1M KI	1M Potassium iodide
4M KI	4M Potassium iodide
0.01M LIS	0.01M Lithium 3,5-diiodosalicylate
0.1M LIS	0.1M Lithium 3,5-diiodosalicylate
Iso pH 4	30% (v/v) Isopropanol, 0.07M glycine pH 4
Iso pH 4.5	30% (v/v) Isopropanol, 0.07M glycine pH 4.5
Iso pH 5	30% (v/v) Isopropanol, 0.07M glycine pH 5
Iso pH 11	30% (v/v) Isopropanol, 0.07M glycine pH 11

Table 5.2: A summary of the eluents used in this study.

The standard association wells demonstrated that the dilution of the eluents after pre-incubation was such that TGF-β2-antibody binding was not significantly affected. It was determined that OD 490nm for the standard association wells divided by the OD 490nm for wells to which no eluent was added varied in the range of 79% to 123%. The binding capacity of antibody 5D4 was rapidly degraded with 0.1M glycine pH 1.5-2.0, 0.1M glycine pH12, 4M $MgCl_2$, 4M KI and LIS. Also the binding capacity of antibody 8A3 was rapidly degraded with 0.1M glycine pH 1.5-2.0, 4M $MgCl_2$ and 0.1M LIS. It is possible that the observed decrease in binding capacity was due to stripping of the coated TGF-β2 from the ELISA plate or due to the degradation of the constant regions of the antibody to which the

secondary antibody binds. Therefore a limitation of this eluent screening method is that some promising eluents may be overlooked because they strip TGF-β2 from the ELISA plate or degrade the constant regions of the antibody whilst leaving the TGF-β2 binding site intact.

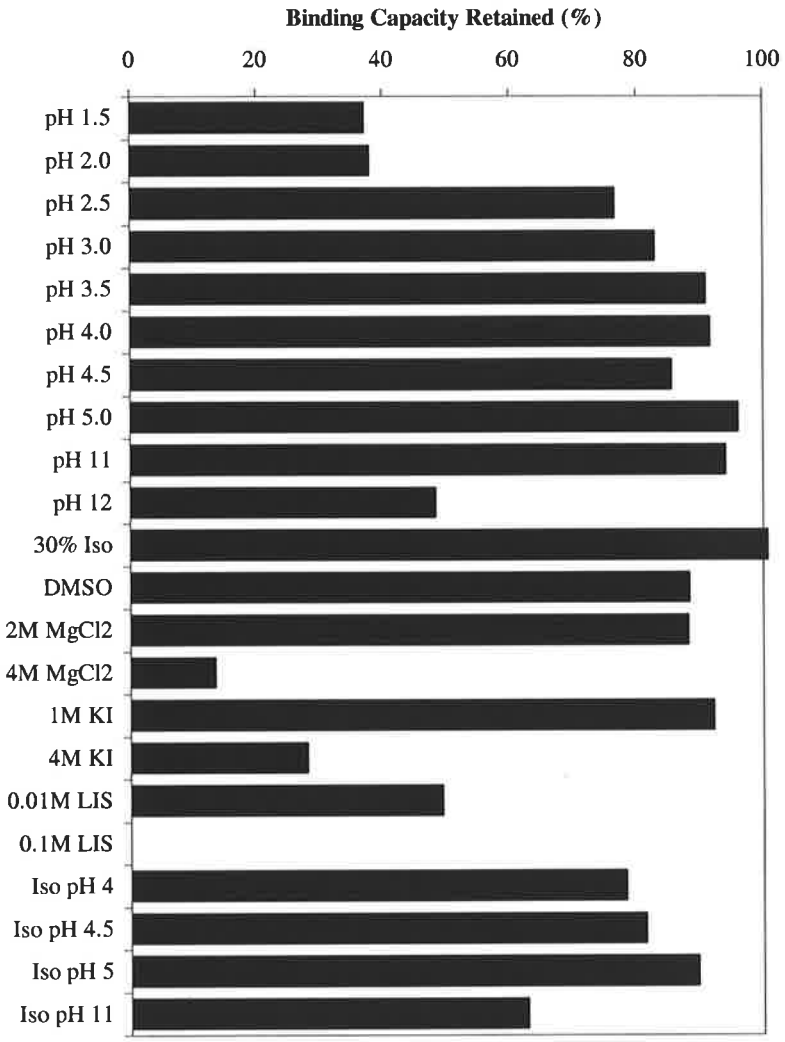

Figure 5.12: Binding capacity of antibody 5D4 retained after pre-incubation with various eluents. *Binding capacity is determined by dividing the OD 490 nm for the pre-incubation wells by the OD 490 nm for the standard association wells. It is a measure of the antibody robustness under various elution conditions.*

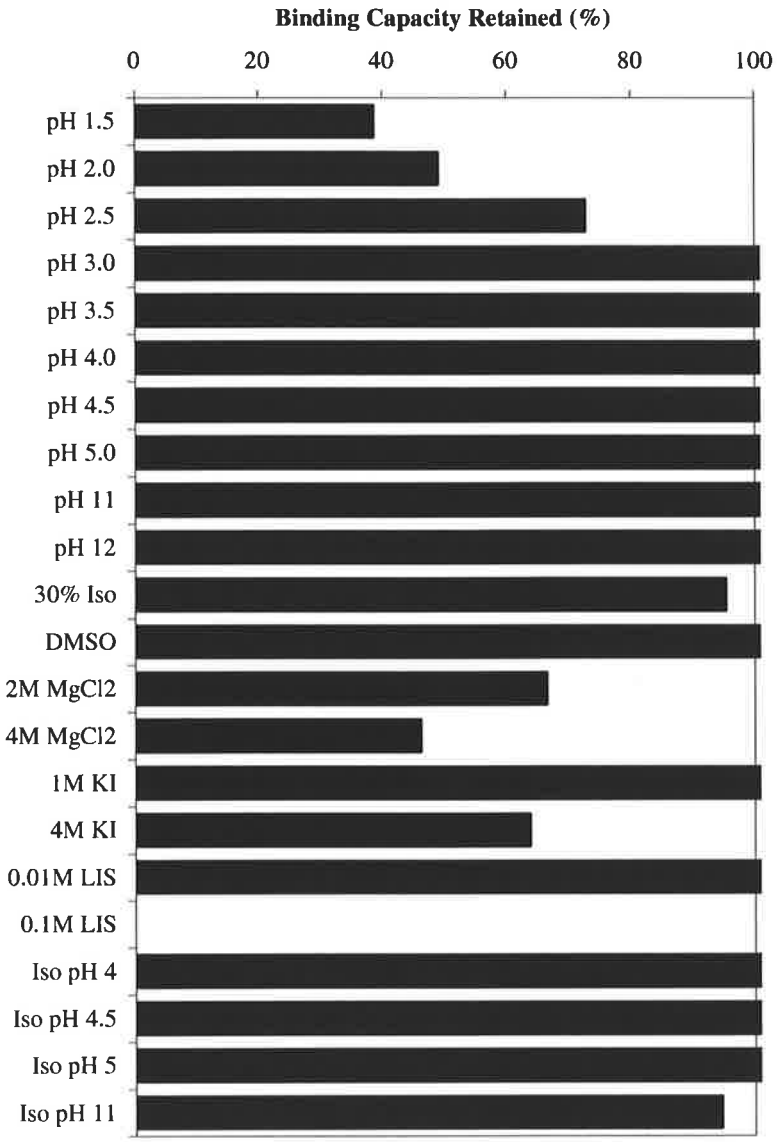

Figure 5.13: Binding capacity of antibody 8A3 retained after pre-incubation with various eluents.

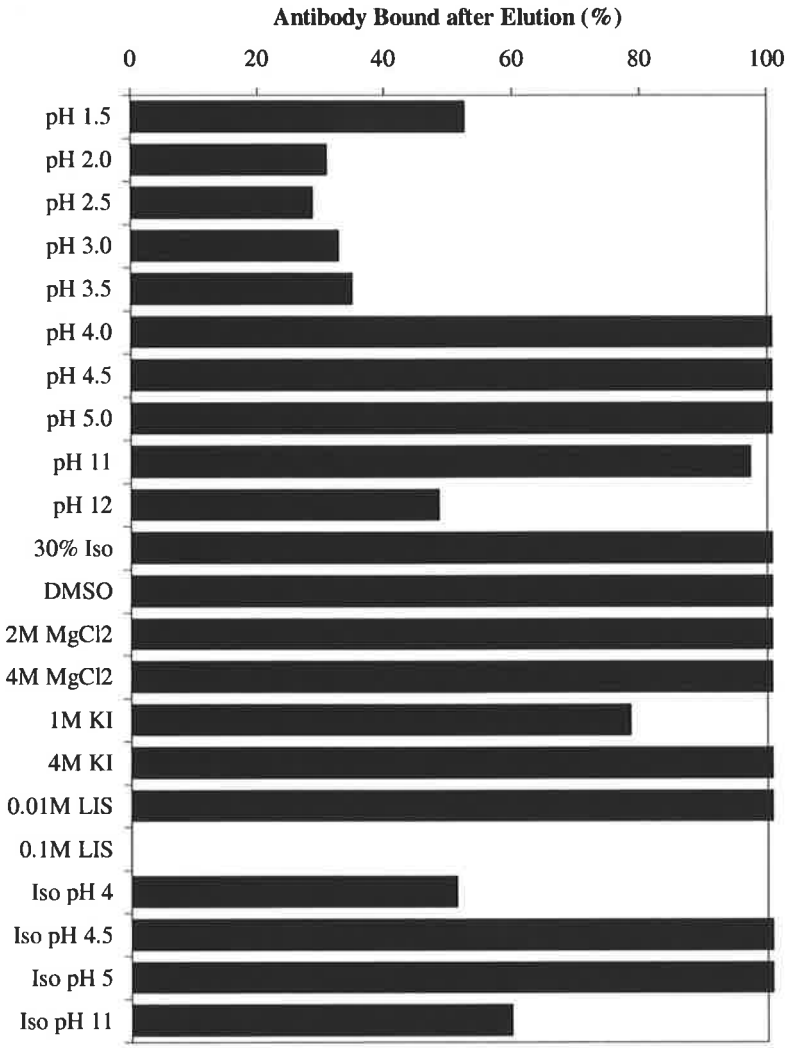

Figure 5.14: Antibody 5D4 bound after elution with various eluents. *Antibody bound was determined by dividing the OD 490 nm for the eluent test wells by the OD 490 nm for the pre-incubation wells. It is an indicator of the effectiveness of the eluent because it measures the amount of antibody that may be eluted reversibly without denaturation.*

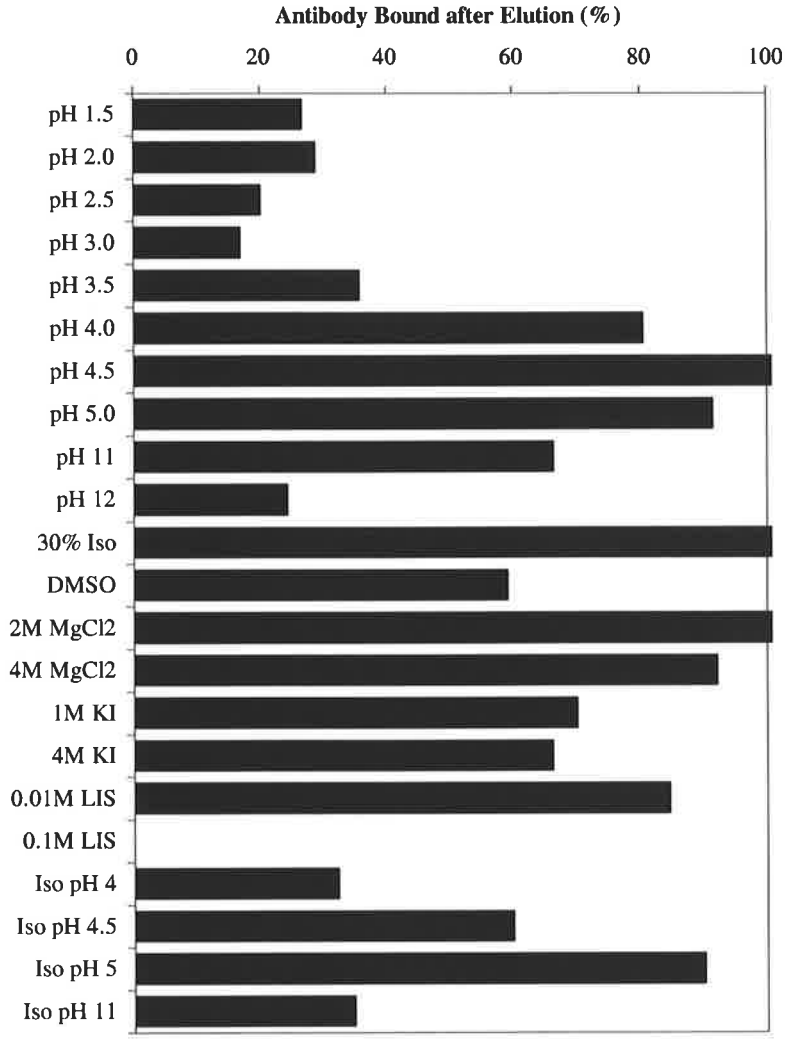

Figure 5.15: Antibody 8A3 bound after elution with various eluents.

In Figure 5.14 it is evident that 0.1M glycine in the pH range 3.5 to 2.5 is the most effective eluent for antibody 5D4 whilst conserving binding capacity. Below pH 3.5 the eluent effectiveness did not improve significantly and decreasing the pH would result in faster binding capacity degradation. Therefore the most promising eluents were 0.1M glycine pH 3.5 and 0.1M glycine pH 3 for antibodies 5D4 and 8A3 respectively.

Pepper (1992) subjected five different monoclonal antibodies against soybean trypsin inhibitor (SBTI) to similar eluent screening. In comparison with the results of Pepper (1992), antibodies 5D4 and 8A3 were difficult to elute. The most promising anti-SBTI antibody for immunoaffinity chromatography had 65% of the antigen eluted with 30% (v/v) isopropanol and 97% of the antigen eluted with 2M $MgCl_2$. Antibodies 5D4 and 8A3 were resistant to elution under these conditions. Therefore this was the first indication that antibodies 5D4 and 8A3 were not well suited for immunoaffinity chromatography.

5.3.3 Long-term Binding Capacity Degradation

The ELISA technique was used to measure the concentration of viable antibody after the eluent incubations. Samples were added in triplicate (100 µl/well) to the coated and uncoated sides of the ELISA plates. Standard curves of viable antibody were included so that the optical densities of the samples could be related to viable antibody concentrations. Tablecurve was used to fit a curve with Equation 2.2 to the viable antibody concentration (x) versus OD 490nm (y) plot. The dose response data for the denatured antibody sample were imported to Tablecurve and viable antibody concentrations (x) were computed from the optical density (y) values with the inverse function of Equation 2.2. The viable antibody concentrations were plotted as a function of time as shown in Figures 5.16 to 5.19. Two theoretical models were considered for fitting the data set. The first assumes that the antibody binding capacity, $Q_m(t)$, degrades in a first order manner and can be described by the equation:

$$Q_m(t) = q_m \, exp(-k_{deg} t) \tag{5.14}$$

where q_m is the initial binding capacity, k_{deg} is the binding capacity degradation rate constant and t is the time. The second model assumes that a non-degradable component of the overall binding capacity, q_{m1}, exists:

$$Q_m(t) = q_{m1} + q_{m2} \, exp(-k_{deg} t) \tag{5.15}$$

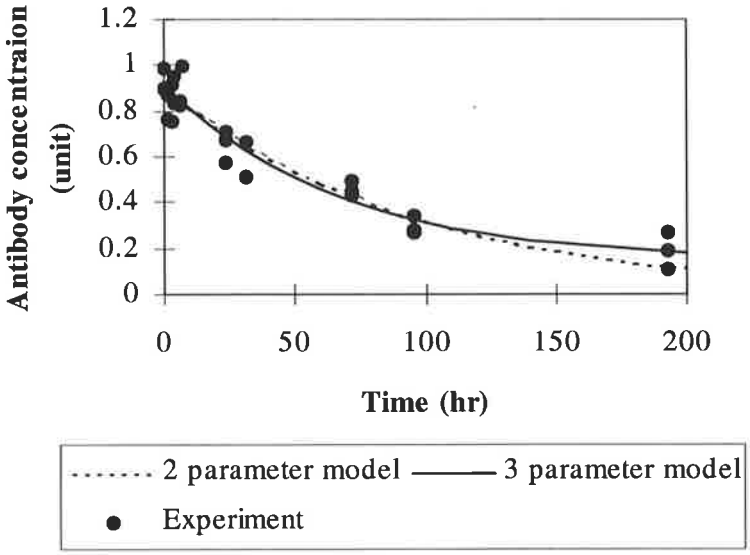

Figure 5.16: Degradation of antibody binding capacity as a function of time for the long-term incubation of monoclonal antibody 5D4 in 0.1M glycine pH 3.5. *Tablecurve regressed the data set to the two parameter model to yield* $q_m = 0.901$, $k_{deg} = 0.0104\ hr^{-1}$ *with* $R^2 = 0.910$. *The data set was also regressed to the three parameter model to yield* $q_{m1} = 0.142$, $q_{m2} = 0.773$, $k_{deg} = 0.0150\ hr^{-1}$ *with* $R^2 = 0.919$.

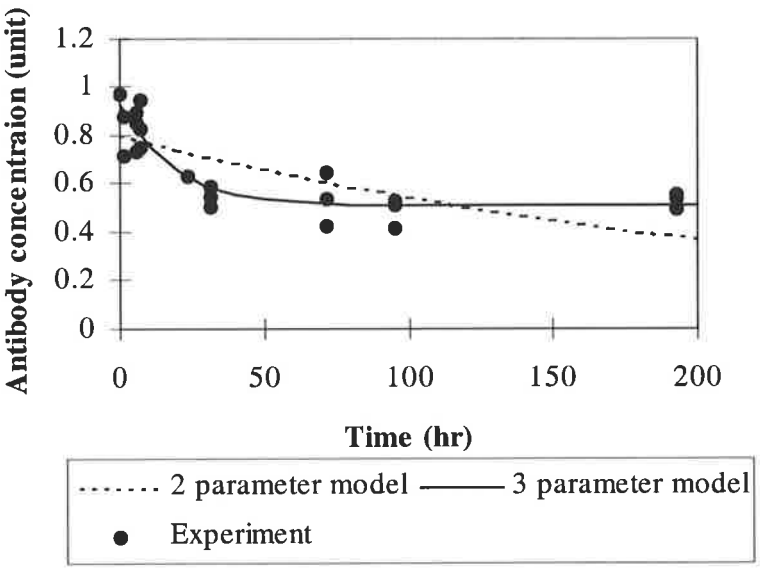

Figure 5.17: Degradation of antibody binding capacity as a function of time for the long-term incubation of monoclonal antibody 8A3 in 0.1M glycine pH 3.0. *Tablecurve regressed the data set to the two parameter model to yield* $q_m = 0.800$, $k_{deg} = 0.0382\ hr^{-1}$ *with* $R^2 = 0.527$. *The data set was also regressed to the three parameter model to yield* $q_{m1} = 0.507$, $q_{m2} = 0.422$, $k_{deg} = 0.0537\ hr^{-1}$ *with* $R^2 = 0.832$.

The two-parameter model (Equation 5.14) is adequate for the description of the degradation process in Figure 5.16 but its prediction is poor when regressed to the data of Figure 5.17. Therefore the three-parameter model (Equation 5.15) is required to describe the binding capacity degradation of antibody 8A3. These observations can be explained if there are two populations of binding interaction, which are either degradable or non-degradable. This is an unexpected result for the binding sites of monoclonal antibodies are by definition homogeneous and the binding capacity should degrade by a first order mechanism. As shown in Chapter 3, the probabilities of monoclonality for hybridomas 5D4 and 8A3 are 98.5% and 99.9% respectively and it is therefore extremely unlikely that two populations of antibody are present. However, variations in the orientation of TGF-β2 on the surface of the ELISA plate may present the epitope to the monoclonal antibody binding site in different ways. Eluent-mediated degradation of the binding site may decrease binding to one orientation of the TGF-β2 epitope but have no effect on binding for another orientation.

Experiments with the Biacore 2000 showed that when monoclonal antibody was immobilised to the chip surface and the TGF-β2 preparation was injected on to the surface, it was not possible to dissociate bound material from the sensor chip with 0.1M glycine pH 3.0. However, it was found that the inclusion of 0.5M NaCl in 0.1M glycine pH 3.0 produced an effective eluent for the bound material for both antibodies. It was to be expected that different elution conditions were required because the ELISA plate and the sensor chip possess different surfaces. The ELISA plate has a flat polystyrene surface and the chip surface consists of a 3-dimensional matrix of dextran chains. In addition, low pH eluents can protonate the carboxylate groups of the dextran chains and increase the hydrophobicity of the surface. In a separate experiment the injection of protein on to the chip surface at pH 2.5 was found to result in the deposition of material at the surface, which was greater than the maximum theoretical specific binding capacity. The material resisted removal by severe eluents, such as 0.1M HCl and 3.5M $MgCl_2$+0.5% (v/v) tween 20. Therefore it can be speculated that the inclusion of 0.5M NaCl minimises these non-specific binding interactions and permits TGF-β2 to diffuse away from the chip surface unhindered. It is thought that the 3-dimensional structure of the sensor chip surface more closely approximates the internal structure of membrane materials than does the flat surface of an ELISA plate. Therefore, it was decided that the optimal eluent for the TGF-β2-antibody systems was 0.1M glycine + 0.5M NaCl pH 3. Therefore the long-term eluent incubations were repeated for the eluent 0.1M glycine + 0.5M NaCl pH 3.

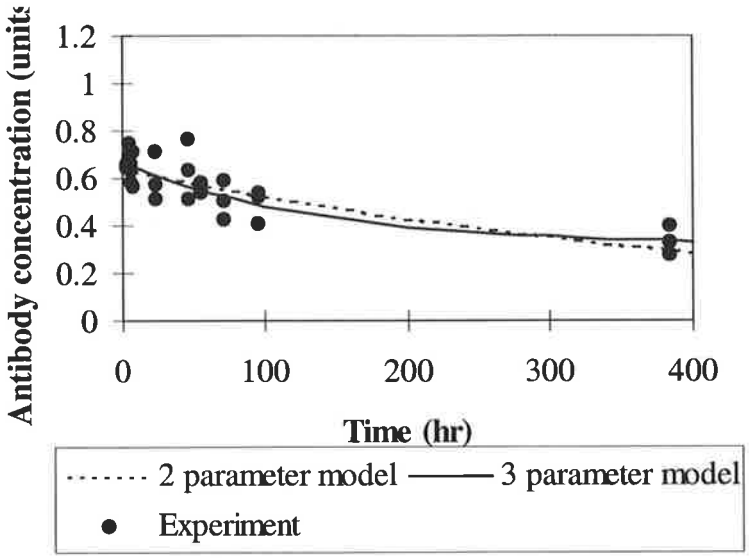

Figure 5.18: Degradation of antibody binding capacity as a function of time for the long-term incubation of monoclonal antibody 5D4 in 0.1M glycine + 0.5M NaCl pH 3.

Tablecurve regressed the data set to the two parameter model to yield $q_m = 0.639$, $k_{deg} = 0.00198\ hr^{-1}$ *with* $R^2 = 0.699$. *The data set was also regressed to the three parameter model to yield* $q_{m1} = 0.316$, $q_{m2} = 0.352$, $k_{deg} = 0.00749\ hr^{-1}$ *with* $R^2 = 0.754$.

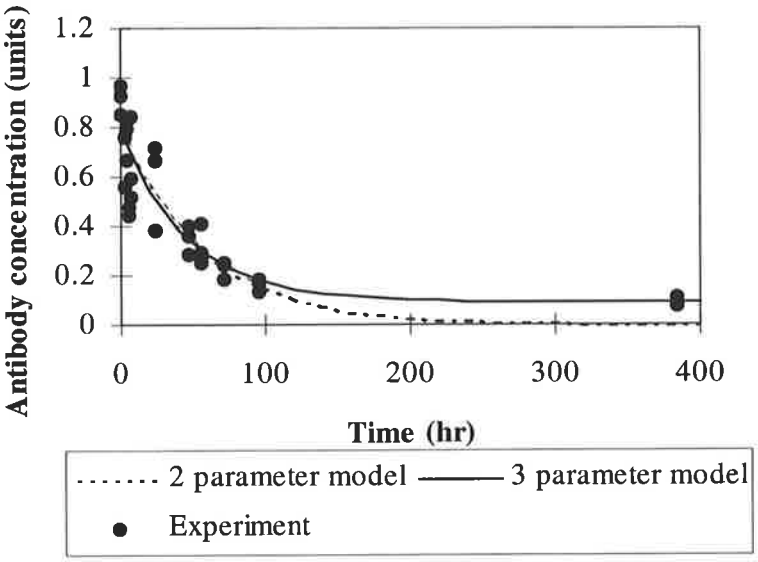

Figure 5.19: Degradation of antibody binding capacity as a function of time for the long-term incubation of monoclonal antibody 8A3 in 0.1M glycine + 0.5M NaCl pH 3.

Tablecurve regressed the data set to the two parameter model to yield $q_m = 0.774$, $k_{deg} = 0.0167\ hr^{-1}$ *with* $R^2 = 0.810$. *The data set was also regressed to the three parameter model to yield* $q_{m1} = 0.0915$, $q_{m2} = 0.692$, $k_{deg} = 0.0215\ hr^{-1}$ *with* $R^2 = 0.823$.

Figures 5.18 and 5.19 show that the two-parameter model (Equation 5.14) is adequate for the description of the degradation process in 0.1M glycine + 0.5M NaCl pH 3 for both antibodies. The binding capacity of antibody 5D4 degrades more slowly than that of antibody 8A3 and therefore the use of antibody 5D4 rather than antibody 8A3 in a TGF-β2 immunoaffinity purification system would be likely to provide an economic advantage.

5.3.4 Kinetics of the TGF-β2-Antibody Interaction

5.3.4.1 Binding to Surface TGF-β2

Anti-TGF-β1,2,3 monoclonal antibody was injected over the sensor chip surface to which recombinant human TGF-β2 was immobilised. Relative to the blank flow path, the TGF-β2 immobilised flow path showed a normal increase in response during antibody binding with a subsequent decrease in response when binding buffer alone was injected, as shown in Figure 5.20. Normal binding responses were also observed when the conditioned media of hybridomas 5D4-1D9 (Figure 5.21) and 8A3-1G3 (Figure 5.22) were injected on to the surface.

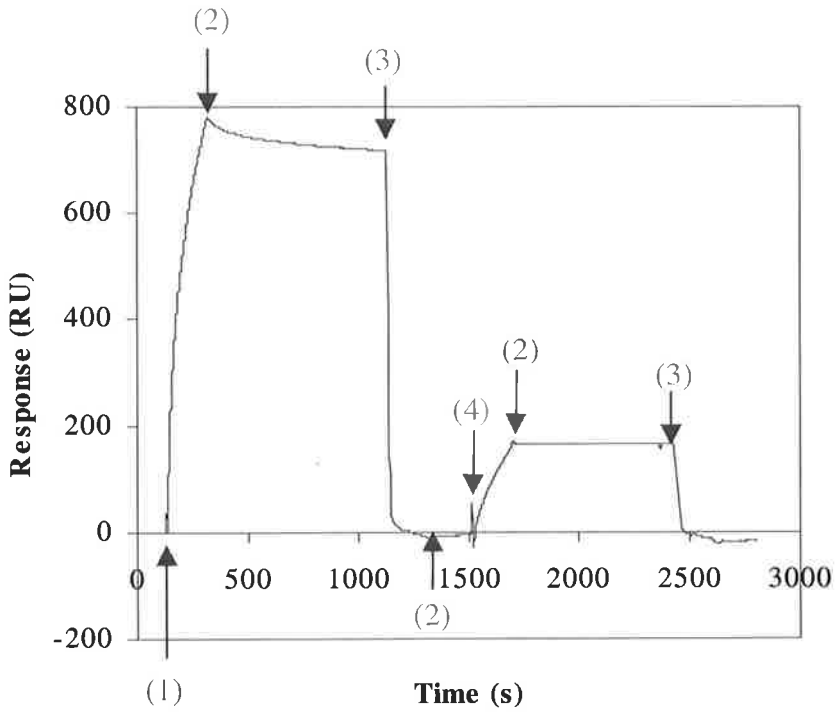

Figure 5.20: Anti-TGF-β1,2,3 monoclonal antibody was injected over the sensor chip surface to which recombinant human TGF-β2 was immobilised. *Fifteen μl of 100 μg/ml antibody was injected (1), followed by HBS running buffer (2), 0.1 M HCl regenerating buffer (3), HBS (2), then 15 μl of 10 μg/ml antibody (4), HBS (2) and 0.1 M HCl (3).*

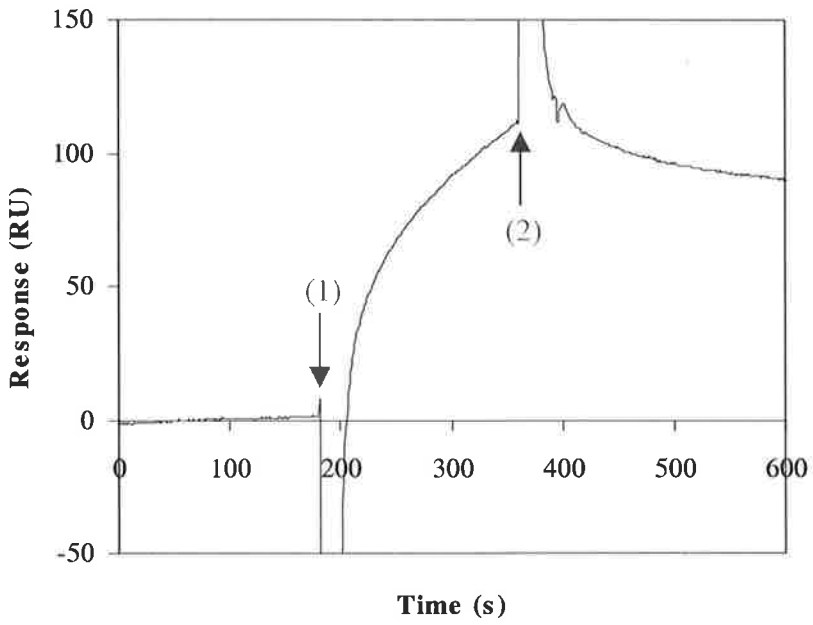

Figure 5.21: Conditioned medium from hybridoma 5D4-1D9 was injected on to a sensor chip to which recombinant human TGF-β2 was immobilised. *Fifteen μl of conditioned medium from hybridoma 5D4-1D9 was injected at 5 μl/min over the surface of both flow paths (1). The surface was then washed with HBS (2).*

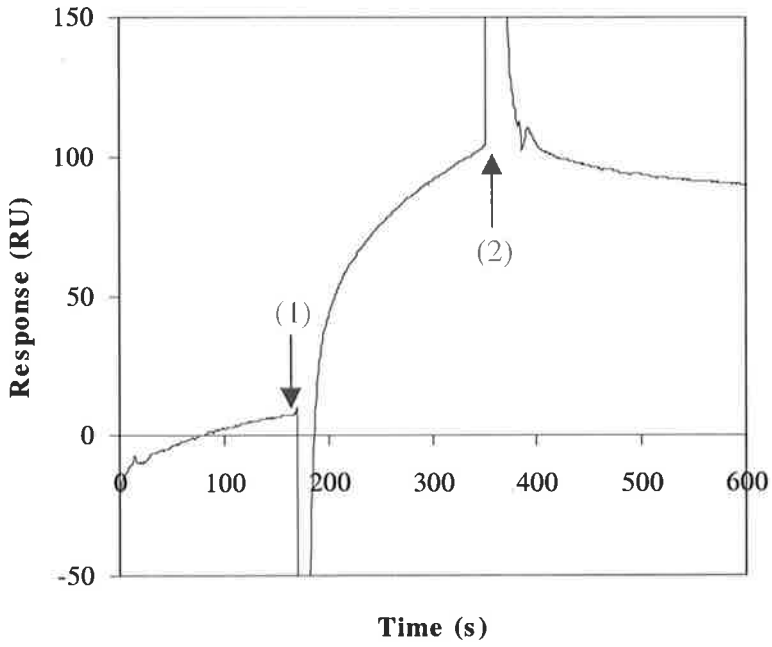

Figure 5.22: Conditioned medium from hybridoma 8A3-1G3 was injected on to a sensor chip to which recombinant human TGF-β2 was immobilised. *Fifteen μl of conditioned medium from hybridoma 8A3-1G3 was injected at 5 μl/min over the surface of both flow paths (1). The surface was then washed with HBS (2).*

5.3.4.2 Surface Regeneration

A series of prospective eluents of volume 200 µl each were injected on to the chip surface; the eluents were 0.1M glycine pH 4.5, 0.1M glycine pH 4.0, 0.1M glycine pH 3.5, 0.1M glycine pH 3.0, 0.1M glycine + 0.5M NaCl pH 3.5 and 0.1M glycine + 0.5M NaCl pH 3.0. Only 0.1M glycine + 0.5M NaCl pH 3.0 was capable of regenerating the surface. As was mentioned in section 5.3.3, this eluent was selected as an improvement upon the previous optimal eluents of section 5.3.2. According to Brigham-Burke and O'Shannesy (1993), buffers that are successful at eluting protein from the Biacore chip are also effective at eluting protein in immunoaffinity chromatography. An attempt was made to determine the rate of dissociation under elution conditions (0.1M glycine + 0.5M NaCl pH 3.0) by fitting a first order dissociation curve to the sensorgrams. However, the dissociation sensorgrams were non-linear and not repeatable and therefore it was not possible to determine the dissociation rate for the mathematical modelling of Chapter 4.

5.3.4.3 Binding to Surface Antibody

The fourth pool of ppTGF-β2 activity was lyophilised, resuspended in HBS and injected on to the chip surface coupled with anti-TGF-β1,2,3 monoclonal antibody. Figure 5.23 shows the binding responses when 10 µl of 1, 5, 10, 20 and 50 µg/ml TGF-β2 in HBS were injected sequentially at 5 µl/min over the surface of both flow paths.

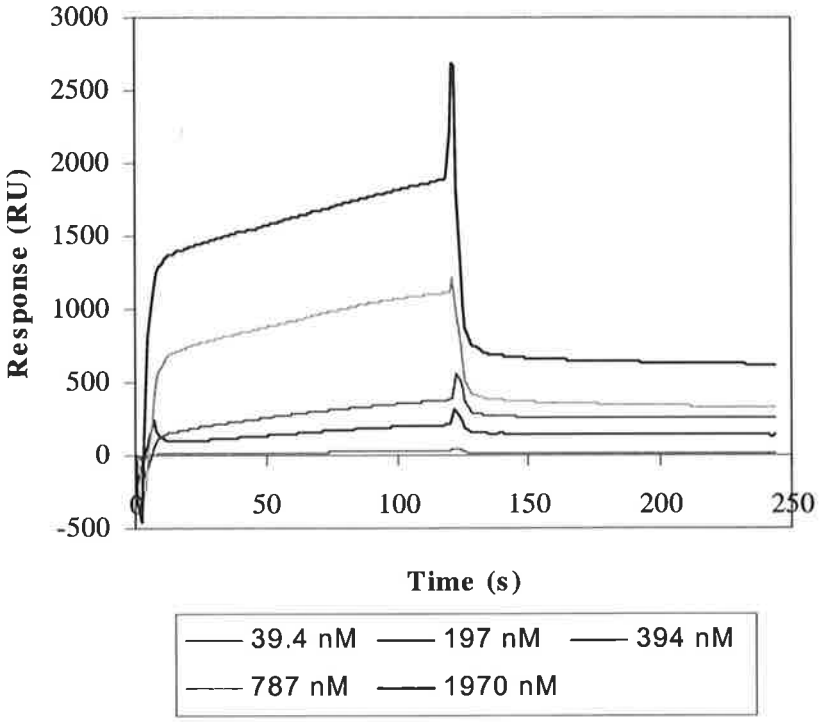

Figure 5.23: Anti-TGF-β1,2,3 monoclonal antibody was immobilised to the sensor chip and ppTGF-β2 was injected over the chip surface. *Partially purified TGF-β2 was injected sequentially over the surface at 1, 5, 10, 20 and 50 μg/ml in HBS at 5 μl/min.*

Four different concentrations of the sixth TGF-β2 pool (Table 2.7) were injected in duplicate over the chip surface to which antibodies 5D4 and 8A3 were immobilised. The sixth TGF-β2 pool was dialysed into PBS and injected over the chip surface at 40 μl/min to minimise the effects of mass transfer. The sensorgram curves of antibodies 5D4 and 8A3 for the binding of ppTGF-β2 were regressed with Biaevaluation 3.0 using two different pre-defined models: a Langmuir 1:1 binding interaction model and a heterogeneous ligand model with parallel reactions. The results of regressing the binding responses of antibody 5D4 and 8A3 to these models are shown in Tables 5.3 and 5.4 respectively. Comparisons between the experimental data and the regressed curves are shown in Figures 5.24 to 5.27.

Regressed value	Langmuir 1:1 model	Heterogeneous ligand model
k_{a1} ($M^{-1}s^{-1}$)	$1.71\times10^{5} \pm 1.28\times10^{1}$	$1.38\times10^{5} \pm 1.03\times10^{3}$
k_{a2} ($M^{-1}s^{-1}$)		$5.5\times10^{5} \pm 1.51\times10^{4}$
k_{d1} (s^{-1})	$2.12\times10^{-3} \pm 5.50\times10^{-6}$	$1.06\times10^{-3} \pm 7.17\times10^{-6}$
k_{d2} (s^{-1})		$0.0372 \pm 5.84\times10^{-4}$
R_{max1} (RU)	337 ± 0.055	204 ± 1.05
R_{max2} (RU)		286 ± 5.48
k_{a1}/k_{d1} (M^{-1})	8.07×10^{7}	1.31×10^{8}
k_{a2}/k_{d2} (M^{-1})		1.48×10^{7}
χ^2	148	44.8

Table 5.3: Regressed values to the experimental data of antibody 5D4 for the kinetic models.

Regressed value	Langmuir 1:1 model	Heterogeneous ligand model
k_{a1} ($M^{-1}s^{-1}$)	$2.41\times10^{5} \pm 2.92\times10^{3}$	$1.64\times10^{5} \pm 9.11\times10^{2}$
k_{a2} ($M^{-1}s^{-1}$)		$7.76\times10^{5} \pm 1.94\times10^{2}$
k_{d1} (s^{-1})	$2.19\times10^{-3} \pm 1.12\times10^{-5}$	$9.04\times10^{-4} \pm 6.07\times10^{-6}$
k_{d2} (s^{-1})		$0.0464 \pm 8.10\times10^{-6}$
R_{max1} (RU)	87.3 ± 0.63	51.2 ± 0.0152
R_{max2} (RU)		87.6 ± 0.317
k_{a1}/k_{d1} (M^{-1})	1.1×10^{8}	1.81×10^{8}
k_{a2}/k_{d2} (M^{-1})		1.67×10^{7}
χ^2	24.9	5.82

Table 5.4: Regressed values to the experimental data of antibody 8A3 for the kinetic models.

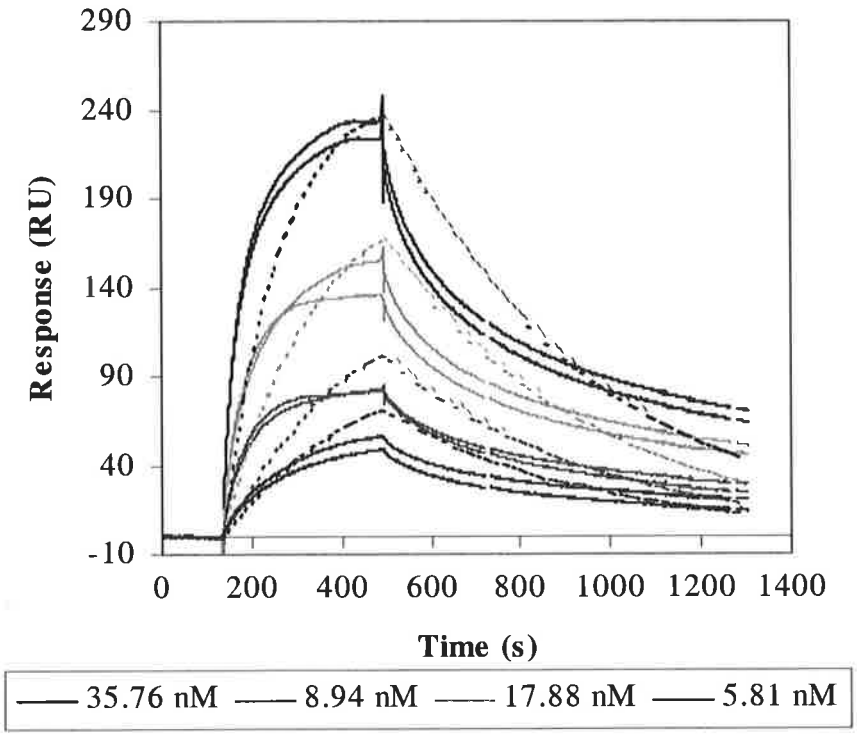

Figure 5.24: Comparison of the curves that were regressed to the Langmuir 1:1 model (broken lines) with the experimental data (unbroken lines) for antibody 5D4.

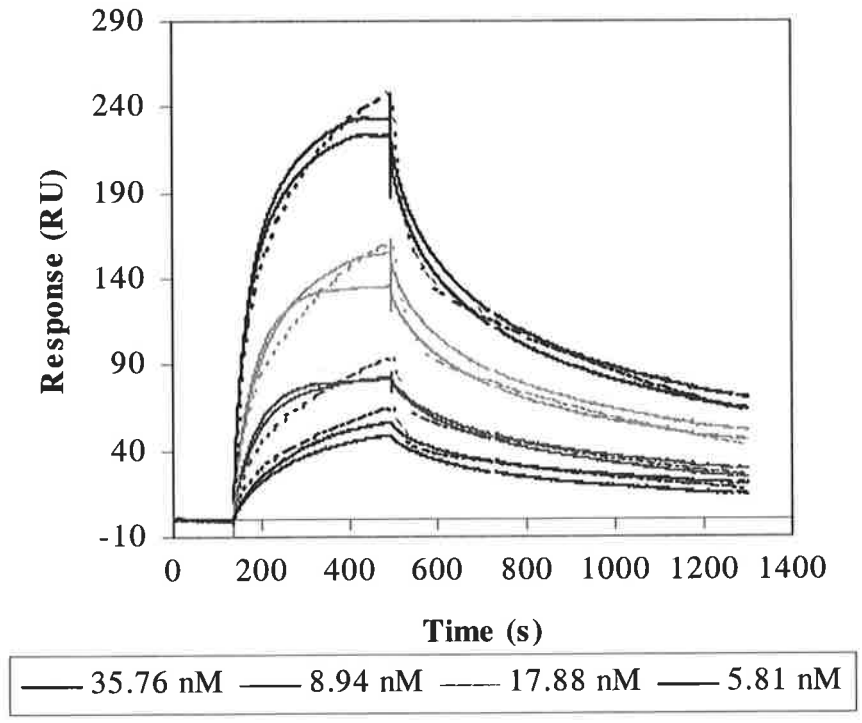

Figure 5.25: Comparison of the curves that were regressed to the heterogeneous ligand model (broken lines) with the experimental data (unbroken lines) for antibody 5D4.

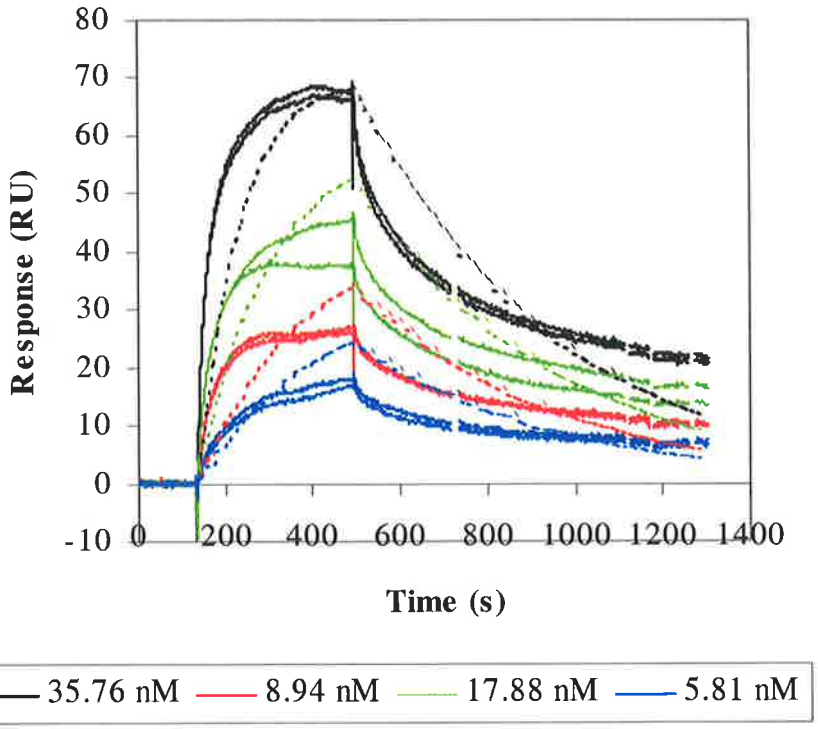

Figure 5.26: Comparison of the curves that were regressed to the Langmuir 1:1 model (broken lines) with the experimental data (unbroken lines) for antibody 8A3.

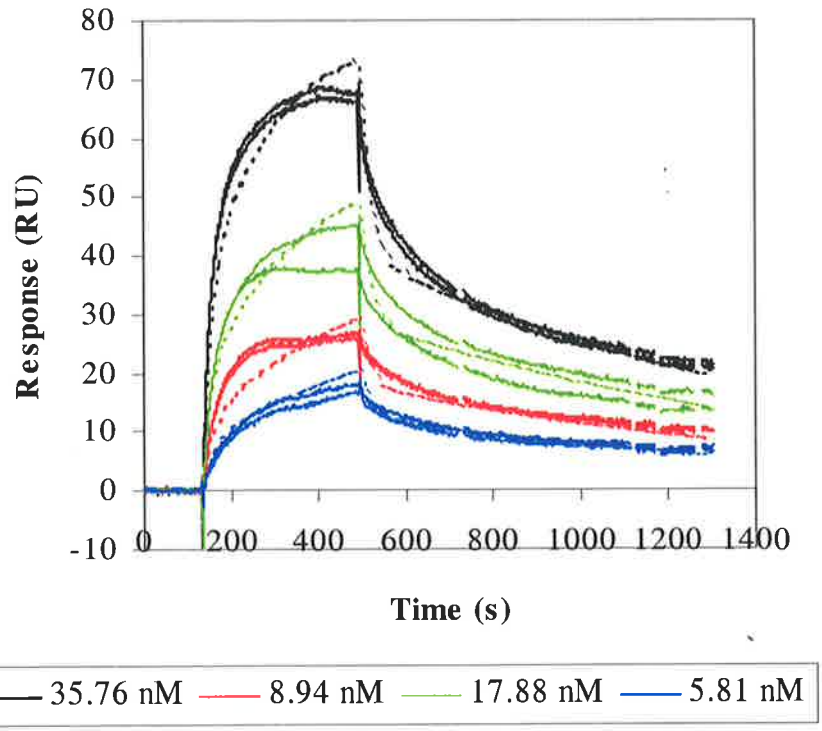

Figure 5.27: Comparison of the curves that were regressed to the heterogeneous ligand model (broken lines) with the experimental data (unbroken lines) for antibody 8A3.

It is evident from the binding curves that the binding event is highly heterogeneous and this phenomenon has been previously reported for monoclonal antibodies (Regnault et al., 1998). The range of orientations in which antibody can be immobilised to the carboxy-methylated dextran could give rise to binding sites with a range of equilibrium association equilibrium constants. Another possible explanation is that contaminating proteins in the partially purified TGF-β2 preparation non-specifically interact with the immobilised antibody. However, this latter explanation is unlikely because a single band was observed when ppTGF-β2 was electrophoresed and subject to western blotting with antibody 5D4.

The kinetic study experiment of section 5.2.4.6 was repeated with recombinant human TGF-β2 (Sigma, St. Louis, MO, USA) at similar concentrations in order to determine whether contaminating proteins in the partially purified TGF-β2 preparation interfere with antibody-TGF-β2 binding to produce heterogeneous binding curves. The rhTGF-β2 was dialysed against 10 mM Na_2HPO_4, 150 mM NaCl pH 7. After dialysis, the rhTGF-β2 concentration was assayed with TGF-β2 ELISA (Promega, Madison, WI, USA). Partially purified TGF-β2 was injected on the chip surface to ensure that the binding capacity of the immobilised antibody had not significantly changed from the previous experiment. Figure 5.28 shows the binding curves for the duplicate injections of five different TGF-β2 concentrations over the chip surface.

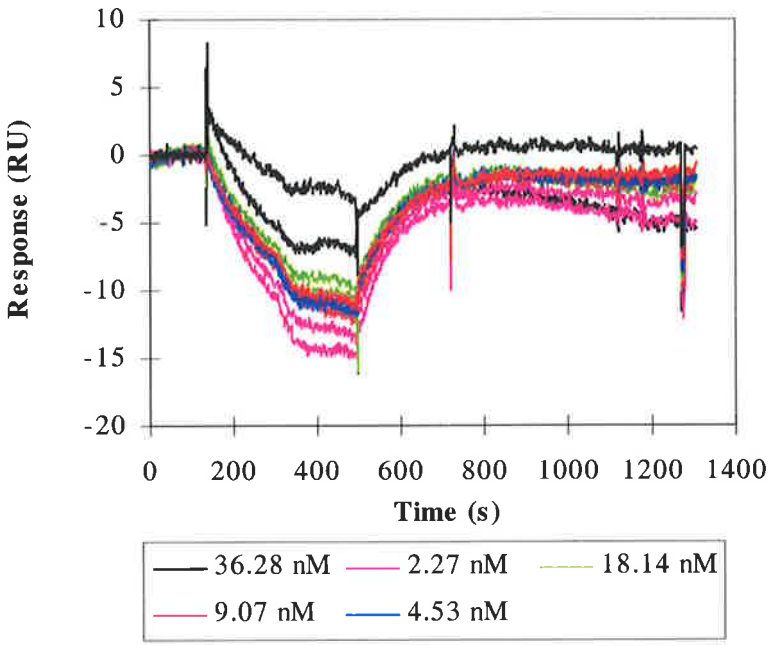

Figure 5.28: Sensorgrams for the injection of recombinant human TGF-β2 over a surface to which antibody 5D4 was immobilised. *Similar behaviour was observed for antibody 8A3.*

No binding was evident when rhTGF-β2 was injected on to the chip surface (Figure 5.28). It was possible that rhTGF-β2 had non-specifically adsorbed to the plastic in the microfluidic cartridge and, when the sixth ppTGF-β2 pool was injected on to the Biacore chip, the contaminating proteins in the sixth ppTGF-β2 pool blocked potential non-specific binding sites. The Biacore manufacturers recommend that analyte concentrations significantly higher than the equilibrium dissociation constant and HBS + P20 detergent running buffer be used to prevent non-specific binding, which were clearly not the conditions here. This potential false negative result was investigated by including carrier BSA protein with rhTGF-β2 (Boehringer-Mannheim, Germany) and injecting it on to the Biacore chip. Again no significant binding was observed in comparison with binding that was observed for the sixth ppTGF-β2 pool. An alternative explanation is that co-factors in ppTGF-β2 are required for the antibody-TGF-β2 interaction and, in their absence, no binding is observed. The possibility that the antibodies had denatured during purification and storage was investigated. A screening ELISA was repeated where recombinant human TGF-β2 (Sigma Chemical Co., St. Louis, MO, USA) was coated on to ELISA plates and used to capture antibodies 5D4 and 8A3. The results were positive and thus confirmed that the antibodies retained their binding capacity for TGF-β2.

5.3.5 Antigen Capture ELISA

The ability of antibodies 5D4 and 8A3 to capture TGF-β2 from solution was investigated and compared with that of the Promega anti-TGF-β2 monoclonal antibody used in the ELISA kit. Figure 5.29 shows the optical densities of the wells in the ELISA after the optical density of the corresponding blank has been subtracted.

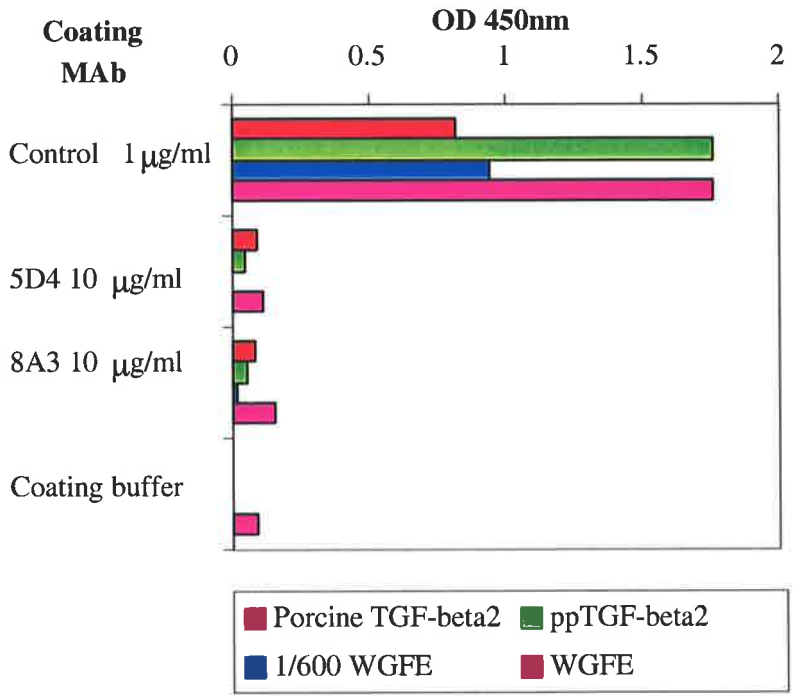

Figure 5.29: Capture of solution-phase TGF-β2 with antibody coated on ELISA plates. *Optical densities of the wells in the antigen capture ELISA after the optical density of the corresponding blank has been subtracted. Solution-phase porcine TGF-β2 (Promega, Madison, WI, USA), ppTGF-β2 and activated WGFE were screened against wells coated with 100 ng/well anti-TGF-β2 monoclonal antibody (Promega, Madison, WI, USA), 1000 ng/well antibody 5D4 and 1000 ng/well antibody 8A3.*

Antibodies 5D4 and 8A3 do not capture TGF-β2 from solution in the ELISA format (Figure 5.29). It is possible that the monoclonal antibody binding site for 5D4 and 8A3 obscures binding of the rabbit polyclonal antibody to the epitope. The source of the polyclonal antibody is unknown but if, for example, the ELISA kit uses the Santa Cruz rabbit polyclonal antibody raised against TGF-β2(50-75), then no response would be observed. Other potential explanations are that antibodies 5D4 and 8A3 possess much lower avidity for TGF-β2 than the Promega monoclonal antibody or that they are highly labile and denature upon coating to the surface.

In view of the failure of coated antibodies 5D4 and 8A3 to bind solution phase TGF-β2, the antigen capture ELISA experiment was repeated with the addition of dithiothreitol to the sample buffer. It was thought that dithiothreitol would reduce and partially unfold the TGF-β2 molecule thereby exposing linear epitopes to which the antibodies had been raised. The

amount of specific binding was determined by subtracting the optical density of the uncoated well from the optical density of the corresponding coated well (Figure 5.30).

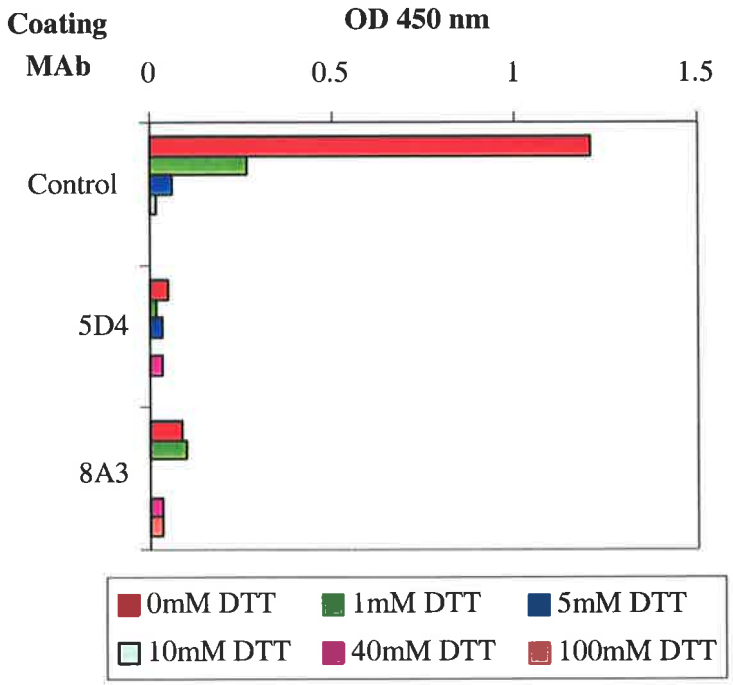

Figure 5.30: Capture of solution-phase TGF-β2 with antibody coated on ELISA plates under reducing conditions. *Optical densities of the wells in the antigen capture ELISA after the addition of dithiothreitol to sample buffer.*

Dithiothreitol denatures the specific binding of Promega antibody to TGF-β2 at a concentration above 1mM (Figure 5.30). No increase in specific binding was observed for antibodies 5D4 and 8A3 in contradiction with the finding of Flanders et al. (1990). However, an increase in non-specific binding was seen for increasing dithiothreitol concentrations.

5.3.6 Antibody Immobilisation to Ultrabind Membrane

5.3.6.1 Antibody Coupling Density

Monoclonal antibodies 5D4 and 8A3 were immobilised to sections of Ultrabind membrane with the aldehyde, hydrazide, tosyl chloride and EDC coupling chemistries. Table 5.5 shows the antibody coupling density of the membrane pieces for these coupling chemistries.

Immobilisation chemistry	5D4 antibody coupling density ($\mu g/cm^2$)	8A3 antibody coupling density ($\mu g/cm^2$)
Aldehyde	5.8±0.2	4.1±0.2
Hydrazide	40.8±3.5	49.4±4.2
Tosyl chloride	25.3±1.8	18.5±1.2
EDC	6.7±1.4	17.2±1.8

Table 5.5: Antibody coupling densities to Ultrabind membrane. *The 95% confidence intervals on the coupling density were calculated by a similar statistical method to that employed in section 5.2.1.3.*

The antibody coupling densities for the aldehyde immobilisation chemistry were significantly lower than the coupling densities reported by Pemawansa et al. (1990). Pemawansa et al. (1990) spot-wetted Ultrabind membrane with 282 $\mu g/cm^2$ of goat IgG and determined that 126 $\mu g/cm^2$ had covalently immobilised. By comparison 56 $\mu g/cm^2$ of antibodies 5D4 and 8A3 were spot-wetted and only ~5 $\mu g/cm^2$ immobilised. Nachman et al. (1992) reported an antibody coupling density of 400 $\mu g/cm^2$ for a hydrazide-activated membrane, which is much higher than the density here. It is thought that the activated groups on the Ultrabind membrane surface had degraded.

5.3.6.2 Static Binding Capacity for TGF-β2

The antibody coupled membrane sections were incubated overnight in the sixth TGF-β2 pool that had been dialysed against PBS. The next day the membranes were washed briefly and then incubated in eluent. The eluent was subject to TGF-β2 ELISA to determine whether TGF-β2 specifically bound to the coupled antibody. Given that the antibody coupling densities were in the range 5-50 $\mu g/cm^2$, the maximum theoretical TGF-β2 binding capacities should be in the range 1.6-16 $\mu g/cm^2$. None of the membranes to which antibody was immobilised demonstrated a significantly higher TGF-β2 concentration in the eluent than the membranes to which antibody was not coupled. Blank membranes adsorbed TGF-β2 at 30-300 ng/cm^2, despite attempts to block the membrane with ethanolamine prior to the binding capacity study. Brown et al. (1990) reported that TGF-β is rapidly lost from solution by adsorption to untreated plastic surfaces. In their work 50% of the TGF-β was lost within 5 minutes and over 70% was lost within 15 minutes from PBS solutions.

It was demonstrated in Chapter 3 that antibody 5D4 binds when TGF-β2 is coated on ELISA plates, blotted on to nitrocellulose membrane or present in tissue sections. However, when antibody 5D4 is coated on ELISA plates, immobilised to a Biacore sensor chip or immobilised to a membrane, it does not specifically bind TGF-β2. Possible explanations are proposed in the following paragraphs.

- Raising of antibodies against "neo-antigens"

It is often the case that a native protein is of insufficient abundance or purity to be used as an immunogen. For this reason, immunisations with synthetic polypeptides corresponding to fragments of native protein are often used to raise an immune response against a particular native protein. However, shorter synthetic polypeptides can only approximate the 3-dimensional conformation of the native protein. If the conformations of the two species are sufficiently different then antibodies against the synthetic polypeptides will fail to bind to the native protein in solution. Antibodies can fail to bind the native protein in solution although the native protein binds when it is coated on an ELISA plate (Altschuh et al., 1985). This is because the hydrophobic polystyrene surface preferentially attracts some regions of the native protein and distorts its conformation. In this way the epitope is revealed to the aqueous environment or distorted into the conformation that is recognised by the antibody. Antigens that possess this characteristic are termed "neo-antigens" (Pepper, 1992). In western immunoblots (section 3.3.4) the heat and SDS detergent provide a denaturing environment that could distort native TGF-β2 sufficiently to yield the epitope that binds to antibody 5D4. However, immunohistochemical staining (section 3.3.4) demonstrated that antibody 5D4 binds TGF-β2 in the microenvironment surrounding cells and that TGF-β2 competes with the antibody from human skin sections. Therefore, antibody 5D4 binds solution-phase TGF-β2 but whether this is at a reduced level relative to binding in solid-phase TGF-β2 formats is unknown.

- Antibodies have low avidity

According to Harlow and Lane (1988), the variation in binding observed for different techniques is common for antibodies. The variation is explained by multivalent binding, which is more likely to occur when the antigen is in the solid phase and antibody in the solution phase. Multivalent interactions permit low affinity antibodies to bind tightly when antigen is coated on ELISA plates or blotted on nitrocellulose membranes.

- Antibodies are highly labile

Solid-phase antibodies can also fail to bind solution-phase antigen because the binding sites are denatured by the immobilisation conditions (Pepper, 1992; Chase, 1984). Chemicals or changes in pH can denature the antibodies because a subtle change in conformation can eliminate binding. The orientation of the antibody upon immobilisation can sterically hinder the approach of the antigen to the binding site. If the antibody density is too high on the chromatography support then "crowding" may similarly block the approach of the antigen. The antibody may be chemically immobilised to the support by multiple attachments that can distort the conformation of the antibody, thereby denaturing the binding capacity. Some antibodies are highly labile and this sensitivity is likely to be related to the original affinity of the antibody-native antigen interaction. For this reason, lower affinity antibodies raised against a synthetic peptide fragment are more likely to be denatured by immobilisation than antibodies raised against the native antigen.

It is not possible to conclude which of these reasons is responsible for the differences in binding observed for the alternative formats. It is more likely that low avidity and high lability explain these results but the "neo-antigen" explanation can not be discounted. The possibility exists that all three influences work in concert to prevent immobilised antibody from binding to solution-phase TGF-β2.

Historically, pre-activated Sepharose (Amrad Pharmacia Biotech) has been the most widely used affinity support. Polyethersulfone membranes and the Biacore instrument are relatively new technologies and therefore will be treated with suspicion. The antigen capture ELISA is not a conclusive method for establishing the absence of solution-phase TGF-β2-binding because of the possibility that the polyclonal antibody was raised against the same epitope as antibodies 5D4 and 8A3. The solution-phase TGF-β2-binding issue will be resolved in Chapter 6 by immobilising the antibody to pre-activated Sepharose and contacting the coupled Sepharose with the antigen.

Chapter Six

Immunopurification of TGF-β2 from WGFE

6. Immunopurification of TGF-β2 from WGFE

6.1 Introduction

It was demonstrated in Chapter 2 that the purification of TGF-β2 from whey with cation-exchange chromatography, acid gel filtration and reversed phase HPLC yielded low specific TGF-β2 activity. Chapter 3 showed that immunisation with partially purified TGF-β2 generated a non-specific titre against contaminants in the preparation and that attaining a specific titre was difficult. Dasch et al. (1989) immunopurified TGF-β2 from partially purified bovine bone. Therefore the small-scale immunopurification of TGF-β2 from ppTGF-β2 was attempted with commercially available anti-TGF-β1,2,3 monoclonal antibody to demonstrate the proof of concept and to immunopurify TGF-β2 for the immunisations.

Although antibodies 5D4 and 8A3 are specific for TGF-β2 and bind to ELISA plates coated with TGF-β2, Chapter 5 showed that no specific TGF-β2-antibody binding occurred when the antibody was coated to an ELISA plate, immobilised to a Biacore sensor chip or immobilised to a membrane. The results of these binding studies suggest that it is unlikely that solution-phase TGF-β2 will bind antibody-coupled gel but they are not conclusive. Therefore, experiments were performed to determine:

- The specific TGF-β2 binding capacity of antibodies 5D4 and 8A3 coupled to Sepharose
- The extent to which TGF-β2 must be partially purified before being loaded on to the immunoaffinity column for an effective purification
- The purity of the eluted TGF-β2
- The pH of the solution at which contaminants are washed from the column without desorbing TGF-β2
- The pH of the solution at which TGF-β2 elutes
- The performance of antibodies 5D4 and 8A3 relative to that of the commercially available monoclonal antibody

The following strategy was adopted to answer these questions. Antibody 5D4, antibody 8A3 and commercially available anti-TGF-β1,2,3 monoclonal antibody were immobilised to NHS-activated Sepharose 4FF. In separate purification runs, activated WGFE (low purity) and ppTGF-β2 (high purity) were loaded on to the antibody-coupled gels. The bound protein was eluted with a linear 0-100% gradient in a 0.1M citric acid pH 5-0.1M citric acid pH 2

buffer system. The eluting fractions were monitored for protein by UV (280 nm) absorbance and for TGF-β by Mv1Lu biological assay.

6.2 Materials and Methods

6.2.1 Immobilisation of Antibodies to Sepharose

Anti-TGF-β1,2,3 monoclonal antibody (Genzyme, MA, USA), purified antibody 5D4 and purified antibody 8A3 were covalently immobilised to NHS-activated Sepharose 4FF (Amrad Pharmacia Biotech) according to the instructions of the manufacturer. The NHS immobilisation chemistry is shown in Figure 5.2.

NHS-activated Sepharose 4FF slurry was poured into a buffer holder above a 1 μm Whatman filter. The degassing equipment was used to remove the isopropanol preservative solution from the gel particles. Six times the volume of cold (4°C) 1mM HCl was added to the dry gel particles and drawn through the filter. The gel particles were scraped off the filter into a siliconised tube. Lyophilised antibody was resuspended in 0.2M $NaHCO_3$-0.5M NaCl pH 8.2. A sample of the antibody solution was taken for the determination of coupling efficiency. The antibody solution was added to the gel and the tube was capped. The tube was taped to a drum that was rotating about a horizontal axis. In this way the gel could not settle because the tube was continually being inverted. The incubation continued at room temperature for 5 hours. One gel slurry volume of 1M Tris pH 8 was added to the gel to block unreacted NHS groups. Blocking continued overnight at 4°C with no agitation.

The next day a column (Vantage L 11×250, Amicon, Beverly, MA, USA) was set up and connected to an FPLC system. The buffers PBS (10mM Na_2HPO_4, 150mM NaCl pH 7), 1M Tris pH 8 and 0.1M sodium acetate-0.5M NaCl pH 4 were prepared. The blocked gel was packed into the column. The packed volume of the gel was approximately half that of the slurry. The gel was washed to remove any non-covalently bound antibody. The gel was washed at 2 ml/min alternately with 1M Tris pH 8 (4 bed volumes) and 0.1M sodium acetate-0.5M NaCl pH 4 (4 bed volumes) a total of three times. Finally the coupled gel was stored in PBS+0.02% (w/v) sodium azide. The column flushes were collected, pooled together and sampled for the determination of antibody coupling efficiency.

The coupling efficiency of the antibody to Sepharose was ascertained by protein estimation (Bradford, 1976) or ELISA. In the protein estimation technique BSA standards were prepared in the range of 0 to 250 µg/ml. Coomassie blue reagent (Bio-Rad, Hercules, CA, USA) was added to the standards and the samples in the ratio of 1:4. The Bradford assay rather than the BCA assay was used to estimate protein because it was found that NHS interfered with colour development in the BCA assay. The standards/samples were vortexed and 100 µl/well was transferred in duplicate to a 96-well microtitre plate. The plate was read immediately with a plate reader (Bio-Rad 450, Hercules, CA, USA) at 570 nm. The coupling efficiency was also determined by ELISA according to the method of section 3.2.2. Serial 1:2 dilutions of the antibody solution prior to immobilisation and the pooled column flushes were prepared. The dilutions were transferred to an ELISA plate that was coated with the ppTGF-β2 pool from the sixth purification. The optical densities of the antibody solution prior to immobilisation and the pooled column flushes were compared. The coupling efficiency was calculated by taking into account the dilutions and volumes of the antibody solution prior to immobilisation and the pooled column flushes.

6.2.2 Immunopurification of TGF-β2 from WGFE

TGF-β2 containing solutions were contacted with anti-TGF-β2 antibody-coupled Sepharose in six separate experiments. Three monoclonal antibodies were immobilised to NHS-activated Sepharose 4FF: anti-TGF-β1,2,3 antibody, purified 5D4 antibody and purified 8A3 antibody. Two TGF-β2 feed solutions were contacted separately with the gels: activated WGFE and ppTGF-β2. The general methodology is described in the following paragraphs.

A column (Vantage L 11×250, Amicon, Beverly, MA, USA) was packed with the coupled gel and connected to the FPLC system. PBS, 0.1M citric acid pH 5 and 0.1M citric acid pH 2 were prepared and degassed. All flows were pumped through the column by the FPLC system at 2 ml/min. The column was equilibrated with PBS until a stable UV (280 nm) baseline was observed. Eluent (0.1M citric acid pH 2) was pumped through the column to dissociate non-covalently bound antibody from the gel to prevent it contaminating the eluting TGF-β2. Once the UV absorbance had returned to baseline, the column was again equilibrated with PBS, which continued until the effluent pH had returned to neutrality. TGF-β2 containing solution was injected into a loop and subsequently loaded on to the column. Two-minute fractions of the column effluent were collected with a FRAC-100 fraction collector (AMRAD Pharmacia Biotech) in siliconised tubes throughout the run. After the

protein was loaded, PBS was pumped through the column in order to wash non-binding species from the column and this was continued until the UV absorbance had returned to baseline. A linear 0-100% gradient was pumped through the column with the buffer system 0.1M citric acid pH 5-0.1M citric acid pH 2 over a period of 30 minutes. The column was equilibrated with PBS until the effluent pH reached neutrality.

The fractions were subject to Mv1Lu biological assay to determine in which fractions TGF-β was present. The purity of the TGF-β activity, that eluted under acidic conditions, was ascertained with analytical reversed phase HPLC and SDS-PAGE.

6.2.3 Static Binding Capacity for TGF-β2

Column experiments established the dynamic TGF-β2 binding capacity of the antibody-coupled Sepharose but this was not equivalent to the maximum binding capacity, q_m. Theoretically, this value can be determined by incubating the antibody-coupled Sepharose with antigen for long periods (overnight) and measuring the depletion of antigen from solution (Pepper, 1992).

Antibodies 5D4 and 8A3 were immobilised to NHS-activated Sepharose 4FF according to section 6.2.1. A negative control gel was prepared in the same manner in the absence of antibody. Rather than wash non-covalently bound antibody from the gel in a column, the tubes were spun at 1000 g in a microcentrifuge for five minutes to separate the gel from the supernatant, which was then removed. The antibody coupling density and efficiency were determined with ELISA.

TGF-β2 was partially purified from WGFE with Cellufine acid gel filtration, reversed phase C4 HPLC (0-80% acetonitrile over 80 minutes) and a second reversed phase C4 HPLC step (20-40% acetonitrile over 200 minutes). The specific activity was determined by a combination of TGF-β2 ELISA and micro BCA assay to be 9.58 μg/mg. The pool of TGF-β2 was partially dried for 90 minutes on a centrifugal vacuum drier in order to evaporate the acetonitrile, which was likely to interfere with TGF-β2-antibody binding. One-ninth the volume of 10×PBS was added to the TGF-β2 pool and the pH was adjusted to 7 with HCl and NaOH. Five TGF-β2 concentrations were prepared in PBS: 3.38, 1.69, 0.845, 0.422 and 0.211 μg/ml. Each sample of coupled gel was divided between five siliconised tubes, to each of which a different TGF-β2 concentration was added. The tubes were capped and secured to

a rotating drum so that the tubes were continually being inverted. The coupled gel was incubated with TGF-β2 overnight at room temperature. On the next day the tubes were spun on the microcentrifuge at 1000 g for five minutes in order to precipitate the gel particles. The supernatant was collected and subject to TGF-β2 ELISA in order to determine the depletion of TGF-β2 from solution.

6.3 Results and Discussion

6.3.1 Immunopurification of TGF-β2 from WGFE

Anti-TGF-β1,2,3 monoclonal antibody was immobilised to NHS-activated Sepharose 4FF, packed into columns and contacted with activated WGFE and ppTGF-β2 in an attempt to immunopurify TGF-β2. One milligram of the antibody was coupled to 1.3 ml of gel and no protein was detected in the pooled column eluates with Bradford protein assay. The ppTGF-β2 pool from the third purification was lyophilised and resuspended in PBS (8.38mM Na_2HPO_4, 1.47mM KH_2PO_4, 2.68mM KCl, 0.15M NaCl pH 7.4). TGF-β2 (37.4 μg) was injected on to the column at 0.2 ml/min. After the effluent absorbance had returned to baseline a flow of PBS+0.5M NaCl at 2 ml/min was started. When absorbance baseline was attained 0.2M glycine pH 2.3 was pumped through the column. The protein corresponding to the loading and elution peaks was collected.

The Bradford technique determined that 29.2 μg and 10.9 μg of protein were present in the loading and elution peaks respectively. Mv1Lu bioassay showed that 14.3 μg of TGF-β was in the elution peak and it did not detect biological activity in the loading peak. TGF- β2 (2.08 μg) from the elution peak was injected on to a C4 narrow bore reversed phase HPLC column (Waters Chromatography Division, Millipore). A linear 20 to 50% acetonitrile gradient was run over 30 minutes at 0.5 ml/min with buffer A (0.1% TFA) and buffer B (80% acetonitrile/0.1% TFA). Twenty-three two-minute fractions were collected with the fraction collector in siliconised tubes and subjected to Mv1Lu biological assay (Figure 6.1).

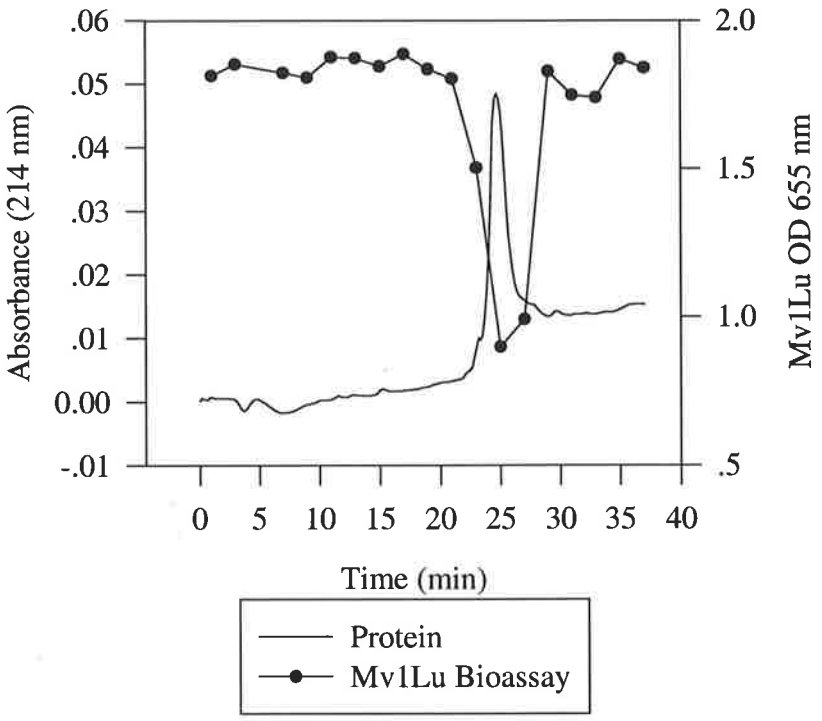

Figure 6.1: TGF-β2 biological activity was measured in the elution peak and subject to analytical reversed phase C4 HPLC to ascertain the purity. *A linear 20-50% acetonitrile gradient was run over 30 minutes and the fractions were assayed for Mv1Lu growth inhibition. The extinction coefficient method (Buck et al., 1989) determined that the integrated peak area (3.49×10^6 μV.s) correlated with 3.06 μg protein.*

The protein concentration of the biologically active fractions of Figure 6.1 was below the limit of detection for dye-binding assays. The integrated peak absorbance was calculated and used to determine the approximate concentration with the method of Buck et al. (1989) and an Excel spreadsheet developed by Dr. Steven Milner of GroPep. The extinction coefficient for TGF-β2 was determined relative to a standard protein (Insulin-like growth factor-I) for which the extinction coefficient was known on this particular instrument. The pool of biologically active fractions corresponding to the absorbance peak was 317 ng TGF-β2 and therefore a specific activity of 103 μg/mg. The specific TGF-β activity of this material was lower than the ppTGF-β2 starting material (531000 μg/mg) despite the obvious separation of non-TGF-β protein in the UV absorbance chromatograms. The possibilities exist that these additional purification steps denatured TGF-β biological activity or that the measurements of protein with BCA assay and integrated peak area are not consistent. The pool was N-terminally sequenced at the Department of Biochemistry, University of Adelaide. The first

five amino acids of TGF-β2 (ALDAA) were correctly identified by N-terminal sequencing (Cox and Burk, 1991). The sequencing demonstrated that the protein was not homogeneous as each round of sequencing revealed contaminating residues. Furthermore there was a significant amount of glycine contamination, which is presumably the result of elution with a glycine buffer in the immunoaffinity step. Therefore an alternate eluent such as citric acid was desired that does not interfere with N-terminal sequencing. Multiple repetitions of these chromatographic steps purified TGF-β2 material from the ppTGF-β2 pools of the second, third and fourth purifications for the immunisations and titre detection of section 3.3.1.

Activated WGFE was also injected on to the Sepharose, to which anti-TGF-β1,2,3 antibody was coupled, in an attempt to immunopurify TGF-β1 and TGF-β2. WGFE was acidified to pH 2.5 with HCl and incubated overnight at 4°C. The next day the pH was increased to 6.5 with NaOH and a considerable amount of protein precipitated. The protein was spun (J6, Beckman, USA) at 1700 g for 30 minutes at 4°C, the supernatant was collected and filtered through 0.45 μm and 0.22 μm membranes (Millipore, Sydney, NSW). The filtered supernatant was assayed using the Mv1Lu cell bioassay (1.46 μg/ml TGF-β) and by BCA protein assays (specific activity 49.3 ng/mg). Ten ml of the protein was injected on to the anti-TGF-β immunoaffinity column at 2 ml/min. The gel was washed with PBS and 0.2M glycine pH 5.3 and then eluted with 0.2M glycine pH 2.3. Twenty-eight fractions (two-minute) fractions were collected and assayed for Mv1Lu growth inhibition.

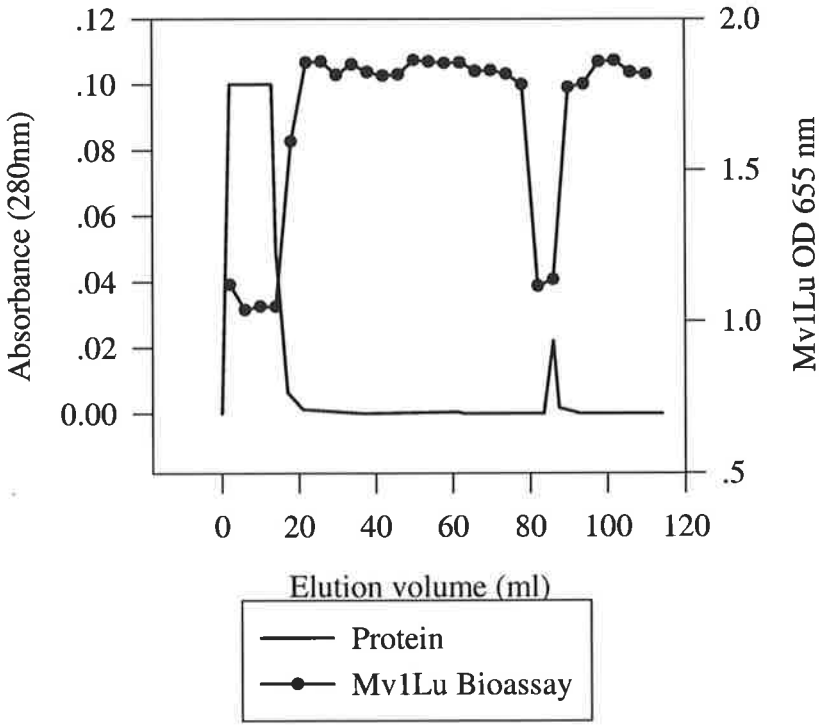

Figure 6.2: Activated WGFE was injected on to the immunoaffinity column, washed with PBS and 0.2M glycine pH 5.3, and then eluted with 0.2M glycine pH 2.3. *TGF-β activity broke through the column early during loading and also eluted under acidic conditions.*

The biologically active fractions that eluted at pH 2.3 were pooled and loaded on to a Radialpak C18 reversed phase HPLC column (Waters Chromatography Division, Millipore). A linear 0-80% acetonitrile gradient was used to elute protein from the column over 80 minutes at 1 ml/min. Fractions were collected and subject to Mv1Lu biological assay.

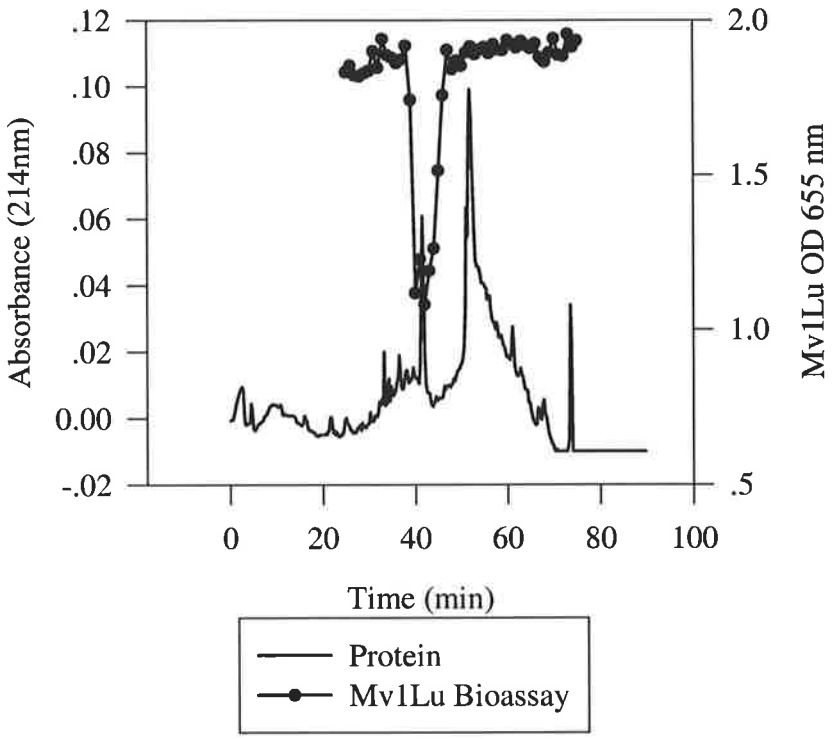

Figure 6.3: The biologically active fractions that eluted at pH 2.3 in Figure 6.2 were loaded on to a reversed phase C18 HPLC column. *Elution was performed with a 0-80% acetonitrile gradient over 80 minutes.*

A peak of biological activity (Figure 6.3) was observed which corresponded to an absorbance peak at 40 minutes. The biologically active fractions were pooled and assayed for Mv1Lu growth inhibition (1.24 μg TGF-β) and protein (specific activity 151 μg/mg). The eluting TGF-β was contaminated with protein that non-specifically bound to the affinity column and then co-eluted with the TGF-β. It was thought that the use of a step gradient (0.2M glycine pH 5.3 followed by pH 2.3) was sub-optimal for purification because contaminating protein, which may have been eluted at pH between pH 5.3 and 2.3, co-eluted with TGF-β. Therefore the use of a linear gradient between pH 5.3 and 2.3 may be successful in eluting the contaminating protein before TGF-β elutes.

Antibodies 5D4 and 8A3 were immobilised to NHS-activated Sepharose 4FF, packed into columns and contacted separately with activated WGFE or ppTGF-β2 in an attempt to immunopurify TGF-β2. Antibody 5D4 (15.5 mg) was coupled to 2.7 ml of gel with a coupling efficiency of 99.95% as determined by ELISA and antibody 8A3 (15.9 mg) was coupled to 2.4 ml of gel with a coupling efficiency of 91%. WGFE was activated by increasing the pH to 11 with NaOH and incubating overnight at 4°C. The pH was adjusted to

7 with HCl on the following day and filtered through a 1 μm Whatman filter. Tween 20 (0.05% v/v) was added to the protein in order to minimise non-specific adsorption to the gel. ELISA determined that the TGF-β2 concentration was 0.7 μg/ml. WGFE was loaded on to the coupled gels and chromatography was performed as described in section 6.2.2 (Figure 6.4).

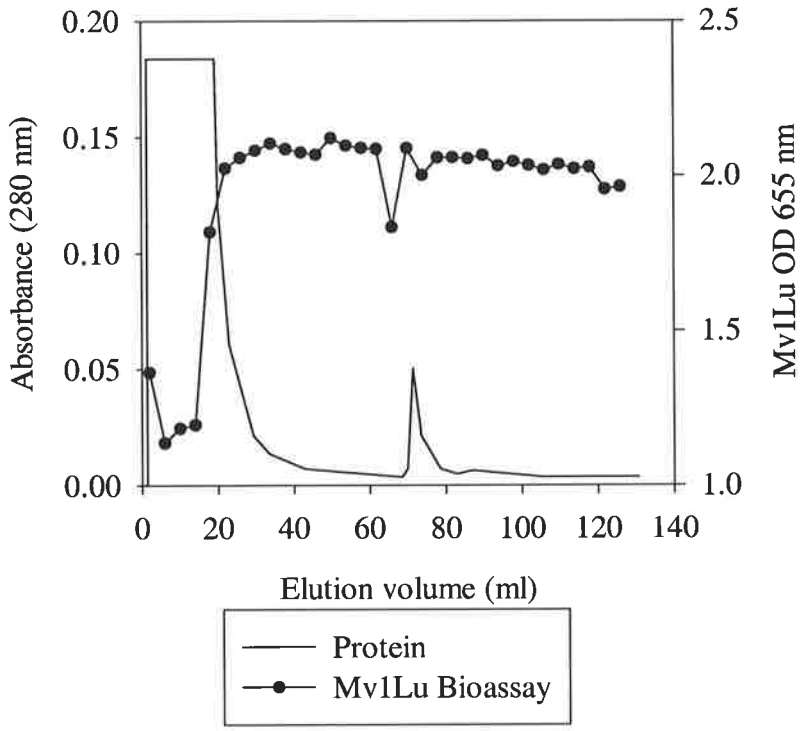

Figure 6.4: Activated WGFE (8.6 μg TGF-β2) was loaded on to 2.7 ml of Sepharose, to which 15.5 mg of antibody 5D4 was coupled. *After loading, the column was washed with PBS (10mM Na_2HPO_4, 150mM NaCl pH 7) and then subject to a linear 0-100% gradient of 0.1M citric acid pH 5-0.1M citric acid pH 2 over 30 minutes. Similar results were obtained for antibody 8A3 and also when Tween 20 was not included in the loading protein.*

The result indicated that it is not possible to capture TGF-β2 from activated WGFE with Sepharose, to which antibodies 5D4 and 8A3 are coupled, unlike the commercially available antibody. Citric acid eluents were screened in a similar manner as described in section 5.2.2 and found to be effective at pH < 3. Evidence from Chapter 5 suggests that these antibodies fail to bind solution-phase TGF-β2 because they are denatured upon coupling or possess low avidity. However, the possibility exists that the complexity of WGFE is such that protein contaminants with similar epitopes to which the antibodies bind prevent TGF-β2 adsorption. Therefore ppTGF-β2 from the sixth purification was loaded on to the coupled gels in an attempt to immunopurify TGF-β2 (Figure 6.5).

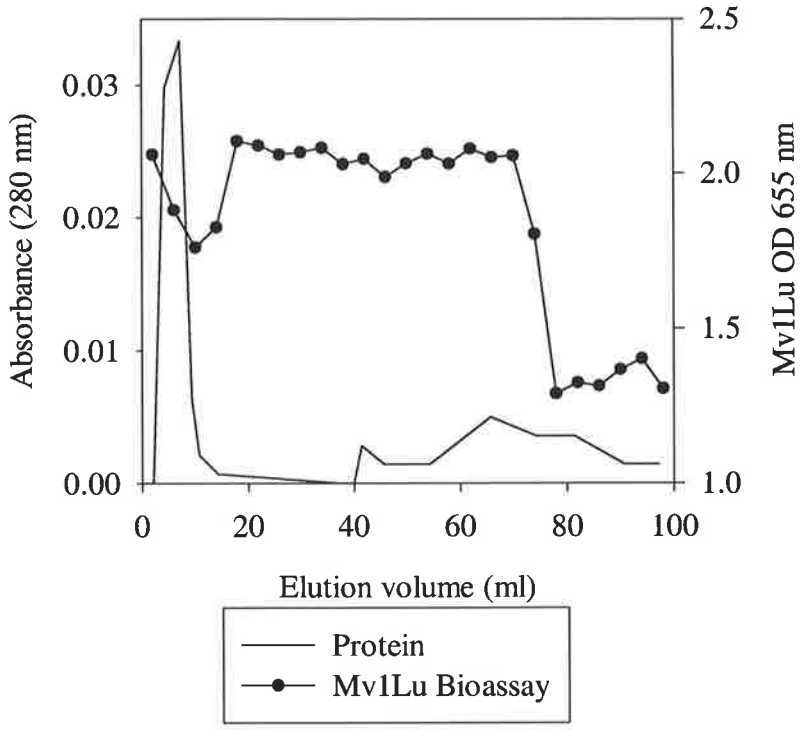

Figure 6.5: ppTGF-β2 from the sixth purification (6.6 μg/ml) was dialysed against PBS and 5 ml was loaded on to the antibody 5D4 coupled gel. *After loading, the column was washed with PBS and then subject to a linear 0-100% gradient of 0.1M citric acid pH 5-0.1M citric acid pH 2 over 30 minutes. Sixteen micrograms of TGF-β2 eluted under acidic conditions. Similar results were obtained for antibody 8A3.*

TGF-β2 specifically bound and eluted from the coupled gels. The purification steps prior to immunoaffinity chromatography removed contaminating proteins from WGFE that possess similar epitopes to TGF-β2 or interfere with the binding. The pH of the fractions in which TGF-β2 eluted were in the range 3.53 to 2.77 (antibody 5D4) and 4.15 to 3.34 (8A3) and these compare with the ranges established in Chapter 5 of 3.5 to 2.5, supporting the hypothesis that a specific immunoaffinity interaction had taken place. Multiple repetitions of immunoaffinity chromatography were performed to purify TGF-β2 from the pool of the sixth purification. The biologically active fractions eluting under acidic conditions were pooled and loaded on to a C4 narrow bore reversed phase HPLC column (Waters Chromatography Division, Millipore). A linear 20 to 50% acetonitrile gradient was run over 30 minutes at 0.5 ml/min with buffer A (0.1% TFA) and buffer B (80% acetonitrile/0.1% TFA). Thirty-six one-minute fractions were collected in siliconised tubes and subjected to Mv1Lu biological assay (Figure 6.6). Protein from the biologically active fractions was electrophoresed on a 10-20% Tricine gel under reducing conditions to determine the purity of TGF-β2 (Figure 6.7).

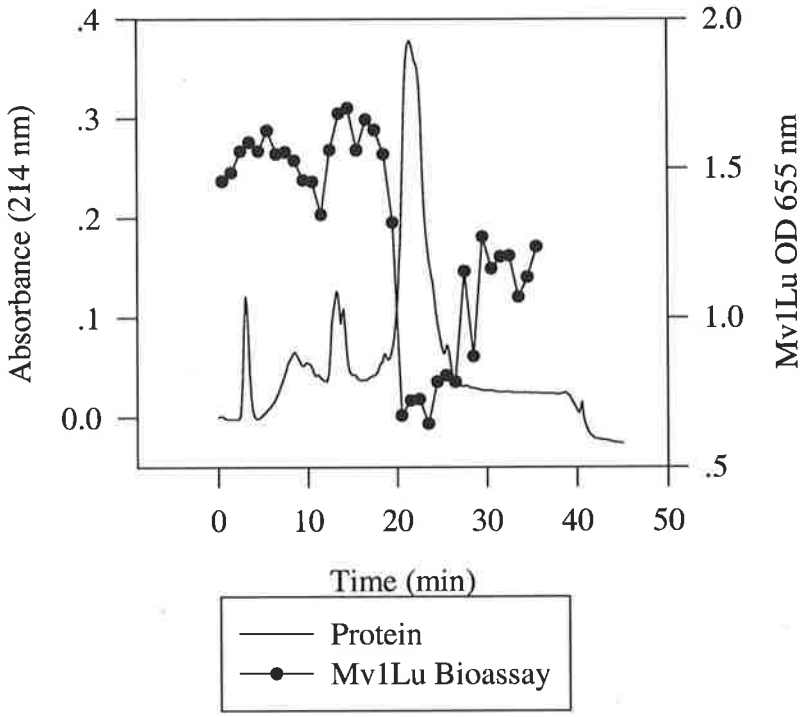

Figure 6.6: The biologically active fractions of immunoaffinity chromatography were subject to analytical reversed phase C4 HPLC to ascertain the purity. *A linear 20-50% acetonitrile gradient was run over 30 minutes and the fractions were assayed for Mv1Lu growth inhibition. The extinction coefficient method (Buck et al., 1989) determined that the integrated peak area (64.5×10^6 μV.s) correlated with 72.9 μg protein.*

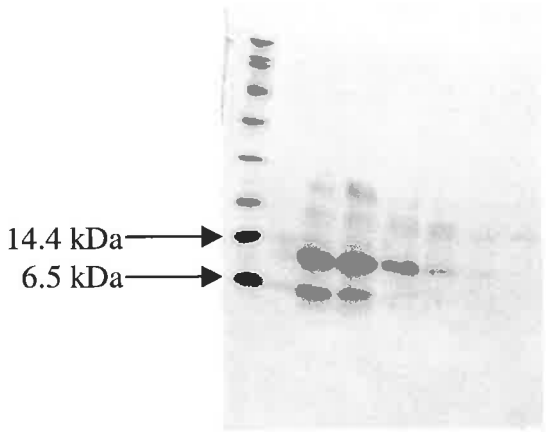

Figure 6.7: The biologically active fractions of Figure 6.6 were subject to SDS-PAGE on a 10-20% Tricine gel under reducing conditions. *A strong protein band runs at the expected molecular weight of reduced TGF-β2 in three fractions, which correspond to 22-24 minutes on the chromatogram. A low molecular weight protein (~6.5 kDa) contaminates the fractions corresponding to 22-23 minutes.*

The fractions that were identified as containing protein bands that ran at 12.5 kDa in SDS-PAGE under reducing conditions were pooled. The protein was loaded on to the Radialpak C18 reversed phase HPLC column in an attempt to purify TGF-β2 from the 6.5 kDa contaminant. A 20-50% linear n-propanol gradient was pumped through the column over 2 hours at 1 ml/min. The buffer system consisted of buffer A (10% n-propanol/0.13% heptafluorobutyric acid) and buffer B (80% n-propanol/0.13% HFBA). Thirty-five four-minute fractions were collected and assayed for Mv1Lu growth inhibition (Figure 6.8). The biologically active fractions eluting with the n-propanol gradient were electrophoresed on a 10-20% Tricine gel under reducing conditions to assess the purity of TGF-β2 (Figure 6.9).

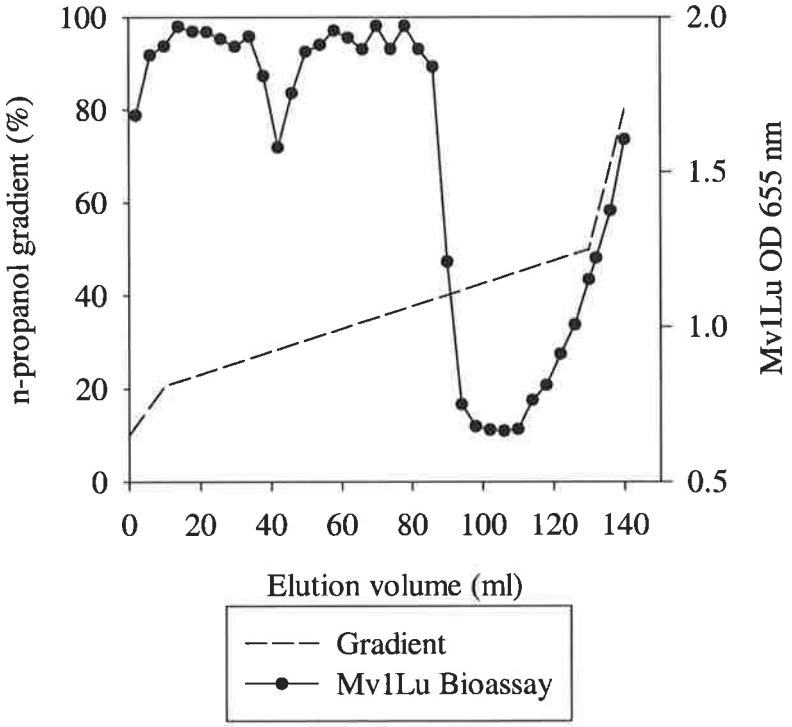

Figure 6.8: The TGF-β2 containing fractions from Figure 6.6 were loaded on to the C18 reversed phase HPLC column. *The protein was further purified with a 20-50% n-propanol gradient. It was not possible to record the absorbance of eluting protein because of the low concentration of protein and the high absorption of n-propanol at 214 nm. Instead, the n-propanol gradient is shown for comparison.*

After two rounds of reversed phase HPLC it was not possible to separate TGF-β2 from the 6.5 kDa contaminant. The possibility exists that the contaminant is the degradation product of TGF-β2 after it was exposed to the denaturing environment of SDS-PAGE. If the 6.5 kDa contaminant is a fragment of TGF-β2 then it may also bind antibody. The fractions corresponding to 94-98 minutes were electrophoresed on a 10-20% Tricine gel under

reducing conditions and electroblotted on to a nitrocellulose membrane. The membrane was probed with antibody 5D4 and developed with enhanced chemiluminescence (Figure 6.10).

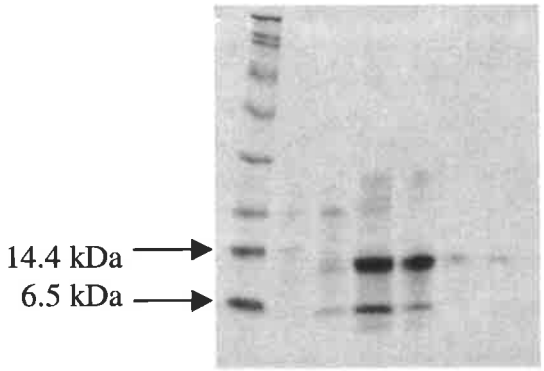

Figure 6.9: The biologically active fractions of Figure 6.8 were subject to SDS-PAGE on a 10-20% Tricine gel under reducing conditions. *A strong protein band runs at the expected molecular weight of reduced TGF-β2 in two fractions, which correspond to 94-98 minutes on the chromatogram. The low molecular weight protein (~6.5 kDa) continued to contaminate the TGF-β2.*

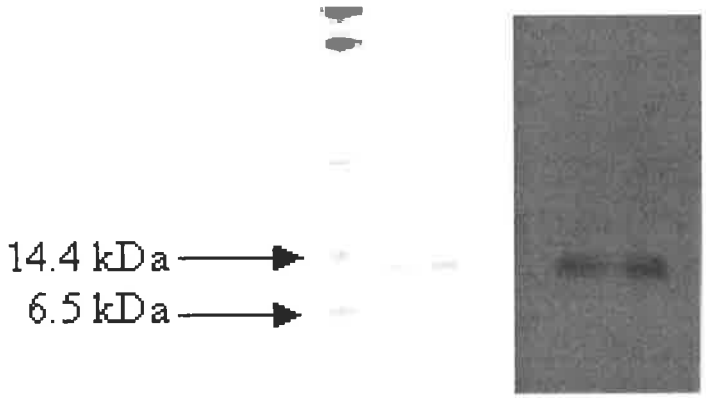

Figure 6.10: The fractions corresponding to 94-98 minutes in Figure 6.8 were electrophoresed on a 10-20% Tricine gel under reducing conditions. *Bands are visible at the expected molecular weight of reduced TGF-β2. The contaminant bands are not visible because a smaller amount of protein remains in the gel than for Figure 6.9 after electroblotting. The blotted protein was probed with antibody 5D4 (1 μg/ml), incubated with a 1:10000 dilution of peroxidase-conjugated anti-mouse antibody and visualised with enhanced chemiluminescence (right).*

The protein bands that run at 12.5 kDa were bound by antibody 5D4 and confirmed as the reduced form of TGF-β2. However, the 6.5 kDa protein contaminant did not bind antibody 5D4 and may be a degradation product of TGF-β2. The purification steps involved in the purification of TGF-β2 to the extent observed in Figures 6.9 and 6.10 were:

- Large-scale Cellufine acid gel filtration
- Small-scale Superdex acid gel filtration
- Reversed phase C4 HPLC with a gradient of 20-40% acetonitrile over 200 minutes
- Immunoaffinity chromatography
- Narrow bore reversed phase C4 HPLC with a gradient of 20-50% acetonitrile over 30 minutes
- Reversed phase C18 HPLC with a gradient of 20-50% n-propanol over two hours

The immunoaffinity chromatography step contributed greatly to the purification of TGF-β2 but substantial purification of TGF-β2 was required prior to loading on to the immunoaffinity column. Furthermore, it did not purify TGF-β2 to homogeneity but required two further HPLC purification steps. These additional steps did not separate the 6.5 kDa contaminant from TGF-β2.

6.3.2 Static Binding Capacity for TGF-β2

The static TGF-β2 binding capacity of the antibody-coupled Sepharose was determined by incubating the Sepharose with different concentrations of TGF-β2 and measuring the depletion of TGF-β2 on the following day with ELISA. The specific amount of TGF-β2 bound (ng/ml) for the blank gel, the 5D4 (6.79 mg/ml) antibody-coupled gel and the 8A3 (2.73 mg/ml) antibody-coupled gel were calculated and plotted as functions of the free TGF-β2 concentration. The adsorption isotherms were assumed to be of the Langmuir type and linearised by plotting $1/C$ versus $1/q$ (Tijssen, 1985). Tablecurve was used to regress a straight line to the data:

$$\frac{1}{q} = \frac{K_d}{q_m}\frac{1}{C} + \frac{1}{q_m} \qquad (6.1)$$

The maximum TGF-β2 binding capacity, q_m, and the equilibrium dissociation constant, K_d, were determined from the regression. The theoretical Langmuir adsorption isotherms were

deduced from the regressed constants and included for comparison with the experimental data in Figure 6.11.

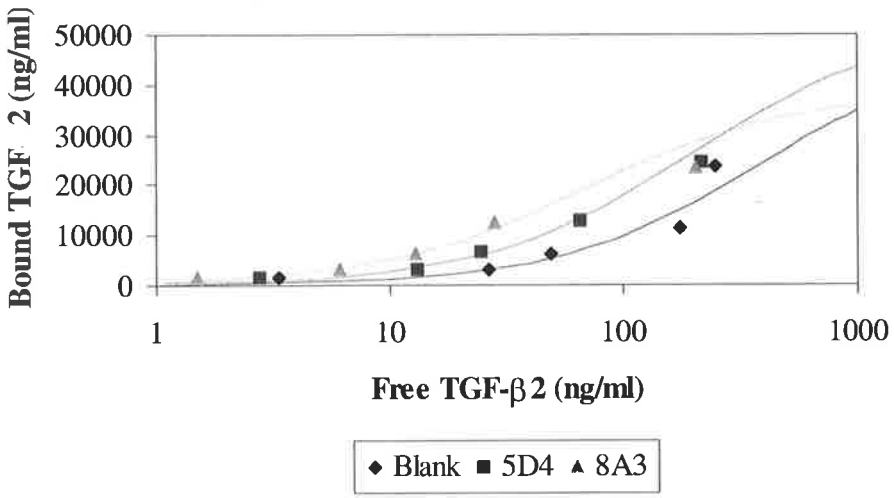

Figure 6.11: Isotherms for the adsorption of TGF-β2 from ppTGF-β2 with blank gel, 5D4 antibody-coupled gel and 8A3 antibody-coupled gel. *The data were regressed to the Langmuir equation to determine K_d and q_m. The lines show the theoretical curves calculated from the Langmuir equation and regressed K_d and q_m.*

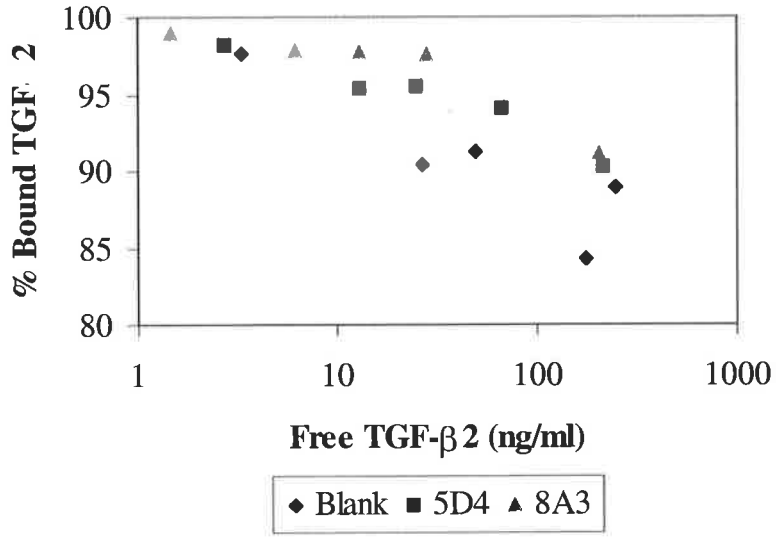

Figure 6.12: Percentage of TGF-β2 adsorbed by the gel as a function of free TGF-β2 concentration.

A high proportion (~90%) of the free TGF-β2 was bound by Sepharose, to which no antibody was coupled (Figure 6.12). There was not a significant increase in the amount of TGF-β2 bound when antibody had been coupled to the Sepharose relative to the negative control gel.

These observations suggest that TGF-β2 adsorption to antibody-coupled gel was not mediated by specific binding to the antibody. Dasch et al. (1989) reported that non-specific binding of TGF-β2 to agarose conjugated goat anti-mouse IgG was a problem and that it was necessary to include 1% (w/v) sodium deoxycholate in order to attenuate this binding. Therefore the static binding experiment was repeated with the inclusion of 1% (w/v) sodium deoxycholate in the binding buffer. Again, no significant increase in the amount of TGF-β2 bound was observed for antibody-coupled gel relative to the negative control gel.

An alternative explanation for the apparent binding of TGF-β2 to Sepharose is that TGF-β2 precipitates at neutral pH and is captured by the gel particles. According to Lucas et al. (1991) it is very important to keep TGF-β at acidic pH during iodination because it is not very soluble above pH 5. It is possible that TGF-β2 resuspends and elutes with acidic buffer giving the false impression that the binding interaction was antibody mediated. However, if this were the case then TGF-β2 would precipitate from activated WGFE and be eluted in acidic buffer in a similar manner to adsorption from ppTGF-β2. It is more likely that sticky more abundant proteins in WGFE bind to the same sites in Sepharose as TGF-β2 but with less avidity and are subsequently eluted at the start of the citrate gradient (pH ~5). Once these sticky contaminants have been removed from the protein, the purification of TGF-β2 from ppTGF-β2 is possible.

Antibodies 5D4 and 8A3, when immobilised to NHS-activated Sepharose 4FF, do not bind solution-phase TGF-β2 in agreement with the finding of Chapter 5 where an absence of binding to solid-phase antibody was also noted. Therefore the antibodies are too labile or possess insufficient avidity for use in immunoaffinity chromatography.

Name	Modified	Size	Ratio	Packed	Path
Title Page.doc	2/02/2000 21:45	19,456	89%	2,063	
Abstract.doc	2/02/2000 23:11	25,088	84%	4,109	
Acknowledgments.doc	2/02/2000 23:14	20,992	86%	2,934	
Appendix page numbers.doc	5/02/2000 13:10	19,456	91%	1,727	
Chapter 5a.doc	6/02/2000 20:50	338,432	72%	95,364	
Chapter 5b.doc	6/02/2000 20:51	274,944	72%	77,334	
Chapter 5c.doc	5/02/2000 13:31	212,992	29%	150,456	
Chapter 5d.doc	6/02/2000 20:53	295,936	33%	197,740	
Chapter 6.doc	5/02/2000 14:53	476,672	69%	146,863	
Chapter 7.doc	6/02/2000 20:40	97,792	79%	20,858	
Errata.doc	12/02/2001 22:08	75,264	85%	11,032	
Reference.doc	3/02/2000 21:42	105,472	74%	27,498	
Statement of originality.doc	22/01/2000 13:41	19,456	88%	2,377	
Table of Contents.doc	7/02/2000 8:43	57,344	84%	9,136	
Table of Figures.doc	7/02/2000 8:43	42,496	80%	8,580	
Table of Tables.doc	7/02/2000 8:43	26,624	83%	4,399	
Abbreviations.doc	22/01/2000 15:05	23,040	83%	3,940	
17 file(s)		**2,131,456**	**64%**	**766,410**	

Chapter Seven

General Discussion

7. General Discussion

7.1 Introduction

Transforming growth factor-β2 is a valuable protein with a wide range of biological activities *in vitro* and a number of potential therapeutic applications. It has historically been a difficult protein to produce recombinantly because it is homodimeric and contains a large number of disulphide bridges. This has resulted in high production costs because of the low refolding yields of bacterially expressed TGF-β2 and hence the requirement for expression in mammalian cell lines. TGF-β2 has been purified from bovine bone (Seyedin et al., 1985; Ogawa et al., 1992), bovine milk (Cox and Burk, 1991; Jin et al., 1991), human glioblastoma cells (Olofsson et al., 1992) and porcine blood platelets (Cheifetz et al., 1987). However, these natural sources are in relatively short supply and require highly involved sequences for TGF-β2 purification. The discovery of high concentrations of TGF-β2 in an abundant and cheap natural source, cheese whey, provided an opportunity to develop a purification system that would potentially be highly profitable (Rogers et al., 1996) because most of the TGF-β2 in milk partitions into whey during cheese manufacture. Francis et al. (1995) developed a cation-exchange chromatography process that partially purified a fraction of proteins from cheese whey that possesses most of the biological activity upon mammalian cells and 1-2% of the protein. This fraction is termed WGFE and is a complex protein mixture consisting of a number of growth factors, some of which are as yet unidentified (Belford et al., 1997). GroPep has patented this process and a GMP pilot-scale facility was recently commissioned in Adelaide. Rogers et al. (1996) demonstrated that TGF-β2 partitions into WGFE and that it was possible to purify it with a combination of acid gel filtration and reversed phase HPLC.

The separation of valuable biologically active molecules from sources of natural or recombinant origin often relies on multiple steps in order to meet the stringent purity requirements imposed by regulatory authorities. Such steps would typically involve ion-exchange chromatography, size-exclusion gel filtration and hydrophobic interaction chromatography, and low yields of the biologically active molecule often result. By contrast, immunoaffinity chromatography can accomplish in one step the same level of purification as the multiple step purification scheme whilst providing higher yields. A limited number of examples of commercial-scale immunoaffinity chromatography have been published in the literature. The obvious impediment to its more widespread use is the requirement of an antibody, usually monoclonal, but the potential for reducing purification costs is considerable. Dasch et al. (1989) demonstrated that monoclonal antibodies could be

generated against TGF-β2 and one of those was used for the immunopurification of TGF-β2 from a preparation that had been partially purified from bovine bone. Therefore the aim of this work was to develop an immunoaffinity separation technique, using monoclonal antibodies against TGF-β2, for the purification of TGF-β2 from WGFE in one step alone or in concert with a number of conventional purification methods.

The specific removal of TGF-β2 from WGFE would also have potential applications. WGFE is used in treatment of wounds and depleting the level of TGF-β2 could reduce hypertrophic scar formation. Furthermore, TGF-β2 is the most abundant growth factor in WGFE and it is likely that its biological activity obscures the detection of as yet unidentified growth factors. Its specific removal would increase the likelihood of discovering novel growth factors.

7.2 Generation of Anti-TGF-β2 Monoclonal Antibodies

The generation of monoclonal antibodies against isoforms of TGF-β has historically been a difficult task because it is an immunosuppressant and is highly conserved between mammalian species. Thompson et al. (1999) circumvented these problems by selecting single chain antibody fragments (scFv) specific for TGF-β2 from repertoires displayed on the surface of filamentous bacteriophage. However, this technology and expertise were not available so conventional hybridoma technology was pursued for the generation of anti-TGF-β2 monoclonal antibodies. TGF-β2 was partially purified from WGFE to varying degrees with a combination of acid gel filtration, reversed phase HPLC and immunoaffinity chromatography with a commercially available antibody. Ten mice were immunised with the partially purified TGF-β2 and poor titres were observed. Only one mouse developed a specific immune response as measured by inhibition of TGF-β2 biological activity in Mv1Lu cells. The fusion between the spleen cells and SP2/0 myeloma cells did not yield anti-TGF-β2 hybridomas because either the titre was insufficient or the fusion efficiency was too low. However, a hybridoma (9B1) was generated against a contaminant in the partially purified TGF-β2. The molecular weight of this protein is approximately 10 kDa and its identity is as yet unknown.

An alternative immunogen was considered for the generation of a titre against TGF-β2. Flanders (1990) reported that a synthetic peptide corresponding to residues 50-75 of TGF-β2 was successful at raising a specific titre for TGF-β2 in rabbits. Ten mice were immunised

with the synthetic peptide and one mouse developed a high titre for TGF-β2. The spleen cells of this mouse were fused with SP2/0 myeloma cells and two anti-TGF-β2 hybridomas (5D4 and 8A3) were generated. The specificity of the monoclonal antibodies was confirmed by coating ELISA plates with recombinant human TGF-β2 (Sigma Chemical Co., St. Louis, MO, USA) and screening the conditioned growth media against this material. The injection of conditioned media over a Biacore chip, to which recombinant human TGF-β2 was coupled, also demonstrated significant binding. The monoclonal antibodies did not cross-react when ELISA plates were coated with TGF-β1 and the conditioned media was screened against this material. This was considered to be sufficient evidence that the antibodies were suitable for the immunoaffinity purification of TGF-β2 from WGFE.

The development of a commercial-scale immunoaffinity purification process requires gram quantities of antibody and therefore a system for producing such quantities was required. Monoclonal antibodies were produced in large quantities by culturing the hybridomas in the CellMax™ artificial capillary cell culture system. The immobilisation of impure antibody to a support is not acceptable because proteins would non-specifically bind to immobilised contaminants thereby reducing the potential purity of the TGF-β2 product. The antibodies were purified from the culture media by Protein G affinity chromatography. In this way 456 mg of antibody 5D4 and 189 mg of antibody 8A3 were produced at a purity of >90%. Further evidence for the TGF-β2 specificity of purified antibody 5D4 was gained by localising TGF-β2 in western immunoblots and in skin sections. Antibody 5D4 is currently available for sale from GroPep.

7.3 Purification of TGF-β2 from WGFE

Commercially available TGF-β2 was prohibitively expensive for use as an immunogen and therefore TGF-β2 was purified from WGFE. Attempts to purify TGF-β2 to homogeneity according to the method of Rogers et al. (1996) were unsuccessful. There are a number of possible explanations as to why the TGF-β2 purification in this work was not as effective as it was for Rogers et al. (1996). The quality of the whey may have differed for the two cases. It is possible that the reversed phase column resolution degraded with age and therefore the purification of Rogers et al. (1996) could not be duplicated. Also the test, for selecting which TGF-β positive fractions to pool, was largely subjective because Rogers et al. (1996) did not publish the extent of Mv1Lu growth inhibition required to distinguish positive from negative

fractions. The difficulties encountered with conventional purification methods necessitated the use of an immunoaffinity step.

Commercially available anti-TGF-β1,2,3 monoclonal antibody was immobilised to NHS-activated Sepharose 4FF. The antibody was expensive and therefore only 1 mg was coupled. The immunoaffinity column was used to partially purify TGF-β2 from activated WGFE and ppTGF-β2 that had been purified by the method of Rogers et al. (1996). It is not known whether the adsorption was mediated by the antibody or by adsorption to the support. The TGF-β2 activity eluting from the immunoaffinity column under acidic conditions after the loading of ppTGF-β2 was subsequently loaded on to a narrow bore C4 reversed phase HPLC column. Protein was eluted from the column with an acetonitrile gradient and the biologically active fraction was also used to immunise mice. This material was N-terminally sequenced and identified as TGF-β2 but contaminating amino acid residues showed that the material was not homogeneous. The partially purified TGF-β2 was used to immunise mice and coat ELISA plates for titre detection.

The most economically attractive immunoaffinity chromatography process would consist of a one step immunopurification from WGFE. In WGFE, TGF-β is bound in a biologically inactive latent complex with latency-associated peptide (LAP) and latent TGF-β binding protein (LTBP) (Miyazano et al., 1990). Polyclonal antisera raised against TGF-β1 do not recognise the latent complex because LAP and/or LTBP surround TGF-β1 with a cage-like structure that prevents the exposure of antigenic epitopes (Wakefield et al., 1989). Therefore it is likely that similar complexes result in TGF-β2 behaving in a similar manner and will require dissociation from the latent complex prior to antibody binding. Subjecting WGFE to extremes of pH or heat increases the concentration of free TGF-β2 by dissociating the latent complex. Acidification to pH 2.5 gives the highest free TGF-β2 concentration in WGFE. However, eluent screening showed that antibody-TGF-β2 binding was poor at this pH and therefore the pH of the activated WGFE would have to be increased above 4 in order for efficient binding to occur. The pH of acidified WGFE was adjusted to various levels in an attempt to define the TGF-β2 concentrations after pH adjustment. A high proportion of the WGFE protein precipitated when the pH was increased above 4 and a reduction in supernatant TGF-β2 concentration was observed. However, the decrease in supernatant TGF-β2 concentration was greater than that accounted for by total protein precipitation alone. It is

possible that TGF-β2 precipitates selectively relative to the bulk of the proteins or that it re-associates with the latent complex when the pH is increased.

In view of the loss of TGF-β2 that resulted upon pH adjustment an alternative activation method was tried. The pH of WGFE was increased to 11 and it was found that the TGF-β2 concentration was substantially higher than unactivated WGFE although not as high as that after WGFE acidification. However, when the pH was adjusted to neutrality precipitation was not observed and the TGF-β2 concentration was unchanged from that at pH 11. More importantly, this TGF-β2 concentration was higher than that after pH adjustment to neutrality for acidified WGFE. In the event that a one step immunopurification should be developed, pH adjustment to 11 followed by pH neutralisation on the following day would be the preferred method of WGFE activation.

After TGF-β2 has bound to the antibody it is eluted from the immunoaffinity column. If a sufficiently large volume of binding buffer were pumped through the column all of the TGF-β2 would eventually desorb. However, the TGF-β2 would be very dilute and require concentration. A chemical eluent is therefore required that quickly dissociates TGF-β2 from the antibody whilst conserving the TGF-β2 binding capacity of the column and maintaining the biological activity of TGF-β2. It is important in immunoaffinity chromatography that the column is reusable as the high cost involved in producing and purifying antibody would make a single use column prohibitively expensive. Obviously the choice of eluent is critical to the economic performance of an immunoaffinity system. Therefore an ELISA format was employed to screen various eluents for their ability to dissociate antibodies 5D4 and 8A3 from TGF-β2 without denaturing the antibody. The best eluents according to these criteria were 0.1M glycine pH 3.5 for antibody 5D4 and 0.1M glycine pH 3.0 for antibody 8A3. In the presence of these eluents the half-lives of the antibody binding capacity were 66.6 hours (5D4) and 41.5 hours (8A3) indicating that these antibodies had potential for immunoaffinity chromatography.

Mathematical simulations of different hypothetical immunoaffinity configurations demonstrated that a membrane support would be likely to have considerable cost advantages over a Sepharose packed bed. The commercially available Ultrabind membrane was considered for the immunopurification of TGF-β2 from WGFE with monoclonal antibodies 5D4 and 8A3. The antibodies were immobilised to the membrane by aldehyde coupling

chemistry, hydrazide coupling chemistry, tosyl chloride coupling chemistry and EDC coupling chemistry. The sections of coupled membrane were incubated overnight in ppTGF-β2, washed and then incubated in eluent in order to determine the static TGF-β2 binding capacity. None of these coupled membranes displayed a significantly higher level of TGF-β2 binding relative to blank membranes.

Mathematical simulations of a hypothetical immunoaffinity system with varying antibody properties showed that the specific binding capacity, the equilibrium association constant and association rate constant of a prospective antibody were critical to the economic performance. The mathematical model could be used with the knowledge of these key antibody properties to identify from a panel of antibodies the antibody with the greatest economic potential. The Biacore instrument can quickly determine these key properties with relatively small amounts of analyte and antibody. In this way the best antibody for commercial-scale immunoaffinity chromatography can be identified without the need for exhaustive bench-scale testing of different flow rates, support dimensions and antibodies. Antibodies 5D4 and 8A3 were coupled to the surface of a Biacore sensor chip. Partially purified TGF-β2 was dialysed into PBS and injected on to the chip surface at different concentrations. Increases in the surface plasmon resonance signal indicated that material specifically bound to the antibody and then desorbed when PBS alone was injected on to the chip surface. Kinetic models were fitted to the sensorgrams and it was found that the binding interaction was highly heterogeneous. This could be explained by different antibody orientations upon coupling to the chip surface or the presence of contaminating proteins in ppTGF-β2 that interfere with the specific antibody-TGF-β2 interaction. The possibility of the latter explanation was examined by injecting recombinant human TGF-β2 over the sensor chip at concentrations similar to that employed in the ppTGF-β2 experiment. In this instance, no binding was observed and therefore confirmed that TGF-β2 alone was not capable of binding to coupled antibody in this configuration. Therefore, co-factors in ppTGF-β2 enable TGF-β2 to bind the coupled antibody by some unknown kinetic mechanism.

The TGF-β2 ELISA kit (Promega, Madison, WI, USA) was employed to determine whether antibodies 5D4 and 8A3, when coated on an ELISA plate, were capable of binding TGF-β2 from solution. The assay was performed according to the manufacturers' instructions except for the substitution of the kit plate-coating antibody with antibodies 5D4 or 8A3. There was

no significant increase in optical density for these wells relative to the negative control wells and therefore antibodies 5D4 and 8A3 do not capture TGF-β2 from solution.

Antibody 5D4 was shown to bind solid-phase TGF-β2 in ELISA, western immunoblots, Biacore binding studies and immunohistochemical localisation. Antibody 8A3 was observed to bind solid-phase TGF-β2 in ELISA and Biacore binding studies. Solution-phase TGF-β2 appeared to bind solution-phase antibody 5D4 and compete it from binding to TGF-β2 in skin sections. Antibodies 5D4 and 8A3, when in the solid-phase, did not bind solution-phase TGF-β2 in ELISA, Ultrabind membrane binding studies or Biacore binding studies. This evidence supports the hypothesis that the solution-phase antibodies bind solid-phase TGF-β2 but solid-phase antibodies do not bind solution-phase TGF-β2. Table 7.1 presents a summary of this evidence.

	Solution Mab-solid TGF-β2	Solution Mab-solution TGF-β2	Solid Mab-solution TGF-β2
ELISA	✓	-	✗
Biacore	✓	-	✗
Immunoblot	✓ (5D4) ✗ (8A3)	-	-
Immunohistochemical localisation	✓ (5D4) ? (8A3)	✓ (5D4) ? (8A3)	-
Mv1Lu assay	-	✗	-
Ultrabind membrane	-	-	✗

Table 7.1: Summary of the various formats in which the interactions between TGF-β2 and the antibodies (5D4 and 8A3) were studied. *The formats were categorised as solution Mab-solid TGF-β2, solution Mab-solution TGF-β2 and solid Mab-solution TGF-β2. Ticks denote that binding was observed and crosses denote a failure to bind. Red indicates that the experiment was conclusive and black indicates that the experiment provided supporting evidence.*

The phenomenon of antibodies binding to solid-phase antigen and failing to bind solution-phase antigen has been previously reported in the literature (Harlow and Lane, 1988). In view of the observations presented in Table 7.1 it is most likely that the antibody avidity for TGF-β2 is low or that the antibody-binding site denatures upon coupling to solid-phase. However, the technologies of Ultrabind membrane and the Biacore instrument are relatively new. Historically, the potential of an antibody for use in immunoaffinity chromatography has been established by coupling the antibody to pre-activated Sepharose. Therefore the conclusive

test as to whether antibodies 5D4 and 8A3 were suitable for immunoaffinity chromatography was to couple them to pre-activated Sepharose.

Antibodies 5D4 and 8A3 were coupled to NHS-activated Sepharose and packed into immunoaffinity columns. In separate experiments, the columns were contacted with activated WGFE or ppTGF-β2, washed with PBS and then subject to a 0-100% linear gradient of 0.1M citric acid pH 5-0.1M citric acid pH 2, in which TGF-β2 would presumably elute. Fractions were collected and assayed for Mv1Lu growth inhibition. Biological activity was depleted from the flow through and observed to elute at low pH for the immunoaffinity columns that were contacted with ppTGF-β2. This was similar behaviour to that observed for the anti-TGF-β1,2,3 monoclonal antibody coupled gel. In addition, the pH at which biological activity eluted was similar to that determined in the eluent screening experiments. This was considered as evidence that the coupled antibody was specifically binding and eluting solution-phase TGF-β2 in contrast to the previous solution-phase TGF-β2 binding experiments. Activated WGFE was loaded on to the immunoaffinity columns, which were washed with PBS and eluted with the linear gradient of citric acid. All of the biological activity was present in the flow through and none was found at low pH in the gradient. It was hypothesised that contaminating proteins in WGFE bound to the antibody-binding sites and blocked the binding of TGF-β2. By partially purifying TGF-β2 these contaminating proteins are removed so specific TGF-β2 can take place.

The purity of TGF-β2 eluting from the immunoaffinity columns was determined by loading it on to an analytical C4 reversed phase HPLC column. The protein was eluted by a 20-50% acetonitrile gradient over 30 minutes. A wide major absorbance peak eluted but there was also a significant amount of contaminating material. The fractions were collected and assayed for Mv1Lu growth inhibition. The biologically active fractions coincided with the major absorbance peak and these were subject to SDS-PAGE under reducing conditions. Two bands were revealed at 12.5 kDa, the expected molecular weight for reduced TGF-β2, and 6.5 kDa, which may be a contaminant or a degradation product of TGF-β2. An attempt was made to separate these proteins by loading them on to a C18 reversed phase HPLC column and eluting with a 20-50% n-propanol gradient over two hours. The fractions were collected and subject to Mv1Lu assay. The biologically active fractions were electrophoresed under reducing conditions, electroblotted on to nitrocellulose membrane and probed with antibody 5D4. The 6.5 kDa and 12.5 kDa bands were not separated by the additional HPLC step and

the 12.5 kDa band was identified as TGF-β2 on the immunoblot. Therefore immunoaffinity chromatography provides a valuable contribution to the purification of TGF-β2 from WGFE but it alone is insufficient to accomplish the purification. The immunoaffinity column was unable to separate TGF-β2 from other proteins unless the feed was partially purified with acid gel filtration and reversed phase HPLC. In this event, the immunoaffinity column was also unable to purify TGF-β2 to homogeneity and subsequently required further purification.

The static TGF-β2 binding capacity of Sepharose, to which antibodies 5D4 and 8A3 were coupled, was determined by incubating the antibody-coupled gel with various concentrations of TGF-β2 in PBS overnight. The Sepharose was spun down on the following day and the supernatant was subject to TGF-β2 ELISA. The depletion of TGF-β2 from solution was calculated for the different TGF-β2 concentrations. There was not a significantly greater amount of TGF-β2 bound by the antibody-coupled gels than the blank gel. All of the gels depleted >90% of the TGF-β2 from solution. This suggests that the TGF-β2 adsorption is not mediated by the antibody but is rather mediated by ethanolamine blocked NHS-activated Sepharose. Dasch et al. (1989) noted that the non-specific binding of TGF-β2 to agarose conjugated goat anti-mouse IgG was a problem and that it was necessary to include 1% (w/v) sodium deoxycholate in order to attenuate this binding. The static binding capacity experiment was therefore repeated with the inclusion of sodium deoxycholate in the binding buffer. However, this did not attenuate the non-specific binding to an extent that demonstrated specific binding to antibody-coupled gel. Antibodies 5D4 and 8A3 are not suitable for use in immunoaffinity chromatography in accordance with the findings of ELISA, Ultrabind membrane studies and Biacore studies where TGF-β2 was in solution-phase. Nevertheless, the serendipitous discovery of TGF-β2 adsorption to ethanolamine blocked NHS-activated Sepharose showed that a useful purification could be accomplished in the absence of antibody mediated binding.

7.4 Mathematical Modelling of Immunoaffinity Separations

Historically the operation of commercial-scale immunoaffinity systems has been optimised by exhaustive bench-scale testing of the apparatus. This is obviously time-consuming and uses relatively large quantities of valuable antibody and antigen. Consequently it is not possible to try every combination of operating conditions and therefore the actual optimal combination may remain undiscovered. A pilot-scale version of the immunoaffinity system is then scaled-up from the bench-scale apparatus. However, the scale-up of an immunoaffinity

system is a complex process and is non-linear. Therefore additional expense is incurred because further testing of the pilot-scale system is required. Obviously it is highly desirable to circumvent exhaustive bench-scale and pilot-scale testing. This could be achieved with the development of a mathematical model that simulates the economic performance of a commercial-scale immunoaffinity system subject to variations in support configuration, operating conditions and antibody characteristics.

The mathematical models of Hiester and Vermeulen (1952), Goldstein (1953) and Arnold and Blanch (1985b) were used to simulate frontal adsorption, zonal elution and frontal elution respectively in a hypothetical immunoaffinity system. A packed bed of Sepharose particles, a perfusive bed of POROS particles and a hollow-fibre membrane were considered to be the three most promising support configurations and were therefore included in the simulations. The feed flow rate (f), the dimensions of the immunoaffinity support (L) and the effluent concentration of the adsorbate at breakthrough (X) influence the potential economic performance. The antibody characteristics include the binding kinetics, the specific binding capacity for adsorbate and the rate of binding capacity degradation. The economic performance of the simulated immunoaffinity system was measured by the adsorbate productivity per unit time per unit volume, Ψ_{prod}, and the dimensionless annual operating cost, ϕ_{tot}. The simulation program calculated Ψ_{prod} and ϕ_{tot} with MathCad 6+ on a 486 computer.

The simulations identified the optimal operating conditions (f, L and X) that minimise ϕ_{tot} for anti-BSA antibody 9.1 (Antonsen et al., 1991) for each of the support configurations. The perfusive bed and the hollow-fibre membrane required less feed protein and antibody in order to satisfy the annual production quota. For this reason, the ϕ_{tot} of these support configurations was 28% lower than for the packed bed. The perfusive bed and the membrane operate with sharper breakthrough curves than the packed bed because mass transfer resistance is much lower in these systems. Therefore higher flow rates and consequently higher production rates may be used without the occurrence of premature breakthrough. Interestingly, the operating conditions that maximise Ψ_{prod} are not identical to those, which minimise ϕ_{tot} in accordance with the finding of Colby (1997). When the adsorbent cost dominates the operating costs, the optimal operating conditions for maximising Ψ_{prod} also minimise ϕ_{tot}. Under such circumstances a short-cut method (Yamamoto and Sano, 1992) can be employed to ascertain the optimal operating conditions. However, in this hypothetical immunoaffinity system the

feed costs are significant in comparison with the adsorbent costs and therefore a more complex optimisation problem arises.

Simulations were performed to determine the effects of antibody property variations upon ϕ_{tot} for the hypothetical Sepharose packed bed operating at the previously determined optimal operating conditions. In this way the key antibody properties that influence economic performance could be identified. The antibody properties were varied one at a time within a realistic range while holding all other properties constant. This study showed that a considerable saving in operating costs could be gained by choosing an antibody from a panel with high binding capacity, equilibrium association constant, association rate constant and low binding capacity degradation rate constant.

Chapter 5 endeavoured to determine the key parameters of the antibody-TGF-β2 system for the mathematical modelling and design of a commercial-scale immunoaffinity system. Eluent screening identified a number of promising eluents for dissociating the antibody-TGF-β2 complex whilst conserving the long-term binding capacity of the antibody. The long-term binding capacity degradation studies showed that the binding capacity of antibodies 5D4 and 8A3 degraded in the presence of eluent but sometimes did not follow the first order model postulated by Chapter 4. A non-degradable component of binding capacity existed in some cases and should be included in future versions of the mathematical model.

In view of the expense and acid stability of TGF-β2 it was considered prudent to couple it to the Biacore chip surface rather than the antibody. However, the injections of antibody yielded heterogeneous binding curves rather than obey Langmuir binding kinetics. The possible explanations were that TGF-β2 was coupled to the chip surface in different orientations, which each yield different binding kinetics, or that each Fab region of the antibody bound to two TGF-β2 molecules simultaneously. Therefore the kinetic rate constants extracted from these binding curves could not be extrapolated to the binding of solution-phase TGF-β2 to solid-phase antibody. Antibodies 5D4 and 8A3 were coupled to the Biacore chip surface, recombinant human TGF-β2 was injected over the surface of the chip and no specific binding was observed. This finding highlights the importance of coupling the antibody to the chip surface if kinetic rate constants are to be extracted for use in mathematical models. Furthermore, the ability of the Biacore to distinguish between homogeneous and heterogeneous kinetics has considerable potential for improving the prediction accuracy of

mathematical models. The simulation of Chapter 4 assumes homogeneous kinetics but future versions of the simulation could include heterogeneous binding kinetics. Such a simulation would be considerably more complex than that presented in Chapter 4 because the analytical solutions would no longer be valid and the simulation of breakthrough curves would require orthogonal collocation to numerically solve the systems of partial differential equations.

In spite of the precautions taken to minimise non-specific binding, contaminants bound to Sepharose. This indicates that it would not be possible to immunopurify TGF-β2 from WGFE in one step, which is not unusual for immunoaffinity chromatography. Rather, additional gel filtration and reversed phase HPLC steps would be required to polish TGF-β2. Future versions of the simulation could consider the additional costs of these purification steps.

The final set of experiments and subsequent analysis showed that a suitable antibody for immunoaffinity chromatography was unavailable and therefore it was not possible to validate the mathematical models. If a suitable antibody were available then future work would involve comparing the actual performance of the system with the predicted performance of the simulation and improving the models so that close agreement is obtained.

7.5 Future Directions

Although the final goal of a complete immunoaffinity system remains tantalisingly elusive, this study yielded a considerable amount of valuable information. No insurmountable impediments to the development of such an immunoaffinity system were encountered. The remaining obstacles to be overcome in the development of a viable immunoaffinity system include finding (1) a monoclonal antibody with better solution-phase binding characteristics; and (2) a support matrix with lower binding potential for TGF-β2 than NHS-activated Sepharose; or (3) a binding buffer that minimises the binding potential to the support matrix. More suitable monoclonal antibodies could be generated by immunising mice with a large number of different synthetic peptides corresponding to partial sequences of TGF-β2. The binding of these antibodies to solution-phase TGF-β2 could then be measured with the Biacore instrument and the best selected for use in immunoaffinity chromatography.

Another issue that requires investigation is the use of an additional purification step that resolves the proteins into two peaks so that homogeneous TGF-β2 is prepared from the six

step TGF-β2 purification process from section 6.3.1. The present process yielded a preparation that consisted of a major TGF-β2 band (12.5 kDa) and a minor band (6.5 kDa). Reversed phase C18 HPLC with a 20-50% n-propanol gradient was unable to separate the two species. The resulting purification process could be used to produce commercially relevant quantities of TGF-β2. According to the extinction coefficient method of protein determination, approximately 570 μg of protein of purity similar to that of Figure 6.7, can be purified from 1860 μg ppTGF-β2 (pool from the sixth purification).

7.6 Conclusions

The multiple step process of Rogers et al. (1996) was followed in an attempt to purify milligram quantities of TGF-β2 to homogeneity. However, much lower specific TGF-β2 activities were observed for the final step of the purification than were reported by Rogers et al. (1996).

Two separate immunisation strategies were employed to raise a titre against TGF-β2. One group of mice was immunised with partially purified TGF-β2. A second group of mice was immunised with a synthetic peptide that corresponds to amino acid residues 50-75 of TGF-β2 and that had been shown by Flanders et al. (1990) to raise a high specific titre. The second immunisation strategy was successful in raising a specific immune response and developing anti-TGF-β2 antibody secreting hybridomas from the spleen of the corresponding immune mouse. The hybridoma cell lines (5D4 and 8A3) were cultured in CellMax Artificial Capillary Modules to produce antibody in the required amounts for the immunoaffinity process. The antibody was purified from conditioned growth medium by Protein G affinity chromatography. Antibody 5D4 stains TGF-β2 in western immunoblots and also localises TGF-β2 in skin sections but the antibodies do not inhibit the biological activity of TGF-β2 in accordance with the findings of Flanders et al. (1990).

It has been demonstrated by a large literature that the economics of an immunoaffinity separation process are influenced by the configuration of the process, the operating conditions and the characteristics of the antibody. A mathematical model of the immunoaffinity process was developed in order to identify the most promising combination without having to resort to laboratory experiments that explore every possibility. A hypothetical immunoaffinity system was simulated with a well-characterised anti-BSA antibody (Antonsen et al., 1991) because the binding kinetics of the TGF-β2-antibody system

were unknown. The immunoaffinity separation simulations showed that a perfusive bed consisting of POROS particles and a hollow-fibre membrane could purify adsorbate with 28% lower annual operating costs than a packed bed consisting of Sepharose particles. A sensitivity analysis on the antibody properties demonstrated that a considerable saving in operating costs could be realised by selecting an antibody with high binding capacity, equilibrium association constant, association rate constant and low binding capacity degradation rate constant.

A number of simple experiments were performed to determine the critical anti-TGF-β2 antibody properties to facilitate the mathematical modelling and rational design of the immunoaffinity system. The optimal method of WGFE activation was found to consist of incubating the WGFE overnight at pH 11 and then neutralising the pH on the following day to realise conditions conducive to TGF-β2-antibody binding. A variety of chemical eluents were screened for the ability to dissociate the TGF-β2-antibody interaction, whilst conserving the binding capacity of the antibody. The eluents 0.1M glycine pH 3.5 and 0.1M glycine pH 3.0 were optimal for antibodies 5D4 and 8A3 respectively and the rates of eluent-mediated binding capacity degradation were determined in these eluents. The TGF-β2-antibody binding kinetics were investigated with the Biacore instrument but no binding was observed when recombinant TGF-β2 was injected over the antibody-coupled surface. Antibody was coupled to membrane and Sepharose but neither of these supports demonstrated specific binding for TGF-β2. However, considerable non-specific TGF-β2 binding was evident for both supports. Interestingly, the Sepharose immunoadsorbent was capable of separating TGF-β2 from contaminating proteins in the absence of monoclonal antibody. In this way TGF-β2 was purified with a combination of acid gel filtration, reversed phase HPLC and Sepharose column chromatography. However, the purification method is complex, time-consuming and no less costly than the method of Rogers et al. (1996).

The immunoaffinity separation of TGF-β2 from WGFE is potentially a very profitable process and remains an attractive commercial goal. However, the generation of suitable antibody for immunoaffinity chromatography was not successful. Dasch et al. (1989) developed a monoclonal antibody that was suitable for this purpose but it was not available. It is believed that the strategy of this project was sound and, if suitable antibodies were available, would have led to a more fruitful outcome. Relative to other proteins, TGF-β2 is intrinsically difficult to immunopurify because it (1) is an immunosuppressant, (2) is highly

conserved between mammalian species, (3) precipitates from solution at pH > 5, (4) binds non-specifically to plastic and (5) binds non-specifically to Sepharose. The literature on this subject has mainly dealt with cases in which immunoaffinity chromatography has been successful but rarely with unsuccessful cases. This work highlights some of the difficulties and pitfalls of immunoaffinity chromatography and it is anticipated that knowledge of these could help future workers to optimise this important technique.

References

Absher, M., Baldor, L. and Kelley, J. "A rapid colorimetric bioassay for TGF-β using a microwell plate reader" J. Immunol. Methods 138 (1991) 301-303

Afeyan, N.B., Gordon, N.F., Mazsaroff, I., Varady, L., Fulton, S.P., Yang, Y.B. and Regnier, F.E., "Flow-through particles for the high-performance liquid chromatographic separation of biomolecules: perfusion chromatography", J. Chromat. 519 (1990) 1-29

Alevizopoulos, A. and Mermod, N. "TGF-β: the breaking open of a black box" BioEssays 19 (1997) 581-591

Altschuh, D., Al Moudallal, Z., Briand, J.P. and van Regenmortel, M.H.V. "Immunochemical Studies of Tobacco Mosaic Virus- VI. Attempts to Localise Viral Epitopes with Monoclonal Antibodies" Molec. Immunol. 22 (1985) 329-337

Ammann, A.J. and Rudman, C.G. (1997) "Method of inducing bone growth using TGF- β" U.S. Patent 5,604,204

Antonsen, K.P., Colton, C.K. and Yarmush, M.L. "Elution Conditions and Degradation Mechanisms in Long-Term Immunoadsorbent Use" Biotechnol. Prog. 7 (1991) 159-172

Arnold, F.H. and Blanch, H.W., "Analytical Affinity Chromatography II. Rate Theory and the Measurement of Biological Binding Kinetics" J. Chromat. 355 (1986) 13-27

Arnold, F.H., Blanch, H.W. and Wilke, C.R. "Analysis of Affinity Separations II: The Characterisation of Affinity Columns by Pulse Techniques" Chem. Eng. J. 30 (1985a) B25-B36

Arnold, F.H., Blanch, H.W. and Wilke, C.R., "Analysis of Affinity Separations I: Predicting the Performance of Affinity Adsorbers" Chem. Eng. J. 30 (1985b) B9-B23

Assoian, R.K. and Sporn, M.B. "Type β TGF in Human Platelets: Release during Platelet Degranulation and Action on Vascular Smooth Muscle Cells" J. Cell Biol. 102 (1986) 1217-1223

Assoian, R.K., Fleurdelys, B.E., Stevenson, H.C., Miller, P.J., Madtes, D.K., Raines, E.W., Ross, R. and Sporn, M.B. "Expression and secretion of type β TGF by activated human macrophages" Proc. Natl. Acad. Sci. USA 84 (1987) 6020-6024

Australian Proteome Analysis Facility Annual Report, Encompassing July 1996-December 1998, p. 13

Ballard, F.J., Francis, G.L. and Regester, G.O. (1992) "Growth-promoting Agent" International Application Published Under the Patent Cooperation Treaty WO 92/00994

Beck, L.S., Chen, T.L., Hirabayashi, S.E., DeGuzman, L., Lee, W.P., McFatridge, L.L., Xu, Y., Bates, R.L. and Ammann, A.J. "Accelerated Healing of Ulcer Wounds in the Rabbit Ear by Recombinant Human TGF-β1" Growth Factors 2 (1990a) 273-282

Beck, L.S., Chen, T.L., Mikalauski, P. and Ammann, A.J. "Recombinant Human TGF-β1 Enhances Healing and Strength of Granulation Skin Wounds" Growth Factors 3 (1990) 267-275

Belford, D.A., Rogers, M-L., Francis, G.L., Payne, C., Ballard, F.J. and Goddard, C., "Platelet-derived growth factor, insulin-like growth factors, fibroblast growth factors and TGF-β do not account for the cell growth activity present in bovine milk" J. Endocrinol. 154 (1997) 45-55

Bernstein, E.F., Harisiadis, L., Salomon, G., Norton, J., Sollberg, S., Uitto, J., Glatstein, E., Glass, J., Talbot,T., Russo, A. and Mitchell, J.B. "TGF-β Improves Healing of Radiation-Impaired Wounds" J. Invest. Dermatol. 97 (1991) 430-434

BIAapplication Handbook, Pharmacia Biosensor AB, Uppsala, Sweden (1995)

Bird, R.B., Stewart, W.E. and Lightfoot, E.N., Transport Phenomena, Wiley, New York, 1960

Border, W.A., Okuda, S., Languino, L.R., Sporm, M.B. and Ruoslahti, E. "Suppression of experimental glomerulonephritis by antiserum against TGF-β1" Nature 346 (1990) 371-374

Boyer, P.M. and Hsu, J.T. "Effects of Ligand Concentration on Protein Adsorption in Dye-Ligand Adsorbents" Chem. Eng. Sci. 47 (1992) 241-251

Bradford, M.M., "A Rapid and Sensitive Method for the Quantitation of Microgram Quantities of Protein Utilising the Principle of Protein-Dye Binding" Analyt. Biochem. 72 (1976) 248-254

Brandt, S., Goffe, R.A., Kessler, S.B., O'Connor, J.L. and Zale, S.E. "Membrane-Based Affinity Technology for Commercial Scale Purifications" Bio/Tech 6 (1988) 779-782

Brigham-Burke, M. and O'Shannessy, D.J., "A Micro-Scale Method Employing Surface Plasmon Resonance Detection for the Determination of Conditions for Immunoaffinity Chromatography of Proteins", Chromatographia 35 (1993) 45-49

Broekelman, T.J., Limper, A.H., Colby, T.V. and McDonald, J.A. " TGF-β1 is present at sites of extracellular matrix gene expression in human pulmonary fibrosis" Proc. Natl. Acad. Sci. USA 88 (1991) 6642-6646

Brown, P.D., Wakefield, L.M., Levinson, A.D. and Sporn, M.B. "Physicochemical Activation of Recombinant Latent TGF-β1,2,3" Growth Factors 3 (1990) 35-43

Buchkovich, K., Duffy, L.A. and Harlow, E. "The Retinoblastoma Protein is Phosphorylated during Specific Phases of the Cell Cycle" Cell 58 (1989) 1097-1105

Buck, M.A., Olah, T.A., Weitzmann, C.J. and Cooperman, B.S. "Protein estimation by the product of integrated peak area and flow rate" Analyt. Biochem. 182 (1989), 295-299

CellMax Instruction Manual, Cellco Inc., Germantown, MD, USA

Cerletti, N., McMaster, G.K., Cox, D., Schmitz, A. and Meyhack, B. (1990) European patent application 90810922.6, publication nr EP 0 433 225 A1, p. 1-35

Cerletti, N., McMaster, G.K., Cox, D., Schmitz, A. and Meyhack, B. (1997) "Process for refolding recombinantly produced TGF-β like proteins" U.S. Patent 5,650,494

Charcosset, C., Su, Z., Karoor, S., Daun, G. and Colton, C.K. "Protein A Immunoaffinity Hollow Fibre Membranes for Immunoglobulin G Purification: Experimental Characterization" Biotechnol. and Bioeng. 48 (1995) 415-427

Chase, H.A. and Draeger, M.N., "Affinity purification of proteins using expanded beds", J. Chromat. 597 (1992) 129-145

Chase, H.A., "Affinity Separations Utilising Immobilised Monoclonal Antibodies- a New Tool for the Biochemical Engineer", Chem. Eng. Sci. 39 (1984) 1099-1125

Cheifetz, S., Bellon, T., Cales, C., Vera, S., Bernabeu, C., Massague, J., and Letarte, M., "Endoglin is a component of the transforming growth factor-beta receptor system in human endothelial cells" J. Biol. Chem. 267 (1992) 19027-19030

Cheifetz, S., Ling, N., Guillemin, R. and Massague, J. "A Surface Component on GH_3 Pituitary Cells that Recognizes TGF-β, Activin, and Inhibin" J. Biol. Chem. 263 (1988) 17225-17228

Cheifetz, S., Weatherbee, J.A., Tsang, M.L-S., Anderson, J.K., Mole, J.E., Lucas, R. and Massague, J., "The Transforming Growth Factor-β System, a Complex Pattern of Cross-Reactive Ligands and Receptors", Cell 48 (1987) 409-415

Chenu, C., Pfeilschifter, J., Mundy, G.R. and Roodman, G.D. " TGF-β inhibits formation of osteoclast-like cells in long-term human marrow cultures" Proc. Natl. Acad. Sci. USA 85 (1988) 5683-5687

Chiang, C.P. and Nilsen-Hamilton, M. "Opposite and Selective Effects of Epidermal Growth Factor and Human Platelet TGF-β on the Production of Secreted Proteins by Murine 3T3 Cells and Human Fibroblasts" J. Biol. Chem. 261 (1986) 10478-10481

Colby, C.B., "Optimisation of Scale-up of Chromatography" PhD Thesis 1997

Coller, H.A. and Coller, B.S. "Statistical Analysis of Repetitive Subcloning by the Limiting Dilution Technique with a View Toward Ensuring Hybridoma Monoclonality" Hybridoma 2 (1983) 91-96

Connor, T.B., Jr., Roberts, A.B., Sporn, M.B., Danielpour, D., Dart, L.L., Michels, R.G., de Bustros, S., Enger, C., Kato, H., Lansing, M., Hayashi, H. and Glaser, B.M. "Correlation of Fibrosis and TGF-β Type 2 Levels in the Eye" J. Clin. Inv. 83 (1989) 1661-1666

Cordeiro, M.F., Gay, J.A. and Khaw, P.T. "Human Anti-TGF-β2 Antibody: A New Glaucoma Anti-Scarring Agent" Investigative Ophthalmology and Visual Science 40 (1999) 2225-2234

Cox, D.A. and Burk, R.B., "Isolation and characterisation of milk growth factor, a TGF-β2-related polypeptide, from bovine milk" Eur. J. Biochem. 197 (1991) 353-358

Creighton, T.E., Proteins, Structures and Molecular Properties p.184 and 268, W.H. Freeman and Company, New York, 1984

Curtsinger, L.J., Pietsch, J.D., Brown, G.L., von Fraunhofer, A., Ackermann, D., Polk, H.C. and Schultz, G.S. "Reversal of Adriamycin®-Impaired Wound Healing by TGF-β" Surg. Gynecol. Obstet. 168 (1989) 517-522

Daopin, S., Li, M. and Davies, D.R. "Crystal Stucture of TGF-β2 Refined at 1.8 Angstroms Resolution" Proteins. Struct. Funct. 17 (1993) 176-192

Dasch, J.R., Pace, D.R., Waegell, W., Inenaga, D. and Ellingsworth, L., "Monoclonal Antibodies Recognizing TGF-β", J. Immunol. 142 (1989) 1536-1541

Denman, J., Hayes, M., O'Day, C., Edmunds, T., Bartlett, C., Hirani, S., Ebert, K.M., Gordon, K. and McPherson, J.M., "Transgenic Expression of a Variant of Human Tissue-type Plasminogen Activator in Goat Milk: Purification and Characterisation of the Recombinant Enzyme", Bio/technology 9 (1991) 839-843

Ding, A., Nathan, C.F., Graycar, J., Derynck, R., Stuehr, D.J. and Srimal, S. "Macrophage Deactivating Factor and TGF-β-1,2 and 3 Inhibit Induction of Macrophage Nitrogen Oxide Synthesis by IFN- γ" J. Immunol. 145 (1990) 940-944

Dunbar, A.J., Priebe, I.K., Belford, D.A. and Goddard, C., "Identification of betacellulin as a major peptide growth factor in milk: purification, characterisation and molecular cloning" Biochem. J. 344 (1999) 713-721

Elder, J.T., Ellingsworth, L.R., Fisher, G.J. and Voorhees, J.J. " TGF-β in Psoriasis: Pathogenesis and Therapy" Ann. NY Acad. Sci. 593 (1990) 218-230

Fanger, B.O., Wakefield, L.M. and Sporn, M.B. "Structure and Properties of the Cellular Receptor for TGF-β" Biochemistry 25 (1986) 3083-3091

Fazekas de St. Groth, S. and Scheidegger, D. "Production of Monoclonal Antibodies: Strategy and Tactics" J. Immunol. Methods 35 (1980) 1-21

Finkelman, R.D., Linkhart, T.A., Mohan, S., Lau, KH., Baylink, D.J. and Bell, N.H. "Vitamin D deficiency causes a selective reduction in deposition of TGF-β in rat bone: Possible mechanism for impaired osteoinduction" Proc. Natl. Acad. Sci. USA 88 (1991) 3657-3660

Flanders, K.C., Cissel, D.S., Mullen, L.T., Danielpour, D., Sporn, M.B. and Roberts, A.B. "Antibodies to TGF-β2 Peptides: Specific Detection of TGF-β2 in Immunoassays" Growth Factors 3 (1990) 45-52

Florini, J.R., Roberts, A.B., Ewton, D.Z., Falen, S.L., Flanders, K.C. and Sporn, M.B. " TGF-β: A Very Potent Inhibitor of Myoblast Differentiation, Identical to the Differentiation Inhibitor Secreted by Buffalo Rat Liver Cells" J. Biol. Chem. 261 (1986) 16509-16513

Foo, S.C. and Rice, R.G. "On the Prediction of Ultimate Separation in Parametric Pumps" AIChEJ 21 (1975) 1149-1158

Fowell, S.L. and Chase, H.A. "Variation of immunosorbent performance with the amount of immobilised antibody" J. Biotechnol. 4 (1986) 1-13

Francis, G.L., Regester, G.O., Webb, H.A. and Ballard, F.J., "Extraction from Cheese Whey by Cation-Exchange Chromatography of Mammalian Growth Factors", J. Dairy Science 78 (1995) 1209-1218

Fulton, S.P., Shahidi, A.J., Gordon, N.F. and Afeyan, N.B. "Large-Scale Processing and High-Throughput Perfusion Chromatography" Bio/Tech 10 (1992) 635-639

Gamble, J.R. and Vadas, M.A., "Endothelial Cell Adhesiveness for Human T Lymphocytes is Inhibited by TGF-β", J. Immunol. 146 (1991) 1149-1154

Glaser, B.M., Michels, R.G., Kuppermann, B.D., Sjaarda, R.N. and Pena, R.A. " TGF-β2 for the Treatment of Full-thickness Macular Holes" 99 (1992) 1162-1173

Goldstein, S. "On the Mathematics of exchange processes in fixed columns I. Mathematical solutions and asymptotic expansions" Proc. R. Soc. Ser. A 219 (1953) 151-171

Grainger, D.J., Metcalfe, J.C. and Weissberg, P.L. (1998) "Prevention and treatment of pathologies associated with abnormally proliferative smooth muscle cells" U.S. Patent 5,773,479

Griffith, D.L., Keck, P.C., Sampath, T.K., Rueger, D.C. and Carlson, W.D. "Three-dimensional structure of recombinant human osteogenic protein 1: Structural paradigm for the TGF-β superfamily" Proc. Natl. Acad. Sci. USA 93 (1996) 878-883

Hannan, R.L., Kourembanas, S., Flanders, K.C., Rogelj, S.J., Roberts, A.B., Faller, D.V. and Klagsbrun, M. "Endothelial Cells Synthesize Basic Fibroblast Growth Factor and TGF-β" Growth Factors 1 (1988) 7-17

Harlow, E. and Lane, D. "Antibodies: A Laboratory Manual" (1988) Cold Spring Harbor Laboratory, New York

Heine, U., Munoz, E.F., Flanders, K.C., Ellingsworth, L.R., Lam, H.Y., Thompson, N.L., Roberts, A.B. and Sporn, M.B. "Role of TGF-β in the Development of the Mouse Embryo" J. Cell Biol. 105 (1987) 2861-2876
Hermanson, G.T., Krishna Mallia, A. and Smith, P.K., Immobilized Affinity Ligand Techniques, Academic Press, London, 1992

Hiester, N.K. and Vermeulen, T., "Saturation Performance of Ion-Exchange and Adsorption Columns" Chem. Eng. Prog. 48 (1952) 505-516

Hjorth, R., Kampe, S. and Carlsson, M., "Analysis of some operating parameters of novel adsorbents for recovery of proteins in expanded beds", Bioseparation 5 (1995) 217-223

Horstmann, B.J. and Chase, H.A. "Modelling the Affinity Adsorption of Immunoglobulin G to Protein A Immobilised to Agarose Matrices" Chem. Eng. Res. Des. 67 (1989) 243-254

Howarth, G.S., Francis, G.L., Cool, J.C., Xu, X., Byard, R.W. and Read, L.C., "Milk Growth Factors Enriched from Cheese Whey Ameliorate Intestinal Damage by Methotrexate When Administered Orally to Rats", J. Nutrition 126 (1996) 2519-2530

Ignotz, R.A. and Massague, J. "Type β TGF controls the adipogenic differentiation of 3T3 fibroblasts" Proc. Natl. Acad. Sci. USA 82 (1985) 8530-8534

Irving, R. and Hudson, P. "Superseding hybridoma technology with phage display libraries" In Monoclonal Antibodies: The Second Generation (Ed. Zola, H.), Bios Scientific Publishers, 1995, p. 119-139

Jakowlew, S.B., Dillard, P.J., Sporn, M.B. and Roberts, A.B. "Complementary Deoxyribonucleic Acid Cloning of a Messenger Ribonucleic Acid Encoding TGF-β4 from Chicken Embryo Chondrocytes" Mol. Endocrinol. 2 (1988) 1186-1195

Jennings, J.C., Mohan, S., Linkhart, T.A., Widstrom, R. and Baylink, D.J. "Comparison of the Biological Actions of TGF-β1 and TGF-β2: Differential Activity in Endothelial Cells" J. Cell. Physiol. 137 (1988) 167-172

Jin, Y., Cox, D.A., Knecht, R., Raschdorf, F. and Cerletti, N., "Separation, Purification, and Sequence Identification of TGF-β1 and TGF-β2 from Bovine Milk", J. Protein Chem. 10 (1991) 565-575

Jones, S.C., Curtsinger, L.J., Whalen, J.D., Pietsch, J.D., Ackerman, D., Brown, G.L. and Schultz, G.S. "Effect of Topical Recombinant TGF-β on Healing of Partial Thickness Injuries" J. Surg. Res. 51 (1991) 344-352

Joyce, M.E., Terek, R.M., Jinguishi, S. and Bolander, M.E. "Role of TGF-β in Fracture Repair" Ann. NY Acad. Sci. 593 (1990) 107-123

Kasper, C., Reif, O-W. and Freitag, R. "Evaluation of affinity filters for protein isolation" Bioseparation 6 (1997) 373-382

Kawakami, H., Shinmoto, H., Dosako, S. and Ahiko, K. (1987) "Method for separating bovine lactoferrin from cow's milk and purifying same", U.S. Patent 4,668,771

Kehrl, J.H., Roberts, A.B., Wakefield, L.M., Jakowlew, S., Sporn, M.B. and Fauci, A.S. "TGF-β is an Important Immunomodulatory Protein for Human B Lymphocytes" J. Immunol. (1986a) 137, 3855-3860

Kehrl, J.H., Wakefield, L.M., Roberts, A.B., Jakowlew, S., Alvarez-Mon, M., Derynck, R., Sporn, M.B. and Fauci, A.S. "Production of TGF-β by Human T Lymphocytes and its Potential Role in the Regulation of T Cell Growth" J. Exp. Med. 163 (1986b) 1037-1050

Keller, J.R., Sing, G.K., Ellingsworth, L.R., Ruscetii, S.K. and Ruscetti, F.W. "Two Forms of TGF-β are Equally Potent Selective Growth Inhibitors of Early Murine Hematopoiesis" Ann. NY Acad. Sci. 593 (1990) 172-180

Kennedy, J.F. and Barnes, J.A. "Immunochemical Studies of the Non-Specific Interaction of Cyanogen Bromide-Activated Macroporous Agarose-Based Immunosorbents" J. Chromatog. 281 (1983) 93-93

Khalil, N., Bereznay, O., Sporn, M. and Greenberg, A.H. "Macrophage Production of TGF-β and Fibroblast Collagen Synthesis in Chronic Pulmonary Inflammation" J. Exp. Med. 170 (1989) 727-737

Klagsbrun, M., "Bovine colustrum supports the serum-free proliferation of epithelial cells but not of fibroblasts in long-term culture" J. Cell Biol. 84 (1980) 808-814

Klagsbrun, M., "Human milk stimulates DNA synthesis and cellular proliferation in cultured fibroblasts" Proc. Natl. Acad. Sci. USA 75 (1978) 5057-5061

Knabbe, C., Lippman, M.E., Wakefield, L.M., Flanders, K.C., Kasid, A., Derynck, R. and Dickson, R.B. "Evidence that TGF-β is a Hormonally Regulated Negative Growth Factor in Human Breast Cancer Cells" Cell 48 (1987) 417-428

Kohler, G. and Milstein, C., "Continuous Cultures of Fused Cells Secreting Antibody of Predefined Specificity", Nature 256 (1975) 495-497

Ksander, G.A., Chu, G.H., McMullin, H., Ogawa, Y., Pratt, B.M., Rosenblatt, J.S. and McPherson, J.M. " TGF-β1 and TGF-β2 Enhance Connective Tissue Formation in Animal Models of Dermal Wound Healing by Secondary Intent" Ann. NY Acad. Sci. 593 (1990) 135-147

Kuruvilla, A.P., Shah, R., Hochwald, G.M., Liggitt, H.D., Palladino, M.A. and Thorbecke, G.J. "Protective effect of TGF-β1 on experimental autoimmune diseases in mice" Proc. Natl. Acad. Sci. USA 88 (1991) 2918-2921

Laiho, M., DeCaprio, J.A., Ludlow, J.W., Livingston, D.M. and Massague, "Growth Inhibition by TGF-β Linked to Suppression of Retinoblastoma Protein Phosphorylation" J. Cell 62 (1990) 175-185

Laiho, M., Saksela, O., Andreasen, P.A. and Keski-Oja, J. "Enhanced Production and Extracellular Deposition of the Endothelial-type Plasminogen Activator Inhibitor in Cultured Human Lung Fibroblasts by TGF-β" J. Cell Biol. 103 (1986) 2403-2410

Laiho, M., Weis, F.M.B., Boyd, F.T., Ignotz, R.A. and Massague, J. "Responsive to TGF-β Restored by Genetic Complementation between Cells Defective in TGF-β Receptors I and II" J. Biol. Chem. 266 (1991) 9108-9112
Lefer, A.M., Tsao, P., Aoki, N. and Palladino, M.A., Jr. "Mediation of Cardioprotection by TGF-β" Science 249 (1990) 61-64

Liu, H-C. and Fried, J.R. "Breakthrough of Lysozyme through an Affinity Membrane of Cellulose-Cibacron Blue" AIChE J. 40 (1994) 40-49

Lopez-Casillas, F., Wrana, J.L. and Massague, J. "Betaglycan Presents Ligand to the TGF-β Signalling Receptor" Cell 73 (1993) 1435-1444

Lucas, C., Fendly, B.M., Mukku, V.R., Wong, W.L. and Palladino, M.A. "Generation of Antibodies and Assays for TGF-β" Methods in Enzymology 198 (1991) 303-316

Lucas, C., Wallick, S., Fendly, B.M., Figari, I. and Palladino, M.A. " TGF-β: a possible autocrine immune regulator" 1991 Clinical applications of TGF-β. Wiley, Chichester (Ciba Foundation Symposium 157) p 98-108

Madisen, L., Lioubin, M.N., Marquardt, H. and Purchio, A.F., "High-Level Expression of TGF-β2 and the TGF-β2(414) Precursor in Chinese Hamster Ovary Cells", Growth Factors 3 (1990) 129-138

Madisen, L., Webb, N.R., Rose, T.M., Marquardt, H., Ikeda, T.,Twardzik, D., Seyedin, S. and Purchio, A.F, "Transforming growth factor-beta 2: cDNA cloning and sequence analysis" DNA 7 (1988) 1-8

Marshall, K.R., "Industrial Isolation of Milk Proteins: Whey Proteins", Developments in Dairy Chemistry 1, Ed. Fox, P.F., Applied Science Publishers, New York and London, 1982, p.339-373

Massague, J., Cheifetz, S., Boyd, F.T. and Andres, J.L. "TGF-β Receptors and TGF-β Binding Proteoglycans: Recent Progress in Identifying Their Functional Properties" Ann. NY Acad. Sci. 593 (1990) 59-72

Masui, T., Wakefield, L.M., Lechner, J.F., LaVeck, M.A., Sporn, M.B. and Harris, C.C. "Type β TGF is the primary differentiation-inducing serum factor for normal human bronchial epithelial cells" Proc. Natl. Acad. Sci. USA 83 (1986) 2438-2442

Mattiasson, B. and Ling, T.G.I., "Ultrafiltration Affinity Purification", Membrane Separations in Biotechnology, Ed. McGregor, W.C., Marcel Dekker, New York and Basel, 1992, p. 99-114

Merril, C.R., Goldman, D. and van Keuren, M.L. "Gel Protein Stains: Silver Stain" Methods in Enzymology 104 (1984) 441-447

Middelberg, A.P.J., "The influence of protein refolding strategy on cost for competing reactions", Chem. Eng. J 61 (1996) 41-52

Miller, A., Lider, O., Roberts, A.B., Sporn, M.B. and Weiner, H.L. "Suppressor T cells generated by oral tolerization to myelin basic protein suppress both in vitro and in vivo immune responses by the release of TGF-β after antigen-specific triggering" Proc. Natl. Acad. Sci. USA 89 (1992) 421-425

Miller, D.A., Lee, A., Pelton, R.W., Chen, E.Y., Moses, H.L. and Derynck, R. "Murine TGF-β2 cDNA Sequence and Expression in Adult Tissue and Embryos" Molec. Endocrin. 3 (1989) 1108-1114

Miller, S.F. and King, C.J. "Axial Dispersion in Liquid Flow Through Packed Beds" AIChEJ 12 (1966) 767-773

Miyazano, K. and Heldin, C-H. "Role for carbohydrate structures in TGF-β1" Nature 338 (1989) 158-160

Miyazano, K., Yuki, K., Takaku, F., Wenstedt, C., Kanzaki, T., Olofsson, A., Hellman, U. and Heldin, C-H. "Latent Forms of TGF-β: Structure and Biology" Ann. NY Acad. Sci. 593 (1990) 51-58

Moses, H.L., Yang, E.Y. and Pietenpol, J.A. "Regulation of epithelial proliferation by TGF-β" 1991 Clinical applications of TGF-β. Wiley, Chichester (Ciba Foundation Symposium 157) p 66-74

Mundy, G.R. and Bonewald, L.F. "Role of TGF-β in Bone Remodelling" Ann. NY Acad. Sci. 593 (1990) 91-97

Munger, J.S., Harpel, J.G., Gleizes, P-E., Mazzieri, R., Nunes, I., and Rifkin, D.B., "Latent TGF-β: Structural features and mechanisms of activation" Kidney Intl. 51 (1997) 1367-1382

Mustoe T.A., Pierce, G.F., Thomason, A., Gramates, P., Sporn, M.B., and Deuel, T.F. "Accelerated Healing of Incisional Wounds in Rats Induced by TGF-β" Science 237 (1987) 1333-1336

Mustoe, T.A., Landes, A., Cromack, D.T., Mistry, D., Griffin, A., Deuel, T.F. and Pierce, G.F. "Differential acceleration of healing of surgical incisions in the rabbit gastrointestinal tract by platelet-derived growth factor and TGF-β" Surgery 108 (1990) 324-329

Nachman, M., Azad, A.R.M. and Bailon, P. "Efficient Recovery of Recombinant Proteins Using Membrane-Based Immunoaffinity Chromatography (MIC)", Biotech. and Bioeng. 40 (1992) 564-571

Noda, M. and Camilliere, J.J. "In Vivo Stimulation of Bone Formation by TGF-β" Endocrinology 124 (1989) 2991-2994

Ogawa, Y., Schmidt, D.K., Dasch, J.R., Chang, R-J., Glaser, C.B., "Purification and Characterization of Transforming Growth Factor-β2.3 and -β1.2 Heterodimers from Bovine Bone", J. Biol. Chem. 267 (1992) 2325-2328

Ohta, M., Greenberger, J.S., Anklesaria, P., Bassols, A. and Massague, J. "Two forms of TGF-β distinguished by multipotential haematopoietic progenitor cells" Nature 329 (1987) 539-541

Okuda, S., Languino, L.R., Ruoslahti, E. and Border, W.A. "Elevated Expression of TGF-β and Proteoglycan Production in Experimental Glomerulonephritis" J. Clin. Invest. 86 (1990) 453-462

Oliver, M.H., Harrison, N.K., Bishop, J.E., Cole, P.J. and Laurent, G.J. "A rapid and convenient assay for counting cells cultured in microwell plates: application for assessment of growth factors" J. Cell Sci. 92 (1989) 513-518

Olofsson, A., Miyazano, K., Kanzaki, T., Colosetti, P., Engstrom, U. and Heldin, C-H., "Transforming Growth Factor-β1,-β2,-β3 Secreted by a Human Glioblastoma Cell Line", J. Biol. Chem. 267 (1992) 19482-19488

Olson, W.C., Spitznagel, T.M. and Yarmush, M.L., "Dissociation Kinetics of Antigen-Antibody Interactions: Studies on a Panel of Anti-Albumin Monoclonal Antibodies", Molec. Immunol. 26 (1989) 129-136

Ongpipattanakul, B., Nguyen, T., Zioncheck, T.F., Wong, R., Osaka, G., DeGuzman, L., Lee, W.P. and Beck, L.S. "Development of tricalcium phosphate/amylopectin paste combined with recombinant human TGF-β1 as a bone defect filler" J. Biomed. Mater. Res. 36 (1997) 295-305

Owen, R.O., McCreath, G.E. and Chase, H.A., "Development and Modelling of Continuous Affinity Separations Using Perfluorocarbon Emulsions", Separations for Biotechnology 3 (1993) p.378-384

Palladino, M.A., Morris, R.E., Starnes, H.F. and Levinson, A.D. "The TGF-β's: A New Family of Immunoregulatory Molecules" Ann. NY Acad. Sci. 593 (1990) 181-187

Pemawansa, K.P.W., Heisler, M.D., Blackwell, S.L., Cymes, L., Mahalak, K.L. and Kraus, M.A. "An Advanced Affinity Membrane for Covalent Binding of Amino Ligands" Biotechniques 9 (1990) 352-355

Pepper, D.S. "Selection of Antibodies for Immunoaffinity Chromatography" Methods in Molecular Biology Vol. 11, p. 135-171, The Humana Press, NJ, 1992

Pierce, G.F., Mustoe, T.A., Lingelbach, J., Masakowski, V.R., Gramates, P. and Deuel, T.F. " TGF-β reverses the glucocorticoid-induced wound-healing deficit in rats: Possible regulation in macrophages by platelet-derived growth factor" Proc. Natl. Acad. Sci. USA 86 (1989) 2229-2233

Polson, A. "Some Aspects of Diffusion in Solution and a Definition of a Colloidal Particle" J. Phys. Colloid Chem. 54 (1950) 649-652

POROS Columns and Media Selection Guide, Perseptive Biosystems

Protein Databank: www.pdb.bnl.gov (1999)

Quaglino, D., Jr., Nanney, L.B., Ditesheim, J.A. and Davidson, J.M. "TGF-β Stimulates Wound Healing and Modulates Extracellular Matrix Gene Expression in Pig Skin: Incisional Wound Model" J. Invest. Dermatol. 97 (1991) 34-42

Recombinant Capital Web site: www.recap.com

Regnault, V., Arvieux, J., Vallar, L. and Lecompte, T., "Immunopurification of human β_2-glycoprotein I with a monoclonal antibody selected for its binding kinetics using a surface plasmon resonance biosensor", J. Immunol. Methods 211 (1998) 191-197

Roberts, A.B. and Sporn, M.B., "Physiological Actions and Clinical Applications of TGF-β" Growth Factors 8 (1993) 1-9

Roberts, A.B., Anzano, M.A., Lamb, L.C., Smith, J.M. and Sporn, M.B. "New class of TGF's potentiated by epidermal growth factor: isolation from non-neoplastic tissues" Proc. Natl. Acad. Sci. USA 78 (1981) 5339-5343

Roberts, A.B., Rosa, F., Roche, N.S., Coligan, J.E., Garfield, M., Rebbert, M.L., Kondaiah, P., Danielpour, D., Kehrl, J.H., Wahl, S.M., Dawid, I.B. and Sporn, M.B. "Isolation and Characterization of TGF-β2 and TGF-β5 from Medium Conditioned by Xenopus XTC Cells" Growth Factors 2 (1990) 135-147

Roberts, A.B., Sporn, M.B., Assoian, R.K., Smith, J.M., Roche, N.S., Wakefield, L.M., Heine, U.I., Liotta, L.A., Falanga, V., Kehrl, J.H. and Fauci, A.S. "TGF-β: Rapid induction of fibrosis and angiogenesis in vivo and stimulation of collagen formation in vitro" Proc. Natl. Acad. Sci. USA 83 (1986) 4167-4171

Robey, P.G., Young, M.F., Flanders, K.C., Roche, N.S., Kondaiah, P., Reddi, A.H., Termine, J.D., Sporn, M.B. and Roberts, A.B. "Osteoblasts Synthesize and Respond to TGF-β in Vitro" J. Cell Biol. 105 (1987) 457-463

Rogers, M-L., Belford, D.A., Francis, G.L. and Ballard, F.J., "Identification of fibroblast growth factors in bovine cheese whey", J. Dairy Res. 62 (1995) 501-507

Rogers, M-L., Goddard, C., Regester, G.O., Ballard, F.J. and Belford, D.A., "Transforming growth factor-β in bovine milk: concentration, stability and molecular mass forms", J. Endocrinology 151 (1996) 77-86

Rook, A.H., Kehrl, J.H., Wakefield, L.M., Roberts, A.B., Sporn, M.B., Burlington, D.B., Lane, H.C. and Fauci, A.S. "Effects of TGF-β on the Functions of Natural Killer Cells: Depressed Cytolytic Activity and Blunting of Interferon Responsiveness" J. Immunol. 136 (1986) 3916-3920

Ruoslahti, E.I., Longaker, M.T. and Whitby, D.J. (1997) "Use of fibromodulin to prevent or reduce dermal scarring" U.S. Patent 5,654,270

Salomon, G.D., Kasid, A., Bernstein, E., Buresh, C., Director, E. and Norton, J.A. "Gene expression in normal and doxorubicin-impaired wounds: Importance of TGF-β" Surgery 108 (1990) 318-322

Sarfert, F.T. and Etzel, M.R., "Mass transfer limitations in protein separations using ion-exchange membranes", J. Chromat. 764 (1997) 3-20

Segarini, P.R. "TGF-β receptors" 1991 Clinical applications of TGF-β. Wiley, Chichester (Ciba Foundation Symposium 157) p 29-50

Segarini, P.R. and Seyedin, S.M. "The High Molecular Weight Receptor to TGF-β Contains Glycosaminoglycan Chains" J. Biol. Chem. 263 (1988) 8366-8370

Seyedin, S.M., Thomas, T.C., Thompson, A.Y., Rosen, D.M. and Piez, K.A., "Purification and characterization of two cartilage-inducing factors from bovine demineralized bone" Proc. Natl. Acad. Sci. USA 82 (1985) 2267-2271

Seyedin, S.M., Thompson, A.Y., Bentz, H., Rosen, D.M., McPherson, J.M., Conti, A., Siegel, N.R., Galluppi, G.R. and Piez, K.A. "Cartilage-inducing Factor-A: Apparent Identity to TGF-β" J. Biol. Chem. 261 (1986) 5693-5695

Shah, M., Foreman, D.M. and Ferguson, M.W. "Control of scarring in adult wounds by neutralising antibody to TGF-β" Lancet 339 (1992) 213-214

Shipley, G.D., Pittelkow, M.R., Wille, J.J., Jr., Scott, R.E. and Moses, H.L. "Reversible Inhibition of Normal Human Prokeratinocyte Proliferation by Type β TGF-Growth Inhibitor in Serum-free Medium" Cancer Res. 46 (1986) 2068-2071

Smiddy, W.E., Glaser, B.M., Green, W.R., Connor, T.B., Roberts, A.B., Lucas, R. and Sporn, M.B. " TGF-β: A Biologic Chorioretinal Glue" Arch. Opthalmol. 107 (1989) 577-580

Soltys, P.J. and Etzel, M.R., "In vivo Characterization of a Membrane-Based Low-Density Lipoprotein Affinity Adsorption Device" Blood Purif. 16 (1998) 123-134

Sonis, S.T., Lindquist, L., Van Vugt, A., Stewart, A.A., Stam, K., Qu, G-Y., Iwata, K.K. and Haley, J.D. "Prevention of Chemotherapy-induced Ulcerative Mucositis by TGF-β3" Cancer Res. 54 (1994) 1135-1138

Soriano, G.A., Titchener-Kooker, N.J. and Shamlou, P.A., "The effects of processing scale on the pressure drop of compressible gel supports in liquid chromatographic columns", Bioprocess Eng. 17 (1997) 115-119

Sporn, M.B. and Roberts, A.B. "Clinical Applications of TGF-β" 1991 Clinical applications of TGF-β. Wiley, Chichester (Ciba Foundation Symposium 157) p 1-4

Sporn, M.B., Roberts, A.B., Wakefield, L.M. and de Crombrugghe, B. "Some Recent Advances in the Chemistry and Biology of TGF-β" J. Cell Biol. 105 (1987) 1039-1045

Stenberg, E., Persson, B., Roos, H. and Urbaniczky "Quantitative Determination of Surface Concentration of Protein with Surface Plasmon Resonance Using Radiolabelled Proteins" J. Colloid Interface Sci. 143 (1991) 513-526

Suardet, L., Gaide, AC., Calmes, J.M., Sordat, B., Givel, JC., Eliason, J.F. and Odartchenko, N. "Responsive of Three Newly Established Human Colorectal Cancer Cell Lines to TGF-β1 and 2" Cancer Res. 52 (1992) 3705-3712

Suen, S-Y. and Etzel, M.R. "A Mathematical Analysis of Affinity Membrane Bioseparations" Chem. Eng. Sci. 47 (1992) 1355-1364

Suen, S-Y. and Etzel, M.R. "Sorption kinetics and breakthrough curves for pepsin and chymosin using pepstatin A affinity membranes" J. Chromat. A 686 (1994) 179-192

Sullivan, K.M., Lorenz, H.P., Meuli, M., Lin, R.Y. and Adzick, N.S., "A Model of Scarless Human Fetal Wound Repair is Deficicent in TGF-β" J. Pediatric Surgery 30 (1995) 198-203

Swiss Institute of Bioinformatics (www.expasy.ch/tools/pi_tool.html) (1999)

Swiss Protein Databank: ftp://ftp.expasy.ch/databases/swiss-3dimage/IMAGES (1999a)

Swiss Protein Sequence Retrieval System: www.expasy.ch/srs5/ (1999b)

Tejeda, A., Noriega, J.A., Ortega, J. and Guzman, R. "Dye Affinity Adsorbent Replacement Optimization" Biotechnol. Prog. 14 (1998) 493-495

ten Dijke, P., Iwata, K.K., Thorikay, M., Schwedes, J., Stewart, A. and Pieler, C. "Molecular Characterization of TGF-β3" Ann. NY Acad. Sci. 593 (1990) 26-42

Thomas, H.C., "Heterogeneous Ion Exchange in a Flowing System" J. Am. Chem. Soc. 66 (1944) 1664-1666

Thommes, J. and Kula, M.R., "Membrane Chromatography- an Integrative Concept in Downstream Processing of Proteins", Biotechnol. Prog. 11 (1995) 357-367

Thompson, J.E., Vaughan, T.J., Williams, A.J., Wilton, J., Johnson, K.S., Bacon, L., Green, J.A., Field, R., Ruddock, S., Martins, M., Pope, A.R., Tempest, P.R. and Jackson, R.H. " A fully human antibody neutralising biologically active human TGF-β2 for use in therapy" J. Immunol. Methods 227 (1999) 17-29

Thompson, N.L., Bazoberry, F., Speir, E.H., Casscells, W., Ferrans, V.J., Flanders, K.C., Kondaiah, P., Geiser, A.G. and Sporn, M.B., "TGF-β1 in Acute Myocardial Infarction in Rats" Growth Factors 1 (1988) 91-99

Tijssen, P. "Practice and Theory of Enzyme Immunoassays" In: Laboratory Techniques in Biochemistry and Molecular Biology (Ed. Burdon, R.H. and van Knippenberg, P.H.), Elsevier (1985)

van Cott, K.E., Williams, B., Velander, W.H., Gwazdauskas, F., Lee, T., Lubon, H. and Drohan, W.N. "Affinity Purification of Biologically Active and Inactive Forms of Recombinant Human Protein C Produced in Porcine Mammary Gland" J. Molec. Recog. 9 (1996) 407-414

Vermeulen, T., LeVan, M.D., Hiester, N.K. and Klein, G., Perry's Chemical Engineers' Handbook 6th ed., Section 16, McGraw-Hill Book Company, 1984

Wahl, S.M., Hunt, D.A., Wakefield, L.M., McCartney-Francis, N., Wahl, L.M., Roberts, A.B. and Sporn, M.B. " TGF-β induces monocyte chemotaxis and growth factor production" Proc. Natl. Acad. Sci. USA 84 (1987) 5788-5792

Wakefield, L.M., Smith, D.M., Broz, S., Jackson, M., Levinson, A.D. and Sporn, M.B. "Recombinant TGF-β1 is Synthesized as a Two-Component Latent Complex that Shares Some Structural Features with the Native Platelet Latent TGF-β1 Complex" Growth Factors 1 (1989) 203-218

Wakefield, L.M., Smith, D.M., Masui, T., Harris, C.C. and Sporn, M.B. " Distribution and Modulation of the Cellular Receptor by TGF-β" J. Cell Biol. 105 (1987) 965-975

Wang, X-F., Lin, H.Y., Ng-Eaton, E., Downward, J., Lodish, H.F. and Weinberg, R.A., "Expression Cloning and Characterization of the TGF-β Type III Receptor" Cell 67 (1991) 797-805

Wilder, R.L., Lafyatis, R., Roberts, A.B., Case, J.P., Kumkumian, G.K., Sano, H., Sporn, M.B. and Remmers, E.F. " TGF-β in Rheumatoid Arthritis" Ann. NY Acad. Sci. 593 (1990) 197-207

Wrana, J.L., Attisano, L., Wieser, R., Ventura, F. and Massague, J. "Mechanism of activation of the TGF-β receptor" Nature 370 (1994) 341-347

Wu, S.P., Theodorescu, D., Kerbel, R.S., Willson, J.K.V., Mulder, K.M., Humphrey, L.E. and Brattain, M.G. "TGF-β1 is an Autocrine-negative Growth Regulator of Human Colon Carcinoma FET Cells In Vivo as Revealed by Transfection of an Antisense Expression Vector" J. Cell Biol. 116 (1992) 187-196

Yamaguchi, Y., Mann, D.M. and Ruoslahti, E. "Negative regulation of TGF-β by proteoglycan decorin" Nature 346 (1990) 281-284

Yamamoto, S. and Sano, Y. "Short-cut method for predicting the productivity of affinity chromatography" J. Chromat. 597 (1992) 173-179

Yarmush, M.L., Antonsen, K.P., Sundaram, S. and Yarmush, D.M. "Immunoadsorption: Strategies for Antigen Elution and Production of Reusable Adsorbents" Biotechnol. Prog. 8 (1992) 168-178

Zale, S.E. and Colton, C.K. (1994) "Method and apparatus for eluting proteins in affinity membrane process", U.S. Patent 5,310,688

Zola, H., "Monoclonal antibodies: a manual of techniques" (1987) CRC Press, Boca Raton, Fl

Errata

Page 36

Page 36 should include the following figure:

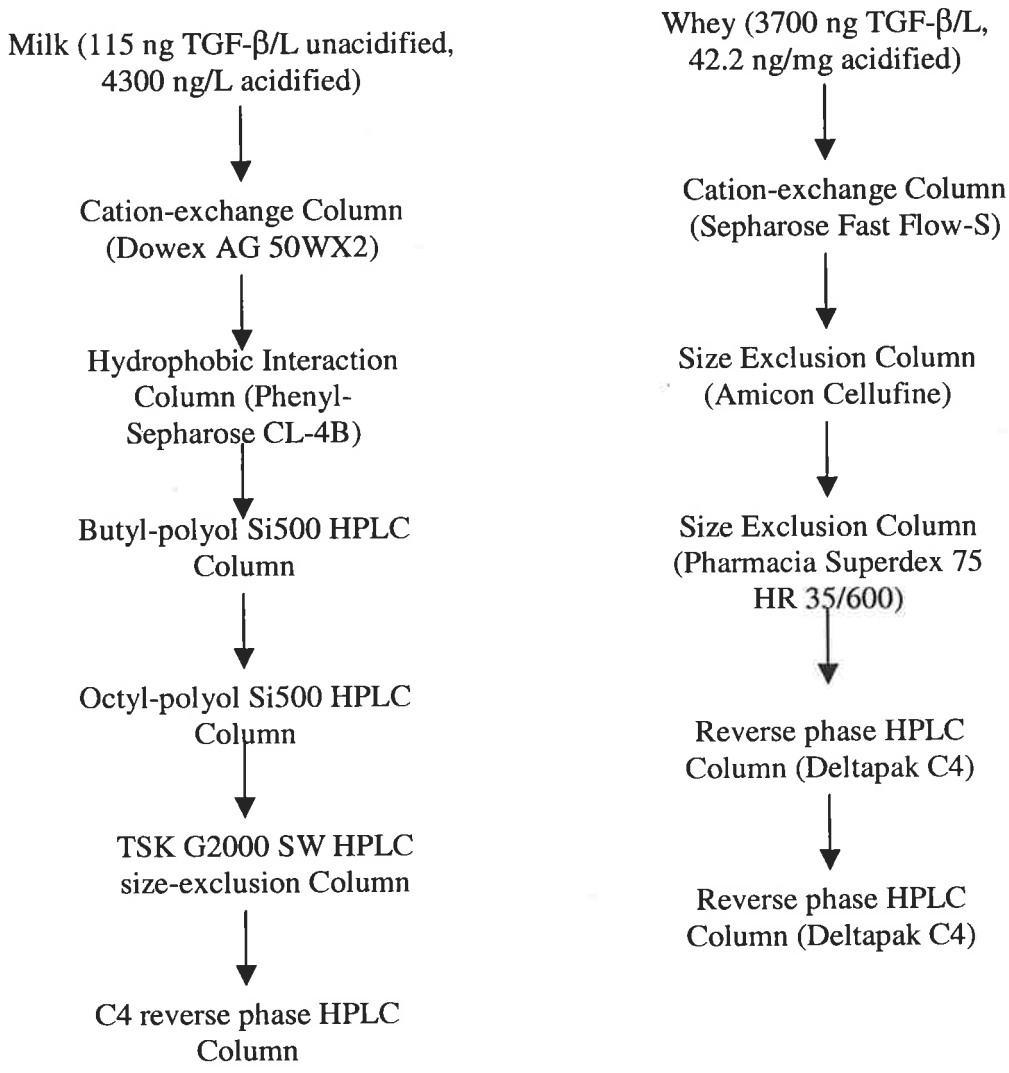

Figure 2.1: Comparison of the TGF-β2 Purification Methods. *The purification method of Cox and Burk (1991) and Jin et al. (1991) at left is compared with the method of Rogers et al. (1996).*

Page 38

On page 38 the rationale for using the TGF-β2 purification approach of Rogers et al. (1996) was given prematurely: "In view of the relative simplicity of the purification method of Rogers et al.

(1996) and the large quantities of WGFE available from the pilot-scale production facility, this purification method was selected for the purification of TGF-β2 immunogen." This statement should be relocated to the first paragraph under Results and Discussion on page 46:

"In view of the relative simplicity of the purification method of Rogers et al. (1996) and the large quantities of WGFE available from the pilot-scale production facility, this purification method was selected for the purification of TGF-β2 immunogen. WGFE was acidified and subject to large-scale gel filtration (page 44). The fractions were analysed for TGF-β2 by biological assay (page 38) or ELISA (page 40). TGF-β positive fractions were pooled and analysed by SDS-PAGE (page 43). The pool was loaded on the small scale gel filtration column (page 45) and TGF-β positive fractions were pooled. The TGF-β pool was then loaded on the reverse phase HPLC column (page 45) and subject to two rounds of purification firstly at 1%/min gradient and then at 0.1%/min. The TGF-β containing fractions were pooled and analysed by SDS-PAGE. In addition to TGF-β, the protein quantity in each pool was estimated by BCA protein estimation (page 42)."

Page 28

Table 1.5 should read:

Support Matrix	Example	Type
Agarose	Pharmacia Sepharose CL-6B	Packed bed, Stirred tank
Cellulose		Packed bed
Controlled pore glass and silica		Packed bed
Polyacrylamide Beads	BioRad Bio-Gel P-200	Packed bed, Stirred tank
Trisacryl	IBF Biotechnics Trisacryl GF-2000	Packed bed
Sephacryl	Pharmacia Sephacryl HR series	Packed bed
Ultrogel AcA	IBF Ultrogel AcA 22	Packed bed
Azlactone beads	3M	Packed bed
TSK-Gel Toyopearl HW	Tosoh	Packed bed
HEMA	Alltech HEMA-AFC BIO	Packed bed
Eupergit	Rohm Pharma Eupergit C	Packed bed
Poros	PerSeptive Biosystems	Perfusive bed

Page 49

The legend to Figure 2.2 is not correct and should read "SDS-PAGE of protein purified on the Cellufine column under reducing conditions".

Pages 98-99

The regions that stain for TGF-β2 in the immunohistochemistry patterns of Figures 3.24, 3.25 and 3.26 should be identified with arrows. The light coloured regions correspond to TGF-β2 staining.

Page 196

The heading "5.4 Chapter Overview" should be included at the top of page 196.

Page 218

The term "titre" is used incorrectly in the last paragraph. The term "antibody" is correct.